

Barbara Misztal

Wooden Domes

History and Modern Times

 Springer

Wooden Domes



Barbara Misztal

Wooden Domes

History and Modern Times

Reviewed by Prof. Zbigniew Kowal, Ph.D., Eng., Dr.H.C.

 Springer

Barbara Misztal
Faculty of Architecture
Wrocław University of Technology
Wrocław
Poland

ISBN 978-3-319-65740-0 ISBN 978-3-319-65741-7 (eBook)
<https://doi.org/10.1007/978-3-319-65741-7>

Library of Congress Control Number: 2017958719

Translation from the Polish language edition: *Kopuly DREWNIANE* by Wojciech Mühleisen, © PWN, Warsaw 2017. All Rights Reserved.

© Springer International Publishing AG 2018. Original Polish edition published by PWN, Warsaw, 2017.

This work is subject to copyright. All rights are reserved by the Publisher, whether the whole or part of the material is concerned, specifically the rights of translation, reprinting, reuse of illustrations, recitation, broadcasting, reproduction on microfilms or in any other physical way, and transmission or information storage and retrieval, electronic adaptation, computer software, or by similar or dissimilar methodology now known or hereafter developed.

The use of general descriptive names, registered names, trademarks, service marks, etc. in this publication does not imply, even in the absence of a specific statement, that such names are exempt from the relevant protective laws and regulations and therefore free for general use.

The publisher, the authors and the editors are safe to assume that the advice and information in this book are believed to be true and accurate at the date of publication. Neither the publisher nor the authors or the editors give a warranty, express or implied, with respect to the material contained herein or for any errors or omissions that may have been made. The publisher remains neutral with regard to jurisdictional claims in published maps and institutional affiliations.

Printed on acid-free paper

This Springer imprint is published by Springer Nature
The registered company is Springer International Publishing AG
The registered company address is: Gewerbestrasse 11, 6330 Cham, Switzerland

Preface

The existing massive population migrations due to wars and forecasted migrations caused by climatic changes result in the need to design an architecture that provides a shelter under difficult conditions of survival. There appeared a humanitarian architecture [99] (2016) looking for building solutions that provide a potential for survival in disasters, also the potential for the development of the society after disasters. The humanitarian architecture creates the process of the balanced growth of the place and the people who live therein. The most advanced technologically and economically types of wooden structures, such as shell roof coverings, are worth adding to the humanitarian architecture. A special variety of such roof coverings are axially symmetrical coverings from solid wood, as discussed in this publication. Wood is the unique building material renewable in a way that it fosters the human environment, even reconstructing that environment, contaminated by the heavy industry products. While consuming carbon dioxide, it delivers oxygen to the atmosphere. Wooden domes collated and described in this publication are a favourable alternative to other building industry types.

The process of moving from post-beam systems up to reaching arches and dome forms, including wooden domes, lasted for centuries. Systems of a very favourable relationship of load capacity to the weight of a structure were developed by evolution. Despite many advantages, there are few records in the references on their subject. The existing information is fragmentary. Many solutions of dome structures vanished jointly with the people who built them. It is the intent of the author to propagate the knowledge of economic and eco-friendly wooden dome structures. For the further development of wooden structures, among others, domes, the author compiled the most urgent topics of theoretic research studies and analyses.

The form of a dome has a minimum outside surface in relation to that being covered. This results in a lower airflow resistance, owing to which domes are more resistant to the interference of wind and climatic impacts. The minimum outside surface limits losses of heat, increases energy savings, and reduces heating costs. The centre of gravity located quite low brings about that they are more stable in the situation of an earthquake. The publication aggregates historical examples and

discusses such shaping of domes that allows to build facilities adapted to the recently occurring climatic phenomena.

The monograph discusses 36 structural solutions of historical domes and compares them to nine examples of the most eminent accomplishments of domes made from glued laminated timber. The structure of some forgotten domes was reconstructed on the basis of the available information remainders. The missing data were supplemented on wooden models or computer visualizations so as to present the most advanced, technologically and economically, types of historical wooden structures. The reconstructed file is all the more precious because it presents the systems characteristic of wooden structures only, perfected over centuries by talented builders. Their characteristic feature is that they are geometrically invariable, being safe in use at the same time. The adaptation of the construction to the dome shape, using the properties of wood, followed over centuries, which resulted in the development of reliable systems. The structural solutions consisting in the multiple prestressing of load-carrying elements brought about the development of systems having a high load capacity at a minor weight of the wood applied, including that of common quality.

The comparison of the accomplishments of a large cubic capacity from glued laminated timber and domes from non-glued laminated timber allows to notice a lower consumption of materials as converted per unit of the projection area for historical domes.

The paper shows that many among historical solutions of dome structures from non-glued laminated timber have had, until this day, an economic, eco-friendly and technological justification. They should continue to be developed based on the improvement of systems characteristic of wood.

In the present-day edition of this monograph, the historical part has been supplemented with new examples of dome structures of facilities, built until the middle of the twentieth century. They have been compared against the largest domes from glued laminated timber built in 1977–2004. The description of the research has been broadened by the testing of wood properties.

I yield thanks to Prof. Zbigniew Kowal, Ph. Eng. from Kielce University of Technology, for the consent to quote extensive fragments of his works.

I yield thanks to the attention of the Director of the Faculty of Wood Construction Engineering, Miyazaki Prefectural Wood Utilization Research Center, Dr. Yutaka Iimura, to the Company's Management Board for making available the drawings of large-cubature space domes from glued laminated timber built in Japan. I thank all the team for the friendly welcome at the Company's seat.

I sincerely thank the readers who have become familiar with my book entitled 'Shaping the Solid Wood Domes' for their favourable feedback. It has motivated me to work on the second edition, supplemented and broadened, entitled 'Wooden Domes'.

I yield my respectful thanks to all those who contributed to the publication of this book.

Contents

1	Introduction	1
	References	4
2	Selected Elements of the Dome Building History	5
	References	13
3	Multi-Shell Domes	15
	3.1 Introduction	15
	3.2 Wooden Scaffoldings for the Building of Masonry Structures from Stone or Brick	15
	3.3 Wooden Covering Domes Developed from the Wooden Scaffoldings of Masonry Domes	20
	3.3.1 Multi-shell Domes Built in the Middle East	21
	3.3.2 Multi-layer Domes Built in Europe	24
	3.4 Multi-shell Domes with an Outside and Inside Wooden Dome	34
	3.5 Ribbed Domes from Arch Centres	38
	3.6 Conclusions	47
	References	49
4	Thick-wall Domes	51
	4.1 Introduction	51
	4.2 Methods of Shaping Log Connections	52
	4.3 Dome-like Log Coverings	53
	4.4 Compilation of Dome-like Forms	61
	4.5 Domes with a Massive Shell	62
	4.6 Examples of Domes with a Massive Shell	63
	4.7 Conclusions	72
	References	74

5	Ribbed Domes	77
5.1	Introduction	77
5.2	Ribbed Domes Built in Switzerland and Germany	77
5.2.1	Ribbed Domes Built in Russia	80
5.3	Conclusions	92
	References	93
6	Shell Domes	95
6.1	Introduction	95
6.2	Shell, Smooth Domes	96
6.3	Shell Domes Prestressed with Steel Tie Rods	101
6.4	Shell-Ribbed Domes	104
6.5	Ribbed-Shell Domes	108
6.6	Conclusions	115
	References	116
7	Gridshell, Ribbed–Shell Domes	117
7.1	Introduction	117
7.2	Sectoral, Gridshell Domes	118
7.3	Gridshell Domes from Arch Centres	121
7.4	Steel-Prestressed Gridshell Domes	126
7.5	Shell Domes on a Grid from Arch Centres Strengthened in the Node with a Flat Plank	128
7.6	Gridshell Dome on a Rhombic Grid from Planks	129
7.7	Testing Gridshell Dome Models from Arch Centres	130
7.8	Meaning of Ribs-Crossheads in the Development of Wooden Gridshell Domes	132
7.9	Conclusions	135
	References	136
8	Selected Examples of Domes from Glued Laminated Timber	137
8.1	Introduction of Wood Gluing to Structures	137
8.2	Examples of Prestigious Domes from Glued Laminated Timber Built in the USA	139
8.3	Examples of Domes from Glued Laminated Timber Built in Europe of a Diameter Higher Than 100.0 m	144
8.4	Examples of Prestigious Domes from Glued Laminated Timber Built in Japan	147
8.5	Conclusions	156
	References	163
9	Issues of the Load Capacity and Stability of Compressed Wooden Bars	165
9.1	Introduction	165
9.2	Static Balance Paths of Wooden Bars in Function of Axial Load	166

- 9.3 Analogy of the Loss of Stability of Wooden Bars to that of Composites Reinforced Axially with Fibre 168
- 9.4 Impact of Transverse Forces on the Critical Load Capacity of Wooden Bars 170
- 9.5 Impact of Compressive Forces on the Destruction of Wooden Bar Ends in Nodes—Cleavage of Compressed Bars’ Ends 174
- 9.6 Impact of the Pasting of Steel Nodular Sheets on the Load Capacity of Wooden Bars 178
 - 9.6.1 Effects Accompanying the Pasting of Steel Sheets into the Extreme Section of Compressed Bars 178
 - 9.6.2 Examples of the Destruction of Wooden Bars’ Ends Fastened in Steel Nodes 179
- 9.7 Impact of the Longitudinal Stiffness Reduction of Compressed Bars on the Dome Node Snap-Through 182
 - 9.7.1 Impact of the Bar-Compressing Strength on the Bar’s Longitudinal Stiffness 182
 - 9.7.2 Effect of the Node Snap-Through in Domes as a Cause of Catastrophes 186
- 9.8 Concentration of Tangential Stresses on the Surface of Fibres in Wooden Beams Loaded Transversally and Axially 188
- 9.9 Warning Properties of Wood Accompanying the Exhaustion of the Load Capacity of Compressed Bars 190
- 9.10 Strengthening of Compressed Wooden Bars Under Load 193
- 9.11 Impact of the Wood Protection Technology on the Load Capacity of Wood 194
- References 202
- 10 Effect of Time on the Mechanical Properties of Wood 205**
 - References 211
- 11 Testing Wooden Elements for the Building of Domes 213**
 - 11.1 Introduction 213
 - 11.2 Dynamic Testing Oriented Towards the Choice and Selection of Wood for the Construction of Domes 217
 - 11.3 Dynamic Testing Results Oriented Towards the Determination of the Modulus of Direct Elasticity E of Wood 225
 - 11.4 Conclusions 230
 - References 232
- 12 Assessment of the Physical Properties of Wood-Based Materials on the Basis of the Measurement of Free Vibration Parameters 235**
 - 12.1 Introduction 235
 - 12.2 Dynamic Testing of Models from Wood-Based Materials 235

12.3 Comparison of the Vibration Period of the Tested Models 242

12.4 Comparison of the Vibration Damping of Dry and Wet
Models in Order to Reveal Wetted Materials 243

12.5 Comparison of Residual and Permanent Deflections
of the Tested Models from Wood-Based Materials 244

12.6 Dynamic Testing Oriented Towards the Determination
of the Coefficient of Direct Elasticity E of Wood
Derived-Materials 245

12.7 Conclusions 248

References 249

Summary 251

End 261

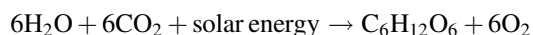
Bibliography 267

Chapter 1

Introduction

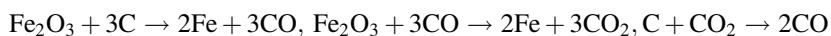
The aim of this monograph is to present the opportunities of using wood as construction material in which both the architects and the designer can achieve various useful, cheap and aesthetic facilities, even for the most fastidious user.

In modern times, wood is a re-discovered material due to its mechanical and eco-friendly properties. Wood is the unique construction material the production of which is accompanied by the absorption of many environmental pollutants, including carbon dioxide. In the photosynthesis reactions, in the presence of light, there follows the bonding of water collected by wood from soil and carbon dioxide from air. The products of this reaction are carbohydrates and oxygen. The generally known reaction follows according to the scheme:



While growing and increasing their weight, trees supply oxygen to the atmosphere. Wood is the unique construction material renewable in a friendly way to the atmosphere, and even reconstructing this environment contaminated by the heavy industry products, which was described by the authors Krutul D., Kozakiewicz P., in the publication [1] (1998).

As a comparison, the production of steel (from ore, e.g. Fe_2O_3 —hematite of the highest iron content), used commonly in building industry, consists in the reduction with coal of oxide ores, supplying huge amounts of carbon dioxide to the atmosphere—CO. The simplified scheme of the metallurgical process is reduced to the reaction:



Besides, wood is a construction material that is relatively easily treatable. Structures made from wood can be combined and adapted on the construction site, sometimes by the economic way, with the use of the simplest tools.

Wood is a particular construction material, richly provided by nature. The detailed learning of the structure, biology, chemistry and mechanical behaviour of wood under various environmental conditions, allows its correct application. The comprehensive testing was conducted within this scope at the Faculty of Wood Technology of SGGW, Warsaw University of Life Sciences. Professor Krutul D. with his team specifies the quantitative share of microelements, including metals, in the wood structure, e.g. [2] (1996) [3] (1996). The chemical structure affects the resistance or susceptibility to corrosion, e.g. biological corrosion.

The increase in the durability of wooden structures, especially prestigious ones, can be achieved by using natural defensive mechanisms of wood, by resigning from some methods that destroy its structure, in particular mechanical properties. The susceptibility of wood to external factors can be used, revealing its beauty, like in the furniture items by Michael Thonet described by Sassone A. et al. in the work [4] (1997) or by impregnating it, e.g. with vacuum-pressure methods, destroying its mechanical properties.

In this area, particularly valuable is the testing carried out by the team of Bednarek Z., Kaliszek-Witecka A., demonstrating the destructive impact of salt impregnates on the properties of wood. The test results were described in the work [5] (2004) revealing that salt preparations used for wood impregnation decrease its strength. This information is of basic importance in the securing of wood used in the construction of thin-wall shells, including domes.

Among many systems built from wood, domes have been selected, as the most advanced technologically types of wooden structures. Their historical development has been tracked, pointing out to optimum solutions, suitable for a general application.

The shaping of domes from solid wood differs from that of domes made from other materials. It requires some knowledge on the realization of wooden elements of load-bearing constructions, on connections, on the geometrical shaping of the dome sphere adapted to the properties of wood.

Since the dawn of the building trade, prestigious building facilities roofed with domes from solid wood have been known. The cases of catastrophes of such domes for causes other than fires are ignored. Unfortunately, the information on the wooden domes burnt down are fragmentary. Neither are unknown reports about the destruction of wooden domes, e.g. due to biological corrosion.

Wars and random cases produced that those works vanished in fire, also due to the human ignorance. For instance, a fire broke out during the overhaul of the roof of the central dome (Fig. 1.1a) on the building of the Trinity-Izmailovsky Cathedral in Petersburg, crowned with 5 domes. The authors Orłowicz R., Kosiorek M. in their publication [6] (2007) described the impact of the fire on the inside masonry dome. Figure 1.1 shows the view of the domes before the fire and the fire of the central dome.

The outside, wooden structure, shielding the masonry shell, burnt down fully. For the analysis of the masonry dome, just a section of the wooden structure shielding it earlier is attached. The figure of the structure of the burnt-down dome is

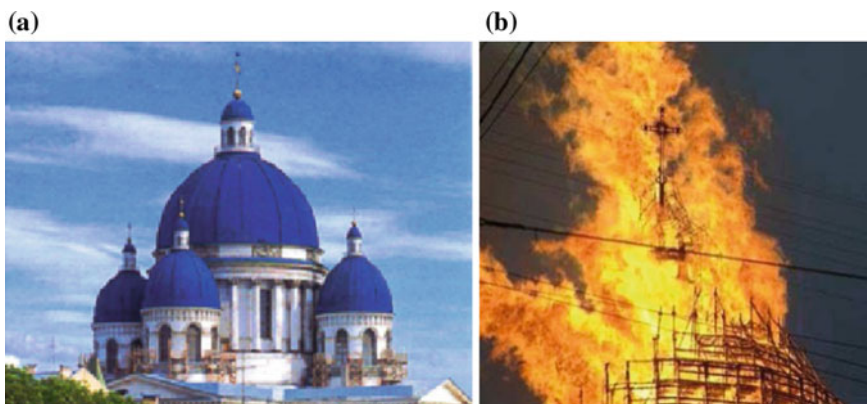


Fig. 1.1 Domes of the Trinity-Izmailovsky Cathedral of 1826 to the design by the architect Stasov V. P. [6] **a** domes of the cathedral before fire, **b** fire of the wooden central dome

shown in Chap. 3 in Fig. 3.17c made up on the basis of [6]. The wooden dome built in 1826 burnt down on 25 August 2006.

Wooden domes are vanishing before our eyes, along with the knowledge that made up their creation. We know about them only from fragmentary, disordered reports by various authors. Most often, the descriptions of the decorations of the dome palate are specified, and not of the structure on which details were made.

Attention, however, should be paid that wooden domes known from laconic descriptions were built with a high feeling of the structural stability and the properties of wood. It is all the more noteworthy that they also were created in the severe, continental climate of Eastern Europe where considerable loads by wind, snow and temperature appear. The research on the development of the structures of wooden domes is not only a tribute paid to the work and skills of the builders, but it also teaches the rational application and fabrication of useful wooden structures in present times.

Domes belong to the building facilities of architecture in which the form was shaped over centuries, while finding the proper structure for them. In this work the development of the structure required to accomplish the form of wooden domes has been discussed. The testing allowing to better learn the properties of wood necessary for their construction have been suggested. The technology based on the mechanics of wood can make the building of domes a cheap and eco-friendly undertaking.

While tracking the development directions in the designing and realizations of domes throughout the world, the author has started her own search for dome structures from solid wood, as eco-friendly structures, created at the minimum wood consumption and associated minimum destruction of the environment. Owing to the research of the literature to describe the existing, but also forgotten facilities, various solutions of domes from solid wood have been tracked, arranging them in a typological series, starting with the roofings of dome-like domes up to thin-wall

shell domes with an imposingly low consumption of material in relation to the surface being covered. Those systems were considered to be an attractive proposal for contemporary researchers, designers and users.

The documentation of many domes from solid wood, and not glued laminated timber, has been reconstructed from rudimentary information found. Models from wood and computer visualizations of forgotten structures have been plotted and built.

It is the intention of the author to summarize the status of the knowledge on the domes made from solid wood, in order to ensure their further transformations based on the contemporary knowledge, using contemporary tools and calculation methods. **Despite many presently accomplished structures from glued laminated timber, the experience in the area of building domes from solid wood is precious and their propagation is recommended.**

References

1. Krutul D., Kozakiewicz P., *Właściwości fizykochemiczne oraz cechy budowy mikroskopowej drewna brzozy porażonej przez Piptoporus betulinus*. SYLWAN 4: 49–59, Warszawa 1998.
2. Krutul D., Kazel-Bek D., Sacharczuk D., *Zawartość niektórych pierwiastków w korze i drewnie sosny zwyczajnej (Pinus Sylvestris L.)*, XIII Konferencja Naukowa Wydziału Technologii Drewna SGGW: “Drewno – materiał o wszechstronnym przeznaczeniu i zastosowaniu”, Warszawa 16–18 listopada 1999.
3. Krutul D., *Rozmieszczenie substancji mineralnych na przekroju poprzecznym i podłużnym pni sosnowych*, Konferencja Naukowa Wydziału Technologii Drewna SGGW Drewno – Tworzywo Inżynierskie, Warszawa 16 lutego 1996.
4. Sassone A., Cozzi E., Griffo M., Sciolla G. *Meble XIX wieku*. Wydawnictwo Amber Warszawa 1997.
5. Bednarek Z., Kaliszek-Wietecha A., *Wytrzymałość drewna impregnowanego ogniochronnym środkiem solnym metodą próżniowo- ciśnieniową*. 50 – ta Jubileuszowa Konferencja Naukowa Komitetu Inżynierii Lądowej i Wodnej PAN i Komitetu Nauki PZTIB “Krynica 2004” 12–17 września 2004 roku.
6. Orłowicz R. B., Kosiorek M. *Skutki pożaru Katedry Troicko - Izmailowskiej w Petersburgu* XXII Konferencja Naukowo Techniczna Szczecin - Międzyzdroje, 23–26 maja 2007.

Chapter 2

Selected Elements of the Dome Building History

The development that was taking place over centuries in the field of the stability of wooden structures and constructions can be analysed by observing the changes occurring in the wooden building trade. Since wooden structures are specific models of geometrically invariable bar structures.

This is applicable both to wooden structures, allowing to build stone and brick structures, and structural systems characteristic of wooden domes. A hypothesis may be formulated that the creation of wooden domes was preceded by the development of scaffoldings for the building of stone domes. In the historical process of the effective use of wooden structures, associated with domes, transformations of architecture, structure and understanding of statics, also the production of structural elements, the methods of their connection and building technologies are noticed.

The prototype of the dome was created already in very remote times when man started building shelters in form of a hut from branches. These first structures—a couple of branches embedded in soil and bound above—have accompanied us from the very beginning of the civilization.

The proven form and structure of a hut from branches also happen to be an inspiration for contemporary architects. In 1986, in Visegrád, a dome from tree stems was built. The author of the project was Imre Makovecz, a Hungarian architect from Budapest. On the basis of the work by Natterer [1], a figure was compiled, Fig. 2.1, presenting its structure. The facility has a span of circa 11.5 m and a height of 9.0 m. The natural appearance of the dome ribs emphasizes the rationalism of the structure and the beauty of the minimalist form.

In the civilizations of the East and the West, domes were built to distinguish the given facility from among other building structures. The sacral and prestigious facilities were crowned with a dome in order to achieve a strong urbanistic accent.

They were built on roofs of the centres of authorities, religious cult and culture. In building structures of a special destination, having extensive meeting rooms, a

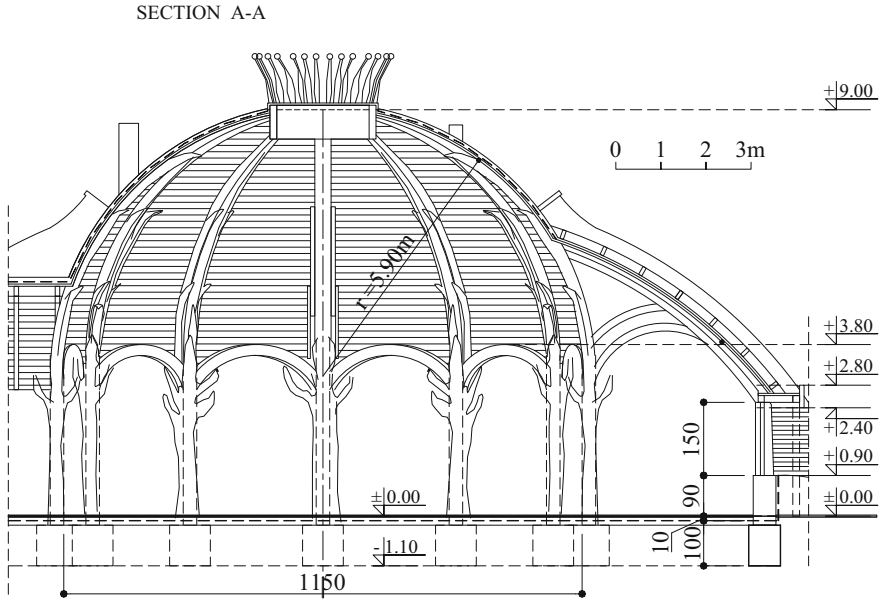


Fig. 2.1 A “hut-like” dome built in 1986 in Visegrád according to [1]

dome was used as a unique, known at that time, roof covering without intermediate supports. The palate of the dome was applied to arrange an exceptionally scenery of the representative interior. It was often covered with paintings with views from the biblical heaven.

Domes are characterized by a minimum outside surface in relation to the volume of the interior. The two-curvature of the dome surface fosters the reduction of materials in relation to the cubic volume of the facility and limits the destructive environmental effects. Its shape ensures the reduction of the load by wind and facilitates a quicker drying of the surface, and the distance of the structure of useful surfaces impedes the formation of fire. This is confirmed by the domes of various historical facilities existing to date.

Depending on the geographical position, in various proportions, the first materials used for the construction of domes were stone, clay and wood. The availability of stone in the Mediterranean area and its greater durability affected its use in the building structures of Egypt, Greece and Rome.

The timeless building facilities of Egypt were formed from stone. Stone, having a high resistance to compression, has a many-time lower resistance to extension and is susceptible to brittle breaking. Hence a huge quantity of pillars in constructions supporting the ceilings of the temples of Egypt where the clear distance between the pillars similar to their diameter is noticed.

The Ancient Greece contributed technical inventions that were using the favourable properties of stone and wood in building trade. Stone walls were built in

the temples of Greece, the thickness of which amounted to $1/20$ of the clear spacing of supports. Such proportions were achieved, for instance, in the Aeschylus temple in Epidaurus, built in ca. 370 BC to the design by Theodorus from Samos [2]. The slight thickness of masonry, stone walls allows to presume that light, wooden roofs were resting on them. The spacing of walls and pillars shows that it could not be simple beam roofs. The clear spacings of supports indicate a truss system or an arch system.

Kuznetsov A.W. in his work [2] described two potential variants of a light roof structure, matching the slim fragments of the walls of the Aeschylus temple from the 4th century BC, which is shown in Fig. 2.2. The author supplemented the Kuznetsov's figures by the dimensions, as specified by himself, of the load-bearing walls burdened by the roof structure: wall thickness and spacing between walls. The roof covering of the temple was based on two rings. The skewback of the central roof covering rested on the internal ring, based on columns. Two masonry vaults and the temple roof rested on the internal wall and the outside colonnade. Those vaults, beside their own weight and that of the roof, probably transferred the strutting caused by the central roof covering, maybe by the dome.

Such solution method of the temple structure would give evidence that Greeks had the knowledge of the polygon of forces and the skills how to use it in the designing of building structures.

The engineers of Rome, using the load capacity of stone to compression, propagated semi-circular arches of a high eminence. They used wood sparingly, just for bent and stretched structural elements.

The development of stone domes in the ancient Rome is associated with the growing demand for prestigious facilities with representatives large-surface halls. With higher dimensions of dome-roofed rooms, the use of full masonry domes was related to a high consumption of material. The illustration of the huge mass of material used for the dome is the hall with the statue of Venus in Rome [3] (Fig. 2.3). Worth noticing in the facility shown in Fig. 2.3a is the execution of the spherical roof covering using the sphere division into caissons having the rhomboid form. The author estimates that the weight of the masonry canopy amounted to more than 7000.0 kg/m^2 of the dome's projection.

Despite the enormous weight, domes from concrete, stone and brick were built due to their durability so that they could outlast wars and barbarian invasions. This ensured the perpetuation of patterns and fostered their imitation. It contributed to the creation of many masonry domes in the south of Europe.

Romans used the static properties of domes. By slightly lifting the dome peak, they approached the dome profile to the chain curvature. In Rome, in 125 AC, it was probably the builder Apollodorus from Damascus [4] who managed the works at the erection of the highest axially symmetrical dome—the Pantheon. The construction of the dome was made from the Roman concrete. Its section and dimensions are shown in Fig. 2.4a. The facility has a diameter of 43.30 m and a height of 43.89 m. The thickness of the walls to support the dome totals $1/6$ – $1/7$ of its diameter—Fig. 2.4 [2]. Over 1300 years, the dome of the Pantheon was the largest dome of the Western European civilization. The search for lighter solutions

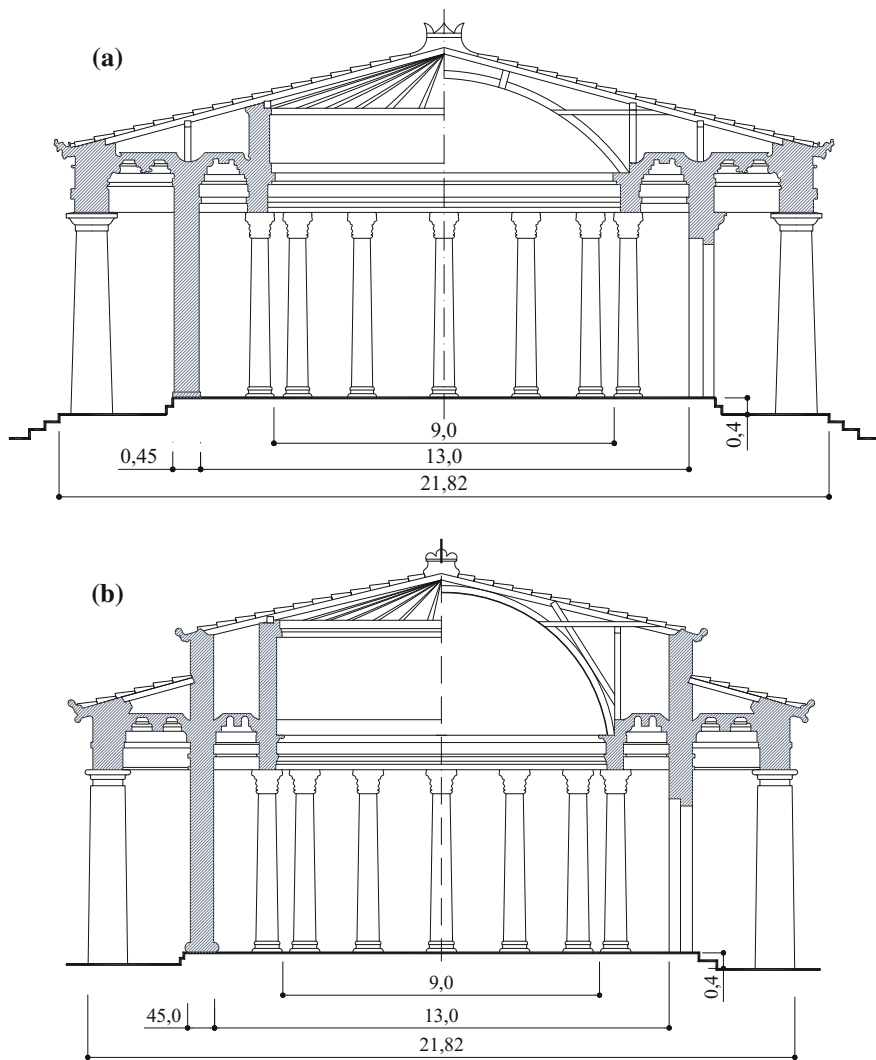


Fig. 2.2 Reconstruction variants of the roof of the Aeschylus temple in Epidaurus, Greece according to [2]

in the masonry dome structures and the need to use wooden scaffoldings to build the domes lasted for thirteen centuries.

In 1412, builders started to proceed with the resolving of the crowning of the Santa Maria del Fiore Cathedral in Florence with a dome [5], the building of which had been started in 1296. The dome of an internal diameter of ca. 42.0 m had been planned on an octagonal tambour of a 17.0 m long side, ending at the height of 55.0 m above the cathedral floor level.

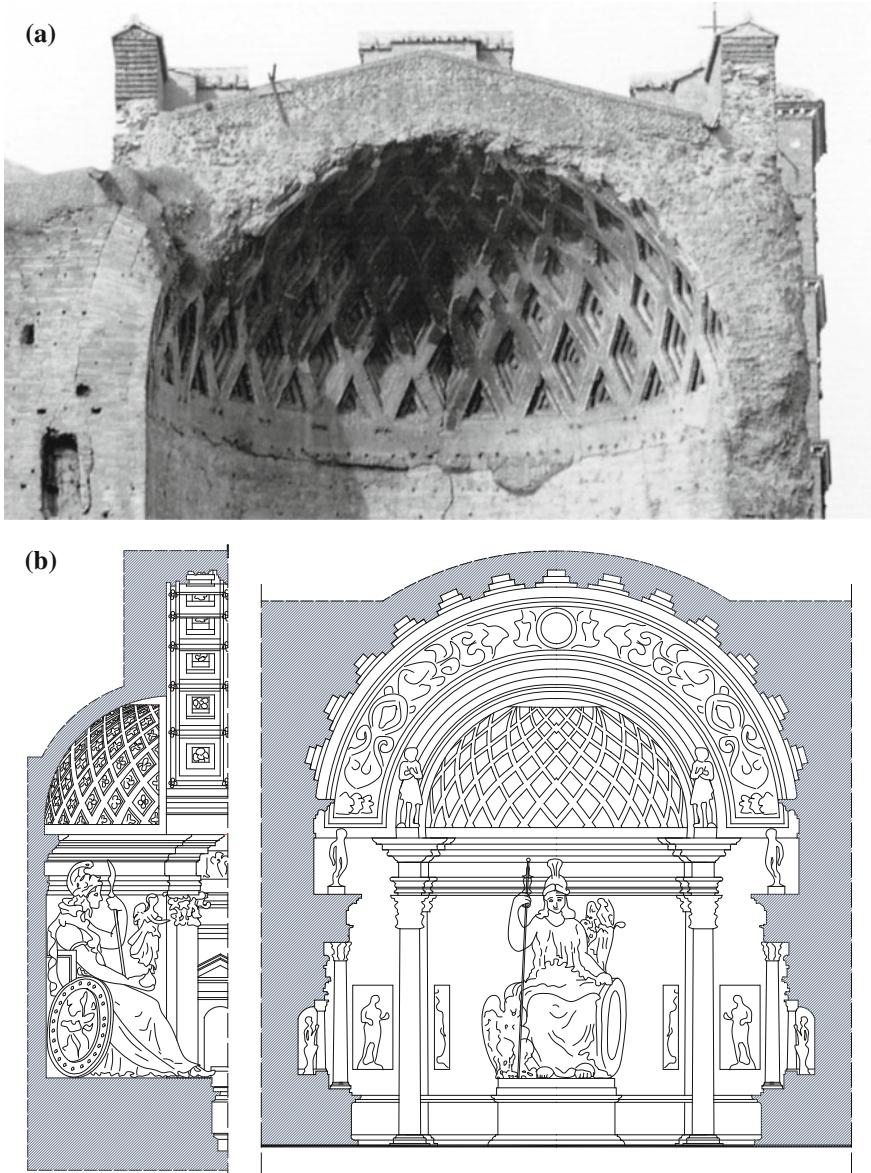


Fig. 2.3 Dome of the Diana Temple of 135 AC. **a** contemporary view of the dome from the inside [3], **b** reconstructed section of the historical interior (figure developed on the basis of the sketch by the German architect Josef Bühlmann of the facility reconstruction project; *Die Architektur des Klassischen Altertums und der Renaissance*; 1913, Verlag; München, Deutschland)

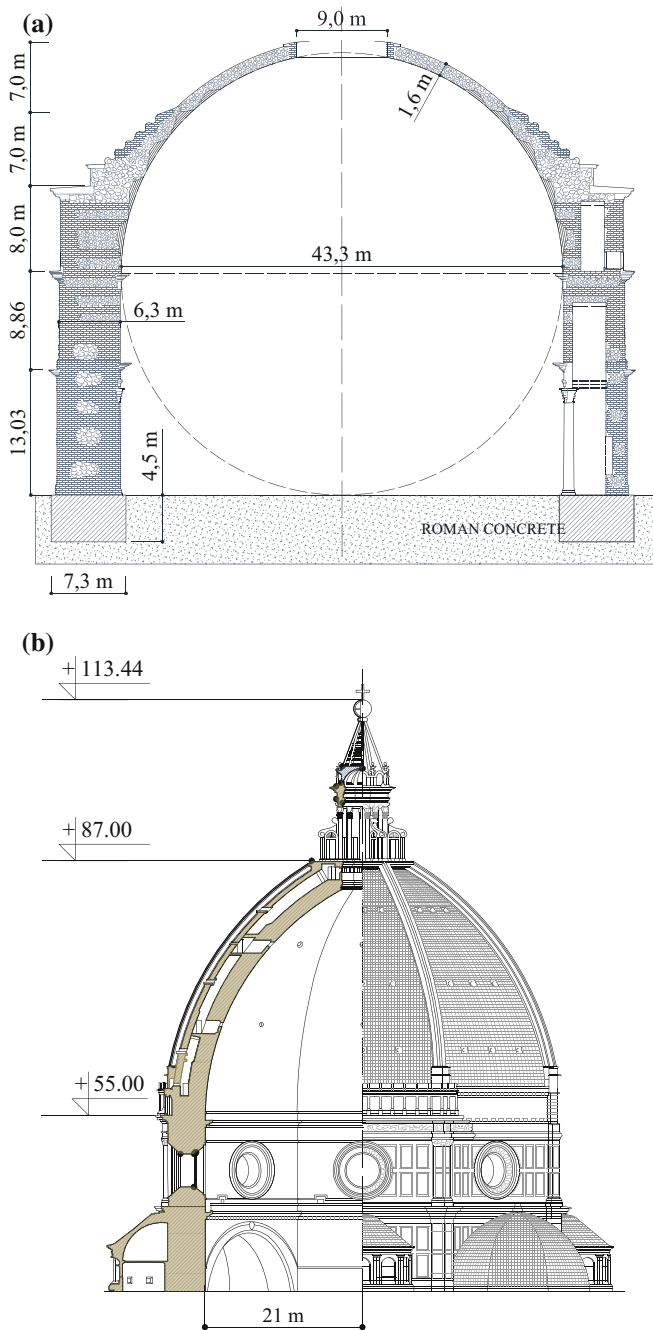


Fig. 2.4 The largest domes of the Mediterranean civilization, **a** section of the dome of the Pantheon in Rome to [2], **b** section of the dome of the Santa Maria del Fiore Cathedral in Florence according to [5]

The attempts to position a scaffolding under the heavy, masonry two-shell canopy of the dome demonstrated how difficult it was to build a sufficiently resistant scaffolding having the wooden construction only known in that time. The task to maintain two massive masonry shells exceeded the technological capacities of the epoch.

The investment project was saved by the idea by the architect Filippo Brunelleschi. In his project, he proposed to build an ogival, two-shell ribbed dome that would be a scaffolding for itself [5]. The idea was innovative and in order to prove its feasibility, F. Brunelleschi built, without scaffoldings, a dome in the Ridolfi's Chapel in the San Jacopo sopr'Arno Church [6].

Brunelleschi F. applied in the construction of the dome of the Santa Maria del Fiore Cathedral eight meridional main ribs and sixteen intermediate ribs, two ribs between the main ribs each. The building of the dome was started in 1420. The constructing of the ribs and the two shells was scheduled to follow in several stages. Each stage of the erection led to the closure of the dome curvature. The completion of each stage was the execution of a horizontal, latitudinal rib to stiffen meridional ribs. The circumferential closure of main and intermediate ribs secured the meridional ribs against twist. Brunelleschi F. made masonry canopies between the ribs as two-shell canopies. The outside canopy protected the inside one against weather effects. The backup facilities of the construction yard was arranged on the horizontal ribs, including a canteen for workers. Two masonry shells rested an octagonal tambour. Brunelleschi F. designed strings of steps and ramps between the masonry shells. The traffic of workers and the transport of materials was carried out over there. Brunelleschi F. developed the structural system of the dome canopies, gutters and drains, inter-connections of the masonry canopies in order to provide the stability of the dome, even during an earthquake. The space between the shells has been, until today, sufficient for the routing in plumb line between the masonry canopies of the dome [6].

During the construction, it turned out that the heavy stone could be used at the dome's base up to the height of seven metres. Lighter materials were used higher, such as porous travertine or brick. The building technique of the shells was described by Brunelleschi F. in his "Rapporto" in 1426. Probably, this was an oriental plot imported by Brunelleschi F. to Europe. This technique consisted in making in the wall of parallel, spiral ribs raising obliquely. Bricks were laid, I quote: "not flat, but upright" so that they protruded from the canopy—Fig. 2.5c. Meridional, inclined spirals of bricks to pressurize and stabilize the bands of bricks were laid in parallel, ensuring a higher coherence and resistance of masonry shells.

The dome of the Santa Maria del Fiore Cathedral was constructed for sixteen years and the building process was completed in 1436 (Fig. 2.4b). Thus, the construction of the cathedral lasting for 140 years was finalised. For one hundred and twenty years it was an expression of the top achievements of the technology of building masonry domes until the creation of the Saint Peter's Basilica in Rome.

The models and the drawings of auxiliary scaffoldings and equipment needed during the construction of the cathedral have outlasted until our times in the Uffizi Museum in Florence. Brunelleschi F. designed many innovative and efficient

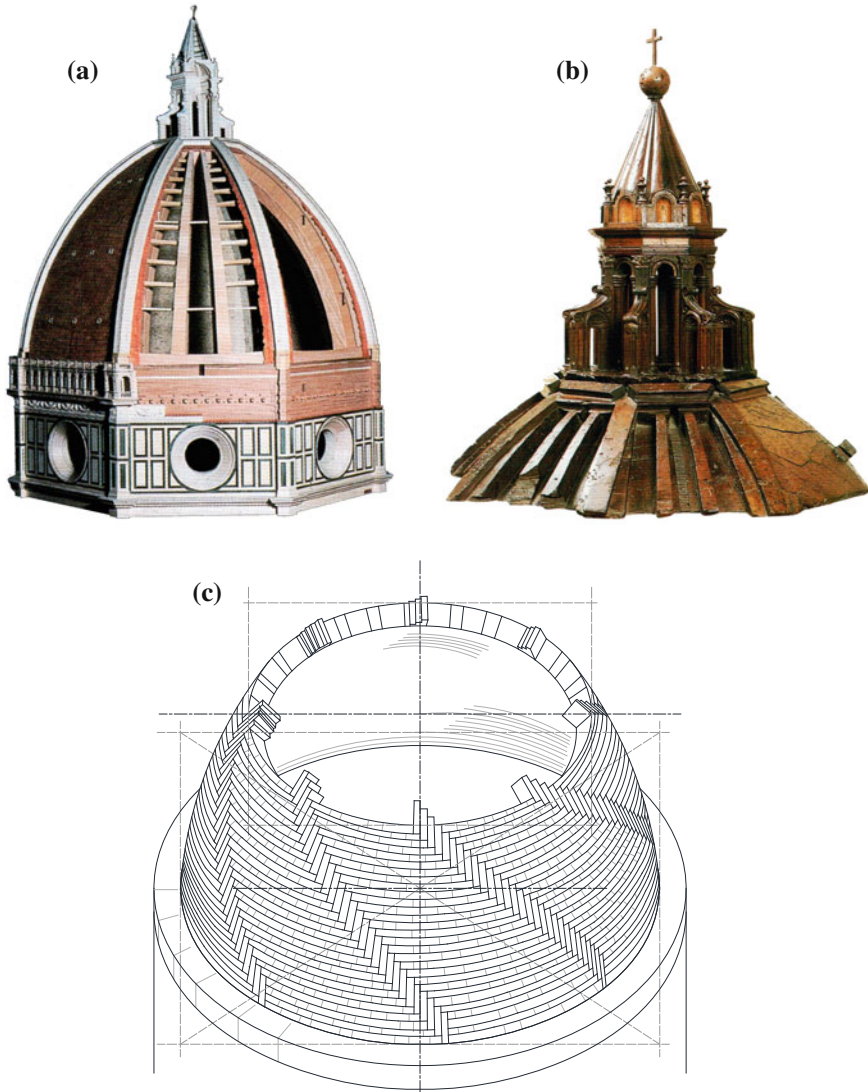


Fig. 2.5 Exhibits of the Uffizi Museum in Florence: **a** wooden model of the dome of the Santa Maria del Fiore Cathedral, **b** wooden model of the lantern to crown the dome, **c** drawing of the brick motif of the dome's masonry shell made on the basis of drawings by Brunelleschi [6]

construction machines, and he even designed, and his own expense, a barge (for which he was awarded with a patent) to convey heavy marbles on the Arno river [7]. We do not know the criterion for the choice of wood. It is known that they were designed sparingly, with a large knowledge of wood statics and features. Of interest is the opinion of another eminent creator of the Renaissance, Leone Battista Alberti,

formulated on the occasion of the inauguration of the cathedral on 25 March 1436. Alberti L.B., full of admiration, wrote, “Whosoever could be so envious and unwilling so as not to praise Pippo, the architect, seeing here such an enormous structure, aerial, able to cover with its shadow all the peoples of Tuscany, made without the support of arch centres and a great amount of wood” [6].

In 324 AC, Emperor Constantine ordered the erection of the basilica in honour of Saint Peter in Rome. The building of the facility was started, the extension and improvement of which lasted for 1200 years when Michelangelo joined the project.

Basing on the sketches by Bramante D. (from 1505), he designed the basilica on the plan of the Greek cross, crowned in the centre by a dome having a double canopy. The Saint Peter’s Basilica in Rome was built in 1506–1626 in the shape known to us. The form and structure of the Basilica changed along with the architects striving for the expression of the papal prestige by the architecture. The work started by Bramante was finally determined by Michelangelo and its construction according to his concept was completed after his death. In 1588–1590, the masonry, two-shell dome of the Saint Peter’s basilica, having a diameter of 42.52 m and a height of 52.0 m, was created. The weight of the dome totals 6800.0 kg/m² of its projection [8].

The domes of: the Diana Temple, the Pantheon, the Santa Maria del Fiore Cathedral, the Saint Peter’s Basilica, are characterized by an enormous weight of the shell and the structure. The accomplishment of such facilities was possible on the rocky soils of the southern Europe.

Proven scaffolding systems of wood were required for their construction. The constructing of resistant scaffoldings to maintain stone and brick structures contributed to the development of geometrically invariable wooden structural systems and statics of bar structures. An essential role was also played by the constructing of wooden models of the facilities projected, required by the founders. The ease of making wooden models of structures and the possibility to adjust the system in order to provide the geometrical invariability of the structure assisted the difficult investment process.

References

1. Natterer J., Herzog T., Volz M., *Holzbau Atlas Zwei*, Institut für internationale Architektur-Dokumentation GmbH, München 1991.
2. Kuzniecowa A., W. *Tektonika i Konstrukcja Ciętriczeskich Zdzanij*, Gosudarstwiennyje Izdatielstwo Architektury i Gradostroitelstwa, Moskwa 1951.
3. Saudan M., Saudan-Skira S., *Coupoles: espaces symboliques et symbols de l’espace*, La Bibliotheque des Arts. Genève Atelier d’édition, “LE SEPTIÈME FOU [B.R.]”.
4. Głab J. *PONTIFEX MAXIMUS. Ponad przestrzenią i czasem*. Wydawnictwo Politechniki Śląskiej, Gliwice 2009.
5. Murray P. *Architektura włoskiego renesansu* Wydawnictwo VIA 1999 r.
6. Pescio C., Carpetti E. *Brunelleschi* Wydawnictwo Rzeczypospolita 2006, seria Klasycy sztuki.

7. Pożgaj A. *Wpływ wymiarów przekroju poprzecznego próbek na ich pęczanie w naturalnych warunkach atmosferycznych* Reologia drewna i konstrukcji drewnianych – Symposium Akademii Rolniczej w Poznaniu. Materiały. Zielonka 21–22 październik 1982.
8. Lisowski A. *Projektowanie kopuł obrotowych* Biuro Studiów i Projektów Wzorcowych Budownictwa Miejskiego, Warszawa 1955.

Chapter 3

Multi-Shell Domes

3.1 Introduction

The Renaissance brought into the Western-European building masonry two-shell domes, lighter than the massive, one-shell Roman concrete or masonry domes from stone or brick. When the requirements for prestige led the dimensions of two-shell domes to a weight exceeding the load capacity of scaffolding systems from wood known at that time, it was necessary to introduce lighter and slimmer double masonry domes. Such shells, susceptible to non-symmetrical and concentrated loads, required a shielding structure to protect against the load by wind and atmospheric precipitation. Outside wooden scaffoldings as shielding structures were introduced. It has been shown in this chapter how the systems deriving from the scaffolding building practice affected the development of the construction of domes.

3.2 Wooden Scaffoldings for the Building of Masonry Structures from Stone or Brick

The daily practice of the building of masonry facilities from stone or brick included various types of ceilings, vaults and masonry shells that were erected on light and resistant supporting structures. Also, smaller stone and ceramic domes were constructed on wooden scaffoldings. Inventive bar structures were erected, having static schemes allowing to transfer high loads. The shaping methods of scaffoldings, proven at the building of heavy masonry vaults, were imitated and propagated. The building of wooden scaffoldings started the optimization process of light engineering structures from wood. Those systems were sort of prototypes of wooden dome structures.

Along with the development of technology and the new challenges of successive epochs, more and more interesting solutions of wooden structures appeared. It may be presumed that the building technology of wooden scaffoldings moved to the general building trade owing to carpenters knowledgeable in various structural solutions, their knowledge practiced in masonry building. The role of bricklayers and skills of carpenters in the forming of masterpieces of architecture is not to be underestimated.

Various wooden truss systems were used for the building of scaffoldings. Shown in Fig. 3.1a) is a sketch of a scaffolding compiled on the basis of the manual by the French architect Eugène Viollet-le-Duc according to [1]. He reconstructed the historical solutions of scaffoldings structures used for the building of shells and vaults. The scaffoldings exhibited were used for the building of masonry vaults of a span up to a dozen or so metres.¹ The floor from planks was built on a scaffolding, with an upper chord from arch centres, with outside edges cut according to the radius of the vault curvature. The vault bricks, connected with mortar, were laid on the floor from planks.

An example of a wooden scaffolding shaped for a heavy, masonry cross vault is shown in Fig. 3.1b according to [2]. The scaffoldings bars were made from several layers of arch centres cut out from planks, according to the methods shown in Fig. 3.2. Load-bearing ribs (bars) were consolidated with the plank shell, creating ribbed shells on which vault bricks were laid. In the example shown (Fig. 3.1b), in order to strengthen the scaffolding, the nodes of bars from arch centres were supported with pillars. Wooden tie rods were applied at the base of the arches of the wooden scaffolding, in order the transfer expansion forces at the stage of bricklaying.

The skill of cutting out arch centres from straight planks and their connection into arch elements affected the development of the building technology of wooden structures. Shown in Fig. 3.2 are the methods of cutting out arch centres from planks and the option of their connecting in flat arches - Fig. 3.2c. The planks cut as in Fig. 3.2a, b were laid and connected with nails as in Fig. 3.2c. Ribs, built from two or more layers of arch centres, constituted the load-bearing structure of the planking to construct headers, cylindrical or ribbed vaults, tiny cupolas or as upper chords of the trusses that supported plank shells of large spans required in the building of massive masonry structures.

The constructing of arched ribs from arch centres also allowed to build apparent vaults in more modest sacral, dwelling or temporary facilities, e.g. built on the occasion of local feasts. The interpenetrating cylindrical shells from wood were used as various cross vaults in sacral facilities. An example of a wooden vault is that of the cathedra of 1192–1280 in the cloister at the Cathedral in Lincoln in UK

¹*Dictionnaire raisonné de l'Architecture française* of 1854–1868.

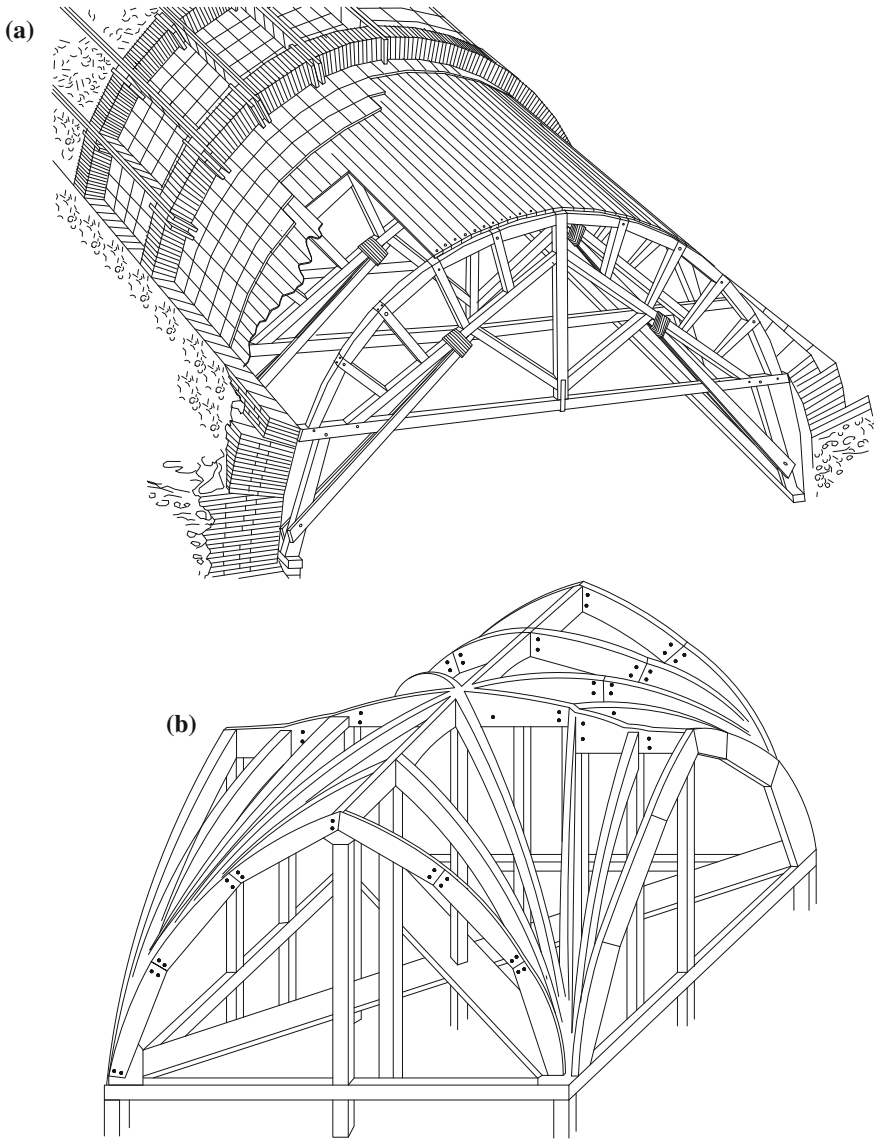


Fig. 3.1 Scaffoldings for the building of vaults, **a** masonry cylindrical vault [1], **b** masonry cross vault according to [2]

[1], as presented in Fig. 3.3. The shell-ribbed vault made in wood in the 13th century has been an instructive example of an open shell roof covering until today.

The architect Philibert de l'Orme, who lived in the years of 1510–1570 in France, introduced to the building trade, arches from arch centres, cut out from

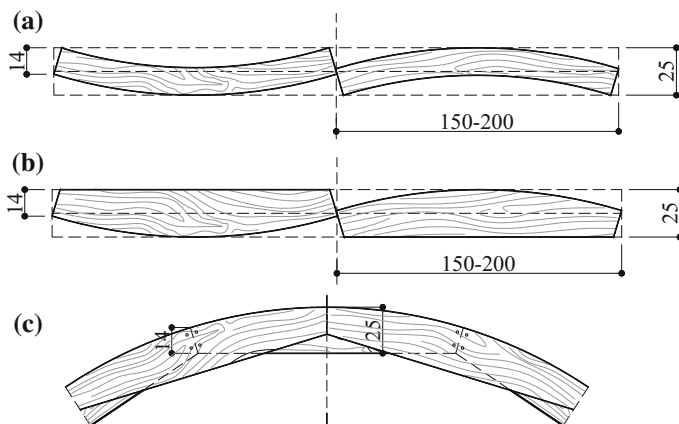


Fig. 3.2 Rules of constructing arches from arch centres [13]: **a, b** methods of cutting out arch centres from straight planks, **c** connecting method process of arch centres into a scaffolding bar. The dimensions are specified in [cm]

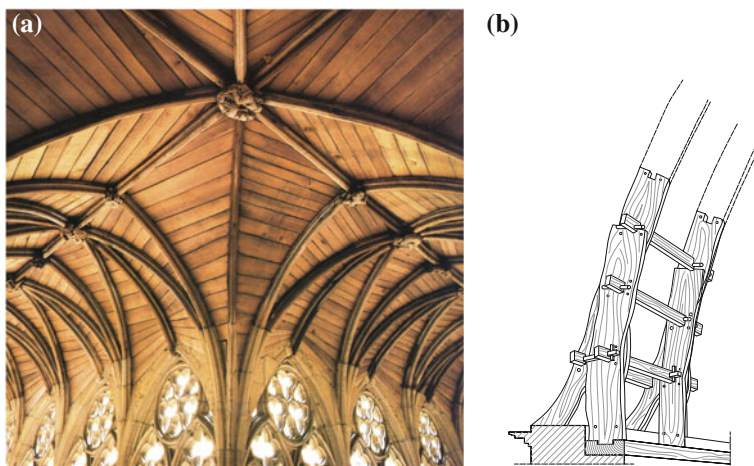


Fig. 3.3 Example of application of arch centres in construction: **a** wooden vault from the 13th century in the cloister at the Cathedral in Lincoln, UK [1], **b** arch by Philibert de l'Orme according to [6]

straight planks following the rules shown in Fig. 3.2. They appeared as single and connected pair-wise arches, as shown in Fig. 3.3b. Double arches from planks were used by de l'Orme to build cylindrical vaults and roofs in the 16th century in France.

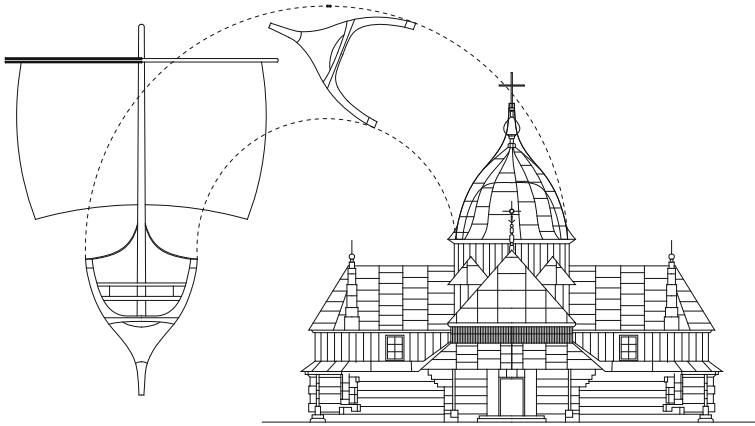


Fig. 3.4 Transfer of experience in sailing into building according to [3] vol. 2

The solutions from various fields of technology were mutually inclusive. Taras J. describes in his work [3] (2007) a solution known from the building of ship ribs encountered in the structure of church domes in north-eastern Europe—Fig. 3.4.

In the International Maritime Museum in Hamburg (*Internationales Maritimes Museum Hamburg, Hafen City*) exhibits were demonstrated illustrating the process of the material selection for the building of ship structures. The criterion of the wood species choice is ignored. Owing to the exposure, it is possible to learn which tree trunks from a wood were selected to fabricate the ribbed structure of vessels. Trees having the shape close to the geometry of ship ribs were looked after, e.g. such as in the example in Fig. 3.4. Shown in Fig. 3.5 are the photographs of the models from the exposure in the International Maritime Museum in Hamburg illustrating how the load-bearing ribs of a ship from selected tree trunks were cut out.

The shaping of ship structures demonstrate that ship carpenters were aware of the meaning to maintain the fibrous continuity of the wood structure. They tried to build the structure using the natural arrangement of wood fibres in selected tree trunks. Intuitively, they appreciate the anchoring of fibres in the mass of parenchymatous cells (visco-elastic matrix). Owing to this, they obtained the elements of the ship structure of an increased strength. The durability of ribs was provided by the cutting-out of elements from the central, heart-wood part of the trunk. The meaning of the maintenance of the natural wood structure, built from fibres anchored in the visco-elastic matrix, is explained by the author basing on the works by Kowal Z. in Chap. 9 of the monograph.

The proven ribbed structure of a boat adapted to overcome the forces of the sea element was introduced to the building trade where considerable climatic loads occurred and a higher load-bearing capacity and durability of the facility was required.



Fig. 3.5 Exposure in the International Maritime Museum in Hamburg illustrating the selection process of trees having a shape favourable for the building of ship rib structures. Photograph by the author, 2017

3.3 Wooden Covering Domes Developed from the Wooden Scaffoldings of Masonry Domes

The scaffoldings used to erect heavy vaults and masonry domes were separated in the course of time as independent wooden structures. Originally, the structure of the scaffolding was just used to support the masonry cylindrical shell or the cross vault (Fig. 3.1). As the structure of the scaffolding was perfected, they started to be used also to cover and strengthen the masonry dome from the outside. The outside

wooden structure, covered the inside single-shell or double-shell masonry dome, protecting it against destructive weather effects.

3.3.1 Multi-shell Domes Built in the Middle East

In the 7th and 8th century AC, two and three-layer structures of wooden domes were built in the Middle East. Shown in Fig. 3.6a is the location of the domes discussed in this chapter: the Dome of the Rock and the Al-Aqsa Mosque in Jerusalem and the mosque in Isfahan, Iran.

Its designer, surely a Byzantine, consciously used the option of splitting outside and inside loads, in order to accomplish the concept of the two-shell dome. 745 years before the construction of the two-shell dome of the Santa Maria del Fiore Cathedral in Florence, an unknown builder designed and executed a two-layer dome.

Probably, this is the first in the history bar structure in which the wooden outside structure transfers climatic loads, and the other shell, the inside one, transfers its own weight and the interior decorations.

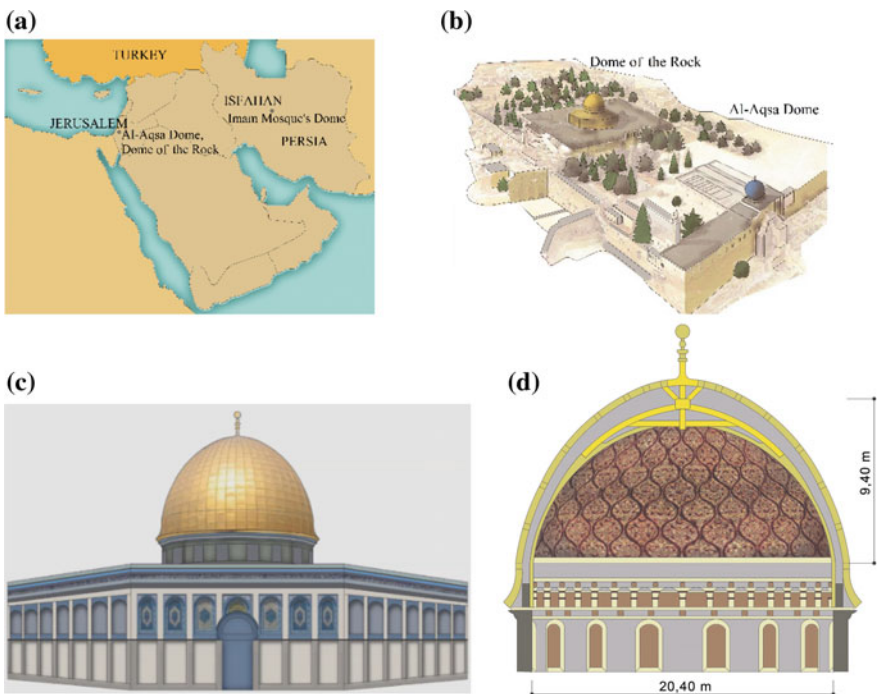


Fig. 3.6 The Dome of the Rock in Jerusalem built in the years 687–691 AC, of a 20.40 m diameter, according to [1, 4], **a**, **b** location of the domes, **c** view of the temple crowned with the Dome on the Rock, **d** vertical section of the structure of the dome ribs and shells

made up of: an outside shell, having the structure of a roof truss arch, and an inside dome connected in the key block using a stiff node with the outside dome. The stability of the structure is provided by a stiff node in the dome key block. It is not known whether this building method was brought in the territories by Arab builders from the areas abounding with woods, or those are examples to confirm the high civilization or technological development of the Byzantine culture.

In Jerusalem, in 715 AC, a two-shell wooden dome was built, crowning the Al-Aqsa Mosque, shown in Fig. 3.6 [4]. Its structure is exceptional due the static operation. It was built from two canopies, made as ribbed shells from planks, and was placed axially the one in the other. The support ring fastening meridional arches was set on a masonry ring of a 11.5 m diameter. The eminent outside canopy transfers the climatic load, the semi-spherical inside canopy transfers the own weight. The outside canopy was made by cutting off the sphere below the equator. The ribbed inside canopy was made as one-half of the sphere. The skilful choice and juxtaposition of the outside and inside canopies led the builders to reduce the horizontal forces on the structures of the supporting walls, built, maybe, from a weak brick dried in the sun. Such shaping of the domes gives evidence of the advanced knowledge of their builders.

The effects of the interference of the compression forces in the ribs of the outside dome were reduced, by introducing sloping bracings—crossheads to protect outside meridional ribs, against buckling. The statics of the dome, legible and simple, creates an exceptionally beautiful structural solution.

The beauty of the dome is exhibited by the model made on the basis of [4] at a 1:50 scale, presented in Fig. 3.7.

Wood in Arab countries was used sparingly. Only in prestigious facilities, erected as a proof of significance and richness, wooden bars to transfer stretching and bending were introduced to the structure. An example is the dome of the mosque Masjed-e Shah in Isfahan originating from the years 1612–1630, shown in Fig. 3.8, developed on the basis of [1]. Two thin-wall, masonry dome canopies were connected with an internal scaffolding from wood. The lower masonry dome of a 21.40 m diameter rises up to the height of 36.3 m above the floor level. The outside dome reaches the height of 51 m from the skewback to the key. The inside wooden bar structure was also used as a scaffolding required to erect and strengthen both the domes. The outside dome was constructed on it. Upon completion of the construction, the scaffolding was left as a bar membrane supporting the light masonry shell, shielding the inside sphere. The split masonry shells were joined with a bar structure from wood and adapted to the transferring of various loads, mainly load by wind by the outside shell and the own weight by the masonry inside dome (Fig. 3.8). The scaffolding from wood also transfers the forces of strutting, stretching and bending.

The significance of the structure shown in Fig. 3.8a, b consists in the creation of the brick-wooden joined domes in which the wooden scaffolding to the joining of the outside and inside brick shell of the dome is used. This concept was initiated by Byzantines in the 7th–8th century, afterwards it was perfected by other, talented builders.

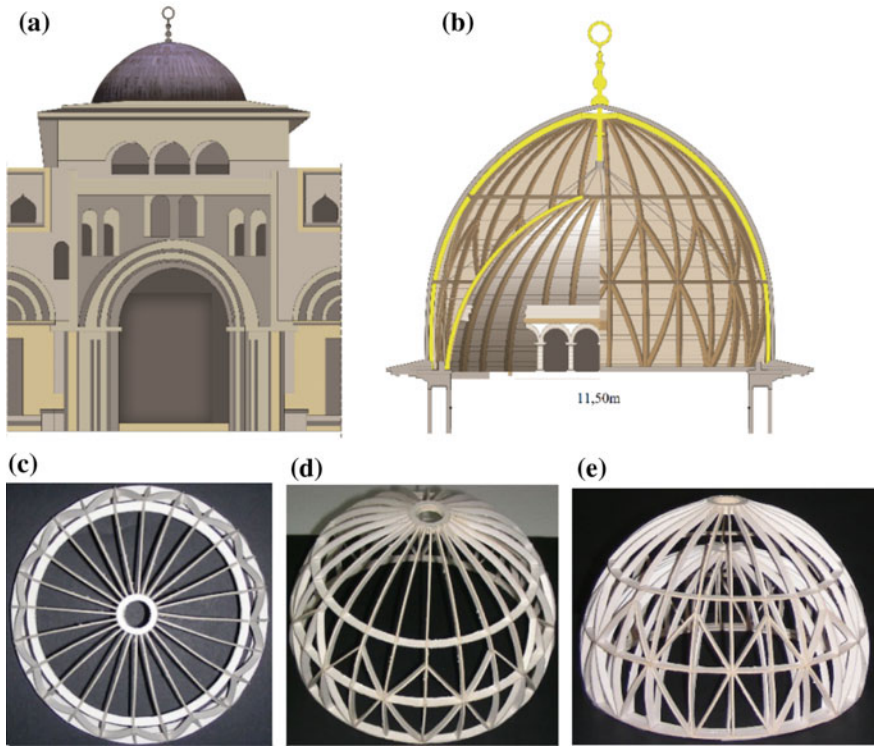


Fig. 3.7 Figure and model of the structure of the dome of the Al-Aqsa Mosque built in Jerusalem in 715 AC to [4], **a** view of the Al-Aqsa Mosque **b**, two-shell structure of the dome of a 11.50 m diameter, **c** model—top view of the outside dome, **d** model—side view of the outside dome, **e** model—view of the inside and outside dome

It is worth noticing the quantity and variety of masonry domes used as roofs of various building structures in Persia—Fig. 3.8c, d. Visible on the photographs are the 3 domes of mosques and those of other building structures. They were generally built due to their effectiveness, from the most available material in those areas—brick from clay dried in the sun.

Perhaps the statics of the domes as presented in Sect. 3.3.1 derives from the need to save wood as construction material, and from the need to reduce horizontal loads on load-bearing walls, also from the wick brick dried in the sun. The brick, the most frequently used as the most available material in the given area, fixed the template of the dome occurring in the architecture of the southern Europe and the Middle East. Shown in Fig. 3.9 and developed according to [5] are the most often achieved forms. It may be presumed that the specific shape of arches, e.g. of Grenada and Cordoba, shown in Fig. 3.9, is not just a decoration characteristic of that architecture, but it follows from the careful use of the system and the material.

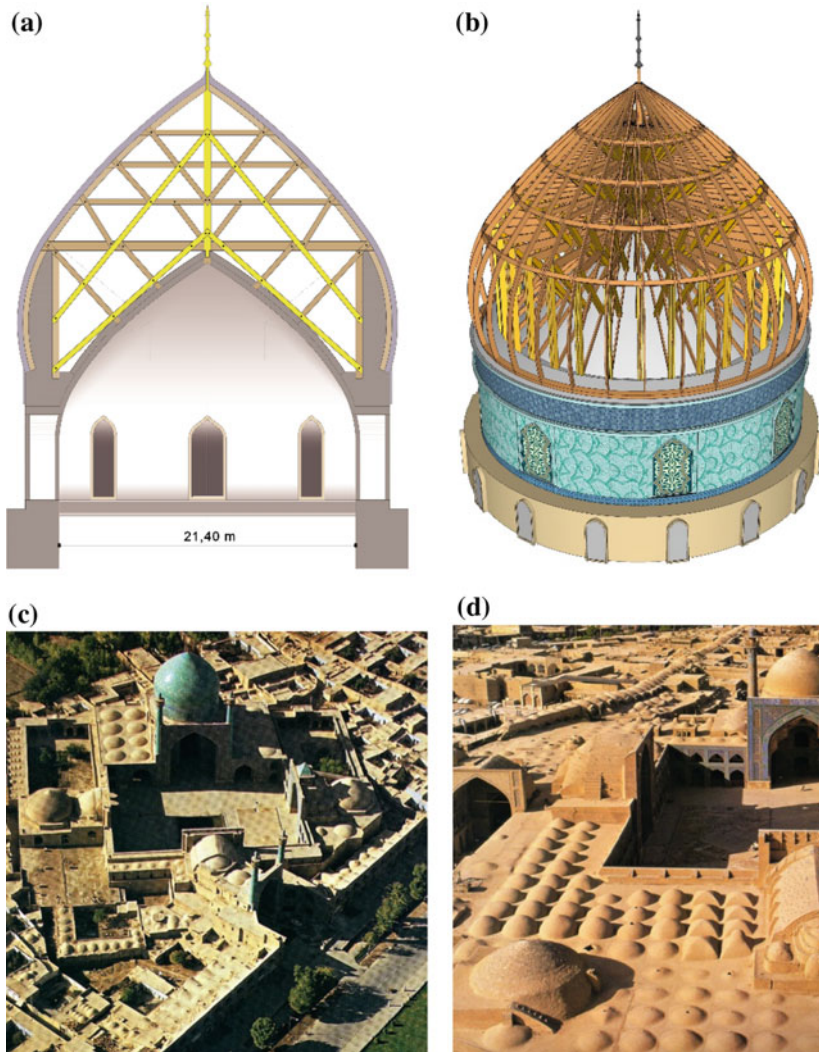
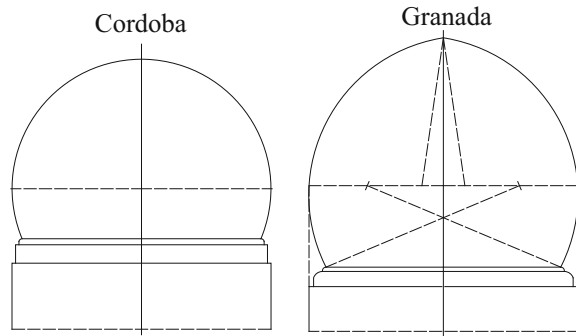


Fig. 3.8 The domes covering the building structures in Isfahan, Iran to [1]. **a** Section of the structure of the central dome of the Masjed-e Shah Mosque, **b** visualization of the structure, **c** top view of the central dome and those in the surroundings of the Masjed-e Shah, **d** top view of the central domes and those in the surroundings of the Friday Mosque in Isfahan [16]

3.3.2 Multi-layer Domes Built in Europe

On the basis of the references retained, it may be noticed that the invention of the two-shell masonry dome in shells joined using an internal scaffolding has been known in Europe since the Middle Ages. At that time, the central bar structure

Fig. 3.9 Shapes of the arches of Cordoba and Grenada [17]



(Fig. 3.10b) covering the inside masonry dome and stiffening the outside dome, bricked or shaped on meridional arches from arch centres, was introduced. The lower masonry shell transferred its own weight and that of the interior decorations, the upper outside shell rested on a wooden scaffolding. The bar structure from wood was constructed so as to transfer the load from the lantern—the conical part of the bars—Fig. 3.10d. The latitudinal ribs supported with pillars with angle braces, supported meridional arches from arch centres on which the latitudinal shell from planks for the elements of the outside roof covering were made. In this way the solutions of three-layer domes, lighter than those of heavy masonry one or two-shell domes were formed. An example are the domes of 1063-1031, as described by Heinle E., Schlaich I. in the work [4] (1996), characteristic of the Saint Mark's Basilica in Venice. The view and the section of the domes are shown in Fig. 3.10. In the crosscut of the aisles of the church, three-layer domes were built, having two shells: an inside masonry shell, an outside shell on ribs from arch centres. A scaffolding from wood was made between the outside shell and the inside shell—Fig. 3.10b. In this way five domes were built, of which the largest, central dome has a span in projection of 13.0 m. Shown in Fig. 3.10c, d is the view and the structure used in the building of the lateral dome of a 10.0 m diameter.

Figure 3.11 shows the three-layer dome crowning the Saint Paul's Cathedral in London to [4]. Upon destruction during a fire of the earlier roof of the tower, the builders feared to erect the conventional heavy masonry structure of the new dome on fire-weakened pillars of the building.

This resulted in a need to assume a lighter structure. The new dome of the Saint Paul's Cathedral in London came into being in the first decade of the 18th century, about 1710, in accordance with the project design by the astronomer and architect Christopher Wren. Two masonry domes and the third outside shell were made on a wooden scaffolding, as a wind shield for two inside domes. The height from the floor level to the highest section of the steel cross positioned on the lantern totals 108.0 m.

The masonry inside domes of the Saint Paul's Cathedral in London: the semi-spherical and the conical dome (Fig. 3.11) operate in tandem in the transfer of vertical loads. The conical dome supports the load of the lantern, transferring the

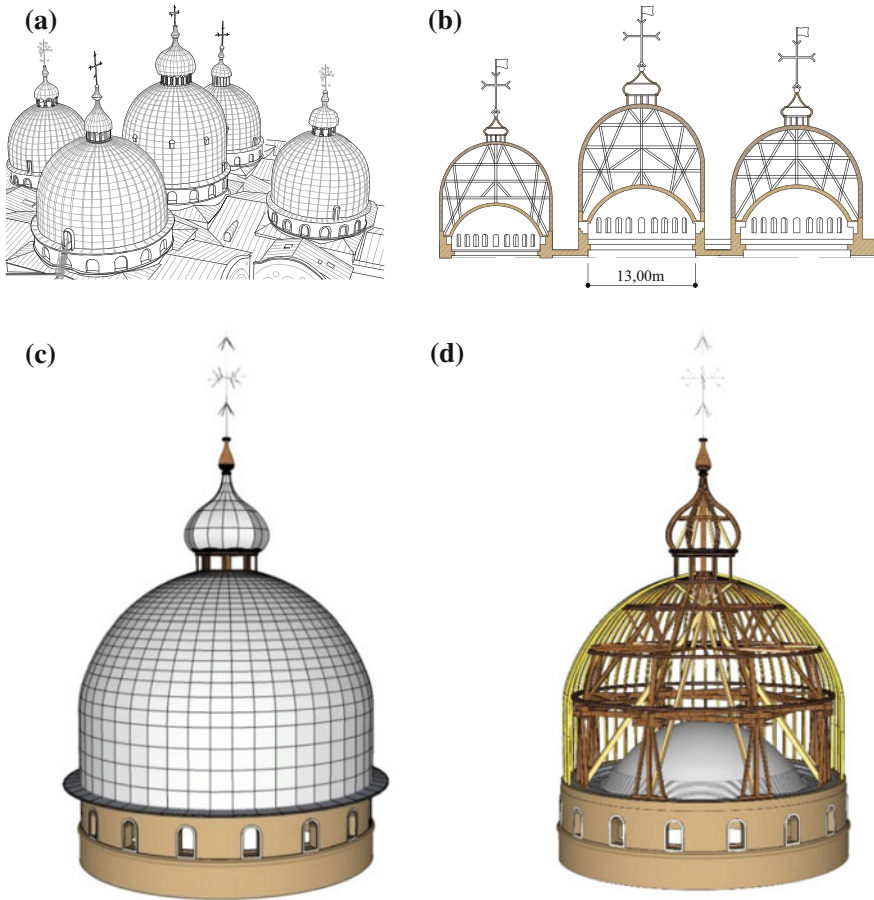


Fig. 3.10 Venice—Saint Mark's Church, 1063-1031 according to [4, 6], **a** view of the roof, **b** cross-section of the three domes, **c** view of the side dome of a 10.0 m diameter, **d** visualization of the dome's structure

vertical forces onto the circumferential ring common with the semi-spherical internal dome, built as a masonry double ring. The bottom dome, of a circa 32.0 m diameter of the horizontal projection, transfers the load by own load and the rich architectonic detail giving evidence of the rank and function of the facility. The pillar-purlin structures of the outside scaffolding, surrounding the conical dome, were helpful at the stage of building both the masonry domes, later on as a shield against the load by wind. The outside arch elements of the domes on which the coating was laid burdened the separate, outside, tensile support ring.

The dome of the Invalids Church in Paris also has a three-layer structure (Fig. 3.12). The outside wooden dome of an 80 ft, i.e. 25.0 m diameter of the horizontal projection and a height 16.0 m to the lantern basis [6] was designed by

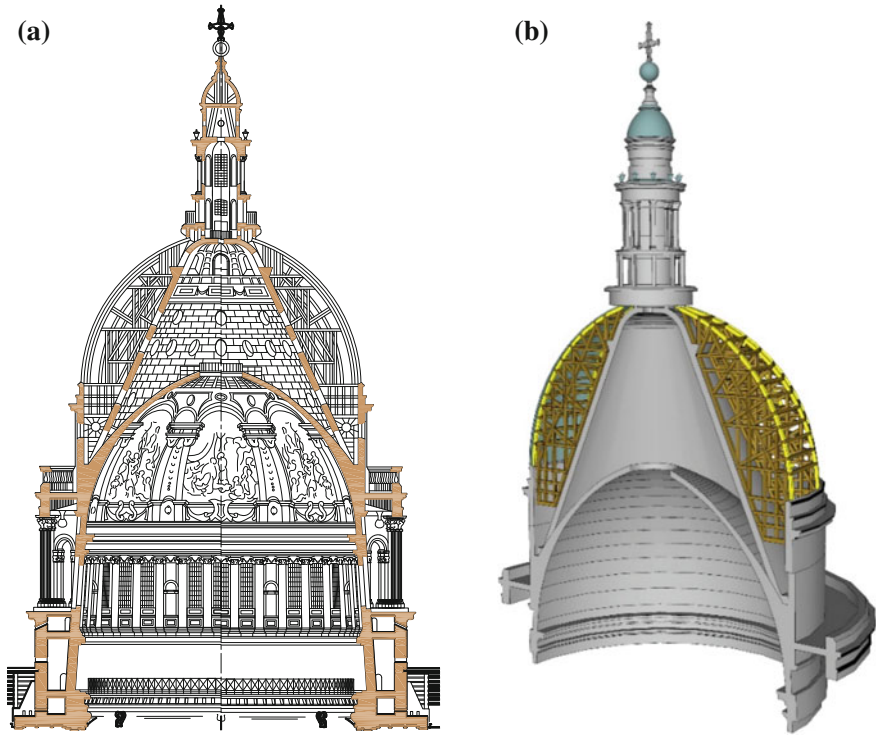


Fig. 3.11 London—St Paul's Cathedral, 1710 to [4], **a** section of the dome, **b** visualization of the structure

the engineer Mansart J. [5], and was built in 1693 until 1706. This talented designer of wooden roofs resolved the outside, wooden bar structure so that it could transfer the vertical load with the lantern and the horizontal load from wind. Two masonry inside domes, set up on a ring of a 25.0 m diameter, have transferred the own weight and the load by the décor of the inside.

The outside dome of the Saint Nicholas' Church in Potsdam (Fig. 3.13) in the wooden version was designed by the master builder and painter Karl von Schinkel [7]. The wooden construction had to shield the inside masonry dome of a 10.0 m diameter.

The outside element of the scaffolding giving the shape to the dome in Potsdam were ribs from arch centres of the dimensions: 5 cm thick, 30 cm wide each. The total thickness of the meridional rib from arch centres amounted to 15.0 cm. On the meridional ribs, at the spacing of 1.50 m each, latitudinal stiffenings from three arch centres of the 5×25 cm dimensions were designed. Finally, the wooden dome was not built due to the interest in iron that at that time was introduced to the building trade. The design of the wooden dome was replaced with another one. The dome was built in 1830–1849 from cast iron [7]. The bar structure of the inside

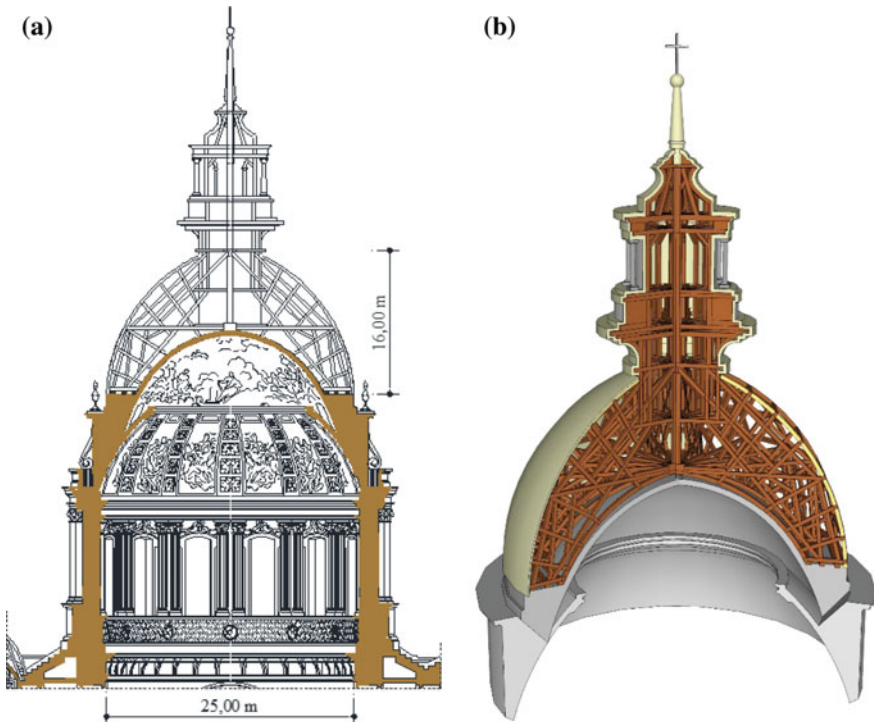


Fig. 3.12 Dome of the Invalids Church in Paris, 1693–1706, design project by the engineer Mansart J. Ch. to [4], **a** section of the dome, **b** visualization of the structure (Bourget P., Cattai G. *Jules Hardouin Mansart* Éditions Vincent&Co, Paris)

casing of the masonry dome of the diameter of the horizontal projection of 10.0 m was made so as it could transfer the vertical loads from the lantern and the horizontal forces from wind.

The data collected in this work on the multi-layer structures of the wooden-masonry domes are incomplete. **The detailed inventory of paintings and the décor, as existing in the referenced literature, is not related to the information on the structure on which those works came into being.** Such is the situation in the majority of domes completed. The data on the structure, especially the outside load-bearing wooden dome, are inaccurate, without numerical sizes. Sometimes, those are fragmentary figures, as for instance in the case of the dome of the church shown in Fig. 3.14 according to Durand J.N. (1800). An interesting structure of the outside dome is shown fragmentarily. One may presume that it was constructed from arches of two chords interconnected with pillar lacings. **The fragmentary figure exhibits, however, that by chance, (without paying special attention), one of the most important technological events of the epoch was shown: the structure of the two-layer shell of a wooden dome.**

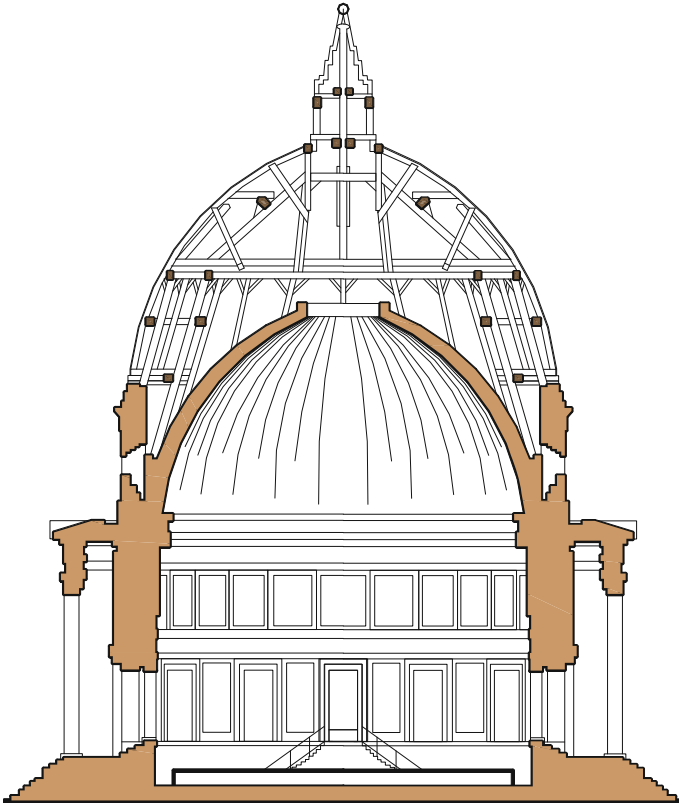


Fig. 3.13 The duplicated structure of the dome of the church in Potsdam according to [7]

In 1631, in Venice, the construction of the Santa Maria della Salute Basilica started. The designer was the Italian architect and sculptor Baldassare Longhena. The basilica is shown in Fig. 3.15. This is a structure in the style of the Venetian baroque, crowned with cupolas, the central cupolas having the diameter of 60 Venetian feet² each, i.e. 20.63 m. The two-coating canopy is supported on an octagonal tambour. The presbytery adjacent to the central part was roofed with a dome of a lower diameter (Fig. 3.15a). The structure of the outside casing from wood of a 23.0 m diameter [6] shields the central inside masonry dome of a circa 20.60 m diameter. The multi-layer dome of the Longhena's basilica was built following the rules discussed in the previous examples. The view is shown in Fig. 3.15a, b, the schematic of the section is shown in Fig. 3.15c), whilst in Fig. 3.15d) the visualization.

²1 Venetian foot is equal to 34.38 cm.

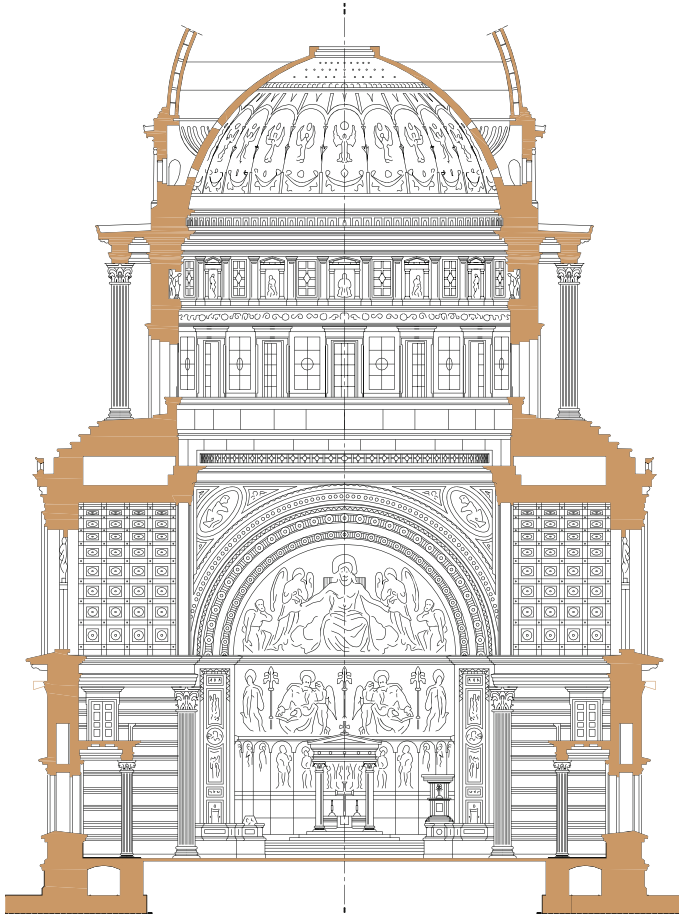


Fig. 3.14 Rich inventory of the church interior to Durand J.N.L. 1800 (Durand J.N.L. *Recueil Parallèle des Édifices de Tout Genre Anciens et Modernes*, Chez l'Auteur, à l'École Polytechnique. 1800)

The Santa Maria della Salute Basilica as shown in Fig. 3.15 was the inspiration for the founders of the church in Gostyń, Poland, in the 18th century [8]. A masonry dome was ordered from Longhena B., of a diameter of 60 ft, like in the Santa Maria della Salute Basilica in Venice. After the construction, it turned out that the dome had an internal diameter of 17.20 m, and an external diameter of 20.0 m. In Poland, when building the dome, 60 ft were measured, but these were Cracow (crown) feet.³

³1 Cracow foot, also called a crown foot totals 29.30 cm.

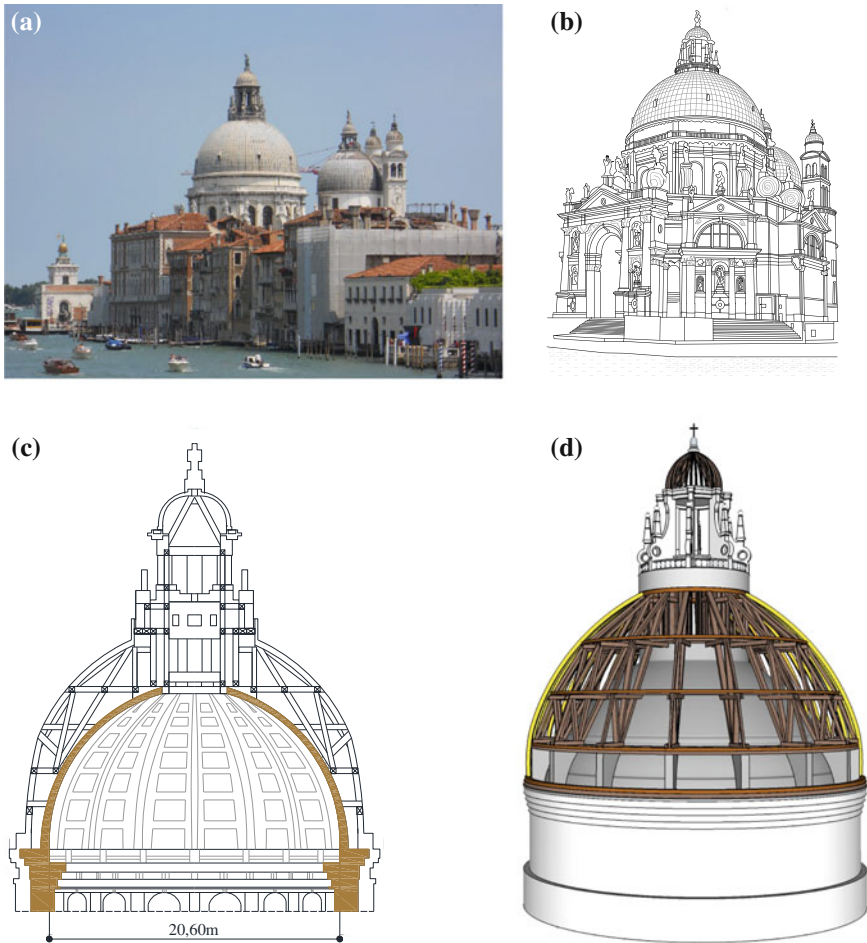


Fig. 3.15 Venice—**a** domes of the S. Maria della Salute Cathedral according to the project by Baldassarre Longhena from 1631 to 1687 [4], photo by the author, **b** view of the central dome, **c** section of the central dome, **d** visualization of the dome's structure [4, 6]

One of the most eminent designers of baroque domes was the architect Balthasar Neumann born on 27 January 1687 in Würzburg [9]. He designed and built in South Germany. He was the Chief Architect of the town of Würzburg. He also died over there on 19 August 1753. Shown in Fig. 3.16a is the view of the Schönborn Chapel in Würzburg, and in Fig. 3.16b the structure of the dome of a 20.0 m diameter crowning the building built in 1722.

A next example of the introduction of meridional trusses to the construction of domes is that of the Saint Mark's dome of a 16.0 m diameter, in Berlin, shown in Fig. 3.17 according to [10]. The design project was completed in 1846–48 by the

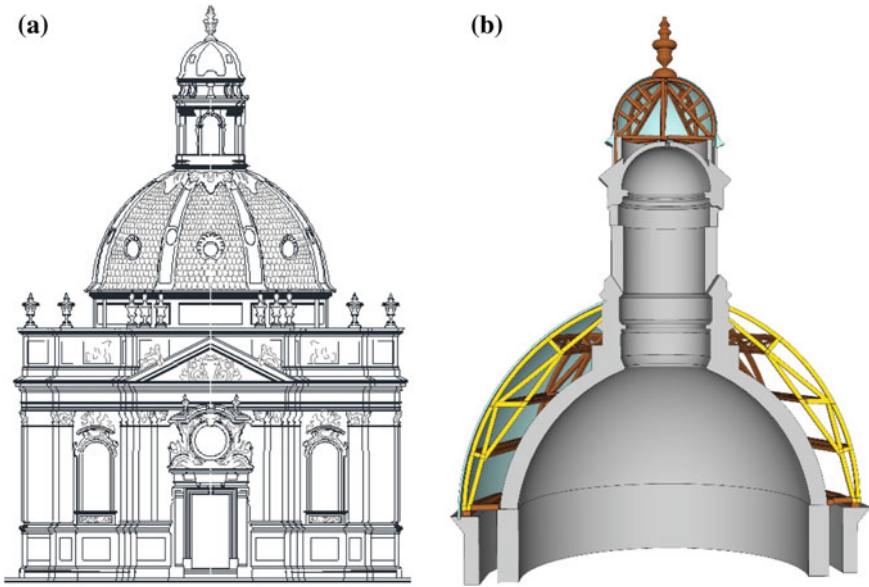


Fig. 3.16 Würzburg—Schönborn Chapel by the architect Balthasar Neumann, 1722, [9], **a** view of the chapel, **b** visualization of the structure

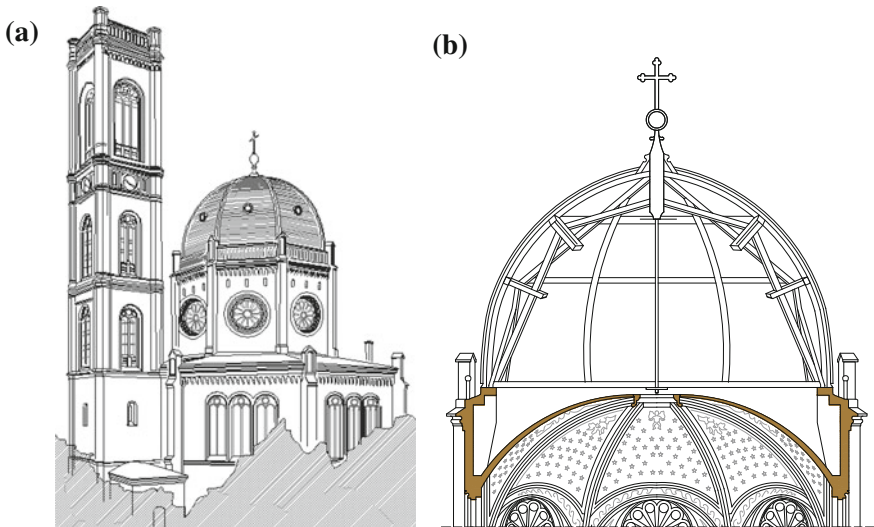


Fig. 3.17 Saint Mark's Church in Berlin built in 1855 [10], **a** view of the church, **b** structure of the dome

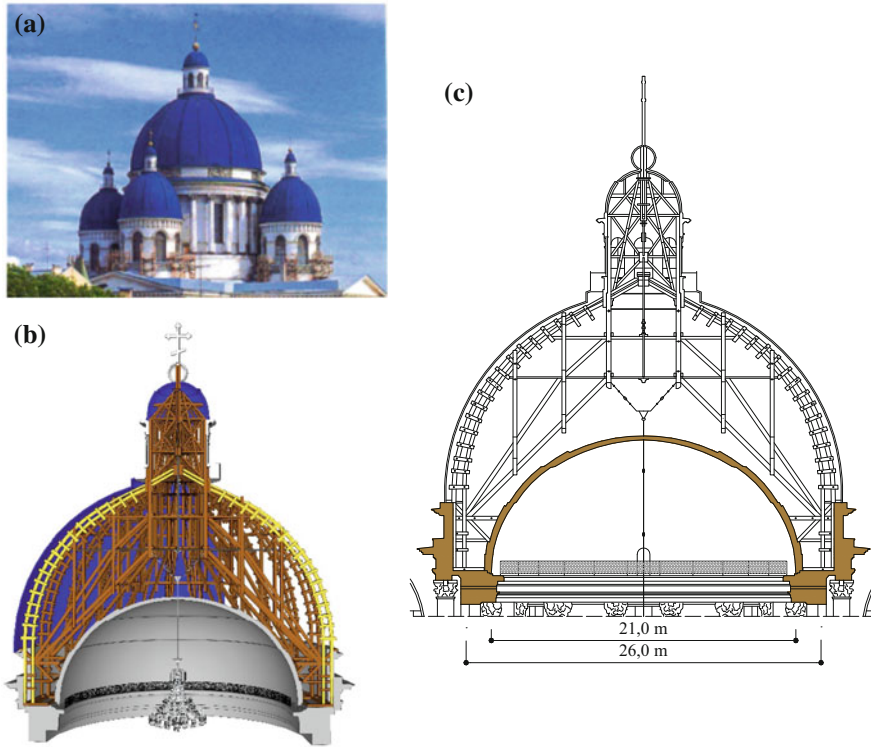


Fig. 3.18 Domes of the Trinity-Izmailovsky Cathedral in Saint Petersburg according to the project by the architect Stasov V.P. [11], **a** view of the domes before the fire, **b** visualization of the structure, **c** view of the structure of 1826

architect Friedrich August Stüler.⁴ The building was erected in 1848–1855. In the solution of the wooden outside dome shielding the masonry canopy roof trusses were used. The reconstruction of the structure was made on the basis of the data acquired from the work [10].

Figure 3.18 a presents five domes that crowned the building of the Trinity-Izmailovsky Cathedral in Saint-Petersburg, designed by the architect Stasov W.P. [11]. The building was erected in 1826. The largest central dome was built to the height of 83.0 m. It is made up of two separate shells. The outside shell, having a wooden structure from arches with two parallel chords interconnected with lacings had a diameter of 26.0 m. Underneath there was a masonry dome of a 21.0 m diameter, 22 cm thick in the key block and 64 cm thick in the supporting

⁴Börsch-Supan Eva, Müller-Stüler Dietrich, *Friedrich August Stüler 1800–1865*, Deutscher Kunstverlag, München Berlin 1997, p. 530–531.

zone. The data on this wooden dome were obtained from the paper [11] written on the subject matter of the inside masonry dome after the fire that totally destroyed the wooden structure of the outside dome. The masonry dome was saved, after the wooden one a sketch was left, as well as the view of the dome before the fire, as shown in Fig. 3.18.

Visible on the sketch of the structure of the wooden dome (Fig. 3.18b) are meridional load-bearing ribs. They form a two-chord load-bearing system not encountered in other, previous solutions of dome structures. Maybe this is the historically first bar system characteristic of the dome form developed in successive years, e.g. by the Karlsruhe school. The inside, conical bar system transfers the load from the lantern. The connection of sloping pillars at the lantern base with steel bars allows to suspend heavy chandeliers of the temple lighting system to the roof structure, without burdening the sensitive masonry dome by concentrated forces.

In multi-shell domes built in the 18th century transformations of the outside, wooden bar structure shielding the inside masonry dome are noticed. Eminent architects introduced trusses with an arched outside chord from arch centres with a curvature adapted to the dome radius.

3.4 Multi-shell Domes with an Outside and Inside Wooden Dome

In 1546, the Italian architect Andrea Palladio, known from the design projects of truss systems in the building of wooden bridges, designed the structure of the dome of the Il Redentore Church in Venice of a 14.50 m diameter [12] as shown in Fig. 3.19. The meridional load-bearing arches were executed as two-chord arches, interconnected with studs and crossheads (Fig. 3.19b). The latitudinal bracing was made from horizontal trusses.

It may be presumed from the inaccurate sketch from the work [12] that the outside arch chords were made from plank arch centres, adapted to the dome radius. The two-chord structure of meridional ribs allows the production of a spherical vault also on the inside, creating a resistant two-layer combined structure. The shell from planks nailed latitudinally on meridional ribs was made on the dome's outside and inside. The combined structure transferred the load by the lantern, own weight and non-symmetrical climatic loads.

The building of wooden multi-layer domes was taught in the 17th century at schools of building trades [1]. The handbook example of a two-shell structure from solid wood is shown in Fig. 3.20. The figure was made on the basis of the building handbook of 1691, by D'Aviler A. C. *Cours d'Architecture*.

As the demand for dome-roofed prestigious facilities was growing, their dimensions were also increased. In order to limit the weight of the structure, heavy

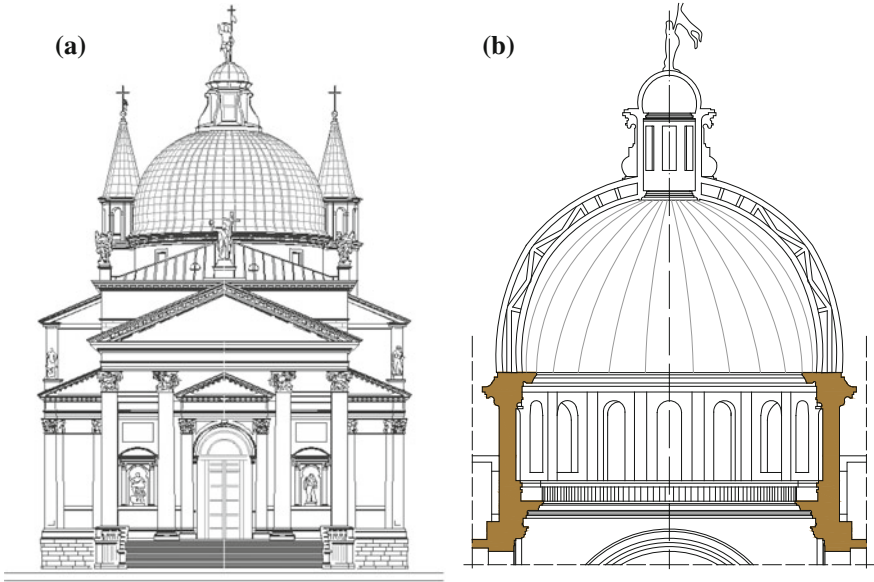


Fig. 3.19 Il Redentore Church in Venice, a view of the church, b section of the dome [12]

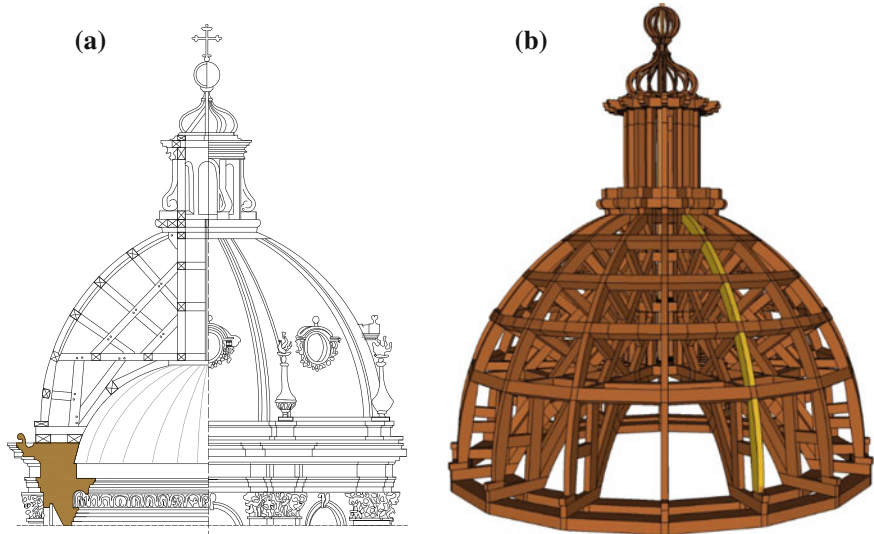


Fig. 3.20 Figure of the dome structure according to [1], a section of the dome, b visualization of the dome's structure

scaffoldings were replaced with lighter bar structures. Trusses with an outside arched chord from arch centres of the outside edge conforming to the radius of the dome sphere were introduced. The inside chord was shaped according to the radius of the sphere of the inside vault being designed. An example of such a structure of the Saint Stephan's Church in Karlsruhe designed by the architect Friedrich Weinbrenner, built in 1808–1814, is shown in Fig. 3.21.

The dome in Karlsruhe (Fig. 3.21) of a span of 30.0 m was built from twenty main meridional truss ribs with upper and lower arched chord made from arch centres. The outside chords were interconnected with studs and crossheads. Three intermediate meridional ribs were built in between each pair of main ribs. In total, eighty wooden ribs, arranged along meridians were made. The main ribs were connected upside with a central ring of a 6.0 m diameter. The latitudinal, truss rib at the middle of the dome height stiffened the structure, constituting, at the same time, a support for meridional intermediate ribs.

The arch centres that connect the outside nodes of meridional ribs shape the dome and maintain the covering (Fig. 3.21). The arch centres that connect inside nodes form the vault, maintaining plasters and paintings. Each of the trusses that form the dome by Weinbrenner F. is based at the bottom on a skewback support by six truss systems. Arches supporting the circumferential construction were made under the trusses. The supporting wooden structure of the dome was encased with a masonry wall. The arrangement of arches over the circumference of the facility allows to unburden the masonry structure of walls, and the adding to the central room of adjacent aisles of a 12.0 m width [13].

This type of the supporting structure for the dome—a lower ring resting on arches of the first storey was developed in successive Western-European building crowned with domes.

The dome as shown in Fig. 3.22 crowned the building erected on the Nordic Exhibition in Copenhagen in 1888 [13]. The dome was set up on the crossing of the longitudinal and cross aisle, close to the main entrance over the representative central hall. The projection of the dome is inscribed into a square of a 26.50 m side. The tambour rests on the arches of lateral aisles of a 17.50 m height. The tambour resting on the arches has a height of 6.0 m. The dome, from the tambour to the top ring, has a height of 11.50 m. A lantern of a 8.0 m height rests on the central top ring. The lantern structure is made of cast iron. At a height of 20.0 m under the tambour a 2.0 m wide circular gallery was located, constituting, at the same time, a horizontal stiffening of the tambour's structure. The clear diameter of the top ring of the dome totals 9.50 m. Meridional trussed rafters were led out from the four corners of the rectangular projection, the chords of which were interconnected with studs and crossheads in each field along the diagonals. The arches are fastened in the supporting zone by several cast iron anchors. The height of the meridional main ribs of a shape approximating a quarter of a circle, the outside chords of which are created from arch centres, totals 1.75 m.

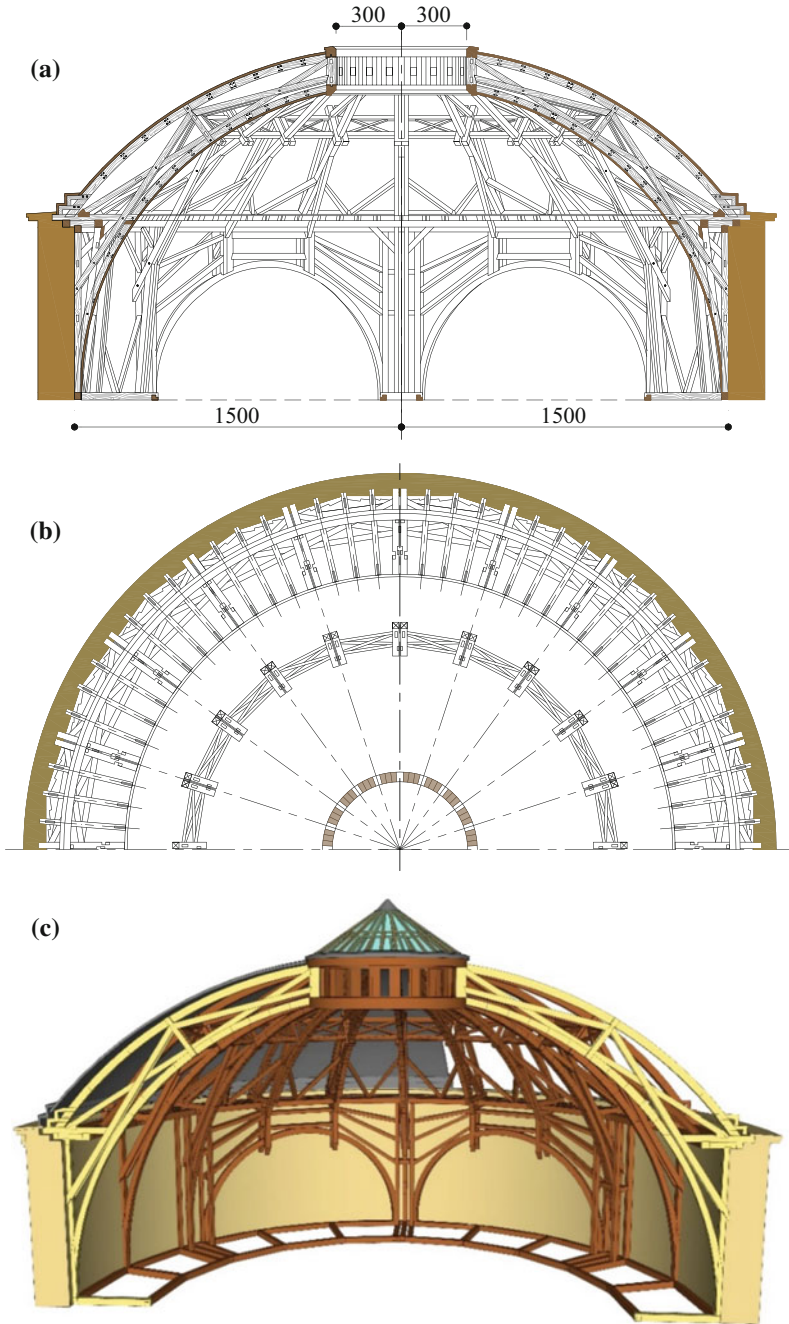


Fig. 3.21 Section and projection of the dome of the church in Karlsruhe by Weinbrenner F. according to [14], **a** section of the dome's structure, **b** projection of the structure, **c** visualization of the structure

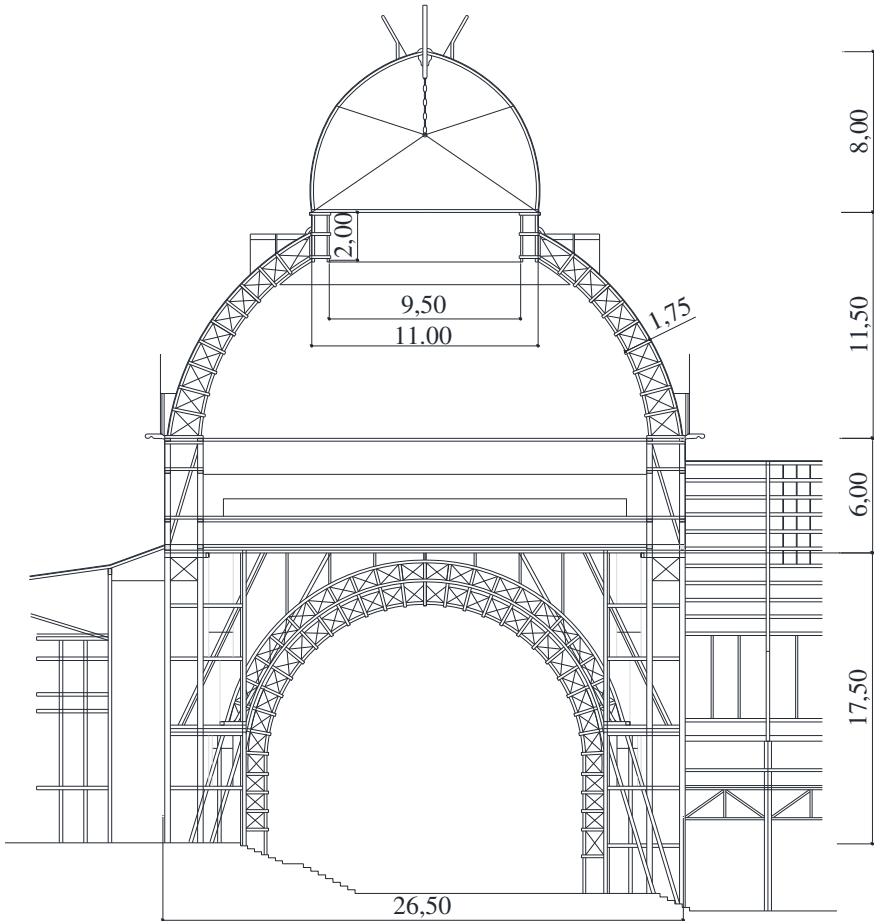


Fig. 3.22 The dome of a temporary facility in Copenhagen was built in 1888 [13]

3.5 Ribbed Domes from Arch Centres

The transformation of the inside scaffolding supporting the meridional arches from arch centres giving the shape to the outside canopy into a meridional-latitudinal system of load-bearing trusses was a breakthrough moment. **The meridional ribs with outside chords conforming to the dome radius were later used by other architects. Weinbrenner F., Neumann B. propagated in the Western-European building trade the dome structures in which already separated load-bearing, both meridional and latitudinal, appeared, characteristic of the dome form as**

shown in Figs. 3.16, 3.17, 3.18, 3.19, 3.20, 3.21, and 3.22. The meridional-latitude systems of trusses with an outside and inside arched chord made from arch centres were adapted to the radius of the outside and inside sphere. Such structures made possible the execution of two-layer domes deemed more solid.

One of the first structures exceeding the barrier of the 30.0 m diameter in which a wooden arch centre had been used for centuries became a separated load-bearing element is shown in Fig. 3.23, the dome structure by Georg Moller of a diameter of 33.5 m [13], built in 1827 for the catholic church in Darmstadt, Germany. A modern, one-layer was built that, according to Prof. Otto Warth from Karlsruhe, constituted simultaneously “a roof and a ceiling”, which was considered more as its defect than success. The dome’s structure rests on a tambour supported by twenty-eight columns.

In the axially symmetrical dome by Moller arched load-bearing ribs in the meridional direction were used and stiffened with latitudinal ribs. One hundred and four meridional ribs were used, including: fifty-two main ribs, and fifty-two intermediate ribs and eleven meridional ribs. One hundred and four meridional ribs were built from several layers of planks of a 5×38 cm section and a 1.60 m length. The main ribs were made from five layers, the intermediate ribs were made from three layers of arch centres, each of a 5×38 cm section. Up to the sixth, lower rib, the main meridional rib was made up of five layers of planks, above the sixth latitudinal rib all meridional were built from three layers of planks. Above the ninth main latitudinal rib, every second was cut off latitudinally, bringing one half of meridional ribs to the top ring of the dome.

The meridional ribs were mounted on a foundation from oak wood laid on walls of the lower storey. The meridional ribs were mounted jointly with the latitudinal ribs, as they were erected. In the first order, in order to support the main ribs, the meridional ribs from a single plank of a 1.25×10 cm section perpendicularly to the plane of the lower stiffness of the meridional rib were mounted. In order to counteract the buckling of arch centres of the meridional ribs, in the contact sections with the meridional ribs, horizontal “plugs” were used, double at the main ribs, single at the intermediate ribs—Fig. 3.23b. **Both the ribs and the “plugs” were made from dry oak wood. Each stage of the dome’s erection process was closed with latitudinal ribs with two chords: an outside and an inside chord from young oak wood.**

Every second circumferential latitudinal rib was made as a beam having two concentric chords, embracing meridional main ribs and intermediate ribs, Fig. 3.23b–d. Those ribs were made from beams of a 2.5×10 cm section from young oak wood. The latitudinal chords of the hoop were connected from drawn iron wire of a 10 mm diameter. **This encountered a critic by Prof. Otto Warth who wrote in his work [13] that rather wooden fasteners should have been used.** In order to prevent an uneven settlement of meridional ribs, horizontal, outside, latitudinal chords were let into meridional ribs to a depth of 1.25 cm, by making cuts in the arch centres of meridional ribs, as shown in Fig. 3.23d.

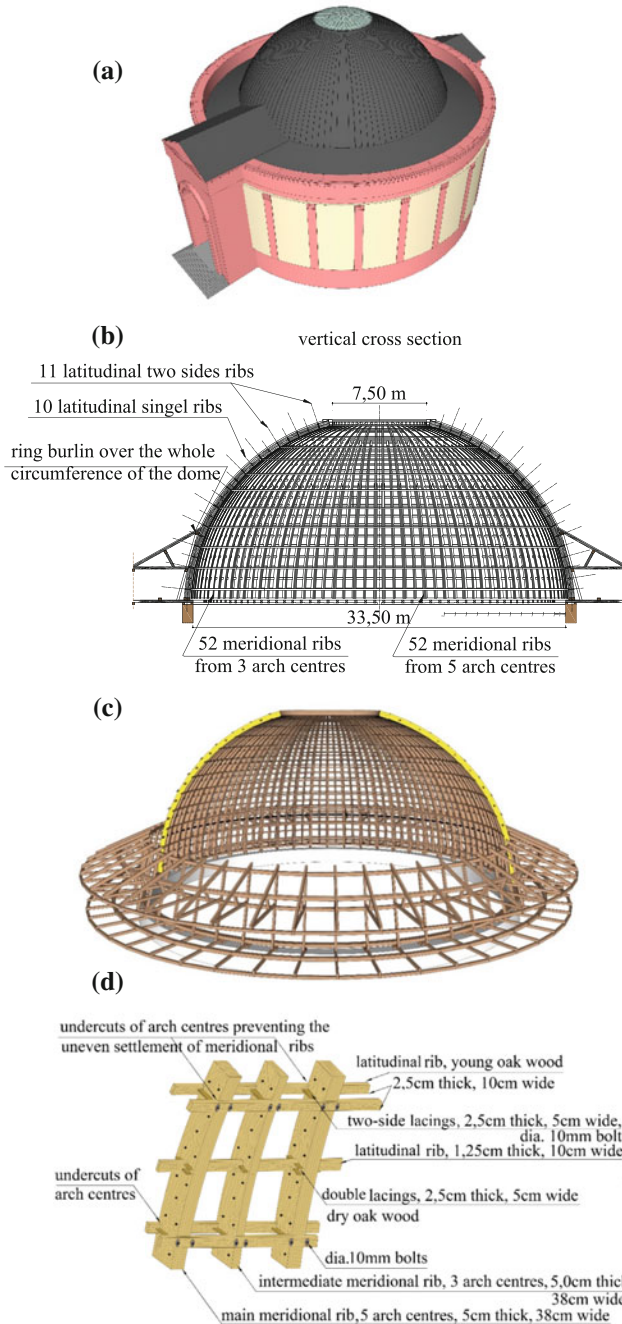


Fig. 3.23 The Moller G.'s Dome in Darmstadt, Germany, of a 33.5 m span according to [13], **a** view of the Saint Louis Church in Darmstadt, **b** vertical section of the structure, **c** visualisation of the dome's structure, **d** details of the connection of the dome's meridional and latitudinal ribs

The horizontal chords surrounds the dome like hoops, protecting it against horizontal distortions and ensuring the mating of mating meridional ribs at an uneven vertical settlement.

The main meridional load-bearing ribs were connected at the dome's peak with a wooden ring of a 7.5 m diameter, made from horizontal beams in which meridional ribs were introduced. This connection method protects ribs against a horizontal shift.

The lower roof of a triangular section shown in Fig. 3.23b, c constitutes a ring that prevents a horizontal shift of the dome. The sloping pillars support a latitudinal double beam that creates a permanent and immobile ring to buckle the meridional ribs in the sphere of the lower dome. The subtly designed and made, geometrically invariable structure ensures a spatial mating of all dome's elements.

The realization of the structure innovative in the 19th century by Moller G. triggered a discussion in the engineering environment. **The use of a single-layer construction and the introduction of iron connectors in rib connections was criticized.** In his work [13] Prof. Otto Warth from Karlsruhe describes two examples of dome structures that he considered correct, as shown in Figs. 3.24 and 3.25. Shown in Fig. 3.24 is the first didactic example placed in [14] of a dome made up of two self-supporting shells: an outside wooden shell of a diameter of ca. 12.0 m, another masonry dome of a 11.0 m diameter. The outside dome has a pure ribbed structure from arch centres, as the dome by Moller G. built in 1827 in Darmstadt (Fig. 3.23). The wooden structure comprises thirty-two main arches made from two arch centres, 4 cm thick and 25 cm wide each, having the character of de l'Orme's arches. The arched ribs of the dome were connected in the key block with a ring of a 3.0 m diameter, at the bottom they were anchored in a masonry wall with cast iron anchors. The stiffening of the wooden ribbed structure constitutes three horizontal latitudinal ribs in a spacing of ca. 2.0 m, also made from arch centres. The connection of vertical ribs and horizontal ribs is shown in Fig. 3.23d.

While comparing the Moller's dome and that shown in Fig. 3.24, Otto Warth wrote so, I quote from his work [13]: "The structure of the dome that creates, at the same time, both the ceiling and the roof is less worth recommending, i.e. the Moller's dome, since in the case of domes it is difficult to recognize leaks of the hardly connected covering since its inside area and its decorative outfit is easily exposed to a damage. Hence, in order to maintain the building it is justified to set one dome above the other so as to be able to recognize necessary repairs on the outside dome in the right time."

Facing up such expectations for the solutions of lighter domes like that shown in Fig. 3.24, Warth O. suggests the other example, i.e. with the two-layer dome from wood shown in Fig. 3.25. Its advantage is the protection of the inside shell against the effects of inundation by precipitation water due to lack of tightness of the outside shell, and the option of using the space between the shells for ventilation,

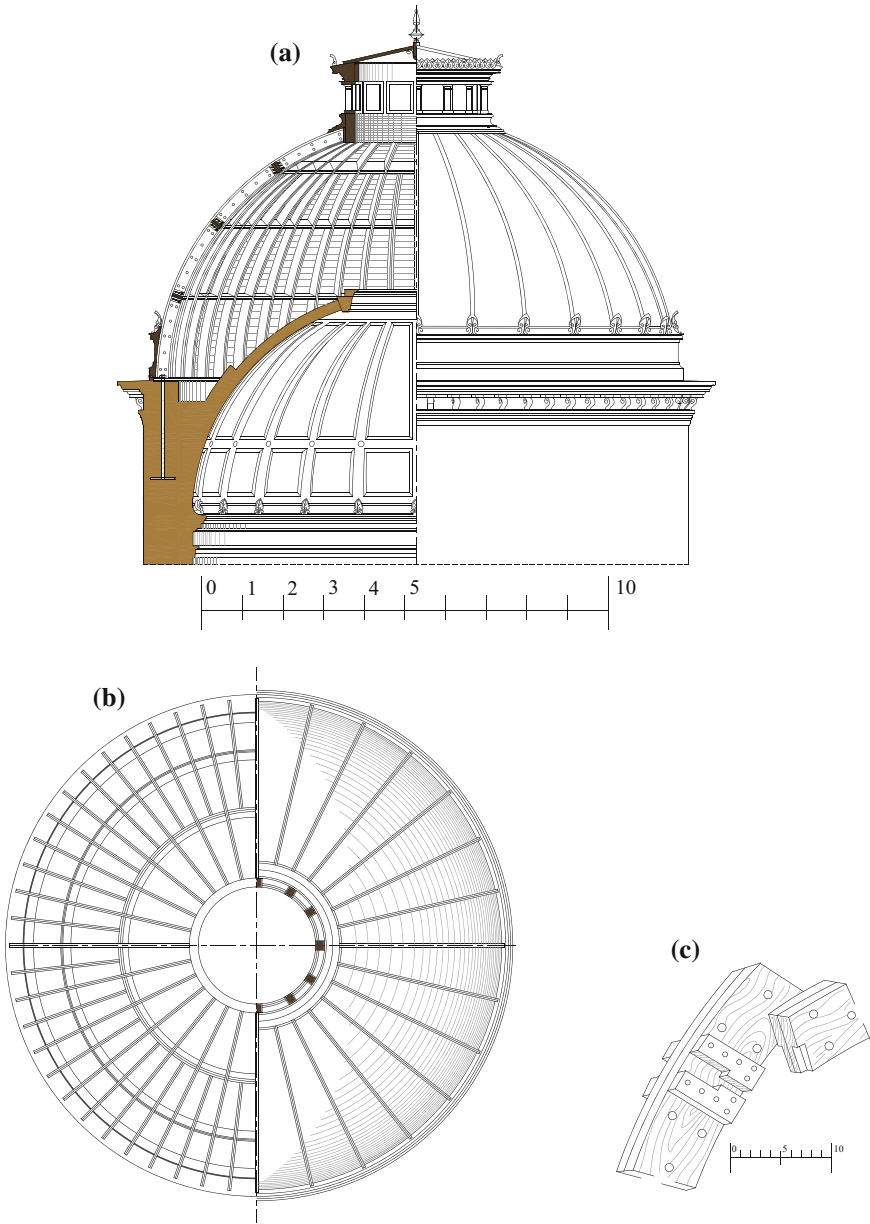


Fig. 3.24 Example of a two-layer dome of a 10.0 m diameter to [14], **a** view and section of the dome, **b** projection and view of the roof covering, **c** connection of meridional and latitudinal ribs in a node

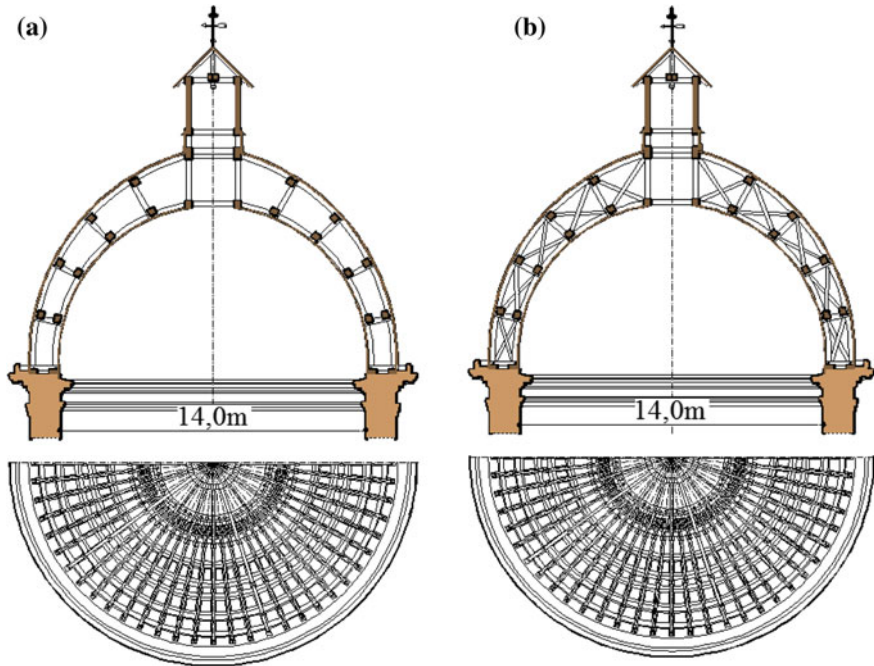


Fig. 3.25 Example of the two-layer dome of a 14.0 m span, with the lantern according to [13] **a** section with the view of meridional ribs, **b** section with the view of the main meridional ribs

maintenance and overhaul purposes. **An essential issued raised by Warth O. is to create conditions for an effective air replacement and ventilation between wooden shells.**

In the structure, meridional ribs from arch centres creating two layers of bars connected with studs were proposed—Fig. 3.25a. The inside diameter of the dome projection is 14.0 m, and the top horizontal stiffening ring under the lantern—ca. 2.30 m. The two-shell dome constitutes both the structure under the roof covering elements and the ceiling over the room covered. Shown in Fig. 3.25a is the section and structure of intermediate ribs. Shown in Fig. 3.25b are meridional, main roof trusses with the dual diagonal framework. The dual-chord, truss meridional bracings in each node of meridional trusses, shown in section, ensure the spatial mating of the meridional elements of the system. At the same time, the calculation of sectional forces was possible without taking into account the effect of displacements. Meridional ribs were embedded on the wall using oak rings from logs. Meridional ribs from logs of 12×25 cm dimensions at a spacing every ca 1.0 m were proposed.

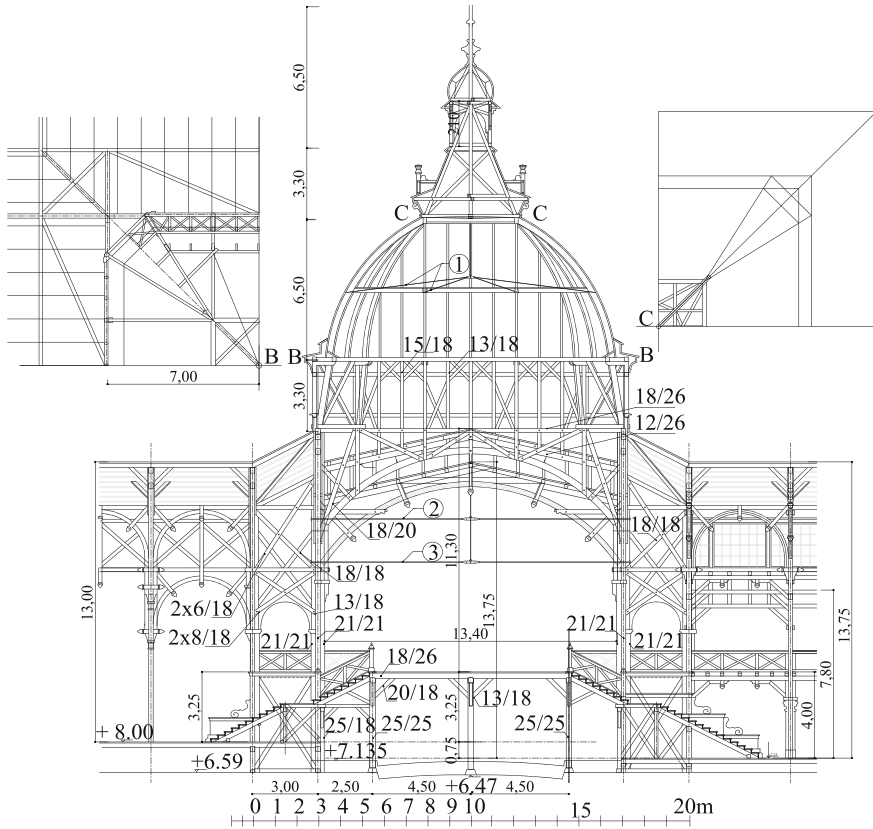


Fig. 3.26 View of the structure crowned with the dome in Görlitz as described in *Deutsche Bauzeitung* 1885. Steel tie rods are designated with numbers 1, 2, 3 [13]

Shown in Figs. 3.26, 3.27, and 3.28 are the examples of later facilities built in the 19th century, having the structure from solid wood, crowned with domes, developed on the basis of the work by Otto Warth [13]. The already illegible drawings have been reconstructed in order to remind of those exceptionally subtle structure, of the sections of load-bearing elements of a height not greater than 30.0 cm and a thickness of several planks.

In Figs. 3.26 an industrial-craftsman's building erected in Görlitz in 1885 is shown. The dome was built over the central room that had been designed on the intersection of the main hall with the cross hall. This fact was designated on the outside through a higher construction crowned with a dome. In the middle of the dome's height steel tie rods were used, anchoring the vertical mast crowning the lantern. Another pair of cast iron tie rods was used at the level of supporting arches of the side aisles supporting the load-bearing tambour of the dome.

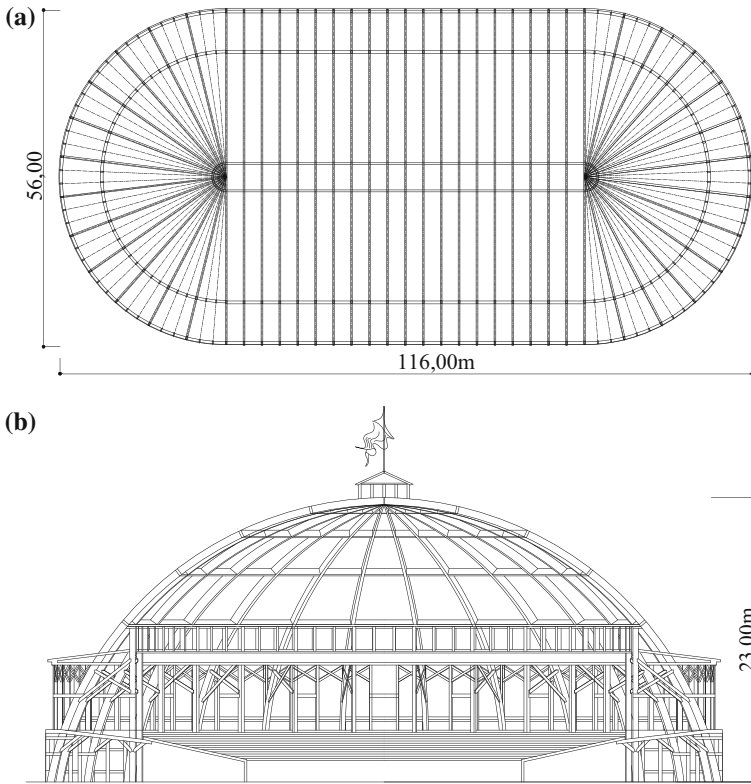


Fig. 3.27 Auditorium built in Vienna in 1890 [14], **a** horizontal projection, **b** section

Beside the dome-crowned buildings, free-standing hall buildings of imposing dimensions were built using ribbed arch centres. Shown in Fig. 3.27 is the auditorium built for the German Federal Festival of Singers in Vienna in 1890. The hall had a span of 56.0 m, a length of 116.0 m and a height of 23.0 m [14]. The hall was dedicated to 20,000 spectators.

The structure was made from arches stiffened with horizontal and meridional beams. The feet of the posts were seated on logs.

Shown in Fig. 3.28 is the section of the building erected for the North-German Industrial Exhibition in Königsberg in 1895. The main entrance led to the central room of a 21.0 m height, crowned with a dome of a 19.0 m diameter. Meridional load-bearing ribs were built from arches from arch centres of 8×30 cm dimensions.

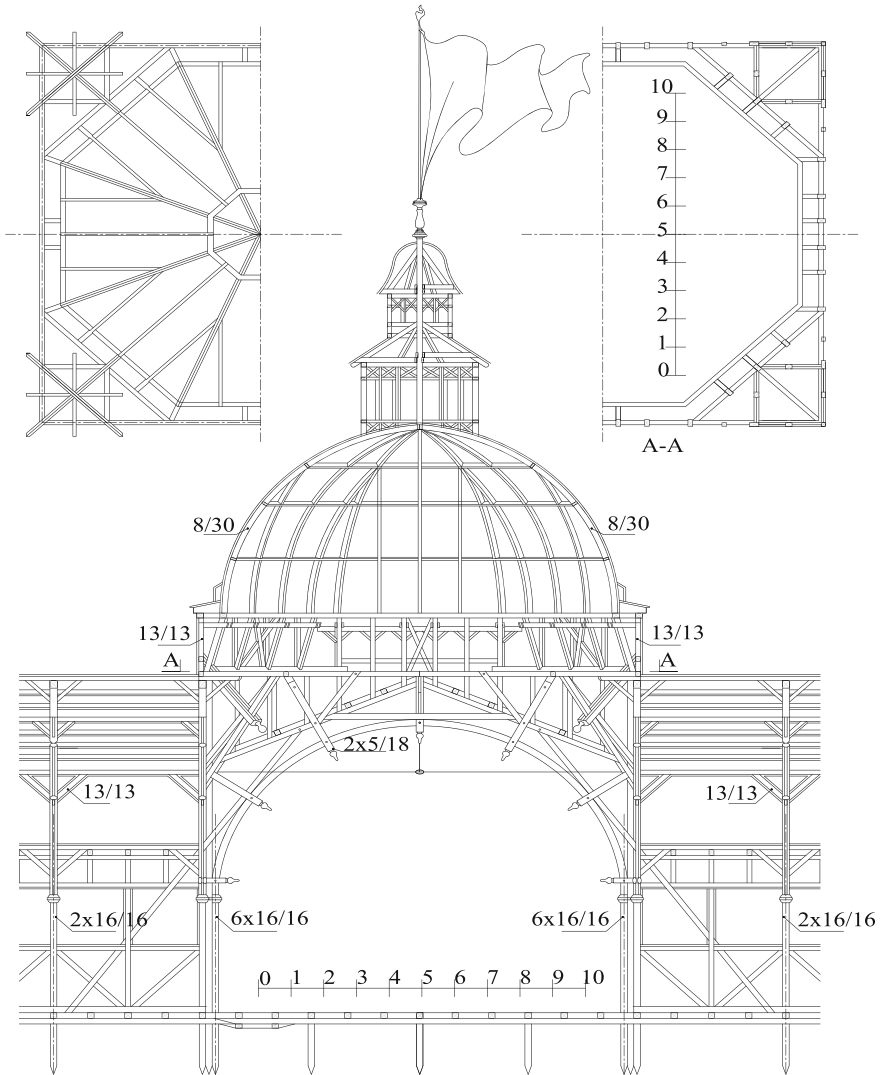


Fig. 3.28 Section of the dome of the building in Königsberg for the North-German Industrial Exhibition 1895 [13]

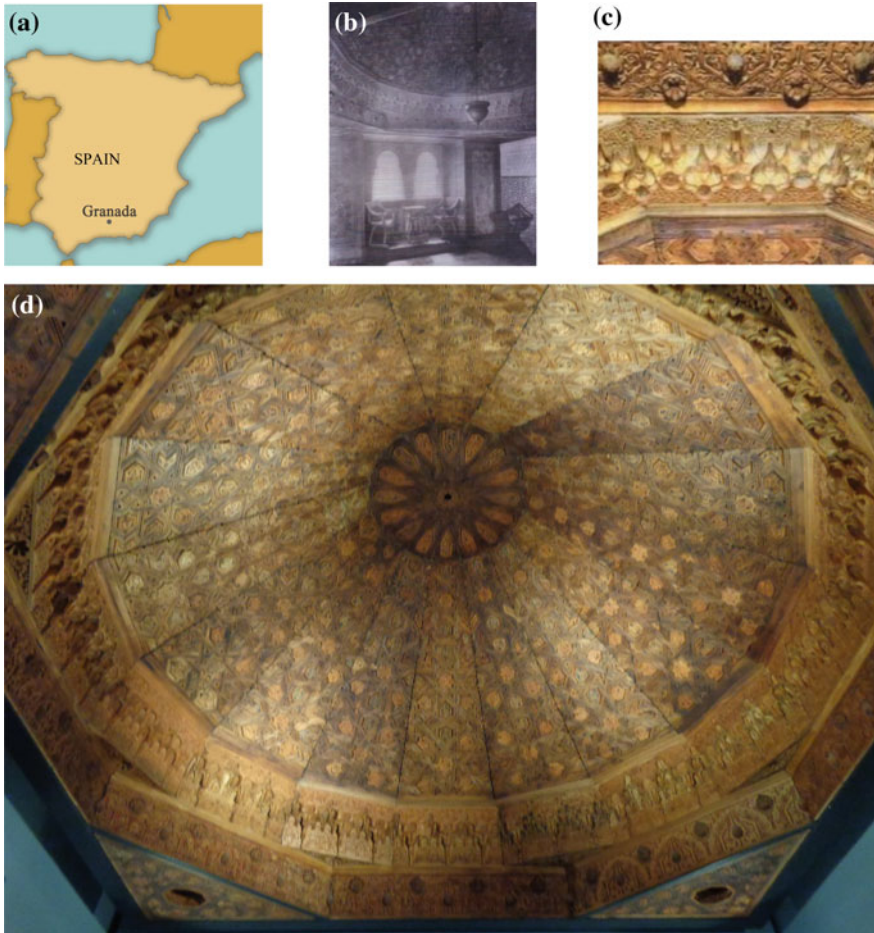


Fig. 3.29 Dome of the Alhambra Palace, Granada: **a** location, **b** view of the dome-roofed inside [18], **c** details in close-up, **d** dome palate, photo by the author

3.6 Conclusions

The lasting centuries of the building of facilities using meridional-latitude structures led to the optimization of the structural characteristic of the dome form. While maintaining the geometrical invariability the system and the connections of wooden elements was perfected, which led to a simple and legible meridional-latitude structure designed and built by Moller G.

Saint Louis Church in Darmstadt is the first facility described in the referenced literature [13] (1900) roofed with a single-layer wooden dome of a 33.5 m span,

made as a regular ribbed structure. The structure designed by Moller is the result of a regular experience in the building of wooden scaffoldings for the building of masonry ceilings and domes. An arch centre, being an outside element of the scaffolding supporting the outside canopy, became an autonomous load-bearing rib of the dome. The scaffolding supporting it vanished. The introduction of a latitudinal stiffening as shown in detail (Fig. 3.23b, c), created the first, ribbed load-bearing system of the dome.

The division of structures into meridians and lines of latitude introduced a legible picture of the distribution of forces in a dome and facilitated the statistical calculations of load-bearing elements.

Today, the Moller's dome arouses admiration due to its subtle sections of the wood used for the construction and its purposeful application. Ripe wood was used for meridional ribs, young wood was used for latitudinal ribs, using differences in the properties of young and old oak wood. Basing on the today forgotten criteria, a wood species was selected to be used for pre-stressing elements or connectors. It is worth quoting here what Moller G. himself, subjected to a critic, wrote on the subject matter of rules applied to increase the durability of a structure. I quote from the work by Otto Warth in Karlsruhe: "The foundations on which meridional ribs from arch centres rest are made from oak wood, the latter standing with their footing not in the plug hole where rain water could collect but in an open and a little bit steep cavity. The entablature that supports the foundation has dilatation openings so that it could quickly dry up in case it got wetted. Located between the rib heads, as near as possible to the top lantern, are dilation openings (in the top ring) having the form of openwork rosettes since, over the roofs, the outside side of the dome is not planked, then long channels are naturally formed between ribs from arch centres, which has to directly contribute to the maintenance."

The Moller's idea was perfected in successive realizations of the facilities roofed with domes.

The susceptibility of wood to the environmental interference produced that for centuries various method of its protection has been used, and Prof. Warth O. called attention to the problem of the durability of wooden domes. He emphasized the meaning in that process of the ventilation of the structure.

Various methods were used, and the most effective turned out to be those methods that protected against corrosion, without destroying the specific anatomic structure of wood. An example of the facility preserved owing to the proper maintenance and operation is the wooden dome made as a roofing of one of view towers of the Alhambra Palace in Grenada shown in Fig. 3.29. The dome was made in 1320, having the dimensions in projection of $3.55 \text{ m} \times 3.55 \text{ m}$ and the height of 1.90 m. It was made from cedar and poplar wood commonly considered as a non-durable species. Owing to the skills of its creators, the dome has subsisted for 700 years and may be admired in the pavilion of the Islamic Art Museum in the Pergamum Museum on the Isle of Museums in Berlin. Shown in Fig. 3.29 are the photographs taken by the author in the museum in Berlin.

An essential role in the issues of durability is played by the conditions under which wood operates in a building facility. Wood located under the settled conditions of temperature and humidity has an unlimited durability. A confirmation of this is the dome shown in Fig. 3.29, as well as wooden items counting several thousands of years, originating from Egyptian tombs [15].

References

1. Saudan M., Saudan-Skira S., *Coupoles: espaces symboliques et symbols de l'espace*, La Bibliotheque des Arts. Genève Atelier d'édition, "LE SEPTIÈME FOU [B.R.]
2. Obmiński T. *Budownictwo ogólne II Atlas* Wydanie i nakład Związku Studentów Inżynierii Politechniki Lwowskiej. Lwów 1925.
3. Taras J. *The Ukrainian Wooden Church Architecture. The illustrated dictionary*. National Academy of Sciences of Ukraine. The Ethnology Institute. Lviv 2006.
4. Heinle E., Schlaich I. *Kuppeln aller Zeiten - aller Kulturen*. Stuttgart. Deutsche Verlags-Anstalt 1996.
5. Bourget P., Cattai G. *Jules Hardouin Mansart* Editions Vincent&Co, Paris.
6. Erler K. *Kuppeln und Bogendächer aus Holz von Arabischen Kuppeln bis zum Zollinger – Dach*, Fraunhofer IRB, Verlag 2013, Stuttgart.
7. Stade F. *Die Holzkonstruktionen*. Leipzig 1904r. Reprint der Originalausgabe 1997.
8. Kowal. E. A. *Kopuła kościoła w Gostyniu*, praca doktorska, Wydział Architektury, Politechnika Wroclawska, 1999.
9. Otto Ch. F., *Space Into Light, The Churches of Balthasar Neuman*, The MIT Press 1979. Würzburg, Schönborn Chapel, 1722 rok średnica kopuły murowanej 20.0 m, arch. Baltashare Neumann.
10. Stüler F. A., Börsch-Supan E., Dietrich Müller-Stüler, *Friedrich August Stüler 1800–1865*, Deutscher Kunstverlag 1997. Berlin, Kościół św. Marka, lata 1848–1855, średnica kopuły około 16.0 m.
11. Orłowicz R. B., Kosiorek M. *Skutki pożaru Katedry Troicko - Izmailowskiej w Petersburgu* XXII Konferencja Naukowo Techniczna Szczecin - Międzyzdroje, 23–26 maja 2007.
12. Cornelius Gurlitt, *Andrea Palladio*, Bibliothek alter Meister der Baukunst zum Gebrauch für Architekten Herausgegeben, DER ZIRKEL 1914, Architektur-Verlag, Berlin, Germany.
13. Timoszenko S. P. *Teoria stateczności sprężystej*. Arkady, Warszawa 1996.
14. Warth Otto *Die Konstruktionen in Holz* Gedruckt von A. Th. Engelhardt, Leipzig 1900.
15. Kozakiewicz P., Matejak M., *Klimat a drewno zabytkowe*, Wydawnictwo SGGW, Warszawa 2002.
16. Sourdel - Thomine J. von Spuler B. *Propyläen Kunstgeschichte die Kunst des Islam*, II. 102a, 102b, Berlin 1973.
17. Chmelnizkij S. *Zwischen Kuschanen und Arabern. Die Architektur Mittelasiens im V.-VIII Jh. Ein Rückblick in die Kulturgeschichte der Sowjetunion*. Felgentreff & Goebel & Co KG, Berlin, November 1989.
18. Brisch K., *Kuppeldach aus dem Aussichtsturm des Torre de las Damas (Damenturm)*, Foto: Bundesarchiv, Staatliche Museen zu Berlin.

Chapter 4

Thick-wall Domes

4.1 Introduction

In parallel with old Mediterranean civilizations, Eastern-European civilizations were formed. In the areas of Eastern Europe, where woods were growing abundantly, marshy soils and heavier conditions for settlement occurred, structures were generally built in wood, including prestigious structures. Unfortunately, there are few historical records on this subject. The first information is to be found in the texts by modern historians.

Vitruvius wrote in his work, “On the Building”, originating from the first years of the Christian Era, found in the library of the Monastery of St. Gall, Switzerland, in 1415, (I am quoting the translation from the 20th century in the work by Obmiński T. according to [1]): “In the nation of Colchis in Pont (over the Black Sea) due to the abundancy of woods, they lay trees on the right and left side (into a square) leaving so much space among them as the length of the tree will allow, on the top they lay transverse trees, surrounding with them the inside dwelling area. Afterwards, they lay alternately to the four sides beams that connect corners between themselves, in this way they lead the walls from wood upwards, vertically, with bottom layers up to the height of a tower, whilst the empty places, left by the roundness of trees, they fill with shingles and clay. Afterwards, they gradually narrow upwards the roofs brought out beyond the four corners and laid crosswise from beams. Thus, they raise, on the four sides towards the centre, a sort of monticules which they cover with branches and clay, and, in a barbarian way, they shape the vaulted roof of the tower” [2].

Shown in Fig. 4.1 is the St. George’s Orthodox Church in Drohobych, Ukraine. It was built on the turn of the 15th and 16th century. The walls and the roof of the temple was made from logs. This facility has been operating until this day in Ukraine. The domes of the Orthodox church’s roof called “globes” were covered using the shingle split from wood.



Fig. 4.1 Domes from logs of the Orthodox church in Drohobych, photograph by the author

The local civilizations worked out their systems of building wooden domes. The main load-bearing element of the original structures was the log made from the single trunk of a tree. Walls and even dome-like roof coverings of various facilities were built from logs.

4.2 Methods of Shaping Log Connections

The framework roofing, also called crown roofing, was shaped on the rectangular or polygonal projection. In the reference literature, there is no subject to justify the nomenclature that facilitates the description of the primary roofings from logs. The names used in this study: dome-like roof coverings, pyramidal coverings, cylindrical coverings, reflect the geometrical form of the facility. The definitions applied result from the attempts to name the basic types and the next development stages of the wooden spatial structures without intermediate supports. The records on this subject are scarce.

Figure 4.2 depicts five selected examples of crown walls, built from horizontally laid logs, hewn from tree trunks.

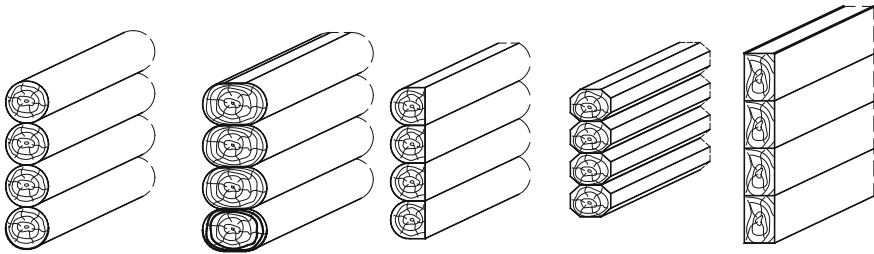


Fig. 4.2 Walls from beams (logs) laid horizontally according to [3]

Walls from beams laid horizontally were joined in the building's corners using various notch connections. Shown in Fig. 4.3, developed according to [3], are several examples of the most connections typical of log walls.

The impact on the spatial stiffness of crown structures will be exercised by nodes. Log daps in nodes were made at various angles. Owing to the skills of shaping notches and fasteners from wood, structures that transfer considerable strutting forces were obtained. In the work [3] (1914) by Obmiński T., examples of the connections of rectangular beams at angle are presented, jointly with the carpenter's designations shown in the left upper corner in Fig. 4.4a–c.

4.3 Dome-like Log Coverings

Originally, a pyramidal covering nearing a monastery vault was erected on the tetrahedron of building's walls made from logs (Fig. 4.5), which could be considered as a dome-like covering. The covering was stiffened with a spatial system of vertical (Fig. 4.5a) and horizontal (Fig. 4.5b) struttings. The cross strutting depicted in Fig. 4.5 stiffens the framework pyramid in horizontal plane and reduces the strutting transferred from the pyramid onto the building's walls. The vertical strutting also plays the role of a wind strutting.

High roofs in form of truncated or stepped pyramids were used in watch towers, bell towers, etc. They were erected in cemeteries, at temples and prestigious facilities, as well as located in fortifications as observation posts. The covering of towers constituted shingle, board planking or metal sheet. The majority of towers gave evidence of the rank of the settlement.

A separate group of framework structures used at a greater height and a higher projection of the structure covered constituted pyramidal "stepped" towers. The height of towers was increased by the stepped overbuilding of pyramids vertically, over straight sections of log walls (Fig. 4.6).

The increased height required a cross vertical strutting (Fig. 4.6) of several storeys. At the base of each pyramid with sloping walls the horizontal elements of

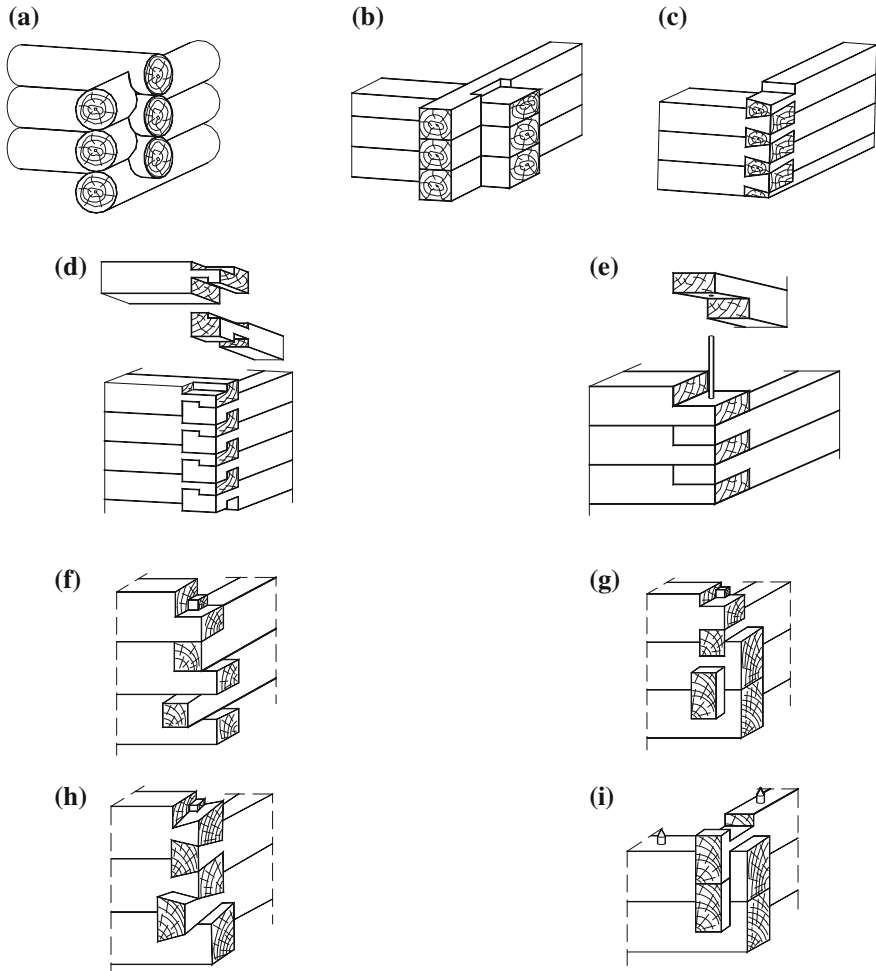


Fig. 4.3 Connections of perpendicular walls from beams laid horizontally [3], **a** saddle framework corner joint, **b** lap, **c** lock on “zincs”, **d** “lock” joint, **e** corner reinforced with a bar, **f** framework joint with tendons, **g** notches with undercuts and tendons, **h** slanting notches and studs, **i** connections of logs using notches and studs

the strutting were fabricated, taking over the thrust of wooden beams. Visible in Fig. 4.6 is the vertical strutting with horizontal tie members at each level of the roof bend.

Demonstrated in Fig. 4.7 are the unique vertical struttings and horizontal tie rods encountered until this day in Orthodox churches [5]. The vertical struttings of domes were fabricated as full membranes (Fig. 4.7a) or lighter wooden vertical trusses (Fig. 4.7b) whose bottom chord operated as a tie rod. The span of eminent roofings of principal houses and places of worship was determined by the length of

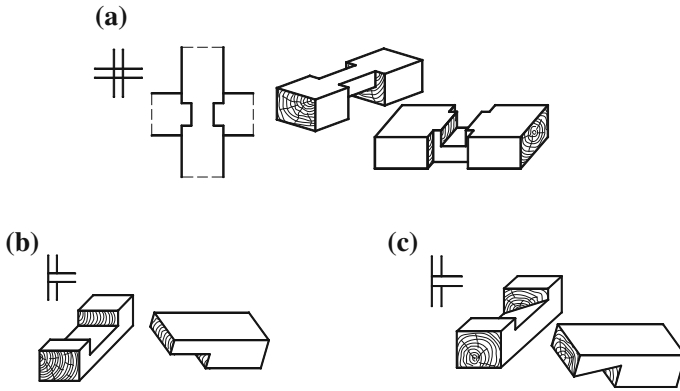


Fig. 4.4 Connections of beams at angle according to Obmiński in [3], **a** straight lap with auxiliary element, **b** straight lap, **c** slanting lap

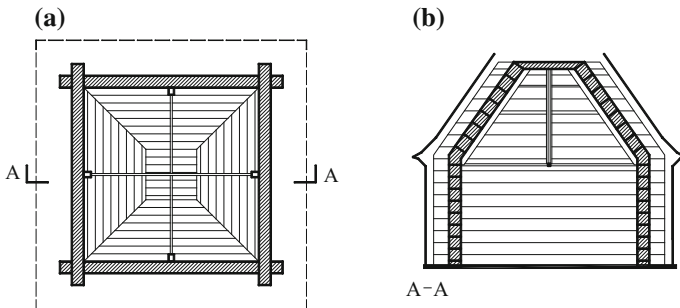


Fig. 4.5 Pyramidal (dome-like) framework structure on the square projection according to [4], **a** horizontal section with the projection of the vault, **b** vertical projection

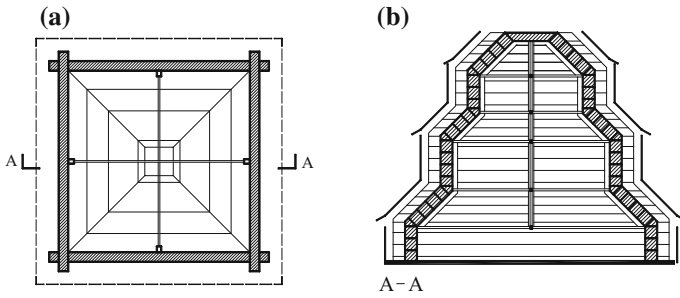


Fig. 4.6 Framework, stepped dome on the square projection according to [4], **a** horizontal section with the projection of the vault, **b** vertical projection

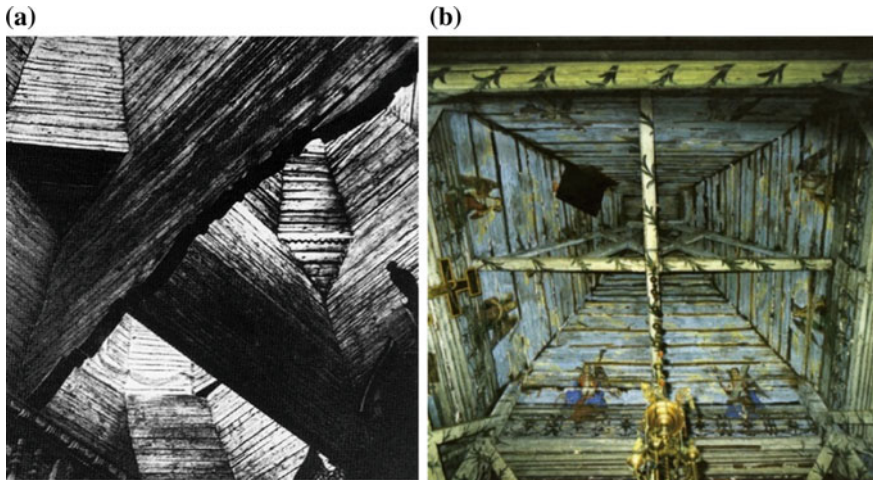


Fig. 4.7 Examples of struttings of a church tower according to [8], **a** with vertical full membranes, **b** with vertical truss membranes

logs acquired from the wood. The full membranes jointly with the increase in the dimensions of the covering base became heavier and heavier (Fig. 4.7a). They were replaced with lighter truss struttings (Fig. 4.7b). A rich collection of figures full of Orthodox church membranes in Ukraine is presented by Taras J. in his work [6] (2016), [7] (2006).

The dome-like roofings built on the plan of a hexagon and an octagon of the same length from logs in one latitudinal layer allowed to increase the surface covered. Figure 4.8 shows an example of a pyramidal facility on the plan of an octagon.

Due to the increased number of the sides of a pyramid, duplicated struttings contracting the opposite walls were used. They were used in the example in Fig. 4.8 in two levels: the bottom level at the base of the pyramid, and that in the middle of the height of the pyramid.

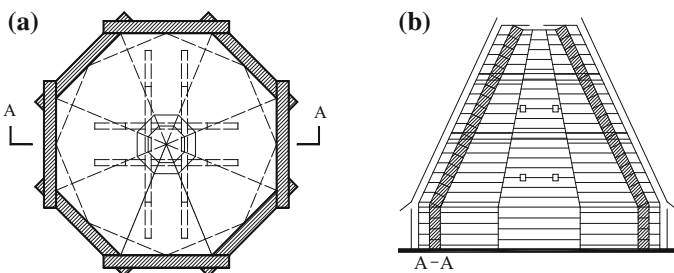


Fig. 4.8 Apparent pyramidal dome laid from horizontal logs on the polygonal projection according to [4], **a** horizontal section with the projection of the vault, **b** vertical section

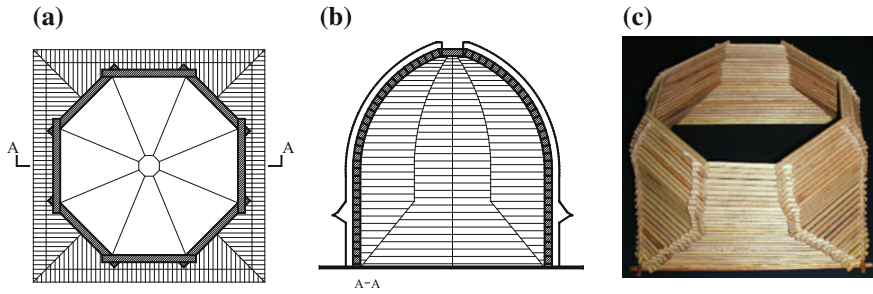


Fig. 4.9 Sectional-cylindrical framework dome on the octagonal projection according to [4], **a** horizontal section with the projection of the vault, **b** vertical section, **c** model of a dome from beech wood

An advanced, eminent dome-like structure having a square base, going over into an octagonal section is shown in Fig. 4.9. It differs from the pyramidal structure from Fig. 4.8 in this way that the sections of the octagonal covering in the plan are cylindrical vertically. Such a solution makes the structure more nearing the stone domes. An advantage of the solution is the resignation from cross struttings interfering with the inside space under the vault. The highest thrust at the dome's base takes over the square framework crown of a projection like in Fig. 4.9a. Shown in Fig. 4.9b is the section of a dome, and in Fig. 4.9c the sectional model of a cylindrical dome made from round bars of a 5.0 mm diameter that reconstruct the actual structure.

Shown on the model—Fig. 4.9c is the passage from the square projection of the log wall to the octagonal horizontal cylindrical vault from logs.

The building of log domes on the projection of polygons with the number of sides higher than eight made difficult the fabrication of connections from logs. The difficulties of the fabrication of notch connections in logs for segmentally cylindrical coverings on the octagonal projection were verified on the model drawn in Fig. 4.10.

The limit of the possibilities to increase the number of sides of the projection of dome-like sprung-arch vaults constituted the connections of logs on notches. The lock that connected the logs were already so complicated that they did not provide the load capacity of connections. Log domes on the octagonal projection were probably the last domes in the series of dome-like facilities. This is evidenced by Orthodox churches preserved still in the 20th century and described in the literature [8] by Brykowski [8] (1995), Kaniowska [9] (2005). Examples of the facilities built with the use of tower structures made according to the scheme as in Fig. 4.9 are placed in Figs. 4.11 and 4.12.

The structure of the Greek-Catholic Church in Krowica Sama, burnt down during the fire in 2002 in Poland [10], described by Rydzewski [11] is shown in Fig. 4.11.

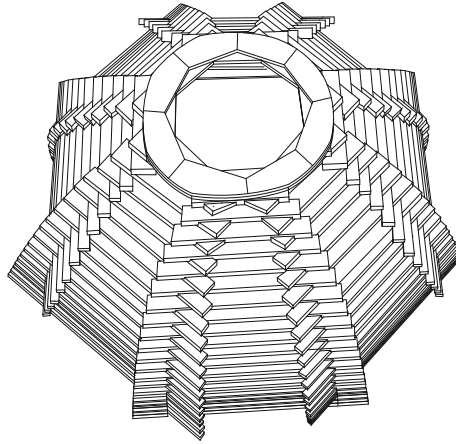


Fig. 4.10 Figure of a model of the dome-like covering from rectangular logs on the octagonal projection

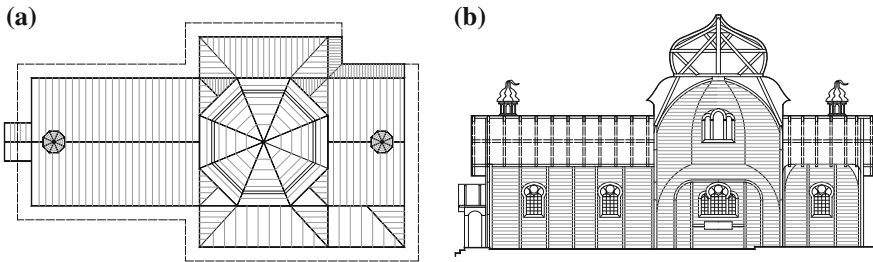


Fig. 4.11 St. Michael the Archangel Greek-Catholic Church in Krowica Sama, Poland, according to [11], **a** projection, **b** section

Shown in Fig. 4.12 is the renovated Transfiguration Orthodox Church in Krechov, Ukraine, built in 1648 to commemorate the visit paid by Bohdan Khmelnytsky to the Basilians' monastery. The view of another dome from logs on the octagonal projection is depicted in Fig. 4.13 according to [8] following the example of the Orthodox church in Korczmin, Lublin voivodship (Poland). The framework domes presented were based on the octagonal tambour resting on the stiff tetragon of log walls.

The building of dome-like coverings on the projections of polygons having the number of sides higher than eight is easier from logs without notches, joined using foreign fasteners. This was verified on the model shown in Fig. 4.14. The dome from rectangular logs, Fig. 4.14, was made on the plan of a dodecagon. The bending of the covering was obtained by arranging each latitudinal layer eccentrically in relation to the lower layer. Logs in each layer were laid in every second cut-out leaving empty every second span over the circumference of the line of latitude.



Fig. 4.12 Wooden dome of the Orthodox church in Krchov, Ukraine, photo by the author

Fig. 4.13 Dome of the Orthodox church in Korezmin [8], photo by Lang J. (1971)



The idea of building the pseudo-dome shown in Fig. 4.14 originates perhaps from Central Asia. Chmelnickij describes in [12] a similar covering on the tetragonal projection in the Turkmenistan architecture. Ceilings in form of apparent

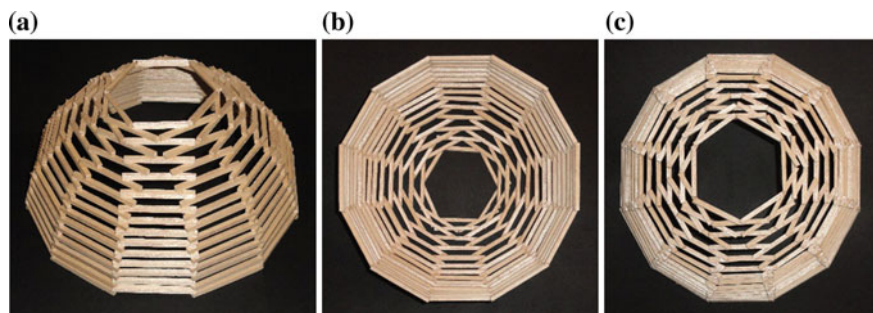


Fig. 4.14 Model of the dome from rectangular logs on the projection of a dodecagon, **a** side view, **b** side from the inside, **c** top view

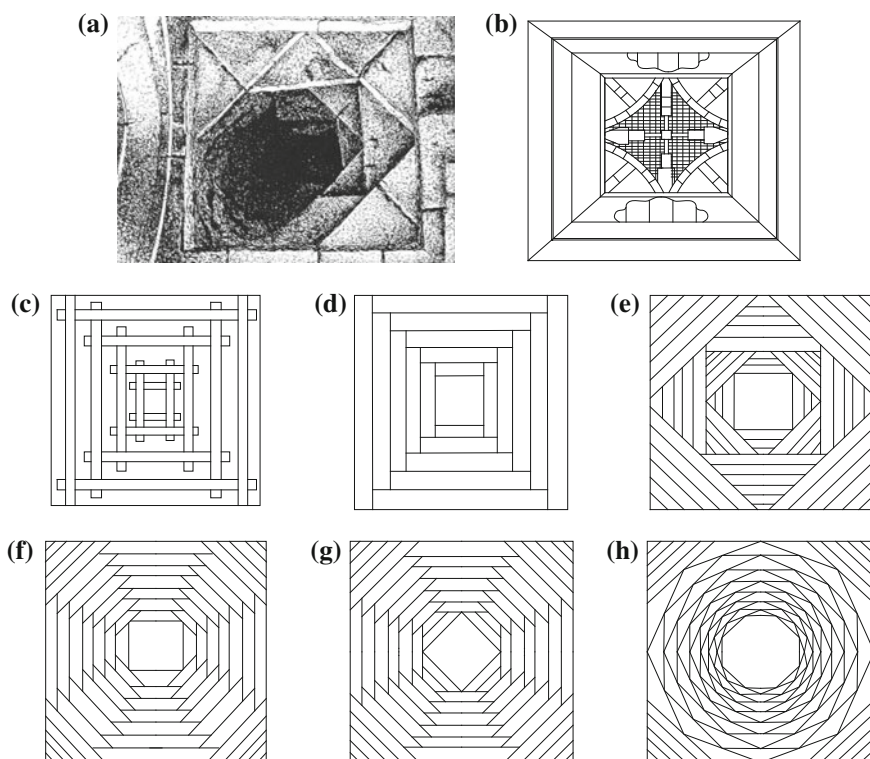


Fig. 4.15 Examples of apparent vaults from blocks: ceramic, stone and wooden, **a** 'rusan'—an apparent dome on the tetragonal projection [12], **b** form of the stone vault from the Mosque of Cristo de la Luz from 999, **c–h** wooden, lantern-type vaults according to [14]

vaults, arranged from large ceramic blocks are encountered in it, as shown in Fig. 4.15a. The covering was closed from the top with a flat stone or ceramic block. Such vaults in the Central Asian terminology bear the name of 'rusan'.

In the locality of P'yauyang, Korea, a form of a vault similar to a 'rusan', originating from the 6th–7th AC was discovered and designated with the name of a dome-like, lantern dome [13].

In Toledo, in the Mosque of Cristo de la Luz built on the turn of 999/1000, nine similar stone, lantern vaults on the projection of a square were built [14]. The sketch of one of them is shown in Fig. 4.15b. The remaining eight vaults were built according to the same scheme, introducing just the differences in the details of the finish particular.

Shown in Fig. 4.15c–h are six apparent vaults described in [14] arranged from wooden logs built in Bukovina, Poland, Moldova and Georgia in circa the 10th century AC. The figures present apparent views of those vaults built from logs without notches, on the tetragonal and polygonal projection. The lantern vault built on the octagonal projection is depicted in Fig. 4.15h.

4.4 Compilation of Dome-like Forms

In the examples specified shown are the transformations of dome-like coverings on the tetragonal up to the dodecagonal projection of a crown and lantern type (Fig. 4.15). Such domes built from logs were joined in the corners of the polygonal projection on notches: straight, inclined, with hidden dovetails and studs from wood.

In the thick-wall domes built from logs, joined with notches, the effects of slenderness of the dome R/g were negligibly small: where: R —radius of the dome, g —thickness of the dome shell. A spatial framework stiffening of dome-like coverings were full or truss membranes, shown in Figs. 4.5, 4.6, 4.7, 4.8 and 4.9. They were used as a protection against “a collapse” to the inside of heavy log walls. The dimensions of the struttings were limited by the length of stretched elements, e.g. of the lower chord of the stiffening (Fig. 4.7). The main obstacle in increasing the span of the construction constituted the stretched connections. **The introduction of the form of a sectional-cylindrical covering, made up of cut-outs of a cylinder on the octagonal projection relieved the inner space under the dome from struttings.**

Depicted in Fig. 4.16 is the compilation of the sections of vertical framework coverings from apparent vaults up to a cloister vault. The last link of the transformation of polygonal projections and stepped projections of pyramidal coverings was a thick-wall from logs, segmentally cylindrical on the octagonal projection demonstrated in Fig. 4.16e, due to the difficulties in fabricating notch connections. **The slenderness of the shells of such domes is measured by the ratio of the radius to the shell thickness R/g amounted to circa 12.**

The horizontal projections of lower thrust rings of the dome-like structures from logs are shown in Fig. 4.17. Each successive polygon made it possible to increase the surface covered. The transfer from the square projection to the circular

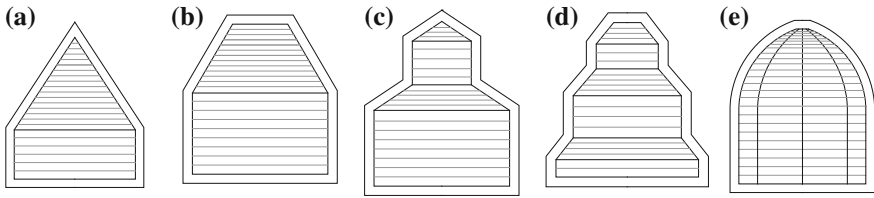


Fig. 4.16 Vertical sections of framework towers: **a** pyramid, **b** truncated pyramid, **c** stepped, **d** stepped duplicated, **e** sectional-cylindrical

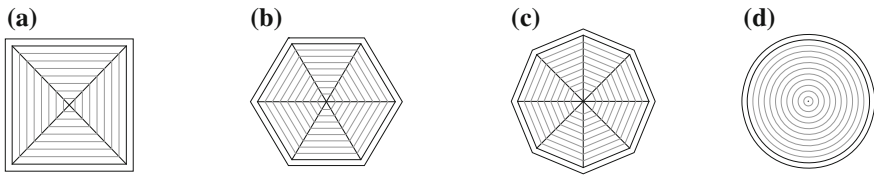


Fig. 4.17 Horizontal projections of dome-like vaults: **a** square, **b** hexagon, **c** octagon, **d** circle

projection was associated with the decrease in the length of logs from which the shell was built.

The decrease of the dimensions of logs, the elimination of notch connections as well as the application of foreign fasteners allowed to build domes of a higher span on a projection nearing a circle. The idea of the nameless author of shells from short quarterings introduced to the building trade wooden thick-wall domes on the plan of a circle, is discussed in Sect. 4.5.

4.5 Domes with a Massive Shell

The experiments on dome-like structures from logs, connected on notches, led to the formation of spherical thick-wall domes (Fig. 4.18). **The increase in the diameter of thick-wall domes became possible owing to the introduction of smaller structural elements in form of quarterings.** Simultaneously, in the place of notch connections, foreign fasteners were introduced, such as wooden studs and nails. **The introduction of foreign fasteners made possible a further development of dome systems.**

The width of quarterings, thus the thickness of the shell was determined from the thermo-insulation weathering conditions. The length of quarterings resulted from the radius of the dome. The easy treatment of wood under the building site conditions allowed to cut the quarterings to fit the shape of the dome. The tendency of the dimensional variations of quarterings in successive latitudinal layers is illustrated in Fig. 4.18a. The quarterings arranged layer-wise were cut to fit the shape of the sphere and connected with nails.

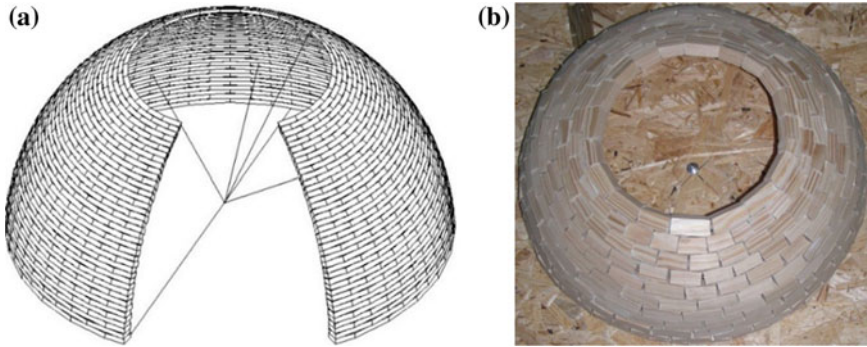


Fig. 4.18 Tendency in the variations of the dimensions of quarterings: **a** building principle of a thick-wall dome, **b** technological model of a thick-wall shell dome

The building of a dome from “identical” quarterings (Fig. 4.18b) does not fill the spherical surface tightly. Shown on the model (Fig. 4.18b) are fissures between thickset, not cut-to-size quarterings. The elimination of fissures consisted in the additional supplementing with wedges or cutting quarterings to fit the outside radius of the dome. The need to cut elements to fit the shape of the dome occurred with the low slenderness of quarterings, e.g. $\lambda = l/b \leq 5$ (l —length, b —width of a quartering). The fissures occurring at the inexact fit of quarterings were also filled with a binding material or closed in the meridional direction with a planking from boards and the covering discussed in Sect. 4.6.

The need to increase the span of domes and the difficulties in fitting the quarterings, requiring experienced carpenters, contributed to the search for a fabrication technology of thin-wall domes. **The further decreasing of the dimensions of quarterings eliminated the defects of the solutions and selected a next system of the economic structures of domes from solid wood as described in Sect. 4.6.**

The slenderness of the shells of thick-wall domes, measured with the ratio of the radius to the thickness of the shell R/g amounted to circa 20. The slenderness of the dome shell R/g became the limit of the span due to the load capacity of single-layer domes made from massive quarterings.

4.6 Examples of Domes with a Massive Shell

In his publication [15], Kashkarov K. P. (1937) presented the structure of two thick-wall domes: (1) the dome of the State Gosippodrom building in Moscow of a 20.05 m diameter, (2) the dome of a 60.0 m diameter. Figure 4.19 presents the building scheme of a thick-wall shell of the dome from quarterings following the example of the dome of the Gosippodrom Palace in Moscow built in 1934.

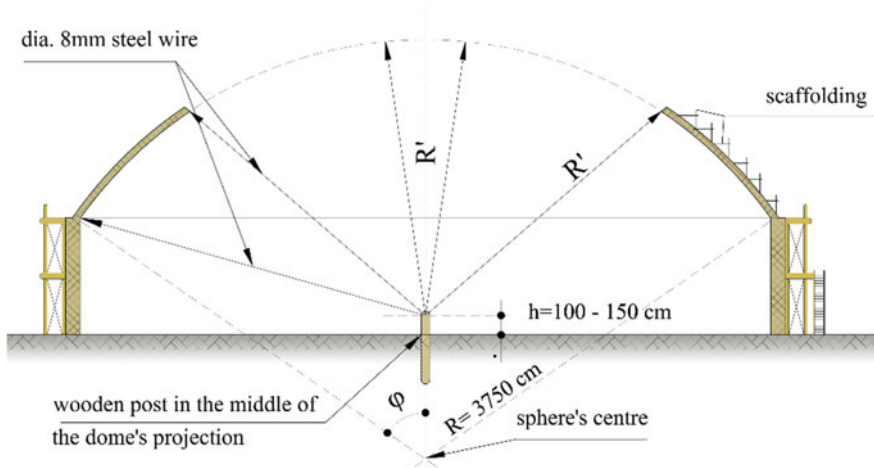


Fig. 4.19 Illustration of the building technology of a thick-wall shell of the dome [15]

Figure 4.20 shows carpenters working on a scaffolding and laying quarterings in form of a shell of the dome according to the scheme in Fig. 4.19. The latitudinal layers of the dome were built from planks laid flat, according to the traced radius of

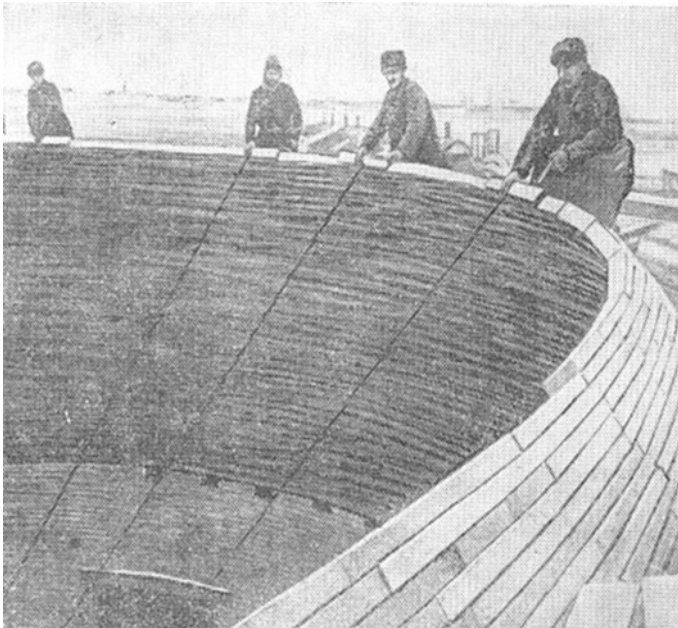


Fig. 4.20 Cutting to size of quarterings to be put into the shell of the dome of a 20.05 m diameter [16]

the layer R'. The length of the radius of the layer was measured off using a wire of a 8 mm diameter, anchored in a wooden post, in the middle of the projection of the dome.

The size of the radius was changed for each layer of the shell. The contact places of quarterings were covered with a next latitudinal layer and fastened with 100 mm long nails of a 4.0 mm diameter. The width of planks (layer thickness) was determined mainly for thermo-insulation reasons.

The length of quarterings was adopted depending on the radius of the canopy. The thickness of planks in one latitudinal layer was invariable, the thickness of the shell (width of planks) was maintained unchanged, only the thickness of plants at the height of the sphere was changed. The highest thickness of planks was used in the bottom rings of the dome, the least in the highest.

In 1934, according to the above-described principles, the dome of the Gosippodrom Palace in Moscow was built. On the basis of the papers [15, 16], the drawings and the data of the unique wooden dome of a 20.05 diameter and a 37.50 m diameter of the sphere were reconstructed. Shown in Figs. 4.21 and 4.22 is the section, projection and details of the already forgotten structure. The drawings of the constructed were used to produce its computer visualizations (Fig. 4.23).

The structure of the dome in Moscow demonstrated in Fig. 4.21 a, b is made up of outside arch centres—1, a thick-wall shell built from three ring-shaped layers of a different thickness—2a, 2b, 2c, as well as from planks 3 of the flat flanking between the outside arches—1. The ring-shaped layers 2a, 2b, 2c were split along the meridional section of the dome into three spheres and made from quarterings of a thickness decreasing from the thrust crown upwards.

In the first bottom zone the thickest quarterings 2a of a 65 × 40 mm section were used. In the central zone the quarterings 2b of a 65 × 30 mm section were used. In the upper zone, of the lower diameter of the meridian of latitude, the quarterings 2c were used, of the highest susceptibility and a 65 × 20 mm section were used. Each ring-shaped layer in the level of one line of latitude has a constant radius and covered the contact place of the quarterings of the previous layer, in the middle of the quartering's length. In order to facilitate the bending in the top zone of the dome being compressed, in the middle of the length of the planks 2c, cuts were made, but no more than to ½ of the plank's thickness.

The strengthening of the shell from quarterings constituted outside meridional elements, that is: twelve arch centres 1 having the nature of de l'Orme's arches and the meridional planking from planks 3, studded every 50.0 cm, when counted along the lower supporting ring, on the outside, as the dome was erected. The quarterings 2 were arranged step-wise along the outside ribs driving the geometric shape of the dome. The arch centre ribs 1 added on the outside constituted the strengthening of the shell. The distance of 5.25 m between the arch centres 1 was determined on the lower supporting ring. The latter was built on a flat plank lying on the wall. It was made up of four planks arranged vertically, which were bent into a ring having the diameter of the dome's projection. Shown in Fig. 4.22b, d is the construction of a rib 1 from arch centres over the meridional direction, allowing the building of a dome from quartering without an inside assembly scaffolding. The ribs driving the

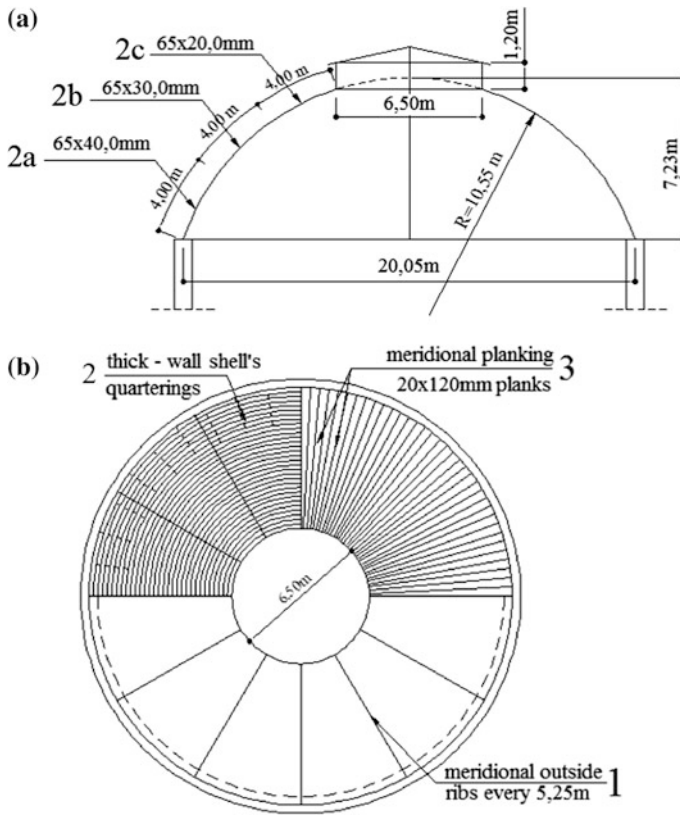


Fig. 4.21 Schematic diagram of a thick-wall dome with outside ribs [15, 16], **a** cross-section of the dome, **b** lay-out of outside ribs, quarterings and meridional planks

geometry of the dome 1 were made from two arch centres of a 50×200 mm section and strengthened on the outside with a flat nailed plank of a 40×100 mm section (Fig. 4.22 b). The connection of the ends of two vertical arch centres of one layer of the meridional rib 1 were fabricated in the middle of the length of an arch centre of the second layer. One half of the quarterings (between ribs 1 from arch centres) was strengthened on the outside with a meridional planking. Those were flat planks 3 (Fig. 4.23 b), laid on a shell from quartering between the outside ribs from arch centres, from the supporting ring to the central upper ring. The planks 3 of a 20×120 mm section were connected with the shell using 100 mm long nails of a 4.0 mm diameter. The coating from metal sheet on the dome's outside was laid on and fastened to the planks 3.

For the better explanation of the construction of the dome its computer visualizations were made, as shown in Fig. 4.23.

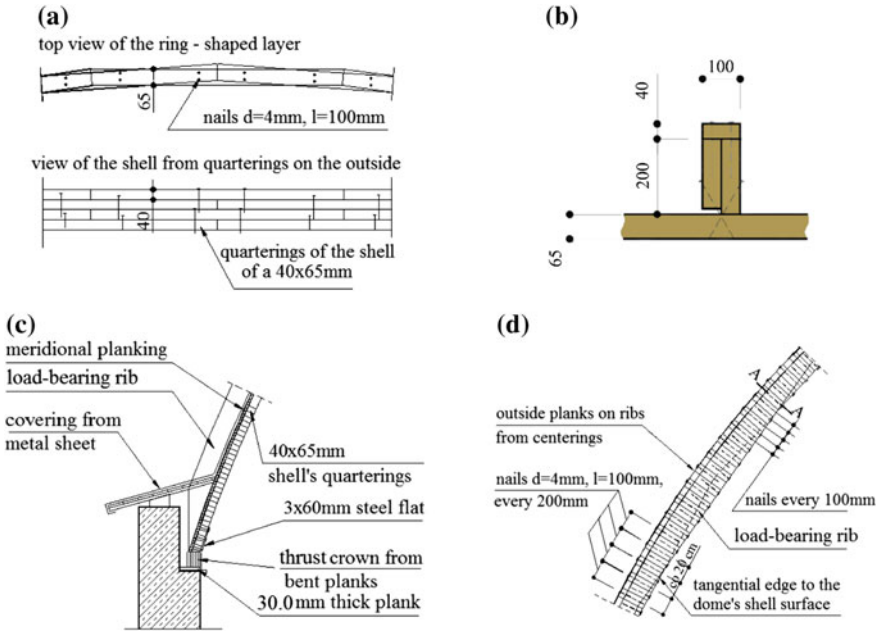


Fig. 4.22 Thick-wall dome with outside ribs [16], **a** arrangement of the shell's quarterings 2, **b** section of an outside rib 1, **c** supporting crown, **d** structure of an outside rib 1

The centring arches 1 increased the load capacity of the shell in the meridional direction. The shell quarterings of the ring-shaped layer assumed the circumferential forces in the dome. The outside centring arches 1 and the meridional planking 3 stabilized the shell from quarterings 2, reducing the dome's distortions due to the drying and swelling of wood. It is worth noticing that the solution shown on the visualization protects the dome against moistening, allows the drying of wood flooded with precipitation water, e.g. due to the wear of the covering from metal sheet.

Another impressive example of a thick-wall dome is the dome of the circular projection's diameter of $L = 60.0$ m, described by the engineer Kashkarov K. P in his paper [15] (1937). Inserted in Fig. 4.24a is the section, in Fig. 4.24b the projection, and in Fig. 4.24c–e the details of the construction, in Fig. 4.24f, g the description and the visualization of the structure developed on the basis of [14]. In the solution of the dome of a 60.0 m diameter all the building principles as discussed in the previous example of the dome of a 20.05 m diameter have been maintained. The difference consists in the introduction of ribs 1 driving the dome's geometry in an expanded form—shutterings, having bipolar coordinates (Fig. 4.24c), instead of the arch centre ribs of de l'Orme following the example of the dome shown in the visualization 4.23.

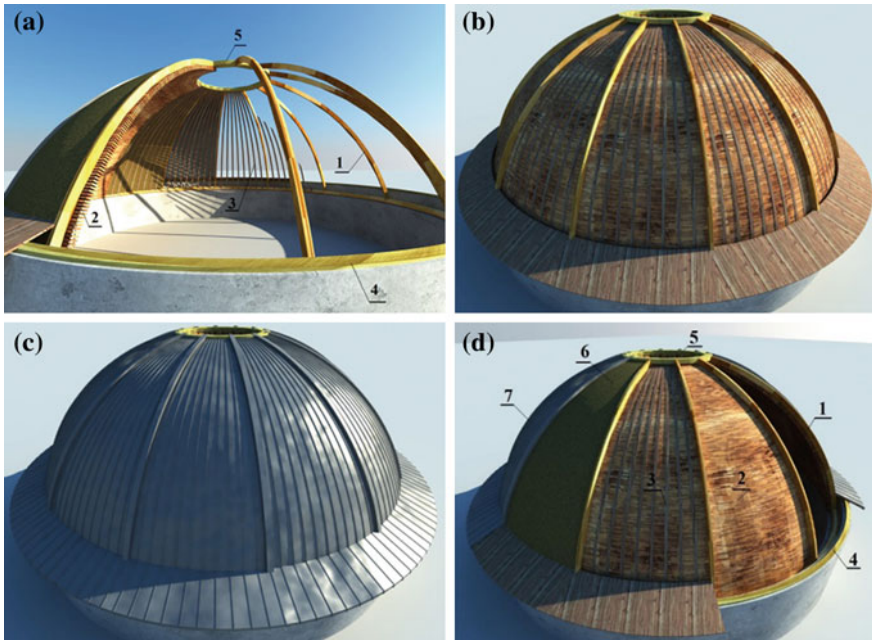


Fig. 4.23 Computer visualization of a thick-wall dome from quarterings with outside driving ribs from arch centres according to [16], **a** section with the view of the dome's inside, **b** shell from quarterings, load-bearing ribs and intermediate ribs, **c** covering from metal sheet, **d** view of dome's elements in successive layers: 1—outside arch centre ribs, driving on the outside the shape of the dome's sphere built from quarterings, 2—shell from quarterings, 3—meridional planking from planks arranged flat on the shell, 4—lower ring from bent planks, anchored to the supporting reinforced concrete ring, 5—upper ring from arch centres, 6—suggesting warming of the dome on the outside, 7—covering from metal sheet

In the dome of a 60.0 m diameter twenty main meridional ribs of bipolar coordinates were used, circa 30.60 m long, of the I-section and of the highest diameter of the section $h = 60.0$ cm, in the middle of its length. The main meridional ribs were disposed on the lower thrust ring in a spacing of 9.42 m. They were connected on the central upper ring every 94.3 cm.

The lower and upper chord of the rib 1 was adopted from 6 cm \times 6 cm quarterings, the web from a 5 mm thick plywood. The ribs 1 were designed from 3.60 m long segments and assembled during the construction on the outside of the shell 2, as it was erected. The assembly of the ribs 1 was conducted from the bottom ring up to the top ring of the dome.

Beside twenty main meridional ribs, sixty flat intermediate ribs were used, three ribs each between the main ribs, also in the meridional direction. The meridional board planking between the ribs strengthens on the outside the thick-wall shell from planks. The distance between the intermediate ribs, as measured over the lower thrust ring was adopted to be 2.35 m. The meridional planking 3 was built from

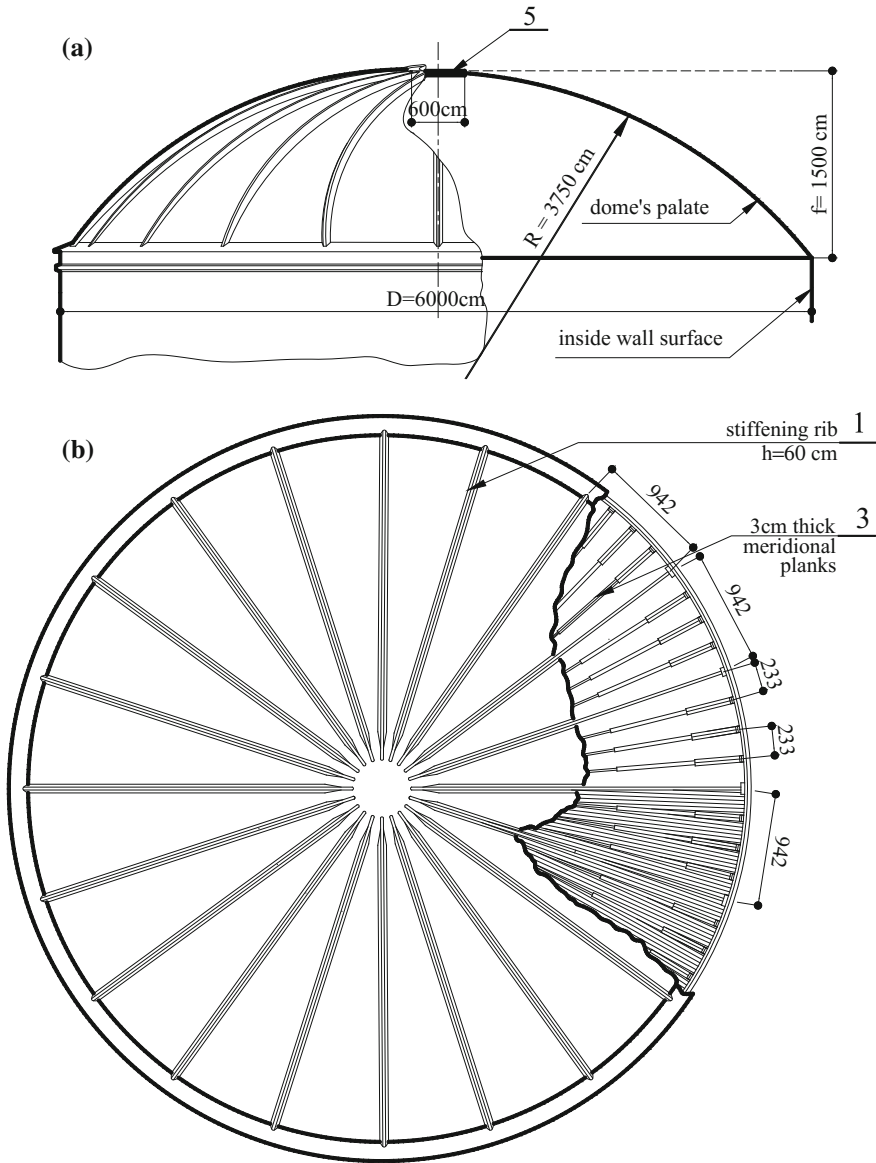


Fig. 4.24 Structure of a thick-wall dome of the projection's dimension $L = 60.0\text{ m}$ according to [14], **a** section of the dome, **b** projection of the dome, **c** view of the outside meridional rib, **d** scheme of the lay-out of the main ribs and the meridional outside planking on the thick-wall shell of the dome, **e** section of the shell and of the ribs, **f** reconstructed arrangement of the outside ribs, **g** view of the thick-wall shell, the meridional ribs and the meridional planking

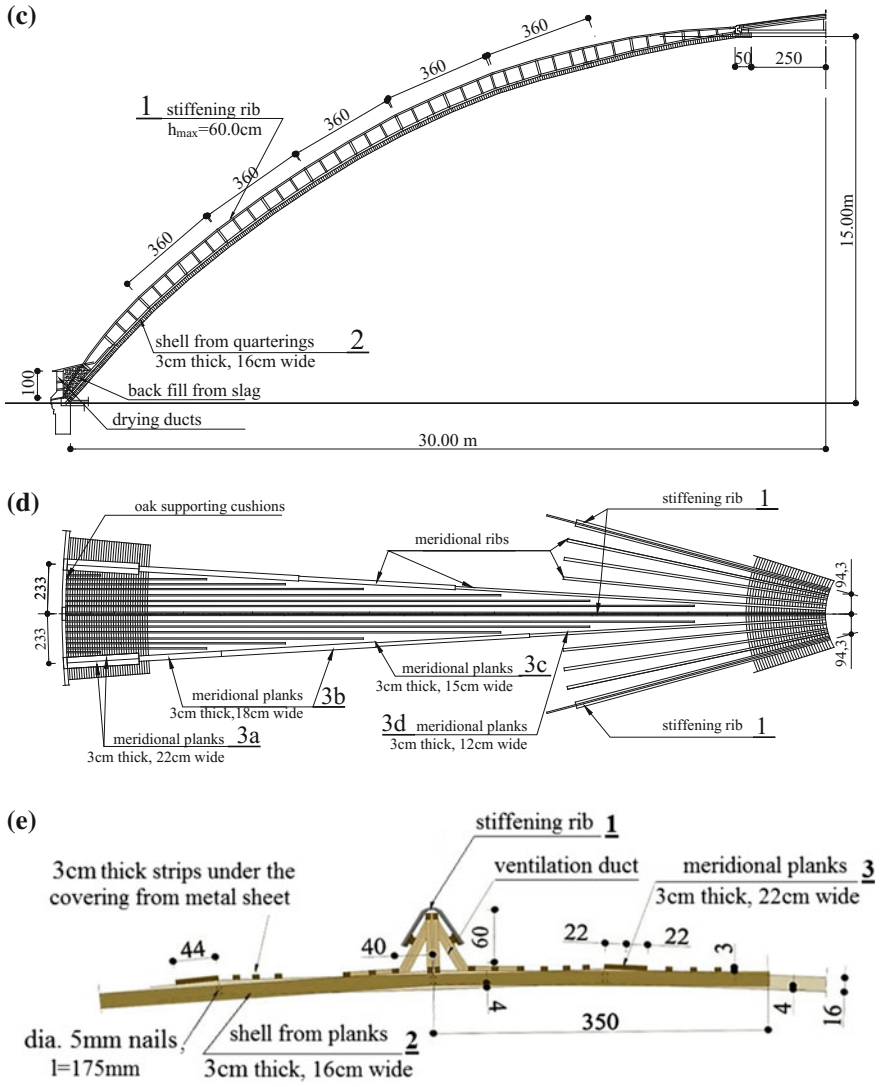


Fig. 4.24 (continued)

3.0 cm thick planks of a various width: the highest width 3×22.0 cm at the lower ring, in the central zone 3×18.0 cm, in the next one 3×15.0 cm, and at the top ring 3×12.0 cm.

The thick-wall shell 2 was arranged from 3.0 cm thick and 16.0 cm wide planks (Fig. 4.24c). The position of each arranged plank of the ring-shaped layer was controlled from the middle of the dome’s projection according to the scheme as in Fig. 4.19. The size of the radius was changed for each layer of the shell form

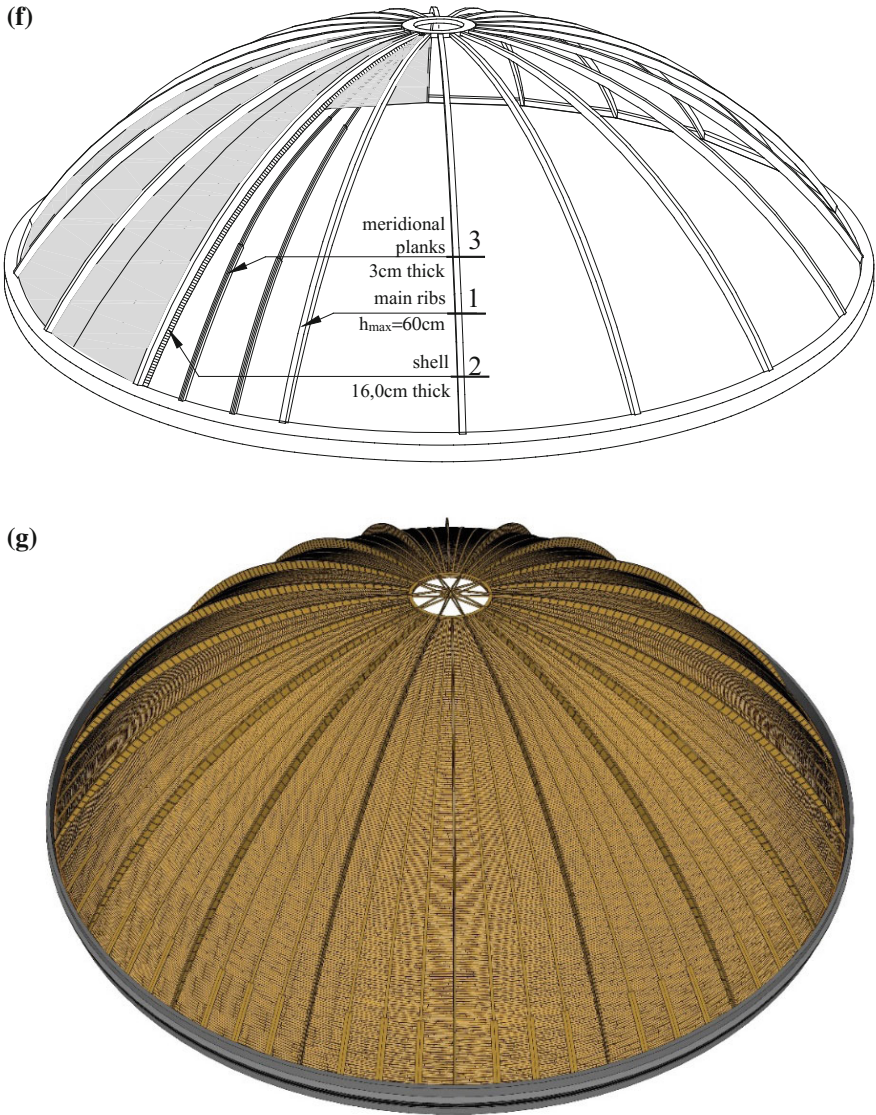


Fig. 4.24 (continued)

planks. The ventilation of the floor and of the ribs was made along the meridional ribs. The detail of the ventilation solution of the main meridional rib is shown in Fig. 4.24c, e. The natural exchange of air via ducts on both the sides of the rib 1 ensured the maintenance of a low moisture content and the drying of the construction impeding the development of biological corrosion.

4.7 Conclusions

The passage from wooden logs as elements to create thick-wall, crown-shaped dome-like coverings, as described in this chapter, to the small-dimensional quarterings joined with nails allowed to build domes on the plan of a circle. Their strengthening on the outside with de l'Orme's arch centre ribs made it possible to erect thick-wall shells of a diameter of the lower thrust ring of 20.05 m up to 60.0 m. The use of outside, stiffening meridional ribs as well as of the meridional planking relieved the inside utility space from the protruding elements of the construction.

The building of a shell with outside ribs did not require the use of a separate central scaffolding.

The thick-wall domes were an important experience on the way of the evolution of the construction of domes from solid wood.

The main advantages of the thick-wall dome are as follows:

1. possibility to build the dome without a central supporting scaffolding,
2. possibility to use low-grade wood for the construction of the shell, even planks of a worse quality,
3. good thermal insulation of the shell,
4. increase of the fire resistance of the facility owing to the minimum inside surface,
5. the slenderness of the shells of such domes between the driving ribs and the flat intermediate ribs, as measured using the ratio g/l_1 , was 8 up to 15. The slenderness of the shell jointly with plank susceptible ribs R/g was 123–197, where R —radius of the shell, g —thickness of the shell.

An enormous importance was attached to the ventilation of ribs and the covering of thick-wall domes. Ventilation ducts from planks were made along the outside arches, which fostered the drying of wood as well as influenced the elimination of the distortions of the shell due to the change in the moisture content of dome-creating elements. The continuous air replacement increase the durability of the facility and the maintenance of the moisture content below 18% impeded the growth of biological corrosion.

As shown in the chart—Fig. 4.25 according to [16], the moisture content of wood changes depending on the ambient temperature and the moisture content. For instance, the equivalent moisture content of wood is 15%, if the relative humidity of air totals 75%, and the temperature circa 20 °C. In his paper [18] (2003), Kozakiewicz P. emphasizes that the moisture content of wood is very essential in the protection against biological corrosion. The majority of technical, biological pests of wood has no capacity to infringe dried or very wet wood.

By convention, there is a distinction between the dry protective state in which the moisture content of wood does not exceed 18–20% and the wet protective state in which this moisture content is higher than 80%. It also results from the foregoing statement that the moisture content within the range of 20–80% contributes most to

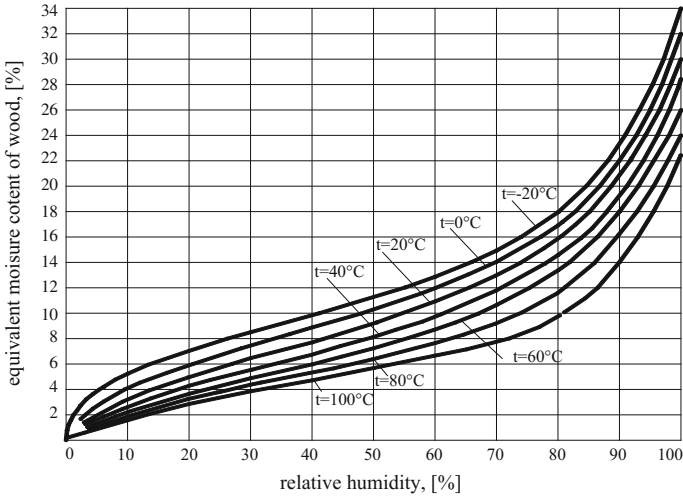


Fig. 4.25 Impact of the temperature on the equivalent moisture content of wood (RH) according to [16]

the destruction of wood. The shaping of a wooden construction, with the possibility to carry away the moisture content, increases the durability of the facility.

As shown in Fig. 4.26, the processes of shrinkage and expansion, dependent on the level of moisture content, influence the maintenance of the shape of the partition wall.

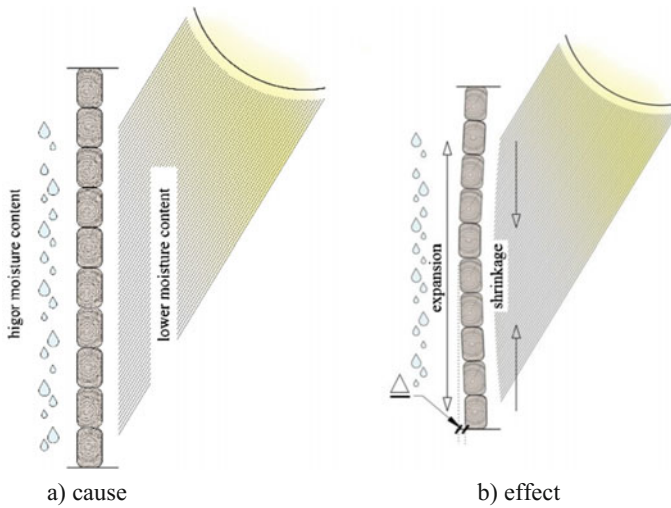


Fig. 4.26 Interference of the environment of a various moisture content with the partition wall from wood, Δ—horizontal distortion of the wall

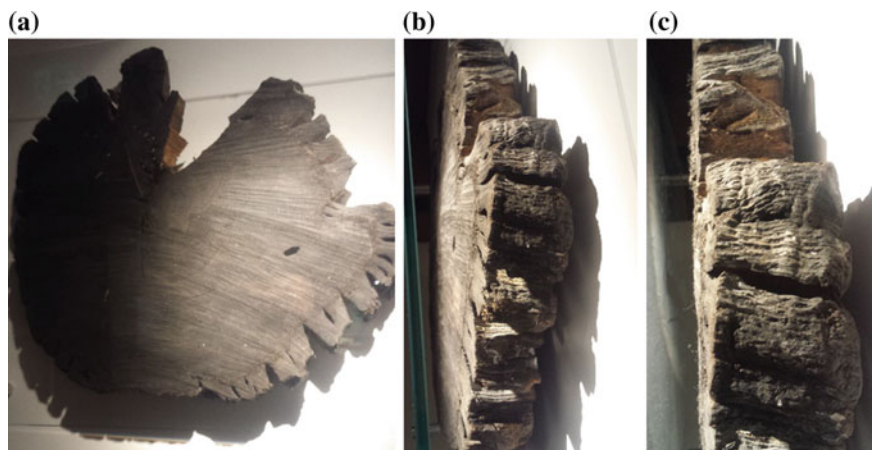


Fig. 4.27 View of the oak wood fragment retrieved from the Baltic Sea exposed in Internationales Maritime Museum in Hamburg, whose age has been estimated to be 8000 years, **a** view of the cross-section, **b**, **c** side view in close-up. Photograph by the author, 2017

A confirmation of this fact are the well-preserved wooden objects found in the Egyptian tombs as well as tree fragments retrieved from the sea.

A good illustration of the wood durability in a wet environment (wet protective state) are wood fragments retrieved from water. In the International Maritime Museum in Hamburg (*Internationales Maritimes Museum Hamburg, Hafen City*) a wood fragment from an oak wood log of a ca. 6.0 m length, retrieved from the Baltic Sea, from a depth of ca. 8.0 m are shown. The testing on the presence of the carbon isotope ^{14}C has demonstrated that the oak wood log is ca. 8000 years old. This is the oldest, preserved and described element from wood (Fig. 4.27).

References

1. Witruwiusz *O architekturze ksiąg dziesięć*, PWN, Warszawa 1956.
2. Widera B. *Dalsze losy radzieckiego konstrukttywizmu*, Wiadomości Konserwatorskie 14/2003, s. 5–10.
3. Obmiński T. *Budownictwo ogólne II Atlas* Wydanie i nakład Związku Studentów Inżynierii Politechniki Lwowskiej. Lwów 1925.
4. Obmiński T. *O cerkwiach drewnianych w Galicyi*. Sprawozdania komisji do badania historii sztuki w Polsce” t. IX, 1914, z. 3 i 4.
5. Brisch K., *Kuppeldach aus dem Aussichtsturm des Torre de las Damas (Damenturm)*, Foto: Bundesarchiv, Staatliche Museen zu Berlin.
6. Szczuko W. *Badania nośności zbrojonych belek drewnianych*. Zeszyty naukowe Nowosybirskiego Instytutu Inżynierjno-Budowlanego im. Kujbyszewa. Nr 624.072.2.011.6 1969 nr 2.
7. Taras J. *The Ukrainian Wooden Church Architecture. The illustrated dictionary*. National Academy of Sciences of Ukraine. The Ethnology Institute. Lviv 2006.

8. Brykowski R., *Drewniana architektura cerkiewna na koronnych ziemiach Rzeczypospolitej*. Towarzystwo Opieki nad Zbytkami Warszawa 1995.
9. www.greenhousedome.com.
10. Cyrankowski M., *Wpływ lakieru silikonowego na zwiększenie trwałości zabezpieczenia przeciwpożarowego drewna Fobosem M-2*. Annals of Warsaw Agricultural University SGGW, Forestry and Wood Technology No 55, Warsaw 2004.
11. Rydzewski P. *Cerkwie których nie ma - ziemia lubaczowska* www.roztocze.horyniec.grid.
12. Chmelnizkij S. *Zwischen Kuschanen Und Arabern. Die Architekturstilarten Mittelasiens im V.-VIII Jh. Ein Rückblick in die Kulturgeschichte der Sowjetunion*. Felgentreff & Goebel & Co KG, Berlin, November 1989.
13. Fontain J. von, Hempel R. *Propyläen Kunstgeschichte die Kunst des China, Korea, Japan*, Berlin 1968 Deskription 241.
14. Sourdel - Thomine J. von Spuler B. *Propyläen Kunstgeschichte die Kunst des Islam*, II. 102a, 102b, Berlin 1973.
15. Kaszkarow K., P. *Kopuły* Sprawocznik projektirowszczyka promyszlennych sooruzienij. Dieriewannyje konstrukciji. Kuzniecowa G. F. Głównaja redakcija stroitielnoj literatury. Moskwa-Leningrad 1937.
16. Karlsen G. G., Bolszakow W.W., Kagan M. E., Świencicki G., *Kurs dieriewiannykh konstrukcij* cz. I i II, G. I. C. L. Moskwa, Leningrad 1943.
17. Jean-Denis Godet *Atlas drewna*, Multico, Oficyna Wydawnicza, Warszawa 2008.
18. Kozakiewicz P. *Fizyka drewna w teorii i w zadaniach* Wydawnictwo SGGW Warszawa 2003.

Chapter 5

Ribbed Domes

5.1 Introduction

The examples of ribbed domes designed by the eminent architects: Neumann B., Weinbrenner F., Moller G. are described in Chap. 3. They introduced to the Western-European building trade the load-bearing systems, still imitating the scaffoldings to build masonry vaults, but also such systems in which separated meridional and latitudinal load-bearing systems already appeared. The impact of the stiffness of the plank floor on the load capacity of the system was omitted considering it to be slight in comparison to the main structure of meridional ribs and latitudinal bracings.

Moller G. (Fig. 3.23), while using the arch centre known for centuries and eliminating the bar systems supporting it, designed in the middle of the 19th century the first modern, ribbed load-bearing system of a dome. By introducing the latitudinal stiffenings, he applied the division of the structure into meridians and lines of latitude. He proposed a legible structural system corresponding to the distribution of forces in the dome, also facilitating the static calculation of load-bearing elements.

5.2 Ribbed Domes Built in Switzerland and Germany

The G. Moller's idea was perfected in successive realizations of many facilities crowned with domes. Shown in Fig. 5.1 is a facility covered with a dome, built in Bern in 1914 for the World Food Products Exhibition. The dome's diameter as measured at the floor level totals 31.0 m. The meridional load-bearing arches were made as full-wall arches from planks. The dome was placed at the height of 22.0 m, on a wooden supporting crown backed on four arches (Fig. 5.1). Each arch starts the adjacent side bay of a 18.0 m span. The photograph of the construction from the paper [1] is shown in Fig. 5.1.



Fig. 5.1 Food products hall at the national exhibition in Bern in 1914 [1]

Figure 5.2 presents the structure of the dome of the hall in Geißweid near Singen made at the beginning of the 20th century using a light Kallenbach's structure.

In the structure presented in Fig. 5.2 the meridional load-bearing ribs were made from flat-arranged planks, glued into an I-section. The supporting piers of arches

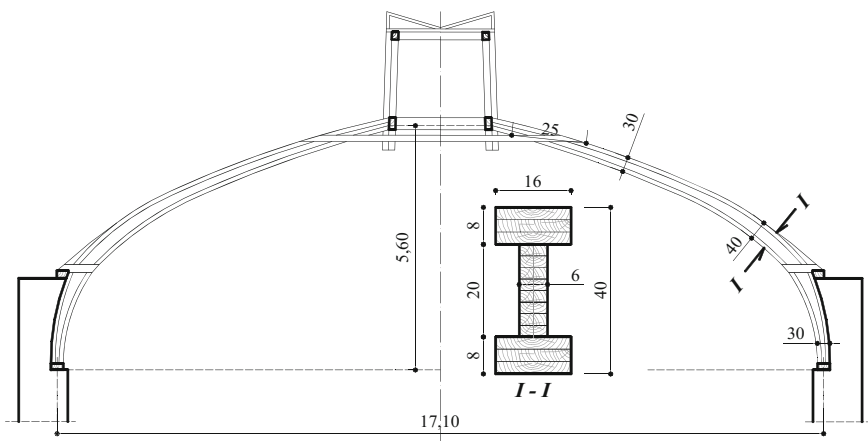


Fig. 5.2 Ribbed dome of a 17.10 m diameter according to the Kallenbach's system [1]

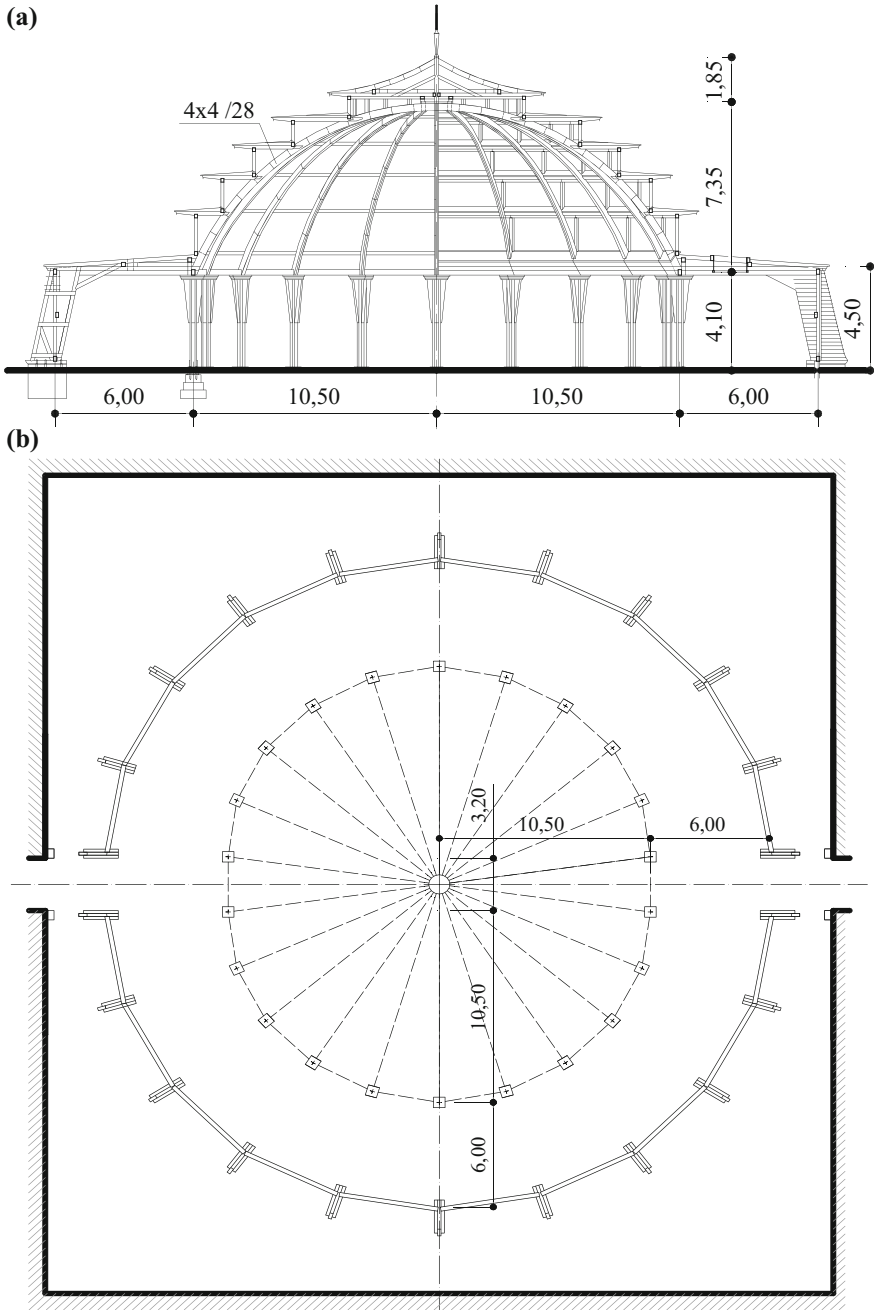


Fig. 5.3 Dome by Hatz F. from 1925 in Munich according to [1], **a** vertical section, **b** projection at the level of the ground floor

were made from concrete reinforced with steel bars. In the supporting section the wooden ribs were reinforced with laps from cast iron. In the static calculations the load of 160 kg/m^2 for own weight, that of snow and wind, including 60 kg/m^2 for own weight itself was assumed. **The characteristic feature of this structure is the use of load-bearing ribs from glued planks forming an I-section.**

The Mail Coaches Hall of an oval dome's horizontal projection is presented in Fig. 5.3. The facility was built by Franz Hatz in 1925 on the occasion of the German Communications Exhibition in Munich. On the ground storey of the building, at the height of 4.10 m (Fig. 5.3a), a dome was situated, having a ribbed structure and a horizontal elliptic projection. The diameters of the ellipse total 21.0 and 24.20 m, respectively, the height from the supporting ring to the upper plate that connects the meridional ribs is 7.35 m.

Twenty-two load-bearing ribs were based on the lower supporting crown made at the height of 4.10 m. At the height of 11.85 m the meridional ribs were connected using a ring-shaped plate from planks. In his paper [1], Kersten C. does not describe the structure of such a board. Boards from planks used as a stiff node, connecting the meridional ribs of ribbed domes, were made familiar from the description by the engineer Kashkarov K. P. in his paper [2] and discussed in Sect. 5.3 following the example of the dome in Baku of 1930.

The additional lighting system and the concentric rings of the casing visible in the section in Fig. 5.3a resemble the section of the Centennial Hall in Wroclaw described by Niemczyk E. in his paper [3] (1997).

5.2.1 Ribbed Domes Built in Russia

In the thirties of the 20th century, the largest domes from solid, and not glued laminated timber were built in Russia. Shown in Fig. 5.4 is the location of just two of them. To reach the paperwork of other facilities ended with a failure.

In 1930, a ribbed dome of the circus-theatre was built in Baku, having a projection's diameter of 67.0 m and a height of 27.0 m [1] (Fig. 5.5). The subtle structure of the dome was reconstructed on the basis of the paper [2], and shown in Fig. 5.6.

The author of the design project was the engineer Kashkarov K. P. The lower supporting ring was made at the height of the second floor of the building. The supporting ring taking over the dome's strutting was connected with the reinforced concrete structure of the ceiling above the 2nd floor. The main gate of the theatre's stage, shown in the section (Fig. 5.5a, h) infringes the symmetry of the dome, at the same time, it constitutes a framework that increases the stability of the dome. Meridional load-bearing arches A were eliminated over the length of the lock of the stage's portal, replacing them with a cylindrical structure based on that of the stage through the intermediary of shorter arches B. The transverse arches are based on shortened lattice arches B, transferring the reactions onto the columns of the stage's



Fig. 5.4 Location of the largest domes from solid wood built in Russia in the thirties of the 20th century

portal. The lay-out of main ribs A and B is shown in Fig. 5.5c. Two arches B are based on the columns of the stage's portal.

Twenty-one main arches A (Fig. 5.6a, b) were disposed along the lower ring every 8.09 m and connected in the key block using the central, multi-layer upper plate shown in Fig. 5.5f, g. The arches A have the form of an arch of bipolar coordinates. The maximum height of the section in the middle of the length of the main meridional arch totals 1.50 m, the width 30.0 cm. The supporting section of the arch has the dimensions of A 30 × 40 cm. The ratio of the maximum height ratio of the main rib $h = 1.50$ m to the dome's diameter $L = 67.0$ m is $\frac{1}{45}L$. The lower and upper chords of the section of the meridional load-bearing ribs A and B were made from 5.0 cm thick planks—the upper chord, from four thick planks—the lower chord from five planks (inside chord—Fig. 5.5i). On the whole, the upper chord was made of 20 × 30.0 cm dimensions, and the inside lower chord of 25 × 30.0 cm dimensions. Duplicated posts and crossheads of a 2 × 5 × 8 cm section were inserted between the layers of the chords.

The intermediate ribs were built from three 10 cm wide and 4.0 cm thick planks, which yielded the total height of the rib of 12.0 cm. The meridional intermediate ribs, required in building of the plank shell of the sheathing were disposed on the latitudinal nodes of the stiffening ribs shown in of the dome's projection 5.5f.

The meridional structure was stiffened horizontally with two latitudinal stiffening chords. The one being latitudinal with parallel chords connected with cross braces, the other having parallel chords with angle braces conducted to the section of the crossing with intermediate meridional ribs, called a brace chord. The view of a brace girder is shown in Fig. 6.13. The latitudinal girders: truss girders and brace girders were connected in nodes with load-bearing ribs. A covering was assembled to the latitudinal girders. The upper ring connecting the meridional ribs A and

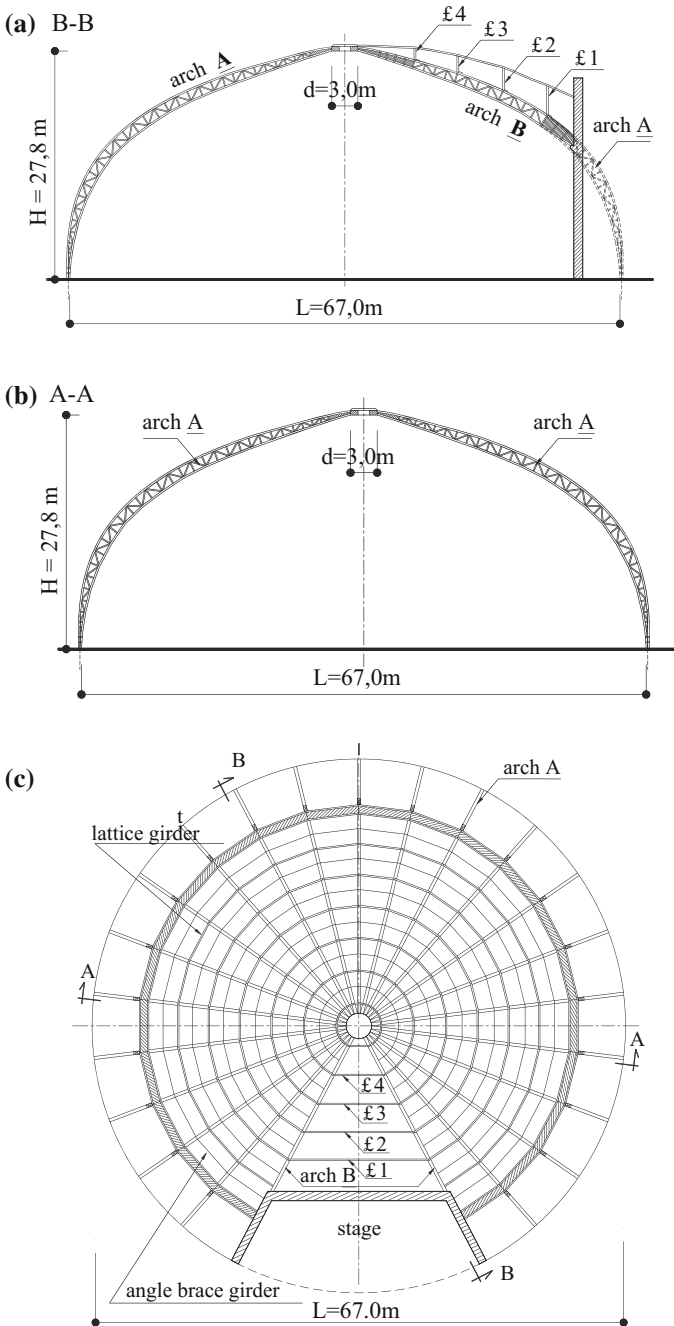


Fig. 5.5 Structure of the Baku dome according to [2], **a** section B-B with the view of meridional arches A and B, **b** section A-A, **c** projection of the dome's structure, **d** structure of the meridional load-bearing rib, **e** structure of the supporting node of the meridional load-bearing rib, **f** structure of the dome's upper plate connecting the meridional ribs, **g** section of the dome's upper ring, **h** view of the reconstructed dome, **i** visualization of the dome's main meridional arch A of a 67.0 m diameter

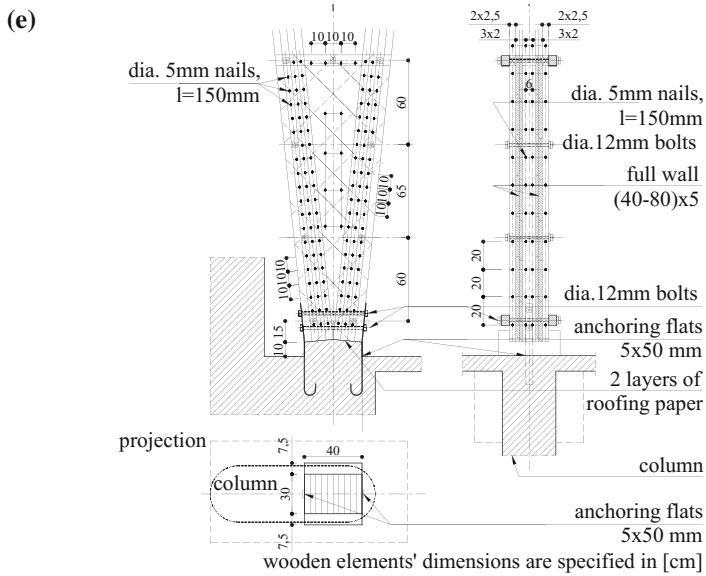
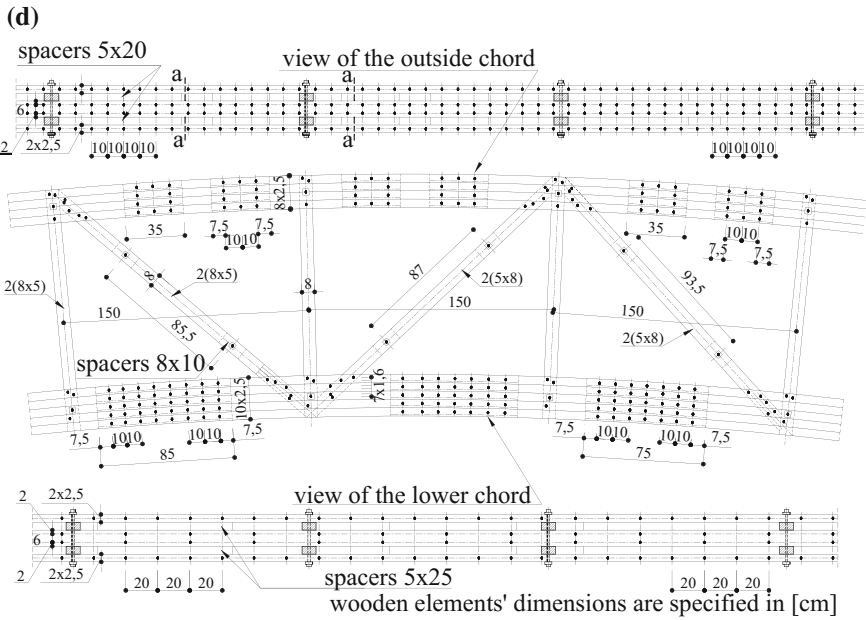


Fig. 5.5 (continued)

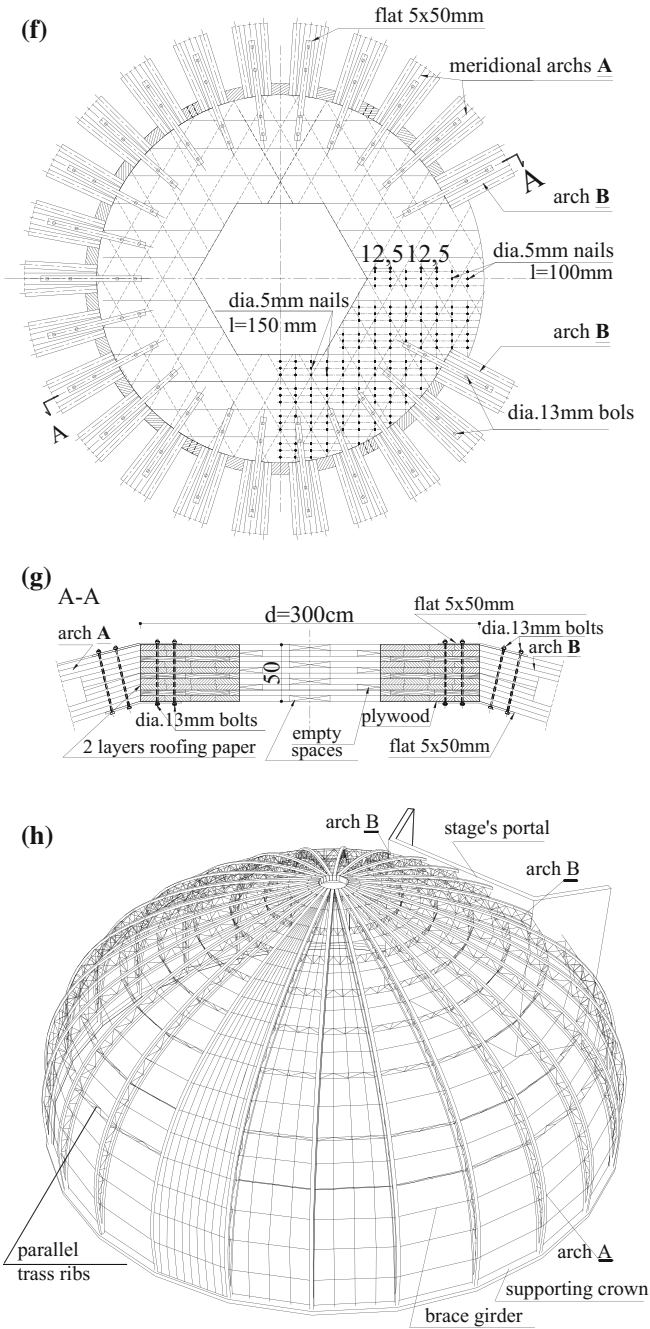


Fig. 5.5 (continued)

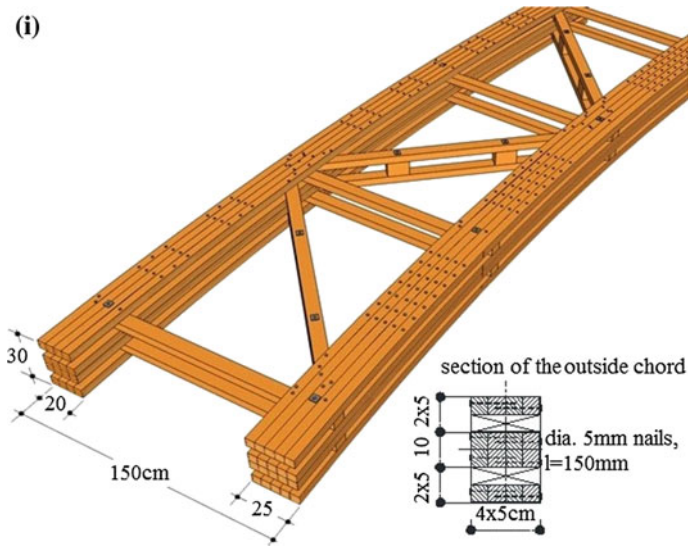


Fig. 5.5 (continued)

B was connected in form of a stiff disk of a 3.0 m diameter, made up of 10 layers of crossed 5.0 cm thick planks. The construction of the ring is shown in Fig. 5.5f, g. It is essential that in the plate of the upper ring empty spaces in various layers and directions have been left as ventilation openings ensuring the exchange of air and moisture on the dome's outside.

The roof sheathing was made from planks in several layers. 2.5 cm thick planks of the first layer were nailed on the outside of the meridional ribs and from below (on the dome's inside) onto the chords of 10 cm wide and 12 cm high latitudinal ribs. The chords of latitudinal ribs jointly with the covering formed a box panel. An inclined roof covering from 1.9 cm thick planks, arranged with an inclined chord over all the arches A, was nailed onto the outside layer of the covering from 2.5 cm thick planks. This is the first example described in the reference literature of the application of box panels from wood as a load-bearing partition constructed to transfer climatic loads.

To connect planks from which the dome's structure (Fig. 5.5) nails of a 5 mm diameter and 150.00 mm long were used. **The consumption of steel for fasteners as calculated per square metre of the dome's projection did not exceed 2.0 kg. Such low consumption of steel for fasteners is not encountered in the presently built wooden structures.** The largest steel fastener used in the node of the lattice construction of meridional ribs are steel bolts of a 12 mm diameter. The steel flats shown in Fig. 5.5d, e connecting the multi-layer upper plate with the meridional load-bearing ribs of the dome were laid on the wooden element. **The most laden supporting sections of bars were embraced with 5 mm thick, 5.0 cm wide metal sheet (uncut).**

An essential issue associated with the discussed domes from solid wood is the ventilation of the structure. Enormous importance was attached to the correct ventilation of elements from wood. Solutions of the exchange of air in the dome’s structure are specified in the description of the Baku dome included in [2]. The figures of the ventilation of meridional arches 5.6a and latitudinal arches 5.6b were compiled according to them. After a closer perusal it is visible that **ventilation ducts along meridians and lines of latitude were built from planks, in a position corresponding to the main ribs of the structure. The dome was covered on the outside with a network of ventilation ducts helping to maintain the thermal and moisture conditions favourable for wood.** Since the durability of the facility depended on the proper ventilation of all wooden elements, especially of the load-bearing structure. The solution of the ventilation of the load-bearing ribs of the Baku dome, built in the thirties of the 20th century is shown in Fig. 5.6.

The method of the drying ventilation of the main ribs of the Baku dome is worth propagation also in the contemporary wooden structures, not only of domes from wood.

In the thirties of the 20th century, steel entered into a broad application in the building trade. The new material was also eagerly used in wooden structures. One of the first examples of the application of steel in the wooden building is the structure of the Ivanovo dome.

The dome of the circus in Ivanovo, Russia, designed by the engineers Minofiev S., Lopatin B., [4] was built from solid wood in the years 1930–1931. The dome has a diameter of the projection of 50.0 m and the height from the floor to the key block of 24.80 m. On the basis of the information from the papers [2, 5, 6], the figures of the dome’s construction were reconstructed (Fig. 5.7) and its computer visualization was compiled (Fig. 5.8).

The dome was built from thirty-two ribs disposed along the meridians.

The assembly of the dome followed using a tower situated in the middle of the horizontal projection. In the building process of the dome in Ivanovo, the strengthening of the assembly tower with inclined posts was used (Fig. 5.7) in order to reduce the horizontal forces acting on the central tower. The assembly of main ribs followed pair-wise on the one and the other side of the tower. The one-sided assembly of more than one half-arch was not permitted.

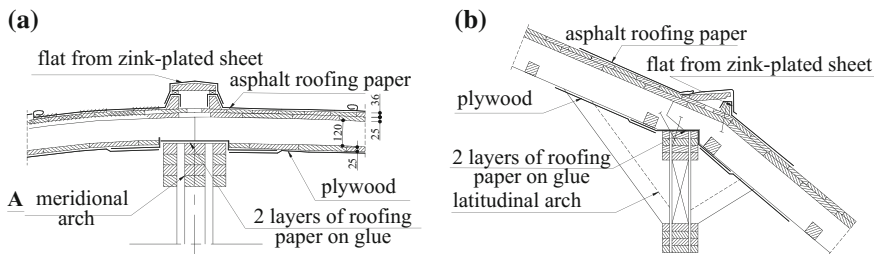


Fig. 5.6 Examples of the ventilation of load-bearing arches in the Baku dome according to [2], **a** ventilation of the main arch **A**, **b** drying opening on latitudinal girders

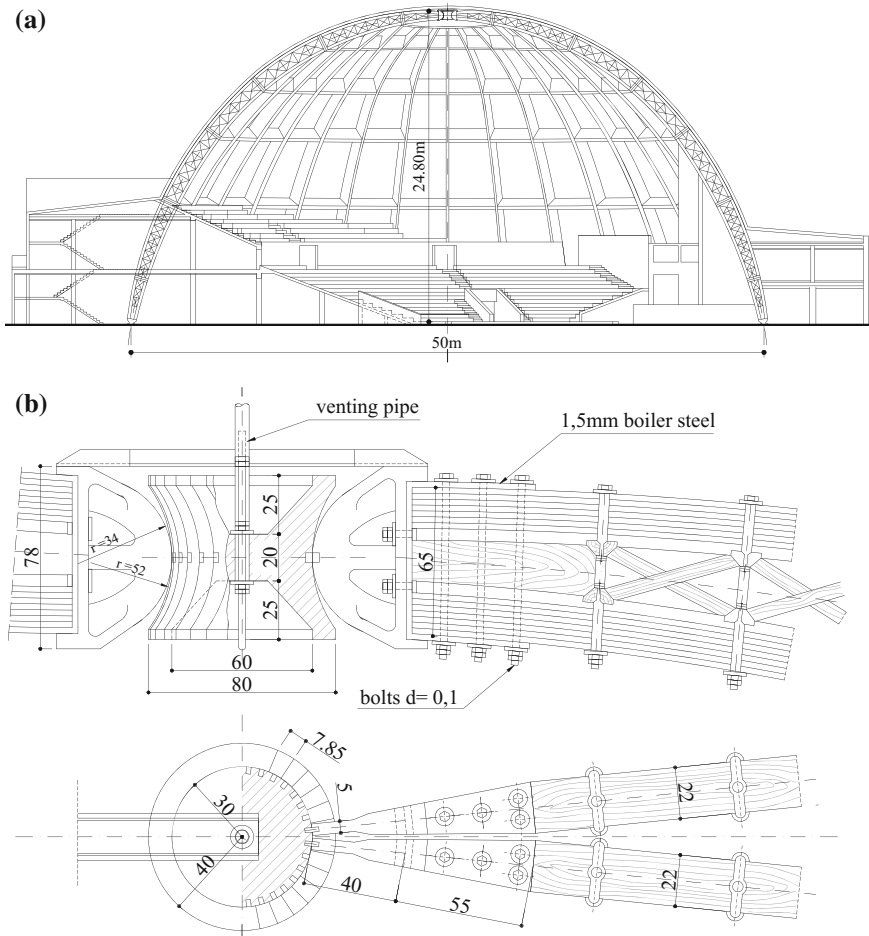


Fig. 5.7 The ribbed Ivanovo dome of a 50.0 m diameter [5, 6], **a** section of the dome, **b** upper steel node connecting 32 ribs of the dome, **c** supporting node of each rib, **d** fragment of the truss of the dome's rib, **e** node to connect cross braces with the chords in the truss of the dome's load-bearing rib

The number of main ribs was determined on the lower supporting crown by dividing the circumference of the dome's projection into circa 4.91 m long sections. The outside chords of bipolar meridional ribs were built from seven 25 mm thick and 220.0 mm wide planks. The planks of the chords were connected using steel clamps, twisting them with steel posts and connecting with wooden crossheads (Fig. 5.7b, d). The multi-layer outside chords of the lattice rib were connected using posts. Crossheads from quarterings as in Fig. 5.8 were built in the field between the posts.

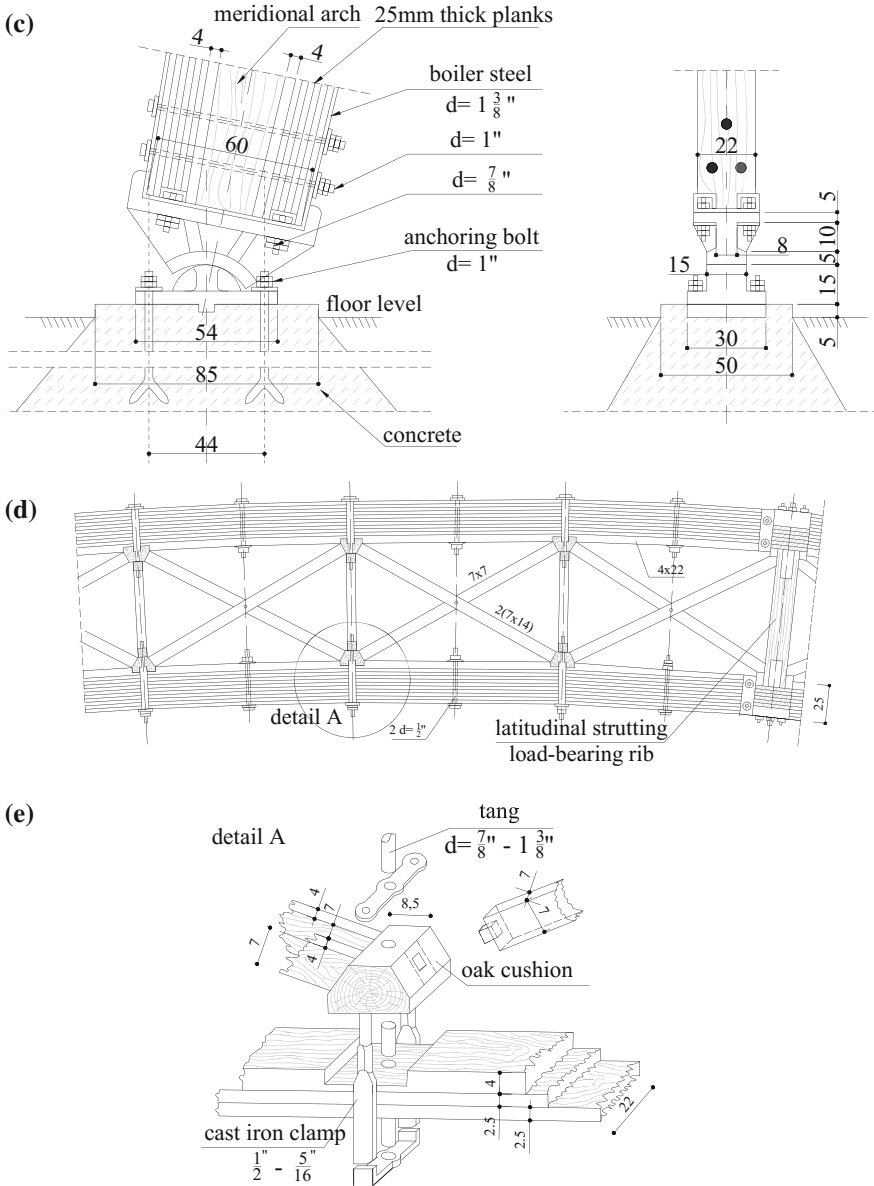


Fig. 5.7 (continued)

The main load-bearing ribs of the Ivanovo dome are trusses of a variable moment of inertia of the section. The maximum height of the section of the dome's meridional rib, in the middle of its length, totals 1.30 m, which in relation to the dome's diameter $L = 50.0$ m yields $\frac{1}{38}L$.

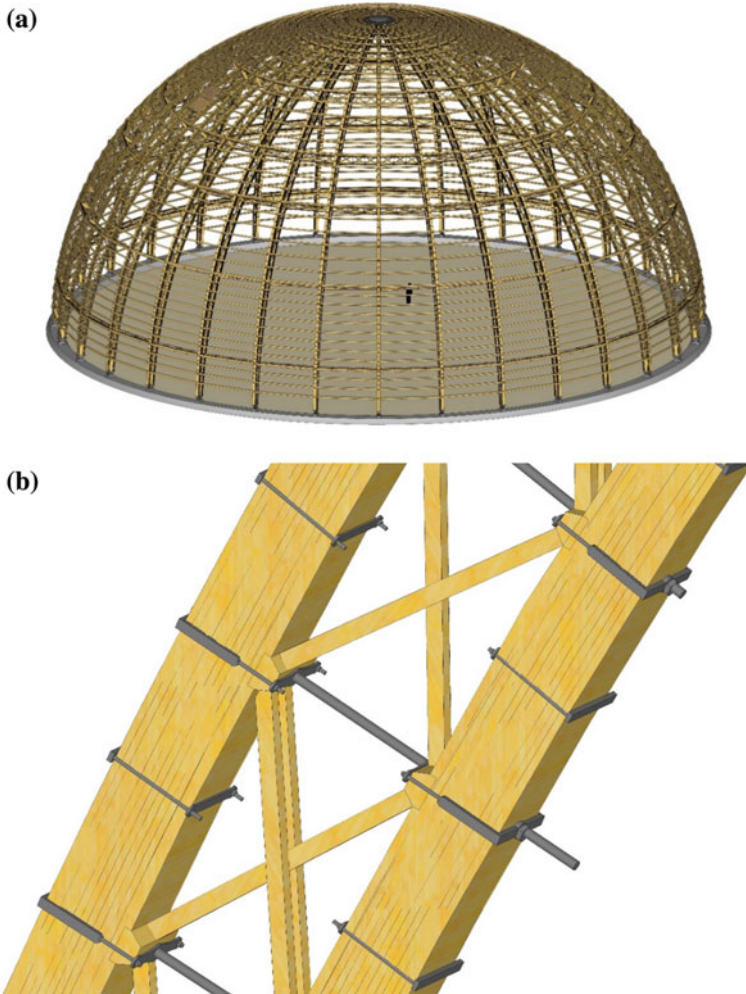


Fig. 5.8 Visualization of the Ivanovo dome according to [6], **a** visualization of the structure, **b** visualization of the structure of ribs

The meridional truss ribs were stiffened in the horizontal line with five latitudinal struttings in form of angle brace girders of parallel chords shown in Fig. 5.8a. Depending on the direction of the occurring deformations of main meridional ribs, the latitudinal struttings operated on compression or extension. Meridional intermediate ribs rested on the outside nodes of angle brace girders, three ribs each between the main meridional ribs.

In the highest node of the dome a steel hinge having the shape of a spool was mounted, in which all meridional load-bearing ribs concurred—Figs. 5.7b and 5.10a. The ends of the ribs connected in the upper hinge were strengthened under a

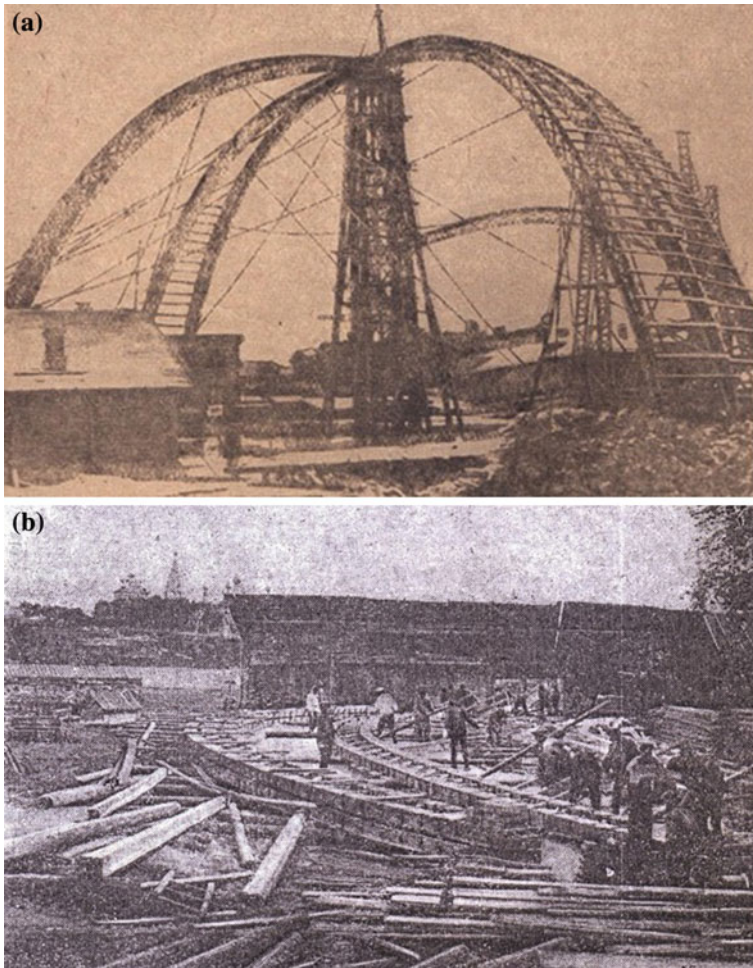


Fig. 5.9 Photographs of the building of the Ivanovo circus dome, **a** pair-wise assembly of the dome's load-bearing arches, [5], **b** construction yard

local pressure with steel clamps. The assembly of the highest node of the dome followed on tower scaffoldings having a vertical axis (Fig. 5.9a). The lower supports of arches were fabricated in form of cast iron hinges (Fig. 5.7c).

In Figs. 5.7, 5.8, 5.10 attention should be drawn to the application method of steel elements in the nodes of the dome. **The characteristic feature of this structure is the shape of nodes from steel and the connection of wood using steel elements. None of the steel elements was pasted in the wooden section.** Steel was used only in sections having the highest local pressure or as clamps introducing the mechanical pressure to increase the load capacity of the wooden element. In the key block and on the lower supports cast iron end pieces embraced

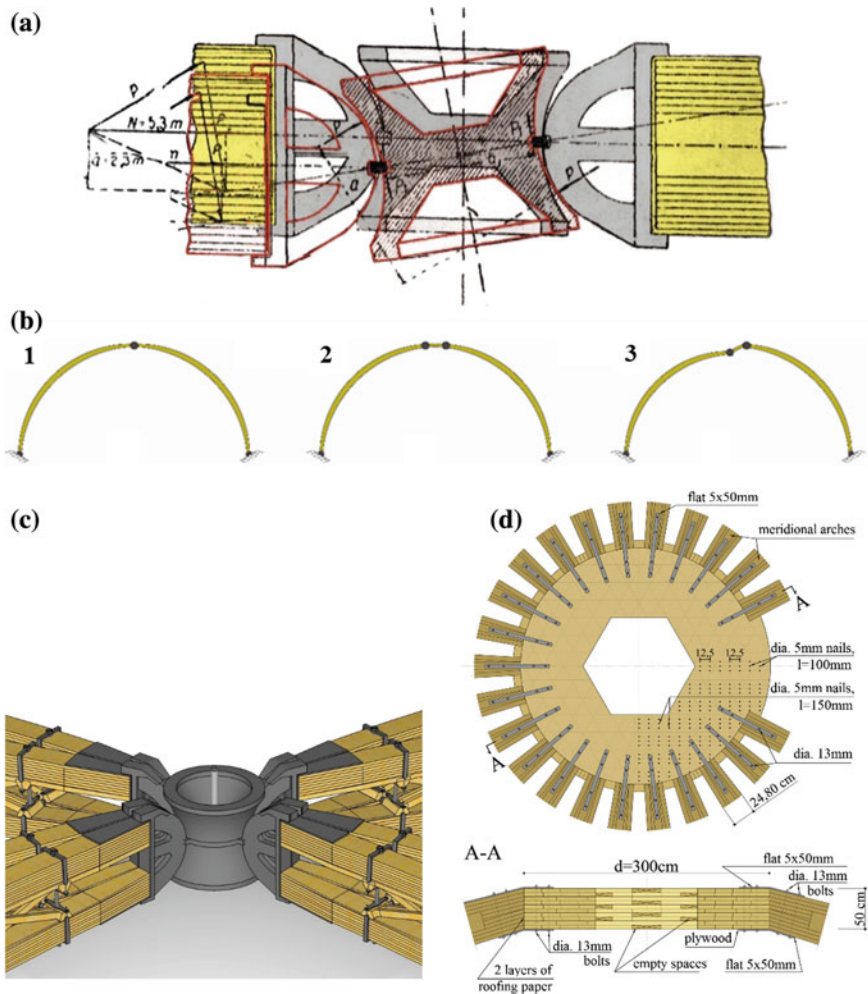


Fig. 5.10 Comparison of the nodes of the domes in Baku and Ivanovo, **a** loss of stability of the upper node of the Ivanovo dome [5], **b** static arrangement of the arches of the Ivanovo dome: 1—arrangement designed, 2—arrangement made, 3—arrangement translocated, **c** steel hinge node not resistant to twist in the Ivanovo dome, **d** upper stiff node from a multi-layer plate from planks made in the Baku dome

the extreme sections of wooden load-bearing ribs. **By using steel, an outside circumferential reinforcement of the section was introduced, protecting wood against delamination.** The historical description of steel included in Fig. 5.7b, ‘boiler steel’ [6], reminds that to protect extreme sections of wooden bars steel of an increased load capacity was used (also resistant to high temperature), used at that time (in the thirties of the 20th century) to build steam-operated industrial boilers. In the calculations of ribs the mating of the plank sheathing with ribs was not

considered. However, in the realization, the plank sheathing was coupled with ribs in order to increase the stiffness of the dome. It was recommended to use the two-layer latitudinal sheathings on which, additionally, the planks of the third layer were nailed in form of a herring-bone pattern at the angle of 45° and 135° in relation to the latitudinal layer.

During the building of the Ivanovo dome—Fig. 5.9, there occurred a failure [5], consisting in the twist of the upper cast iron node, laid on a sand cushion placed on the central assembly tower. The scheme of the node's twist is shown in Fig. 5.10a, b. This happened after the assembly of arches and after the installation of 50% of the sheathing from planks. The arches curved in the horizontal direction. After a discussion of the problem with Professor Karlsen, a decision was taken to stiffen the arches with meridional trusses and to change the structure of the sheathing from planks. In the design project the sheathing from planks was supposed to be fabricated as a two-layer direct sheathing on meridional arches.

In order to stiffen the dome a two-layer sheathing [5] having a nature of a panel made on the outside and inside chord of meridional arches was introduced. The sheathing was made in the following way: on the arches, on the outside, planks with notches were laid latitudinally, from the centre another latitudinal layer was laid. A two-layer shell was formed, stiffening and, at the same time, effectively ventilating the wooden construction. On the outside, the metal sheet covering of the dome was made.

Upon completion of all the works, the central assembly scaffolding was removed. The vertical translocation of the central upper node was measured. It totalled 25.0 mm.

Conclusions related to the failure of the Ivanovo structure, related to the building of the central upper ring, were drawn. They were used in the structure of the Baku dome, as shown in Fig. 5.6. It consisted in the fabrication of a stiff node in form of a plate from 5.0 cm thick planks, laid in ten layers.

The paper [5] specifies the weight of the materials used to produce dome's load-bearing elements. **According to the compilation attached to [5], 5.45 m³ of wood and 869.5 kg of steel and steel fasteners per meridional load-bearing arch were used. When calculated per m² of the dome's horizontal projection, this yields the wood consumption of circa 40.0 kg/m² and steel consumption of circa 15.0 kg/m². Such minimum consumption of materials does not occur in the contemporary realization of domes from layer-wise glued laminated timber.**

5.3 Conclusions

The structure of ribbed domes from solid wood constitutes an essential stage in the development of wooden domes, falling on the thirties of the 20th century. In the calculations of the structures of such domes the coupling of load-bearing ribs with the plank floor or the box panels of the covering was not considered. In reality, the

planks of the covering connected with ribs participated in the spatial operation of the dome, essentially relieving the load-bearing ribs [5]. Kashkarov K. P. specifies in his paper [2] that the own weight of ribbed domes of a span of 20.0–50.0 m totals 50–75 kg per m² of the dome's horizontal projection, without the roofing material and thermal insulation. **An essential element of the structure of the Baku dome, as described by the engineer Kashkarov K. P., is the use of low-dimension fasteners and lack of steel nodes, like for instance in the Ivanovo dome.**

In the thirties of the 20th century, in the domes of the projection's diameter of 50.0 m and more metres, builders started to introduce steel elements, mainly in the supporting zones of the dome's meridional ribs. However, steel was used sparingly. The consumption of steel in the papers by Kaszkarow [2] and Łopatin [5] is minimal and not encountered in the structures from glued laminated timber—Table 14.1. Attention should be drawn to the shape of steel elements used in the nodes of the domes in Baku and Ivanovo: Figs. 5.5, 5.7, 5.8, 5.10. **Cast iron fittings embrace bars from planks, not destroying by the intersection wood fibres and the matrix of the domes' load-bearing elements.**

The mechanical pressure applied increased the load capacity of bars from planks. In this way the wooden load-bearing bars were protected against the delamination of fibres.

The Baku dome, of a 67.0 m circular projection's diameter, closed the development of domes from solid wood built without using steel nodes.

References

1. Kersten C., *Freitragende Holzbauten*, Verlag von Julius Springer, Berlin 1926.
2. Kaszkarow K., P. *Kopuly Sprawocznik projektirowszczyka promyszlennych sooruzienij. Dieriewannyje konstrukcji.* Kuzniecowa G. F. Głównaja redakcija stroitielnoj literatury. Moskwa-Leningrad 1937.
3. Niemczyk E. *Die Jahrhunderthalle in Breslau – ein Triumph des Eisenbetonbaus* Beiträge zur Geschichte des Bauingenieurwesens 8, Technische Universität München, 1997.
4. Warth Otto *Die Konstruktionen in Holz* Gedruckt von A. Th. Engelhardt, Leipzig 1900.
5. Łopatin B. *Postroika Zdanija Goscirka w Gorodie Iwanowo.* Dieriewo w Stroitielitelstwie, Stroitielnaja Promyszlennost, nr 1, s. 46–50, styczeń Moskwa 1934.
6. Karlsen G. G., Bolszakow W. W., Kagan M. E., Świencicki G., *Kurs dieriewiannykh konstrukcij cz. I i II*, G. I. C. L. Moskwa, Leningrad 1943.

Chapter 6

Shell Domes

6.1 Introduction

The striving for the use in the operation of dome structures of all the elements creating the dome: ribs and the plank shell led to the creation of a dome having the form of a thin-wall rotating shell. **Thin-wall domes were called such domes in which of an essential importance in the load capacity of the structure is the shell from planks nailed onto the meridionally laid assembly ribs.** The dome's geometry was formed using assembly ribs, creating at the same time a technological scaffolding of the plank shell. The use of meridional technological ribs also allowed to maintain the computational, mathematical shape of the shell. The ribs, upon consolidation with the shell from several layers of planks, substantially increased the load capacity of the complex structure of the dome.

Thin-wall shells from wood were built from several layers of planks connected using nails. The system of planks of the sheathing and the structure of plank ribs was differentiated depending on the required dome's diameter. Thin-wall, complex spatial structures were built in which all layers of the shell and the ribs participated in the transfer of loads. The thin-wall domes are characterized by the shape nearing a sphere, the spatial stiffness, a favourable indicator of the material consumption for the construction in relation to the surface covered by it, as well the minimum surface of the casing in relation to the projection's area. The minimalist form of shell domes was also favourable in relation to the load from wind. Shell domes of a tiny eminence were built in Central and Northern Russia over gas tanks, at a height of 33.0 m above the ground level in regions exposed to strong and frequent winds [1] (1937).

In the axially symmetrical thin-wall domes from wood discussed in this chapter the ratio of the rise of arch (height) f to the diameter of the base's circle according to the proportion: $\frac{f}{L} = \frac{1}{4} \div \frac{1}{6}$ was adopted.

Depending on the required strength of the shell and ribs, thin-wall domes, axially symmetrical, were built in four systems. A designation was adopted for each system in this publication, emphasizing the essential load-bearing element of the system. Depending on the features of the complex section,¹ thin-wall domes were split into:

- smooth shell domes, on ribs from one, flat plank,
- smooth shell domes, prestressed with steel tie rods,
- ribbed domes on layer ribs (from three planks),
- ribbed shell domes, on ribs having the form of bipolar girders.

6.2 Shell, Smooth Domes

The three-layer thin wall plank shell was built on meridional ribs from a single plank being tangential to the sphere. The lower sections of ribs were connected using steel clamps with the lower supporting ring. The upper sections of ribs were built into central rings, made from several layers of arch centres. Meridional arches in the domes of a projection's diameter up to 20.0 m were made from one plank.

Shown in Fig. 6.1 is the assembly method of the system 1 thin-wall domes. The meridional plank ribs 2' were laid along the radius. The ribs were based on the lower ring 1 and bent to the shape of the plank shell into the position 2.

The conical profile of the ribs 2' in Fig. 6.1a illustrates the initial position of assembly ribs from planks which, upon bending downwards, adopt the shape of the circular section's arc.

The bent ribs 2 were connected by means of the central rings 6, 7, 8 (Fig. 6.1c), supported on a light scaffolding from arch centres. Upon fastening the ribs 2 in the lower and upper ring, the rib was undergoing a prestressing.

The ribs 2 shown in Fig. 6.1b are assembly planks and were used in order to obtain the proper geometry of the dome.

The even number of meridional ribs 2 from 3.0 cm thick and 12.0 cm wide planks was adopted. The number of ribs was calculated according to the lower supporting crown, adopting a spacing of circa 0.80 m to 1.5 m between them. The lower supporting ring 1 was built from three beams laid vertically—Fig. 6.2c. Meridional ribs 2 were disposed on the lower beam of the crown 1. In order to prevent the shift of ribs 2, spacing beams were arranged between them, that is the spacing beam, of the supporting crown 1,—Fig. 6.2c. The lower and the central beam of the ring 1 were used to fasten and to adjust the spacing of plank ribs 2 of the dome. The task of the upper beam of the ring 1 was to hold down from above the ribs 2, as well as to prevent the tearing-off of ribs from the supporting ring during the formation of the dome's shape.

¹The designation “structure of the rib consolidated by the shell” defines the structure type and not the connection type.

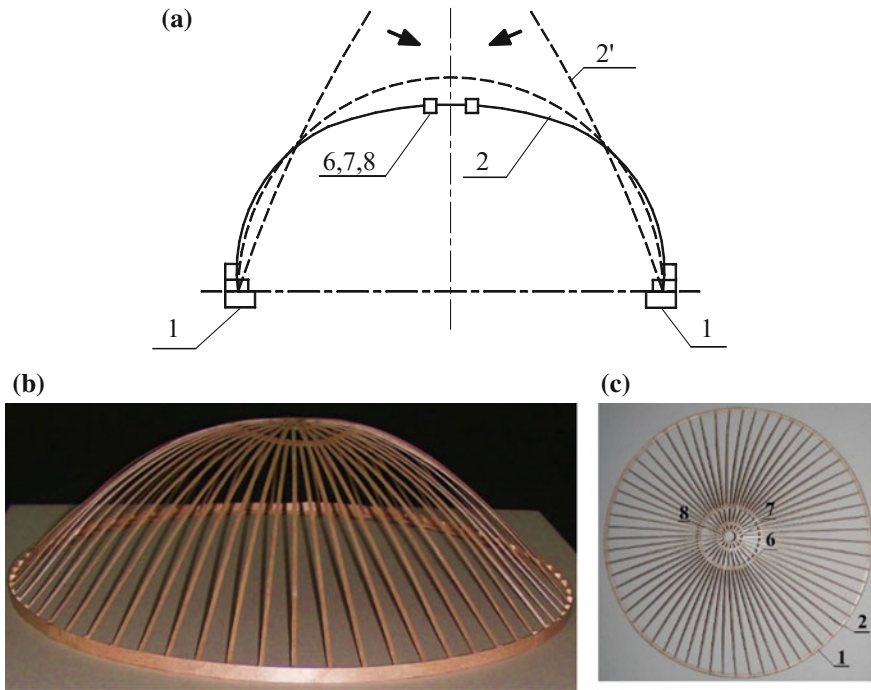


Fig. 6.1 Building rule of structures from flat ribs for thin-wall domes according to [2], **a** schematic diagram of the assembly of the dome's scaffolding: **2'**—initial arrangement of planks, **2**, position of planks after the bending, **b** assembly scaffolding **2** shown on a model, **c** structure of ribs with the top view of the, central rings 6, 7, 8 to connect flat ribs

The rings **6**, **7**, **8** were also used to make such a connection of the ribs that every second meridional rib passed beyond the ring. The rings **6**, **7**, **8** were built from two layers of arch centres that embraced the bilaterally flat planks of the ribs **2**. Each ring let pass every second flat rib of the dome. The longest ribs were connected in the key block by means of the last ring **8**.

The three-layer shell from planks was nailed onto the bent flat ribs **2**. The direction of the layer was determined in parallel to the generatrix of the dome passing through the upper ring **8**. The generatrix of each layer was reversed in relation to the generatrix of another layer by 60° . The construction of the three-layer shell, made according to [2], is shown in Figs. 6.2, 6.3, and 6.4. Three inclined sheathings **3**, **4**, **5** were built from planks of a thickness of 1.9–2.5 cm and an 8–12 cm width. All the three sheathings were connected with nails of a dia. 5 mm diameter between them and the meridional ribs. Each layer of the floor from planks was laid on the sphere in parallel to the generatrix passing through the upper ring of the dome, creating an arch along the meridian.

To illustrate the building technology of the dome's structure two models at a scale 1:50 were made, as shown in Figs. 6.3, and 6.4.

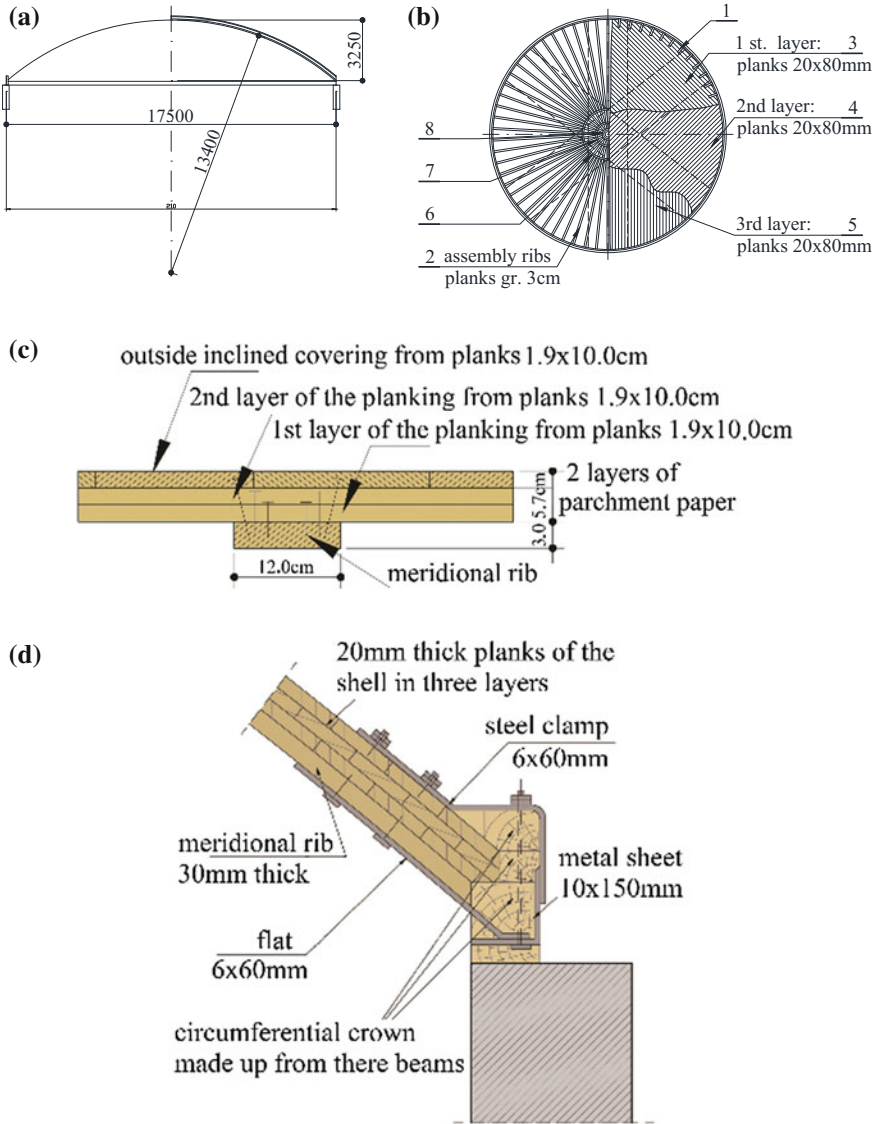


Fig. 6.2 Structure of a dome from planks of a 17.50 m span and a 3.25 m height according to [2], **a** section of a shell dome of a 17.5 m diameter, **b** schematic diagram of the plank shell's projection, 6, 7, 8—upper rings to connect the meridional ribs of the assembly layer, **c** section of a meridional rib, **d** supporting node of a dome using steel flats

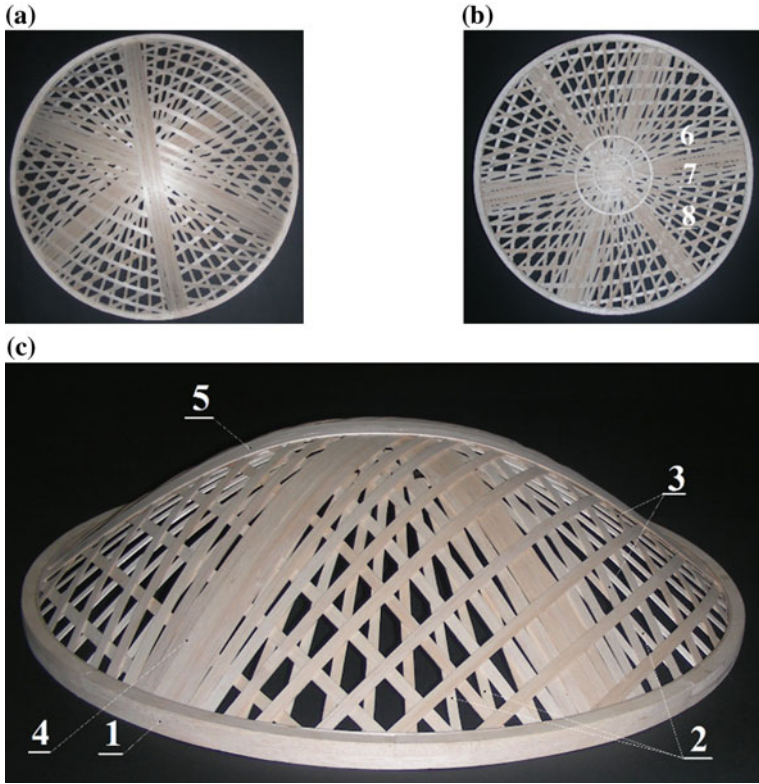


Fig. 6.3 Shell dome from three layers of planks according to [3], a top view, b view of the palate, c side view of the dome



Fig. 6.4 Model of a shell dome of a 17.5 m diameter at a scale 1:30 according to [3]

Three arches intersecting at 60° are shown on the model (Fig. 6.3), each of them being positioned in a different layer. Each layer of the sheathing was fabricated from long planks branching off fan-wise from the arch passing through the dome's peak towards the lower supporting ring. As they go off from the main direction of the layer's arch, the position of planks was nearing the meridional direction. Due to the need to maintain the continuity of the shell, the planks were hewn, or the sheathing was fabricated from planks of a fixed length, with the inclusion every several rows of hewn planks in form of flat wedges.

The model shown in Fig. 6.3 illustrates three layers of the sheathing from planks parting fan-wise from the peak towards the lower crown.

The operation of this dome may be presented in the following way: in each sheathing the layer of planks, positioned along the meridian passing through the upper ring of the dome, creates an arch and takes over the meridional forces in the shell. In this way three main arches in the dome are formed. Depending on the deviation of planks from the meridional direction, the planks of sheathings gradually approach the meridional direction, taking over the circumferential forces in the shell of the dome (Fig. 6.3c).

As verification of the correctness of the reconstructed system, another similar model of a dome of a 17.50 m diameter at a scale 1:30 was made, as shown in Fig. 6.4. The elements of the floor from planks were designated with numbers: lower ring 1 built from three planks, meridional ribs 2, as well as the layers of the plank floor 3, 4, 5.

The models presented were used for the analysis of the operation of shell domes. On the basis of Fig. 6.2 and the models fabricated, the weight of wood required to make thin-wall shell domes was assessed. The results obtained are very attractive in comparison to how much wood is necessary to build domes in other systems or from other materials, also including those from glued laminated timber. The volume of wood required to make ribs, rings or the three-layer shell of the dome of a 17.50 m diameter totals according to Fig. 6.2 circa 14.45 m^3 . The area of the dome's horizontal projection totals 240.41 m^2 . **The weight of solid wood as calculated per m^2 of the dome's projection amounts to circa 30.0 kg/m^2 . The amount of the steel consumed for nails required to join the layers of planks is also lower. It totals circa 1.5 kg per m^2 of the dome's projection.**

The amount of wood required to make the construction and the casing of the facility is much lower than that required to make domes from other materials. The cheapest type of wood used for the construction are planks. The three-layer shell built according the foregoing description allows an additional use of planks without the expensive selection, even the building-in of planks of a worse quality. The execution of plank shell from solid wood is not associated with such a huge mass of waste of structural elements from layer-wise glued laminated timber, requiring the elimination of natural defects of wood. The selection of natural wood in the production of layer-wise glued laminated timber is associated with the production of a huge mass of waste.

6.3 Shell Domes Prestressed with Steel Tie Rods

The system of shell domes prestressed with tie rods from steel bars was patented in Russia under the number 14822, cl. 37a,6, **in 1907, by the engineer Kaliepa [4]** (1947). In accordance with this patent, the dome that covered the building having a rectangular projection did not have a thrust ring and is made up of two layers of planks. The next authors: Wiazemski O. W., Smrczek L. L., Wiesolowski W. W., Chamasuridze G. W, in the authors' certificate 68,121, cl. 37a, 6, from 1947, I quote after Tshichachiev [4], propose using a dome roof shown in Fig. 6.5 as a removable roofing of the hydroelectric power plant's generator. **In practice, the roof was removed during the assembly and the next reviews of the equipment. In summer, the roof was raised for ventilation [4]. It is also known that the shell domes were raised and positioned above gas tanks.**

The three-layer thin-wall plank shell as discussed in Sect. 6.2 was built on meridional ribs from a single plank, bent to the shape of a sphere with steel tie rods. The systems of shells prestressed with steel tie rods were built on projections at the level of a lower thrust ring having a diameter of circa 20.0 m. The solution as described in the paper [4] demonstrates the use of the prestressing of plank ribs, round steel rods of a 8 mm diameter, bending the ribs from planks and taking over the additional horizontal strutting forces. The schematic drawing of the construction of a shell dome using ribs from planks prestressed with steel tie rods is shown in Fig. 6.5.

In Fig. 6.5, the number designations are: 1—triple, lower circumferential ring, 2–3.0 cm thick, 12.0 cm wide ribs, bent using a tie rod 9, and 3, 4, 5—layers of a shell from planks, 9—steel tie rod, 10—hook to raise the dome, 11—steel ring to hold together tie rods, 12, 13—steel clamps of the supporting ring.

The structure of shell domes prestressed with steel tie rods allowed a comfortable assembly of the roof covering using cranes. It is known from historical descriptions that the shell of the domes as described in Sects. 6.2 and 6.3 may be made up of a higher number of layers than it was described in the examples specified. The minimum number of the applied layers of planks amounted to 2.

The approximate calculation of such shells was conducted following the algorithms known since the beginning of the 20th century. The central sheathings of each layer were separated, as marked off with dotted lines in Fig. 6.2b. Those chords were considered to be the basic load-bearing element of a thickness equal to that of the plank in each layer (2.0 cm up to 2.5 cm). Owing to the consolidation (through the connection using nails) of all the layers of the shells, the planks of the layer were considered in increasing the stiffness of the chord being calculated.

The shell dome systems discussed (Figs. 6.2, and 6.5) bring to mind the connotations with the contemporary realizations of Swiss facilities having a structure designed by Natterer [5] (1991). In the solution shown in Fig. 6.6 the flat meridional assembly ribs were eliminated, using just the shell from two layers of planks.

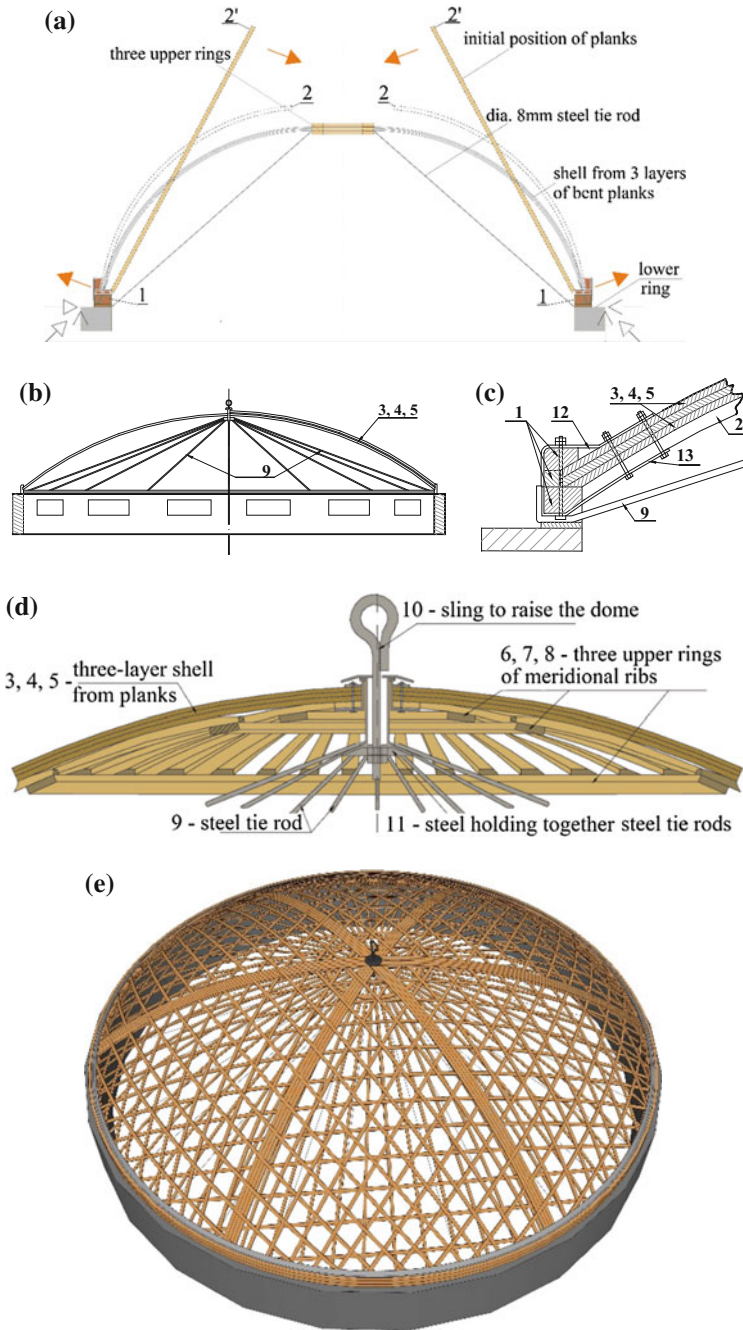


Fig. 6.5 Shell dome prestressed with steel bars according to [4], **a** schematic diagram of the structure, **b** section of the dome, **c** supporting node, **d** anchoring of tie rods in the upper node, **e** reconstructed view of the dome

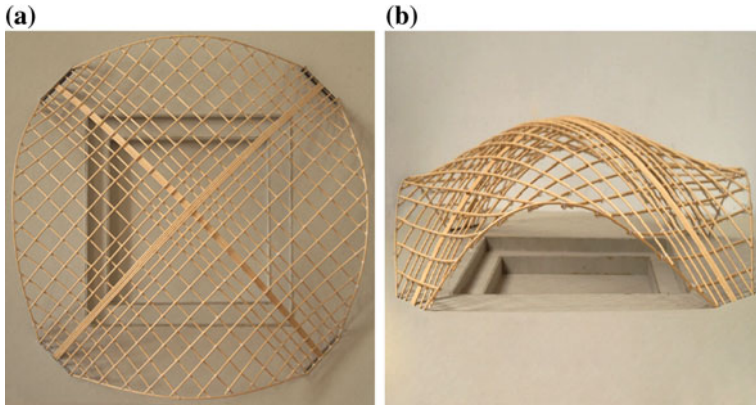


Fig. 6.6 Model of the shell by Natterer J. made from wood, [6], **a** projection of the shell, **b** side view

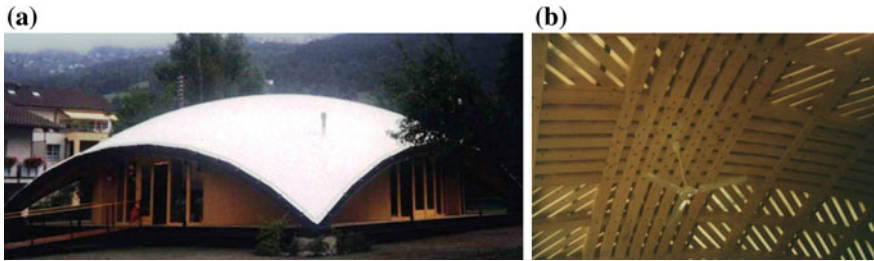


Fig. 6.7 Kindergarten's building in Lausanne roofed with a shell from planks, **a** view of the building, photograph by the author, **b** view of the plank shell from the inside, photograph by the author

Hidden ribs were made in the shell along the diagonal of the square projection. Two main load-bearing arches were made along the generatrices of the shells, shifted in relation to each other at 90° (Fig. 6.6a). The planks of the floor were laid in parallel to the central arches.

Shown in Fig. 6.7 is the covering of the kindergarten's building near Lausanne, Switzerland, built in 1998, according to the design project described in [5] (1991). The construction of the shell was made following the rules presented in Fig. 6.6.

Steel tie rods were eliminated from the structure of the roofing, and the strutting from main ribs was taken over onto the pyramidal reinforced concrete supports in four supporting corner points of the shell.

6.4 Shell-Ribbed Domes

In this system the three-layer thin-wall shell was built on meridional ribs from three planks tangential to the sphere. Such systems were built on circular projections having a diameter of 19.5 m up to 40.0 m [3].

Shown in Fig. 6.8 according to [2] is the example of a thin-wall dome built in the shell-ribbed system, of a diameter of 30.0 m and a height of 6.0 m. The technology of the dome's assembly is similar to that discussed in Sect. 6.1 and illustrated therein. The difference consists in the introduction of multi-layer meridional ribs (Fig. 6.8c) and a different structure of the layers of a shell from planks. In the domes of a 20.0 m up to 35.0 m diameter arches were built from several planks (three or four), laid flat one on another and connected using nails. The distance between the axis of ribs on the lower supporting ring was adopted to be circa 1.0 m. In the example from Fig. 6.8 the distance of 1.27 m was adopted.

In the shell-ribbed domes the ratio of the height of the meridional rib \underline{h} to the dome projection's diameter \underline{L} within the range of $h/L = 1/200 \div 1/270$ was used. The dome shown in Fig. 6.8 was built on seventy-four meridional ribs from three 4.0 cm thick planks of a total height of 12.0 cm, a width of 15.0 cm. The ratio of the height \underline{h} of the meridional rib's section to the dome projection's diameter \underline{L} is $\frac{h}{L} = \frac{1}{250}$. The ribs were bent to the dome sphere's radius (e.g. in Fig. 6.8 this is the radius 21.75 m) and connected at the top at the height of 6.0 m using a ring made from arch centres shown in Fig. 6.9.

The connection of ribs with the upper ring followed on an assembly scaffolding. The sections of the connection spots of meridional arches were moved over the length of ribs, whereby the contact spots of the upper and lower plank were disposed not closer to 3–4 m from the upper ring made from arch centres.

Ring-shaped sheathings were nailed onto the bent meridional planks of ribs, which helped shaping the sphere as well as protected the fragile load-bearing ribs against lateral translocations.

The ring-shaped (meridional) sheathings were used in order to transfer the compressive and tensile, meridional forces. They were built from two layers of planks: the lower layer laid directly on the meridional arches of the dome, and the upper layer, covering the contact spots of the lower layer. This first layer of 19.0 cm thick planks stiffened the scaffolding from meridional ribs. The accurate positioning of the first layer determined the geometry of the whole dome. The slight assembly inaccuracies of the first layer's planks nailed onto ribs introduced the horizontal translocations of ribs, which resulted in a deformation of the dome's sphere. Such deviations became particularly dangerous at the occurrence of non-symmetrical loads. In order to prevent this, a second latitudinal layer was nailed, shifted in relation to the first latitudinal layer by one half of the plank's width. The contact spots of the ring-shaped sheathing's planks were placed in the axis of meridional

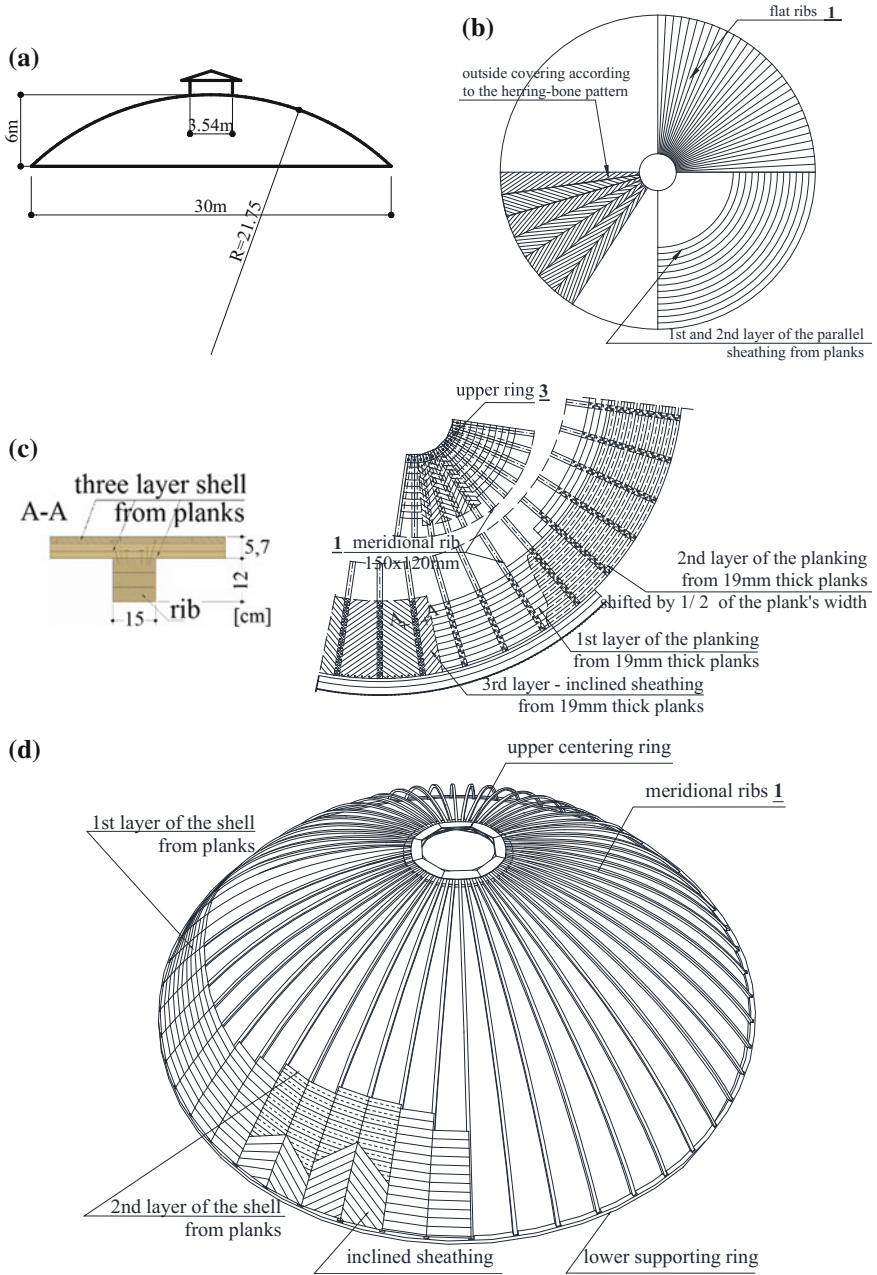
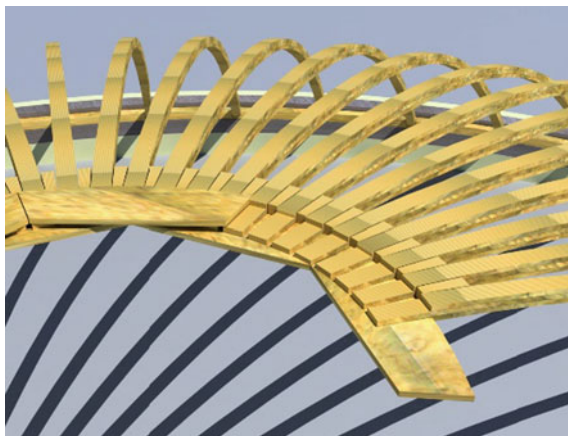


Fig. 6.8 Shell-ribbed dome of a diameter of the circular projection of 30.0 m according to [3], **a** schematic diagram of the dome's section, **b** projection of the dome, **c** lay-out of ribs and planks of the floor, **d** reconstructed view of ribs and the sheathing from planks

Fig. 6.9 Building of the central upper ring of thin-wall domes



ribs. Both the layers of the ring-shaped sheathing were connected using nails of a 5.0 mm diameter, up to the meridional ribs of the dome. Usually, the thickness of 1.9–2.5 cm, the width of 10–16 cm width of the planks of the ring-shaped sheathing was adopted. In the upper part of the dome, at the arch centre ring, the duplicated ring-shaped sheathing was substituted for a single sheathing from planks of a thickness equal to the sum of the thicknesses of the duplicated sheathing.

The elasticity of ribs produced a reciprocal meridional and circumferential tightening of the shell, from the lower supporting ring up to the upper crown. The shape of the dome was maintained owing to the reciprocal equilibrium-maintaining prestressing of the planks of ribs and those of the three-layer shell.

The sloping (outside) sheathing was used to transfer the shearing forces resulting from the non-symmetrical load of the dome. They were laid on latitudinal rings at 45°. They were built from one layer of planks of a 1.9 to 2.5 cm thickness, positioned at circa 45° from one meridional arch to another one. In the outside view, the inclined sheathing fell on the dome into the “herring-bone” pattern.

The upper arch centre ring that anchors meridional ribs and assumes the forces from meridional arches (Fig. 6.9) were made from two or more chords of arch centres embracing the central plank of three-layer, flat of meridional arches. If the number of arches was adopted to be m , and the width of a plank b , then the diameter of the arch centre ring was calculated from the formula $d_0 = \frac{mb}{\pi}$. In order to reduce d_0 , a slight undercutting of the planks of arches was used at the place of their junction with the arch centre ring. The layers of the arch centres of the central ring were connected with the meridional ribs using steel bolts of a 12 mm diameter. The view of the upper ring and the junction of the arch centres of the ring with the planks of ribs is shown in Fig. 6.9.

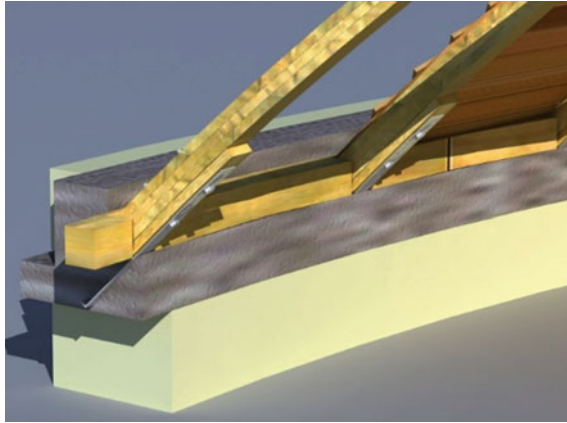


Fig. 6.10 Connection of ribs with the wall plate and the lower reinforced concrete crown

The opening of the upper arch centre ring was covered with a skylight. In some solutions a lantern with a wooden roof was placed on the ring. The weight of the lantern whose walls were placed on the arch centre ring favourably influenced the maintenance of the shape of the dome.

The lower support of the meridional ribs of the shell constituted a circumferential reinforced concrete crown—Fig. 6.10. The supporting ring—the lower circumferential ring of the dome, operating on the extension originating from the strutting of the dome, was made as a reinforced concrete, steel or wooden triple ring (for domes of a diameter up to 20 m, Fig. 6.2d). In this crown, using steel flats, the supporting triple wooden ring of the dome's diameter was anchored. The flat ribs of the dome were fastened in it following the rules and the figures described in Sects. 6.1 and 6.2. The bent planks of the ribs were protected against tearing-off with steel flats of a thickness of circa 5–6 mm. The connection was fabricated with dia. 2 mm bolts. In order to reconstruct the modern (unfortunately forgotten) structure of the dome, the view of the structure of ribs and the covering was reconstructed using incomplete sketches from the referenced literature [3] (1943), [1] (1937), and demonstrated in Fig. 6.8.

Following the above-discussed rules, the dome of the gas tank building of the Berezhnikovsky Chemical Complex in Russia, having the structure as shown in Fig. 6.11, was also reconstructed. The designer of the dome was the engineer Milvitsky [1] in the thirties of the 20th century. The dimensions of the dome were as follows: the diameter of 32.50 m, rise $f = 7.20$ m, the proportion of the rise f to the projection's diameter L was adopted: $f/L = 7,2/32,5 \div 1/4,5$. The shell was built, following the rules discussed in the previous example, on eighty-eight meridional ribs, spaced every 1.15 m on the lower supporting ring.

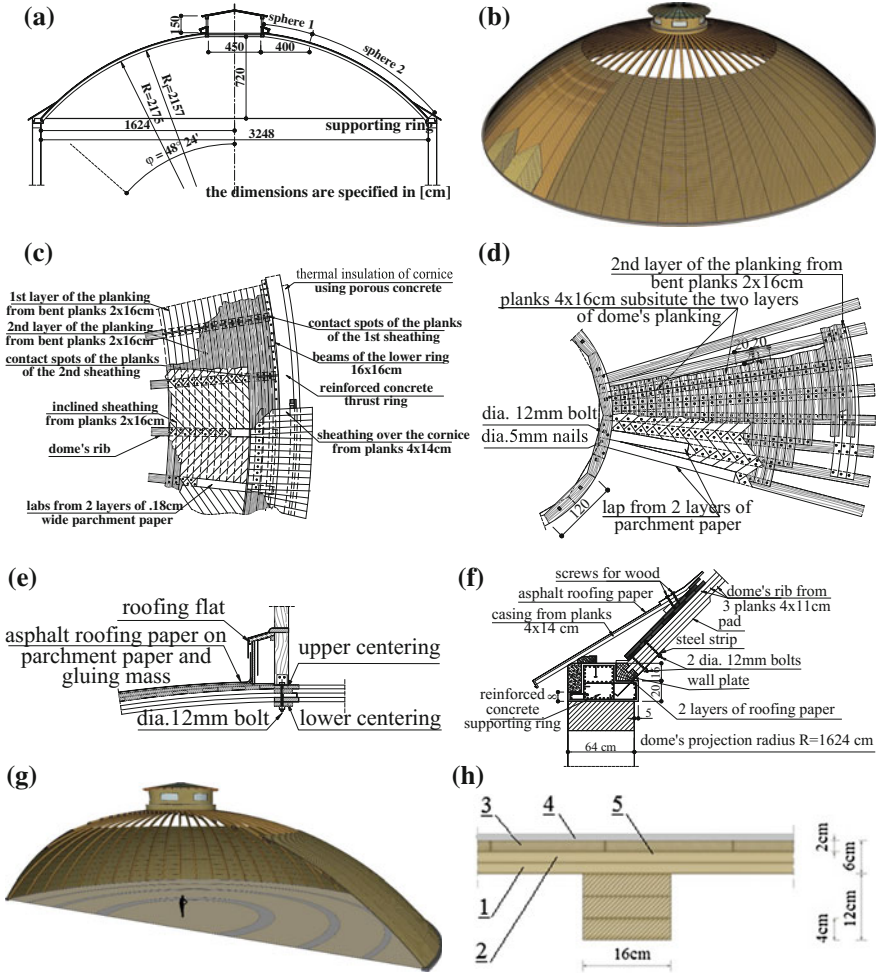


Fig. 6.11 Structure of the Berezchnikovsky's dome of a 32.48 m diameter according to [1], **a** section, **b** general view of meridional ribs and the three-layer shell, **c** shell at the lower supporting ring, **d** shell at the upper supporting ring, **e** connection of the layers of the floor shell with meridional ribs and connection of the meridional rib with the dome's upper ring, **f** supporting ring, **g** reconstructed section of the dome, **h** section of the rib joint with the shell: **1, 2**—1st and 2nd layer of the latitudinal sheathing, **3**—3rd layer of the inclined sheathing, **4**—covering using roofing paper, **5**—spacers from 2 layers of parchment paper

6.5 Ribbed-Shell Domes

The ribbed revolving domes developed from thin-wall shells and were used for domes of a higher stiffness when in order to raise the stability of the shell ribs should have been given a higher stiffness. Besides, the stiff ribs proved correct as an

assembly skeleton when erecting the dome. Such systems were built on circular projections of a diameter of 35.0 m up to 60.0 m.

In the ribbed-shell system the three-layer shell from planks was built from two ring-shaped layers and one inclined layer, like in the thin-wall shells described in Sects. 6.3 and 6.4. In the ribbed shell domes the ribs raise the load capacity to bending, and are characterized by a massive structure as compared to the flat ribs of shell ribbed domes. At the higher diameters of shell domes the stiffness of meridional ribs driving the dome's geometry was increased through spreading apart the chords tangential to the sphere and through introducing a web from two planks between the chords. The main load-bearing ribs were given an I-section, and over the length along the meridian, a form of bipolar coordinates. Meridional intermediate ribs from several planks bent to the sphere's curvature were placed between the stiff main ribs. A three-layer shell from planks like in the system discussed in Sect. 6.4 were nailed on the main and intermediate ribs. The three-layer shell jointly with the stiff and intermediate ribs operated as a complex element.

The forms of ribbed-shell domes, dimensional dependencies and the construction of intermediate ribs and of the dome are assumed to be the same as in thin-wall domes. The difference consists in the introduction of meridional ribs of a higher stiffness and bipolar coordinates. The main meridional ribs of domes required at their erection a support on the central scaffolding in the vertical axis of the facility.

In 1930, a ribbed-shell dome of the circus in Saratov (Russia) was built, as described by Kashkarov K.P. in his paper [1] (1937). The author does not specify the precise description of the dome. It is limited just to some pieces of information. I quote: "Crescent-shaped meridional ribs of the dome were made to have an I-section and a height of 1.00 m in the highest section, which in relation to the diameter $L = 46.0$ m totals $h/L = 1/46$ ". Attached to the text was one photograph that, presently, is almost illegible. On the basis of the intuition and the data on other ribbed-shell domes a model at a scale 1:50 was made, which recalls the view of a light structure of the Saratov dome. Perhaps it looked like as shown in Fig. 6.12. Due to lack of information (at the present-day stage) about the construction of the lower supporting crown of the dome, it was designed in such a way as to suggest a solution meeting also the requirements of the modern user. Let us hope that the model will recall and rescue from oblivion the subtle and modern construction of the Saratov dome.

Shown in Fig. 6.13 is the structure of the ribbed-shell dome as described by Karlsen G. G. in [3]. A facility of a 50.0 m diameter was designed on shuttering bipolar ribs and a plank shell consolidated with them. A ring-shaped shell from two layers of 2.5 cm thick planks laid latitudinally and a third 1.9 cm thick inclined layer was made on 32 meridional ribs and 96 flexible intermediate ribs (from three planks) (Fig. 6.12e).

The main, bipolar rib of the dome shown in Fig. 6.13a was made with the upper chord of a curvature conforming to the radius of the dome's sphere, i.e. 31.85 m. Demonstrated in Fig. 6.13b is the lay-out of the main ribs on the dome's projection. The main meridional ribs were disposed every 6.04 m as measured on the lower ring of the dome. The flexible ribs, made from flat laid planks of the sectional

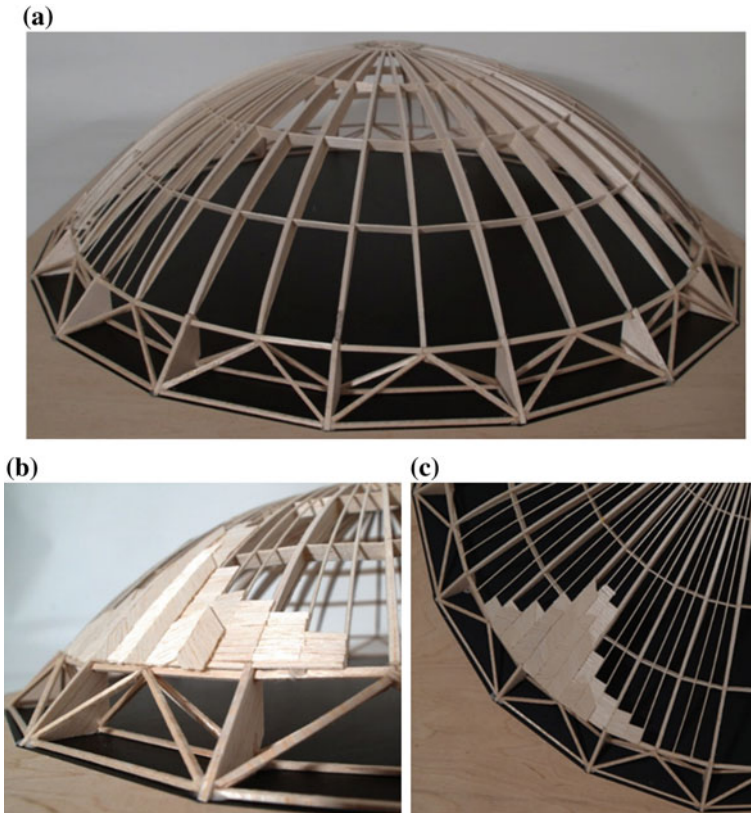


Fig. 6.12 Model of a shell-ribbed dome of a 46 m diameter according to [1], **a** structure of ribs and the supporting ring, **b** detail of overlaying the layers of the sheathing, **c** main, intermediate ribs and the covering

dimensions, 15×16 cm width \times height, were placed between them every 1.51 m. Each of the intermediate ribs was composed of four 40.0 mm thick and 150.0 mm wide ribs each (Fig. 6.13e). The spacing of the intermediate ribs resulted from the length of planks required to make the meridional layers of the shell.

Shown in Fig. 6.13d, e is the structure of a shell made up of two ring-shaped layers from 25 mm thick planks, and of a third, inclined layer from 19 mm thick planks. Quarterings of 40 mm \times 40 mm dimensions, in a spacing of 50.0 cm as battens from zinc-plated sheet were nailed on the three-layers of the shell. Figure 6.13c–e depicts the view and the section of meridional ribs: the main rib and the intermediate rib. The upper and the lower chord of shuttering meridional main ribs were built from four planks of a section of 80×40 mm each, and the web from two layers of 2.5 cm thick planks laid at 90° one to another. The support of meridional ribs on the lower thrust crown was made on a massive reinforced concrete ring. The connection of the main ribs at the top in the key was made on a

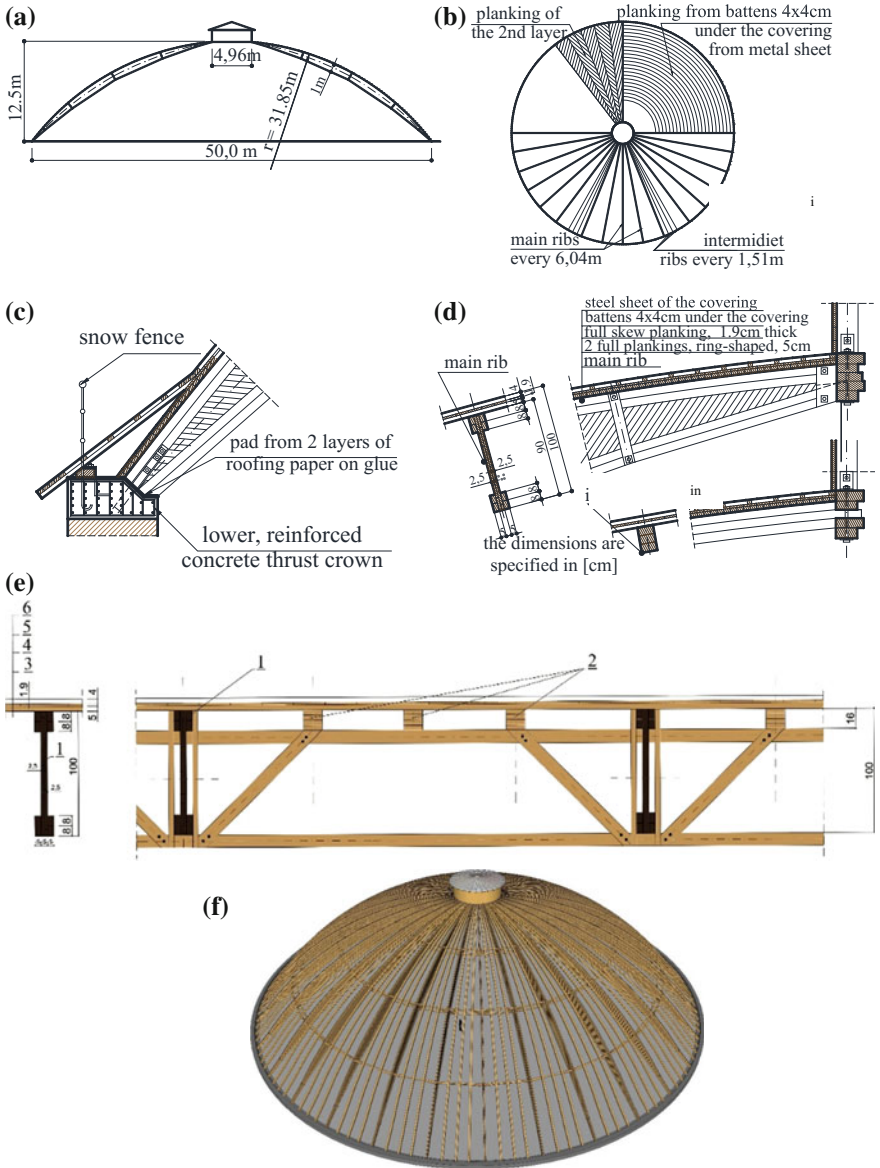


Fig. 6.13 Ribbed shell dome of a 50.0 m diameter according to [3], **a** schematic diagram of the dome, **b** lay-out of ribs and planks of the floor as well as of batters under the covering from metal sheet, **c** structure of the supporting node, **d** structure of the load-bearing and intermediate rib, **e** structure of the latitudinal brace rib between meridional ribs, **1**—main rib, **2**—intermediate rib, **3**—latitudinal planking from planks $2 \times 2.5 \text{ cm}$, **4**—inclined planking from 1.9 cm thick planks, **5**—batters from 4.0 cm thick quarterings, **6**—covering from metal sheet, **f** reconstructed view of the dome with meridional ribs demonstrated

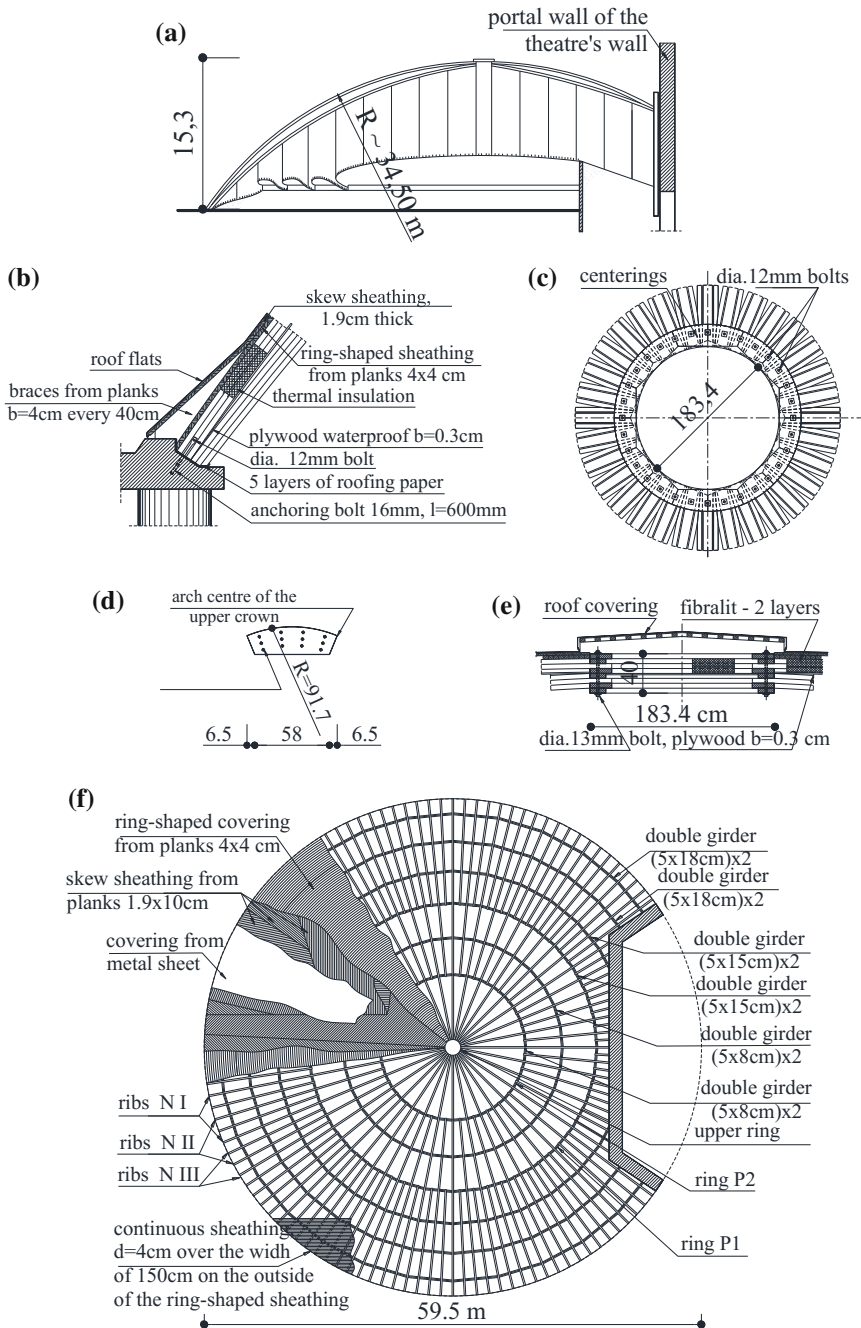


Fig. 6.14 Dome of a 59.50 m diameter on the building of the Simonov Palace of Culture in Moscow according to [1], **a** section of the dome, **b** structure of the supporting node, **c** upper ring, **d** arch centre from which the upper ring was fabricated, **e** section of the upper ring, **f** main ribs projection of the dome, **g** main rib No. NI, **h** construction of latitudinal struttings of main ribs **NI** and intermediate ribs **NI**, **NI**, **NI**, **i** section of the load-bearing rib **NI** in the middle of the span, **j** supporting section of the load-bearing rib, **k** reconstructed view of the structure of ribs and the shell, **l** section of the facility crowned with a dome

wooden ring built from five layers of flat laid arch centres. The view in Fig. 6.13e shows the span of a meridional angle brace strutting between the main ribs, preventing the twist of the main ribs. The braces of the meridional strutting were placed under the meridional intermediate ribs.

In 1933, at the Central Research and Development Centre of Industrial Structures the engineer Kashkarov [1] was the author of the design project of the ribbed-shell dome of the Simonov Palace of Culture in Moscow. The section of the dome is shown in Fig. 6.14a. The diameter of the dome's projection was 59.5 m, and the height was 15.3 m. The ratio of the dome's rise to the diameter amounts to: $f/L = 15.3/59.5 \approx 1/4$.

The dome was built from one hundred and twenty-eight meridional ribs of which thirty-two are brought to the central upper ring. Thirty-two longest load-bearing ribs are designated in Fig. 6.14f, g with the symbol N1. Figure 6.14c, d presents the section of ribs, and Fig. 6.14 the disposition on the dome's projection of the ribs N1, the ribs of an average length N2, as well as the shortest meridional ribs N3. All the ribs N1, N2, N3 were fastened on the lower thrust ring in a distance of circa 1.45 m when calculated over the circumference of the crown. The upper supporting sections of the meridional ribs were connected using ring-shaped latitudinal ribs P1, P2. Only every second meridional rib was let pass beyond the rings. The last longest meridional ribs were connected in the upper, central ring of the dome. The main meridional ribs N1, having in the side view the form with bipolar coordinates, are shown in Fig. 6.14g. They were designed as having a length of circa 30.0 m and the maximum height in the middle of the length $h = 1.15$ m, which yields a ratio of the rib's height to the dome's projection diameter of $h/L = 1.15/59.5 \approx 1/52$.

The cross section of the meridional rib is made up of an upper chord and a lower chord from planks of 5.0×10 cm and 4.0×5.0 cm dimensions. The web to connect the chords is duplicated and was made from a 6 mm thick plywood—Fig. 6.14h–j. The meridional, intermediate ribs, similarly to the example demonstrated in Fig. 6.13, are made up of three planks of 5.0×8.0 cm dimensions using nails. The ring-shaped sheathing of the first meridional layer of the shell was made from quarterings of a 4.0 cm \times 4.0 cm section and placed on the meridional ribs. Three inclined layers from 1.9 cm thick planks each were fastened using nails onto the latitudinal layer (Fig. 6.14f). The structural elements: ribs, the shell, the upper crowning ring and the lower supporting ring were designed following the building rules for ribbed-shell domes and shown in Fig. 6.14.

In the dome of the Simonov Palace of Culture in Moscow 58.3 kg of solid wood were used for the construction and the casing per m^2 of the projection. Steel fasteners were used in the connections: dia. 5 mm nails and dia. 12 mm bolts whose total mass was 1.71 kg per m^2 of the dome's projection [1] (1937). This is such an economical consumption of steel that its repetition in a contemporary produced dome was a failure.

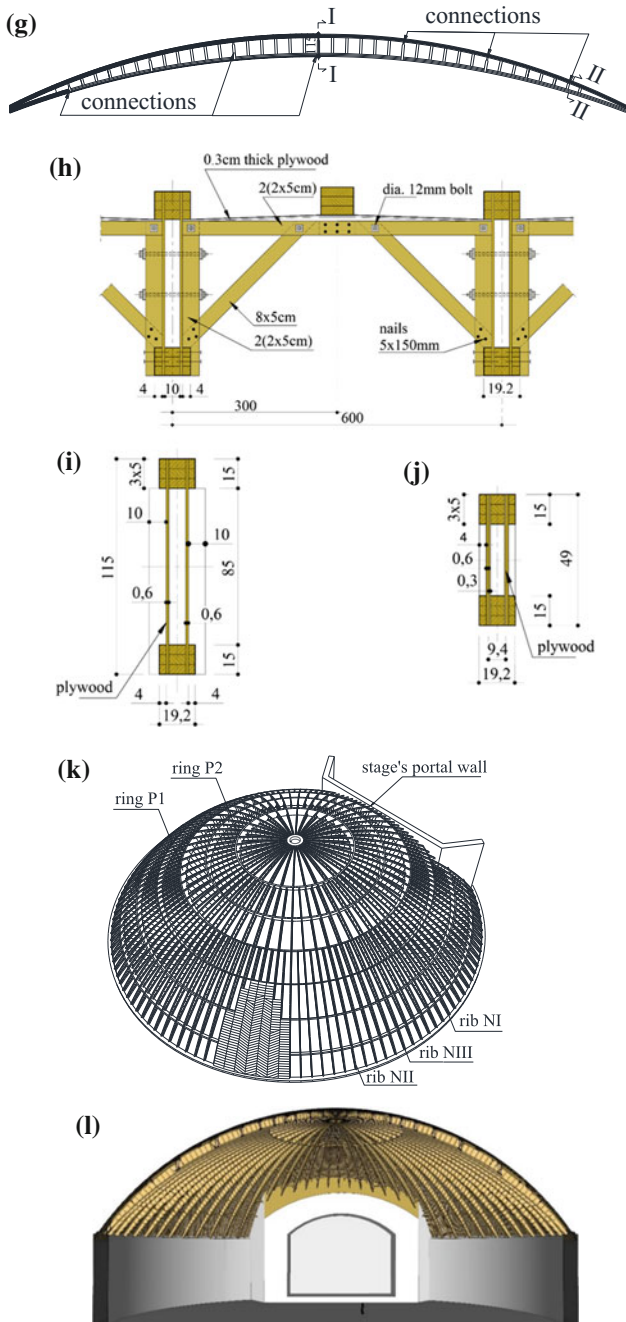


Fig. 6.14 (continued)

6.6 Conclusions

The domes from solid wood described in this chapter constitute an important stage in the search for an optimum structure of roof coverings of a small and average-sized span, as well as of a low eminence. **Among the most important advantages of those rational and economical, worth recalling and reusing structures are:** (1) low consumption of wood and metal fasteners, (2) possibility to use low-grade materials, (3) limitation of wood selection and reduction in waste amount, (4) increase in the span of domes even up to 60.0 m, without changing the assembly technology, (5) increase in the height of load-bearing ribs through nailing several layers of the covering's planks, (6) possibility to join the plank shell with assembly ribs, which considerably increases the load capacity and the stiffness of the construction, (7) possibility to build domes of a low eminence amounting to $h/L = 1/3$ up to $1/6$ of the base's diameter. According to the recommendations in the paper [1], the rise of the dome should not be, however, lower than $1/6$, (8) possibility to limit the scaffoldings at the stage of the dome's erection, (9) possibility to make openings in the shell and reinforcements around the opening even after the building of the dome, (10) possibility to bend planks to the required shape of ribs or the shell.

The system of the layers of covering's planks stiffened the shell in tangential planes, making it almost homogenous, and prevented the translocation of ribs in the plane tangential to the shell, whilst the flexibility of the construction allowed a uniform translocation of forces, created due to thermal and moisture-related deformations. After the consolidation of the three-layer shell with meridional ribs the elements of the central scaffolding to support the central rings were relieved. In the examples discussed in Sect. 6.4 the mass of the lantern placed on the upper ring counterbalanced the prestressed dome's ribs that were tending to straighten.

The fundamental load-bearing element of thin-wall domes are flat ribs made up of three to four planks, bent along the meridians, of a slenderness counted by the ratio of the rib's height h to the dome's diameter L amounting to $h/L = 1/200 \div 1/270$. The ribs were disposed every 1.0–1.5 m over the circumference of the lower supporting crown. The two or three-layer shell, joined with ribs, built from 1.9 to 2.5 cm thick planks, of a total thickness of 5.7 up to 9.7 cm, complements the load-bearing structure of the system.

Steel fasteners of a type: nails, bolts and cast iron clamps were used in order to introduce the mechanical pressure. In the zones of the highest extension, e.g. on the lower supporting ring clamps from steel metal sheet were used, embracing, and not cutting through the wood of the shell's rib.

The production of shell domes and ribbed-shell domes was distinguished by the use of meridional ribs as assembly scaffoldings to be consolidated with the plank shell, prominently increasing the load capacity of the dome. After the years, the light and economical shell systems, shell-ribbed systems, ribbed-shell systems fell into a total oblivion jointly with the people who built them. They were reconstructed after 90 years and described in this work.

In the shell systems domes of a span up to 60.0 m were built (dome of the Simonov Palace of in Moscow), without using steel nodes, which may be considered as a large structural achievement.

The engineers: Kaszkarow K.P. and Sventistky G.W. used plywood for the first time in the construction of domes of a projection's diameter higher than 50.0 m. Worth noticing is the note written in the paper [1] (1937), I quote: "The possibility to use plywood, like in other cases, is dependent on the total exclusion of its moistening after the commissioning".

The described constructions of shell domes and ribbed-shell domes constitute exquisite examples that should presently inspire to work on the solutions of environmentally beneficial contemporary domes.

References

1. Kaszkarow K., P. *Kopuly* Sprawocznik projektrowszczyka promyszlennych sooruzienij. Dieriewannyje konstrukcji. Kuzniecowa G. F. Gławnaja riedakcija stroitelnoj literatury. Moskwa-Leningrad 1937.
2. Jean-Denis Godet *Atlas drewna*, Multico, Oficyna Wydawnicza, Warszawa 2008.
3. Karlsen G. G., Bolszakow W.W., Kagan M. E., Świencicki G., *Kurs dieriewiannych konstrukcij cz. I i II*, G. I. C. L. Moskwa, Leningrad 1943.
4. Czichacziew H. A. *Dieriewiannyje konstrukcji* Gosplanizdat, Moskwa 1947.
5. Natterer J., Herzog T., Volz M., *Holzbau Atlas Zwei*, Institut für internationale Architektur-Dokumentation GmbH, Munchen 1991.
6. Niemczyk E. *Die Jahrhunderthalle in Breslau – ein Triumph des Eisenbetonbaus* Beiträge zur Geschichte des Bauingenieurwesens 8, Technische Universität München, 1997.

Chapter 7

Gridshell, Ribbed–Shell Domes

7.1 Introduction

Shown in Fig. 7.1 is the schematic of the development of the covering geometry, starting with a cylindrical shell up to a polygonal shell formed from the series of intermingling cylindrical surfaces.

A spherical open covering (Fig. 7.1b) or a spherical closed covering (Fig. 7.1c) on the projection of a square can be built from two intermingling cylinders. An open shell covering (Fig. 7.1d) or a closed shell covering (Fig. 7.1e) from several intermingling cylinders on a polygonal projection can also be formed.

In stone structures it was customary to call domes axially symmetrical, masonry closed coverings. In wooden structures there occurs an enormous number of differentiated two-curvature coverings, both open and closed. In this work the scope of considerations covers the closed shell coverings in form of domes.

The covering shown in Fig. 7.1e is made up of sections of a cylindrical vault supported on meridional ribs as well as the lower and the upper ring. The intersection edges of the cylinders separate a section of the sphere limited by edge ribs called chords. The building of main ribs on the intermingling lines of the cylinders determined the essential stiffening and increasing of the load capacity of the covering at a small weight of the structure. Shown in Fig. 7.2 is the model of a sectoral dome from arch centres made on the projection of an octagon. The model is the visualization of a sectional dome having a span of 30.0 m at the scale of 1:50.

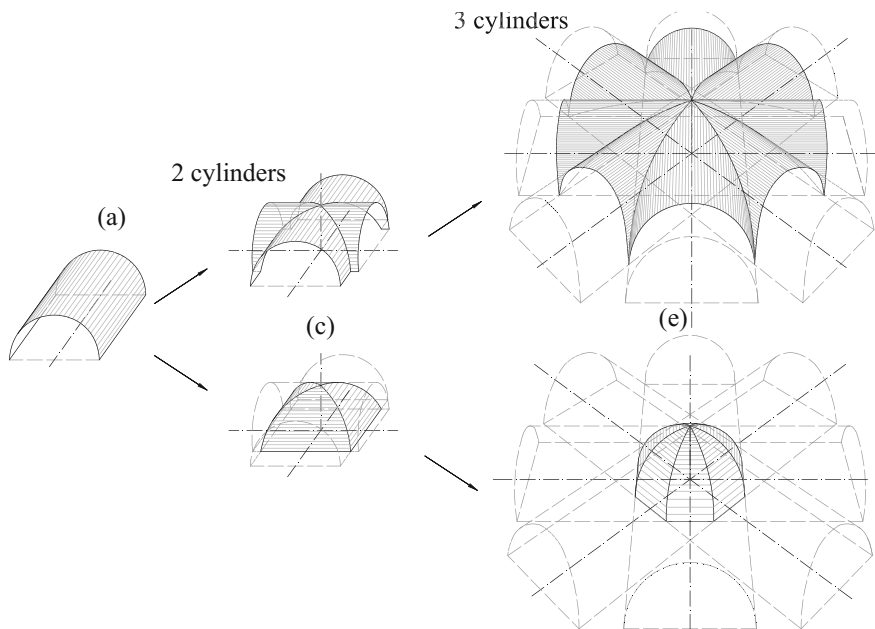


Fig. 7.1 Shaping of the geometry of open and closed shell coverings on polygonal projections

Fig. 7.2 Model of the gridshell covering, closed, on the projection of an octagon
 1—arch centre, 2—chords,
 3—lower supporting crown,
 4—upper chord-connecting ring

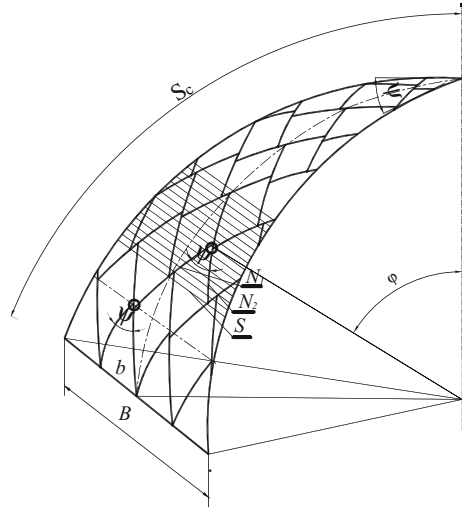


7.2 Sectoral, Gridshell Domes

In coverings built on polygonal projections, in the intermingling lines of cylindrical surfaces there occur main ribs called chords, concurring in the upper ring of the dome [1]. The height of the load-bearing chords was adopted as $h \geq \frac{1}{150}L$, where L —the diameter of the circular projection of the dome. The fields between the chords was filled with a rhombic network of bar ribs using which the shell of the covering from planks was connected, transforming it into a complex construction (Fig. 7.3).

In such system it was recommended to determine the number of the sides of a polygonal projection of the closed vault (Fig. 7.1c, e) in accordance with the adopted angle ψ between the arch centres of the network so that the helices

Fig. 7.3 “Spherical” triangle of a sectional gridshell ‘dome’ [1]



(from crossheads) reach as far as possible the side edges of the chords in one section (Fig. 7.2). This condition is met at the maintenance of the Eq. (7.1) according to [2]:

$$B/S_c = tg(\psi/2) \tag{7.1}$$

where

B—length of the side of the polygonal vault base, Fig. 7.4b.

S_c—length of the arch as shown in Fig. 7.4a.

ψ_m — $360/m$, where *m*—the number of the sides of the base’s polygon. The Eq. (7.1) results from the similarity of the dome’s section limited by ribs to the geometry of the arrangement of crossheads and can adopt the form:

$$s = b/2 \sin \frac{\psi_m}{2} \tag{7.2}$$

where: ψ_m —apex angle of the section. Attention should be drawn to the adjustment of the geometry of crossheads from their joining technology.

At the given number of the sides of the covering’s polygonal projection, the angle between the arch centres of the rhombic shell was determined from the Eq. (7.1), whereby the angle should not go beyond the range of angles between the ribs recommended for cylindrical arch centre-gridshell vaults. This angle, designated in this work as α , should be included within the range of 30° up to 50° [1]. The variable thickness of chords in the projection was obtained using laps of various thicknesses nailed to the side edges of the chords at the place of the chord’s connection with arch centres. While conferring a variable width on main

ribs (chords) (Fig. 7.4b), a bilateral convergence of the helices from arch centres with the chord's axis in one section was obtained, thus providing the full normalization of the length of arch centres. However, if at the pre-set number n of the sides of the polygonal plane of a closed vault it was impossible to adopt the angle ψ between the arch centres, chords of a constant width were built, and the arch centres differently joining them were connected with chords at various levels, or the length of the crossheads was changed. At an inaccurate accounting and the constant thickness of chords, the helices from crossheads, converging with chords of the constant length produce an unfavourable loading of the chords. The chords reinforced with side laps were also used at the assembly of the covering. An example of the gridshell sectoral covering from arch centres is shown on the projection of an octagon is shown in Fig. 7.4.

Visible in Fig. 7.4 are chords of a variable width in the intersection lines of cylindrical width. The assembly of the vault was conducted in the following

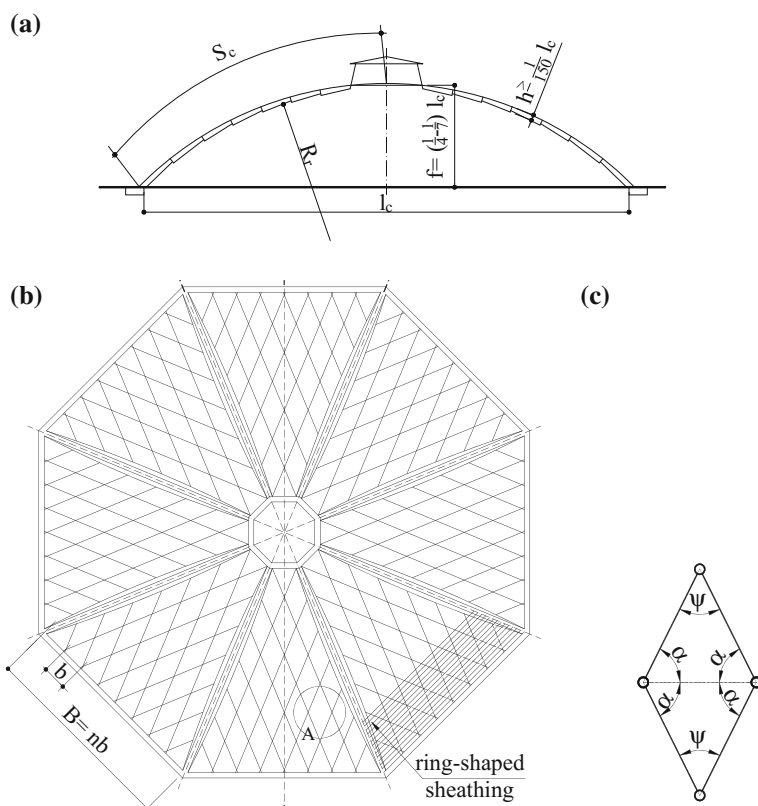


Fig. 7.4 Arch centre-gridshell dome on the projection of an octagon according to [3], with eight sectors; **a** section of a polygonal dome from crossheads, **b** projection at the level of the lower supporting ring, **c** angles of the rhombic network

sequence: first, the lower supporting ring and the central tower, on which the upper ring was laid, were placed and strengthened. Afterwards, the strengthened chords of the vault were disposed, and it was recommended to raise the chords and to place on the central tower of the scaffolding, pair-wise, in order to give the dome the spatial stiffness during the assembly. The chords were strengthened with mounting spacings from planks, afterwards a small scaffolding within one sector or its part was suspended to them.

The assembly of the vault was conducted sector-wise. Two oppositely lying sectors were mounted on a one-off basis.

7.3 Gridshell Domes from Arch Centres

At the realization of domes of large dimensions fabricated from wood, the load-bearing elements happen to be heavy and difficult in the assembly. Their transportation becomes uncomfortable and expensive. One of the most comfortable types of the structures of spherical domes are those made from separate crossheads. An essential stage of the development of wooden domes were domes built from a network of small ribs replacing meridional main ribs. Of particular importance was the introduction of crossheads called in the Russian references ‘**kosjaks**’ [2], in the Polish references ‘**plant slants**’ [1] (1959), which were used to model the surface between the main ribs of sectional-cylindrical domes built on a polygonal as well as circular projection (Figs. 7.1, 7.2, and 7.4). In this work the name ‘**crosshead**’ was suggested for an element made from an element of the arch centre creating the grid of the shell.

Closed axially symmetrical coverings were built from wooden crossheads assembled into a rhombic spherical grid were called gridshell domes. This type of grid occurs in wooden structures only. The dimensions of such domes were selected, like gridshell coverings, on the projection of a polygon, that means that the ratio of the rise of arch f to the dome diameter L is included within the range of: $f/L = (1/7 \div 1/4)$.

Mischke D. in his paper [1] specifies that if in the sectional ribbed-gridshell coverings the condition $B/S_c \leq 1$ is met (where B —length of the polygon’s base side, S_c —length of the arch of the dome’s vertical section (Fig. 7.4a), then the sectoral dome may be treated as a rotary dome on the circular projection. Owing to the transformation of the polygonal projection into a circle, the edge of the intersections of cylindrical surfaces was eliminated, removing ribs off the construction. This required the strengthening of the lower supporting ring and the upper ring in the dome’s key block. The lower supporting ring and the upper ring determined the stiffness of the gridshell dome’s structure from arch centres on the circular plan. Shown in Fig. 7.5a, b are examples of domes built from arch centre gridshells on the circular plan.

The shaping of a shell made up from rhombuses, thus axially symmetrical gridshell domes from wood, followed through such calculation of the angles

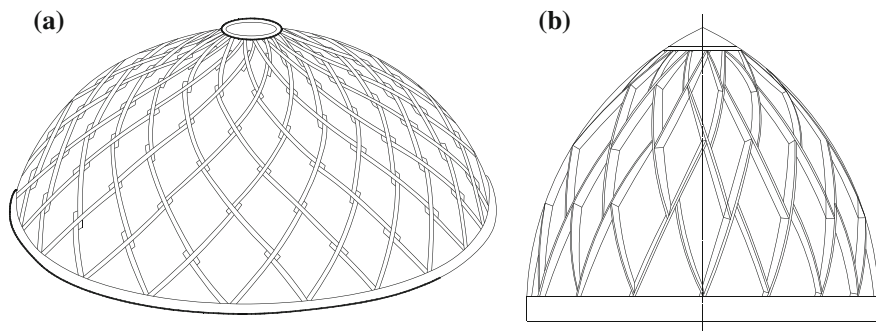


Fig. 7.5 Gridshell domes: **a** gridshell dome on a circular projection, **b** ogival dome on a circular projection

between ribs–arch centres “ ψ ”, their inclination to the level of the dome’s line of latitude “ α ”, as well as the inclination angle to the dome’s interior “ φ ” so as to obtain the closure of the last layer of crossheads in the central upper ring (Figs. 7.3 and 7.4c).

Shown in Fig. 7.6 is the axially symmetrical gridshell dome built at the beginning of the 20th century in Koblenz [4], Germany.

The dome on the side of its interior is demonstrated in Fig. 7.6. The ribs forming the rhombic gridshell of the dome are connected with a plank floor of a latitudinal arrangement of planks. This first layer of the shell was strengthened with successive inside layers of a spiral arrangement of planks. The connection of the ribs with the plank shell provided a spatial operation of the structure. The stiffness of the multilayer shell from planks joined with ribs allowed to make openings in the fields between crossheads in order to enhance the lighting of the interior.

The shape of a ‘crosshead’ used in the construction of gridshell domes from wood derives from an arch centre used for centuries (shown in Fig. 3.2 in Chap. 3), enriched at its end with tangs, and in the central section with an opening (key)—Fig. 7.5a. The proper cutting to size of the edges of the opening and tangs allowed to shape the spherical shell. The distinguishing feature of such shells are nodes in which three bars of a variable moment of inertia of the section converge. Such structure ensures the stiffness of the shell and makes possible the division of the wooden zone of the covering into rhombuses. **The rhombic division of the sphere distinguishes the gridshell domes from glued laminated timber from contemporary steel gridshell domes and those from glued laminated timber.**

Figure 7.7 exhibits a gridshell dome as described by the engineer Kleymienov B. in his paper [5] (1935). The dome was built in 1933–1934 over a gymnasium of the Palace of Physical Culture in Moscow. The sphere was built from crossheads made from factory-prefabricated planks and mounted on the construction yard. High quality wood, dried up to the moisture content of 17–18% was used, which ensured a higher stabilization of dimensions during the construction and operation of the facility. The nodes of the gridshell were fabricated according to the schematic in

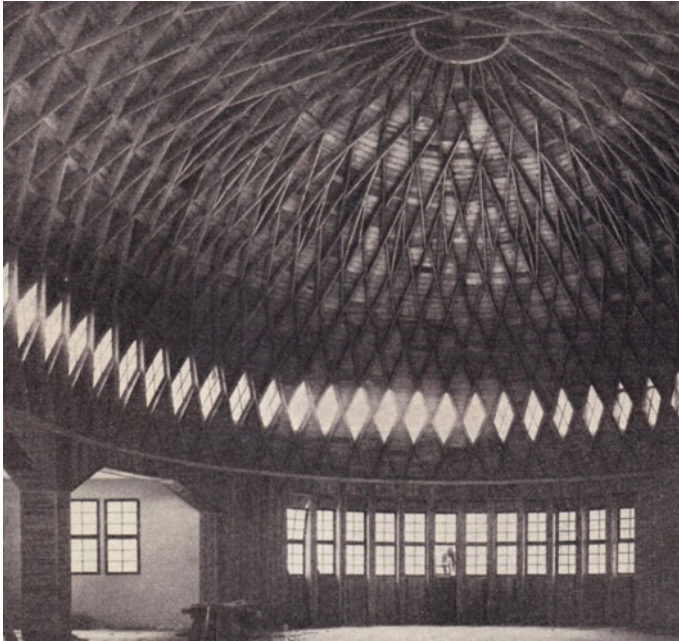


Fig. 7.6 Gridshell dome from cross braces of the Customs Office hall in Koblenz [4]

Fig. 7.7d. The connection of crossheads in the nodes were strengthened with steel bolts. The important condition of the durability of such structure is the exact adherence of crossheads in the nodes, as well as the securing of such adherence during the operation of the facility. This may be achieved owing to the meeting of three conditions: the wood has to be dry, the crossheads have to have an exact geometry, the connection in the nodes has to be careful and straightened with a fastener. Crossheads of thirteen various types were prefabricated. In each latitudinal chords crossheads of one type were used. Demonstrated in Fig. 7.7a is the mounted sphere from crossheads. Still visible on the sphere are horizontal assembly chords from planks to which the scaffolding platforms are screwed, allowing the cutting of crossheads to the shape of the sphere according to the template. Oval openings in planks required to make a node were cut on the construction yard—Fig. 7.7d, as well as the tang ends were cut off in two directions: α —inclination to the line of latitude and φ —inclination to the inside. The setting of crossheads followed in horizontal chords, forming closed circles, in accordance with the radius of the given line of latitude. Each circle was built by two working gangs going separate ways in opposite directions until their meeting. The setup of the first-level crossheads followed on the lower ring in nests designated with triangular laps determining the position of the lowest cross braces. Circa one hundred and twenty nodes were made on the lower ring. A need occurred to reduce the number of nodes at the height of the row 7 and 8 so that less bars of the gridshell reached the central upper metal

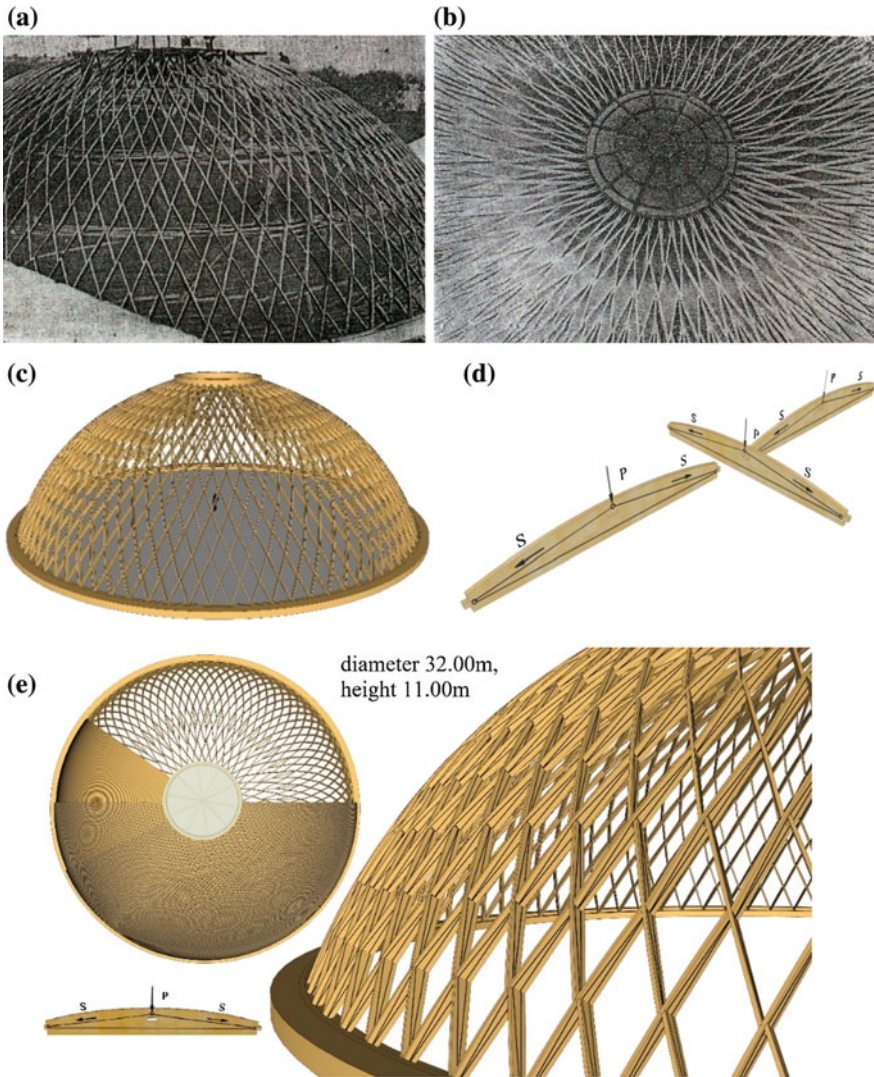


Fig. 7.7 Moscow, 1933/34, Gridshell dome from crossheads of a 32.0 m span, over the gymnasium of the Palace of Sports in Moscow [6], **a** archival photograph during the construction, **b** central, metallic upper node, **c** gridshell from crossheads reconstructed on a 3D model, **d** principle of the construction of a node of the shell from crossheads in which the bars of the Mises' truss were inscribed, **e** projection of the dome of a 32.0 m diameter and a magnification of the gridshell showing the Mises' trusses inscribed in arch centres

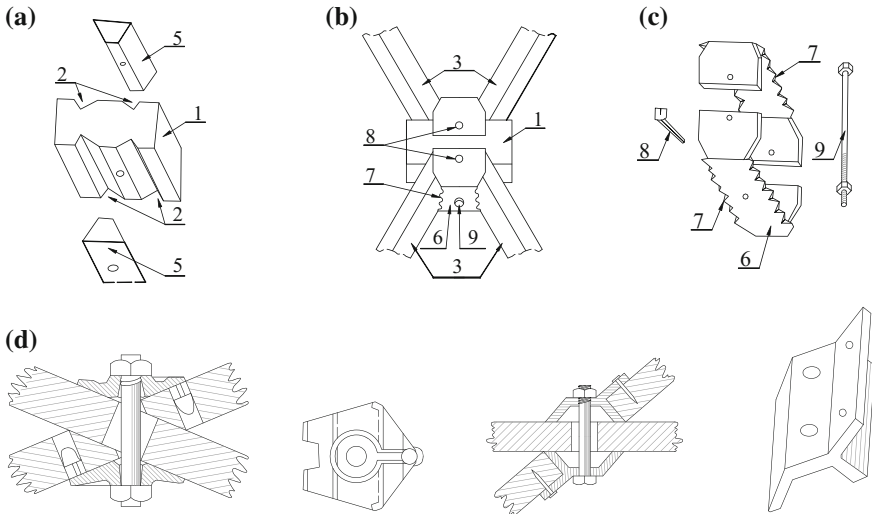


Fig. 7.8 Foreign fasteners used in the connections of arch centres according to [7], **a** wooden elements of the node **b** inclusion of the steel fasteners **c** steel elements of the node **d** iron castings connecting the crossheads of the gridshell

ring. After the reduction, circa forty nodes were made on the central metal ring. The planking was made upon prefabrication of the whole gridshell and the central upper ring, as well as the verification of all connections.

The latitudinal planking in the first-row sphere was made from quarterings of a 10–11 cm thickness. Starting with the second row until the sixth row, the planking from 5.0 cm thick planks, and higher, from 2.5 to 2.0 cm thick planks was applied. In order to make the latitudinal planking of the highest, ninth row, 2.0 cm thick planks were subjected to the interference of steam in order to achieve the required curvature. After the full planking of the dome with two layers of planks, its covering on the outside with metal sheet, the central scaffolding was removed. During the disassembly of the scaffolding, the deflection of the shell was monitored. The highest lowering of the central upper ring of a 1.50 cm value was recorded. The subsequent observations did not record an increase in the deflection.

The connections of arch centres in nodes used in the construction of axially symmetrical domes, like in closed domes, were strengthened using external foreign fasteners, e.g. pins from oak wood, (Fig. 7.8) (Pieselnik [7]), nails, iron castings and bolts.

A characteristic feature of the steel fasteners shown in Fig. 7.8 used in the wooden nodes of gridshell domes from solid wood is the strengthening of the ends of wooden bars through the clamping of the extreme sections of load-bearing elements from wood using iron castings.

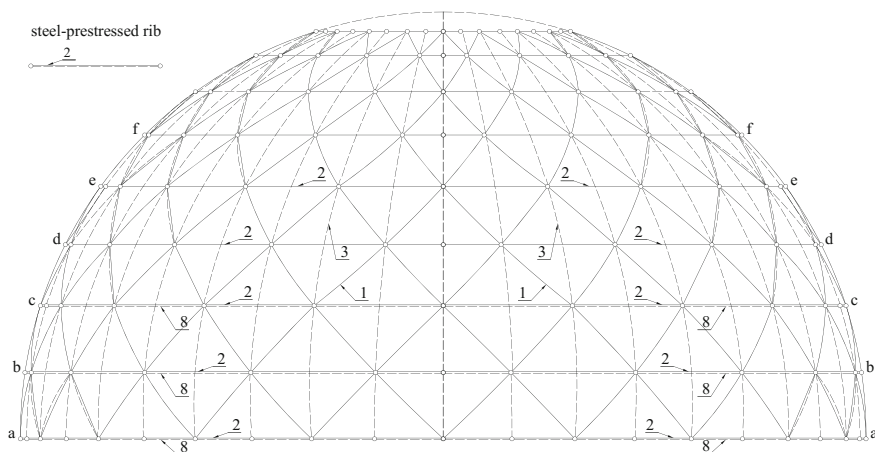


Fig. 7.9 Geometry of the gridshell dome designed by Sackur W. (1927), according to [7]

7.4 Steel-Prestressed Gridshell Domes

In the thirties of the 20th century steel-prestressed wooden domes were built. Examples of a steel-prestressed shell dome are described in Sect. 6.3 and shown in Fig. 6.5. Tshihatshiev H. A. described in his paper [7] (1947) a steel-prestressed gridshell dome as depicted in Fig. 7.9. The gridshell dome by Sackur W., protected by the German patent No. 415870 cl. 37b, 3₀ 1 from 1927, features steel tie rods in lower latitudinal layers. The wooden load-bearing construction of the Sackur's dome constitute the ribs: 1, 2 and 3 from arch centres set perpendicularly to the sphere. The elements: 1 are cross braces, 2 are latitudinal elements, prestressed at the level a, b, c, with steel bars, 3—meridional ribs.

In each dome of the dome four diagonal bars 1 and two bars of the ring-shaped chords 2 converge. In each node a short plank 4 with angular cuts made from one piece of wood or from several planks were used, as shown in Fig. 7.10. At the top and at the bottom the short plank has two angular cut-outs each place according to the template. Diagonal bars 1 were inserted in those cut-outs. The short plank 4 has side cut-outs to insert latitudinal bars 2. The strengthening of the node was achieved using side laps 6 and embracing clamps 7.

Steel bars 8 strengthening the lowest positioned wooden ribs 2 against stretching were used in the lower tensile parts of the dome. An essential role in the maintaining the shape of the dome is played by meridional ribs 3 nailed on the outside of the nodes of the dome in a distance $\underline{d} \sim$ circa 5 cm. (Fig. 7.10g) **A plank shell of the dome covering was nailed to meridional ribs 3, maintaining the distance d of the plank shell from the construction of the wooden dome. This is a next example of the care for air exchange and the provision of the ventilation for the wooden shell and ribs.**

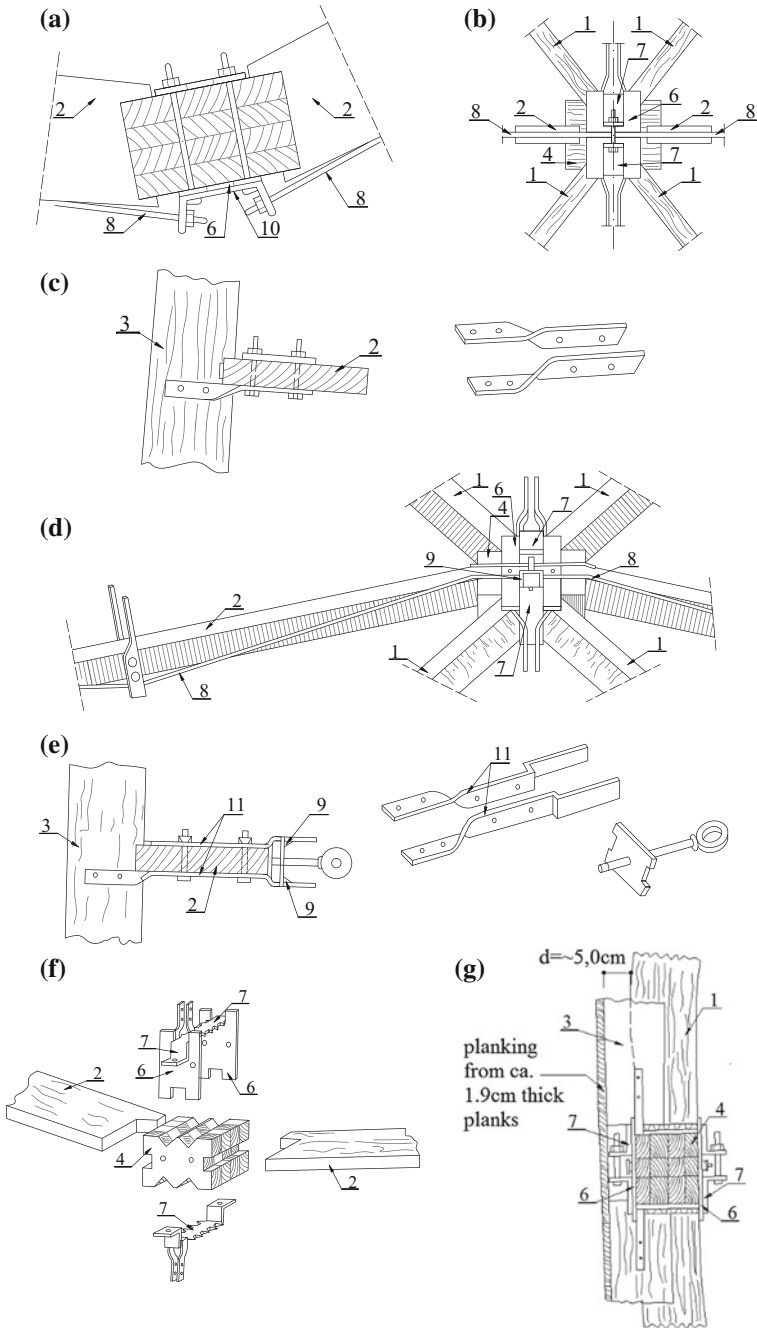


Fig. 7.10 Solutions of the nodes' structure in the Sackur's gridshell dome according to [7] (1927), **a** node from wood with mechanical clamp, **b** top view of a node, **c** connection of a rib with a steel tie rod, **d** prestressing of a latitudinal rib 2 with a steel bar 8, **e** connection of a rib with a steel tie rod, **f** construction of a dome's wooden-steel node, **g** d —distance of the covering from the structure of ribs

The meridional ribs **3**, bearing the planks of the sheathing, facilitate the air flow, exchange of humidity and drying of the wetted elements of the dome. Not flammable fire-proof boards can be mounted into the crossheads **1** on the interior inside.

The nodes of the dome are demonstrated in Fig. 7.10 compiled according to [7]. In each case, the steel elements strengthen the ends of wooden bars through the induction of a mechanical clamp. The stress of the bars **8** was achieved with threaded grip handles on ring-shaped bars **2** strengthened using laps **11** (Fig. 7.10).

Described in the paper [7] is the patent of the solution of the dome's structure, focusing on the building principle and the joining of elements. The details are not shown, including the dimensions of structural elements. It can be stated from the assessment made on the basis of Fig. 7.10 that the dimensions of load-bearing wooden elements are values calculated in several or a dozen or so centimetres.

The structure of the nodes of the Sackur's dome is complicated, however, its solution is conforming to the properties of wood. The steel elements applied strengthen through the mechanical clamp the most loaded, extreme sections nodal sections of wooden bars. Steel sheets are not introduced in the section from wood, but they embrace the most loaded extreme sections of wooden bars. Low-dimensional fasteners of a nail type are only driven into wood. The assembly of the Sackur's dome is described in the paper [7]. The building of the dome followed without an internal scaffolding. Halves of short planks **4** were laid on the lower thrust ring and the connection was made using halves of clamps **7** with the supporting ring. The lower ring from bars designated in Fig. 7.9a, b was mounted on the nodes thus built, afterwards the ring b and c was mounted, successively, up to the central upper ring.

7.5 Shell Domes on a Grid from Arch Centres Strengthened in the Node with a Flat Plank

A next example of gridshell domes is the system to cover tower water tanks used in Germany until World War II, called the GREIM system [8]. A model of such a dome from the paper [4] is shown in Fig. 7.11.

This system differs from the previously described gridshell domes from crossheads in the planks above the node being nailed on crossheads (perpendicularly to the sphere), along the helix resulting from the position of ribs. The shell of the covering of the dome shown on the left of the photograph were nailed on the planks at the angle of 60°. The planks nailed on the crossheads of the gridshell shell level the shape of the spherical coating, stiffening the nodes from arch centres, and facilitate the nailing of the second outside layer of the plank shell at the angle of 60°.

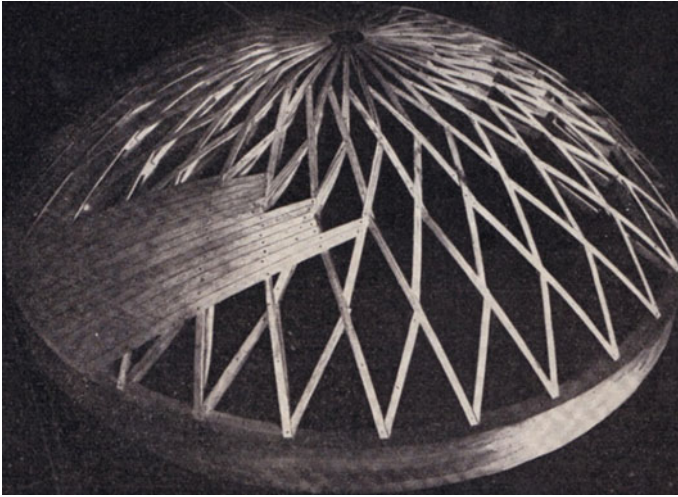


Fig. 7.11 Model of the gridshell dome of the Greim system from the paper [4]

7.6 Gridshell Dome on a Rhombic Grid from Planks

Gridshell domes made from flat planks were also built. An example of the dome of the Zollbau system, the German patent No. 456323 from 1928. Shown in Fig. 7.12a–c is the rule of building the network, as well as the geometry of the shell's grid from planks, according to [7] (1947). The dome was erected without a scaffolding. At the beginning, cross braces 1 and 1' were set on the lower supporting ring, and fastened using wooden inserts. Afterwards, bars 2' were positioned, being fastened to the ring and the ends of bars 1', and in the middle of bars 1. In a similar way the bars of successive layers were connected according to the figure of the node shown in Fig. 7.12d.

The system shown in Fig. 7.12 is distinguished by the crossheads 2 and 3 connected in the middle of the length of the lower layer's crosshead. The planks f to strengthen the node and to level the gridshell shell of the dome were nailed along the helix (quasi-meridionally) on the ends of crossheads positioned on the outside of the shell (Fig. 7.12c). The planks of the covering's shell were nailed to the spiral planks at ca. 60°. The operational rule of the dome was verified on a model made from pine wood at the scale of 1:50 and shown in Fig. 7.12c. The outside planks f, nailed spirally over the nodes of the network protect (the bars of a constant section) the sphere against the node snap-through.

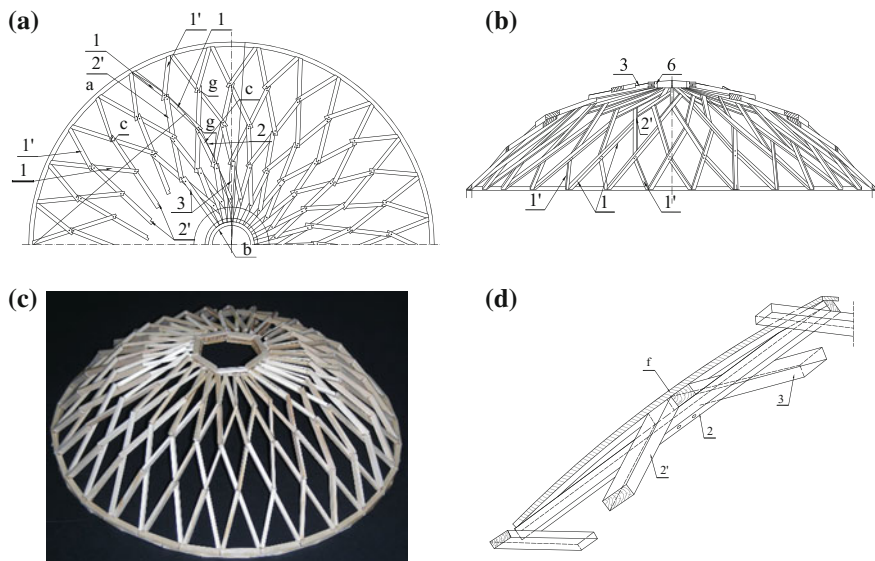


Fig. 7.12 Gridshell dome from arch centres fabricated following to the rules of the patent No. 456323 (1928) according to [7], **a** projection of the dome, **b** side view, **c** model of the dome made from pine wood, **d** rule of connecting the bars

7.7 Testing Gridshell Dome Models from Arch Centres

The author conducted the testing of shells and gridshell domes on models from various wood species and produced their computer visualizations. At each stage of building the model from wood the geometrical invariability and the spatial stiffness of the structure was verified. The models from wood were watched for many years, while checking random geometric deviations of nodes caused by the variable moisture of the environment. Attempts were also made to determine the standardization capacities of ribs-crossheads. To this aim, various models from crossheads of a similar length were built. The term ‘of a similar length’ was introduced for crossheads shown in Fig. 7.7d, f, having a similar geometry of the central part. A differentiated length of tangs made at the ends of the crosshead was assumed. This allowed to fit in a better way the ribs in the nodes of the gridshell. The models shown in Fig. 7.13 were made from arch centres ‘of a similar length’. The differences between the models consist in the differentiation: (1) angle of contact ψ between crossheads, (2) angle α of the inclination of the small arch centre to the level of the equator, (3) angle φ of the inclination of small arch centre to the dome’s inside.

The rhombic shell of the dome shown in Fig. 7.13a was built from ribs-crossheads of a similar length. The shell was shaped through changing the angle between the ribs “ ψ ” and their inclination to the level of the line of latitude

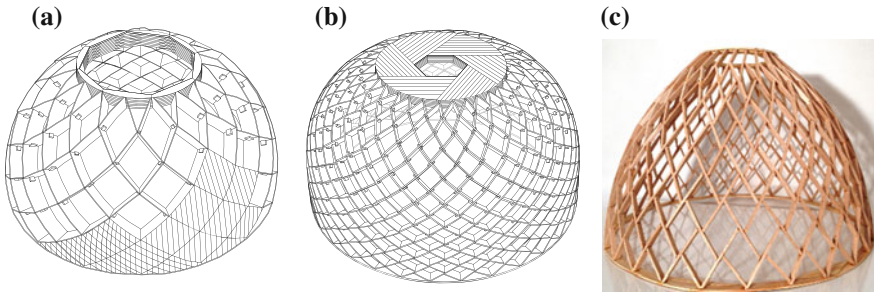


Fig. 7.13 Models of gridshell domes made from elements of a similar length, **a** hemi-spherical shell, **b** cylindrical shell combined with the hemi-spherical shell **c** ogival shell from pine wood

“ α ”. In the first lower layer the crossheads were set up at an angle $\alpha = 36^\circ$ to the level of the lower ring. The change of the angles “ ψ ” between the sides of the sphere’s rhombuses and their inclination to the dome’s inside “ φ ” leads to the closing of the vault. The closure of the last layer of crossheads in the upper ring made from horizontally laid layers of arch centres determines the shape of the dome’s sphere. The stiffness of the upper ring of the dome determines the stiffness of the gridshell of the sphere made from ribs-crossheads.

Shown in Fig. 7.13b is the model of a gridshell dome of an outside diameter of 30.0 m, made at the scale of 1:50. Crossheads of a similar length were used to build the model, the angle “ ψ ” of the arch centres’ connection and the inclination angle “ α ” to the line of latitude’s level was changed. The lower layers of crossheads were set up at an angle of 36° to the level of the lower crown. Several lower latitudinal layers of the dome were made without using the inclination of the crossheads to the inside, i.e. the angle $\varphi = 90^\circ$ was used. In the rhombuses of the lower part of the sphere just the angles “ ψ ” and “ α ” in successive layers were changed. The differentiation of the area of the rhombuses and the inclination of crossheads at an angle $\varphi < 90^\circ$ leads to the closure of the shell, as shown in Fig. 7.13b. In order to stiffen the gridshell of the sphere in the dome’s key block a multi-layer board from small planks was made. The use of the board stiffened the gridshell from crossheads better than the ring shown in Fig. 7.13c.

The differentiation of the values of the angles α , ψ , φ at a similar length of crossheads led to the building of an ogival dome, demonstrated in Fig. 3.13c.

The testing made on the models indicated difficulties in the maintaining of a fixed length of ribs-crossheads. The full standardization of the ribs of the rhombic gridshell can be maintained in single latitudinal chords at one level of the dome. The lower and the upper ring of the dome will ensure the spatial stiffness and the geometrical invariability of the gridshell structure. Many years’ observations of the models of gridshell domes from wood demonstrated that the structure of a cross-head, provided with tangs on the ends, as well as the structure of the gridshell node allow to level the changes in the geometry of ribs-crossheads due to the impact of the moisture content and ambient temperature variations on wood.

7.8 Meaning of Ribs-Crossheads in the Development of Wooden Gridshell Domes

The possibility of using transformed into crossheads of a geometry adapted to the building of double-curvature, gridshell coverings seems to be extremely advantageous (Fig. 7.16a). Probably, this is why in the Polish and foreign bibliography no descriptions of failures of such type of ribbed-gridshell domes from wood were found. It may be presumed that they succumbed to fire and biological corrosion, however, no message is available on the occurrence and course of the failure.

The phenomena of the domes' disasters are known from the descriptions of the catastrophes of the steel structures of bar domes. They consisted mainly in the collapsing of spherical domes to the inside of the facility. Illustrated in Fig. 7.14 is the catastrophe of a steel, gridshell bar dome in the exhibition area in Chorzow as described by Augustyn J. in his paper [7] (1976). The sliding-down of snow due to wind, Fig. 7.14b led to the non-symmetrical load and non-symmetrical shifts of the bar dome's nodes, which produced a dynamic node snap-through to the dome's interior.

The collapse process of the steel dome of a 30.0 m diameter, of a curvature of $1/R = 1/25 = 0.04$,¹ built from bars of a length 1091 mm up to 1026 mm, lasted for 8.0 min. The failure created due to the action of loads as well as the following errors in the design project: a low curvature of the sphere, a minor angle of the intersection of bars $\alpha = 2^\circ 32'$, as well as clearances (ca. 1.3 mm) in the openings for the bolts in nodes [9].

In the designing of steel gridshell domes polyhedrons of an identical length inscribed into a sphere were looked for. Figure 7.15 exhibits the basis divisions of the sphere used in the designing and building of gridshell domes.

The number of regular polyhedrons of the identical lengths of edges, inscribed into the sphere, is limited. Practically, the following comes into consideration: a 12-hedron built from pentagons, a 20-hedron built from triangles and a 32-hedron, semi-regular, built from 12 pentagons and 20 hexagons. The tendency is visible on the examples shown in Fig. 7.15 to design steel domes to divide the ball-like sphere into identical polygons, being the bases of pyramids the apices of which are located on the sphere. In order to form a technically useful gridshell dome various polygons having edges of a similar length, adjustable during the assembly, are used. The edges of those pyramids, are arranged at slight angles, e.g. at an angle of $2^\circ 32'$, as in the dome described in [9]. Such minimal inclination of bars, of a constant section and the moment of inertia, determines the sensibility of steel domes to the effect of the node snap-through.

As distinguished from steel structures, the effect of the node snap-through has not been noted up to the present in the bibliography related to the gridshell wooden coverings.

¹Curvature—the inverse of a radius.

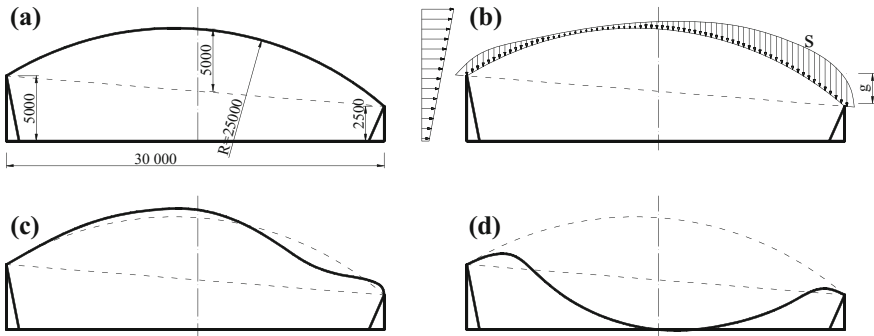


Fig. 7.14 Failure of the steel dome caused by the node snap-through, following the example of the steel dome in Chorow (Poland), (Augustyn [9])

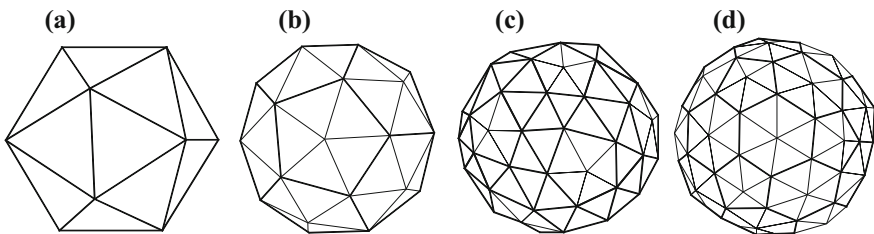


Fig. 7.15 The output polyhedrons to shape the optimum bar nets (*Poradnik projektanta konstrukcji metalowych*, Vol. 2, Part 2, Ch. 10, p. 203 Warszawa, Arkady 1982) **a** icosahedron **b** 60-hedron **c** 140-hedron **d** 180-hedron

The rib—crosshead, cut out from a beam having the geometry shown in Fig. 7.16a, has an advantageously variable moment of inertia of the section, impeding the node snap-through. The shape of the load-bearing element, the use of the variable moment of inertia of the crosshead’s section, the largest one in the section of the potential node snap-through, the combination of ribs-crossheads with the plank shell of the dome, all this immunized the wooden gridshell domes to the node snap-through. The shell combined with the ribs became many times internally statically not determinable, and the structure of the node shown in Fig. 7.7d allowed slight local random deformations associated with the natural properties of wood.

Shown in Fig. 7.16 is the shape of a ‘crosshead’ made from one plank, as well as the schematic diagramme of the distribution of internal forces at the impact of a concentrated load. Figure 7.16b illustrates the schematic diagramme of the node snap-through occurring in steel structures. It consists in the shortening of bars concurring in a node and the lowering of the node, which produces a strong rise of forces in bars, leading to the node snap-through from position “C” to position “C’”. Figure 7.16b depicts the phenomenon occurring in the so-called Richard von

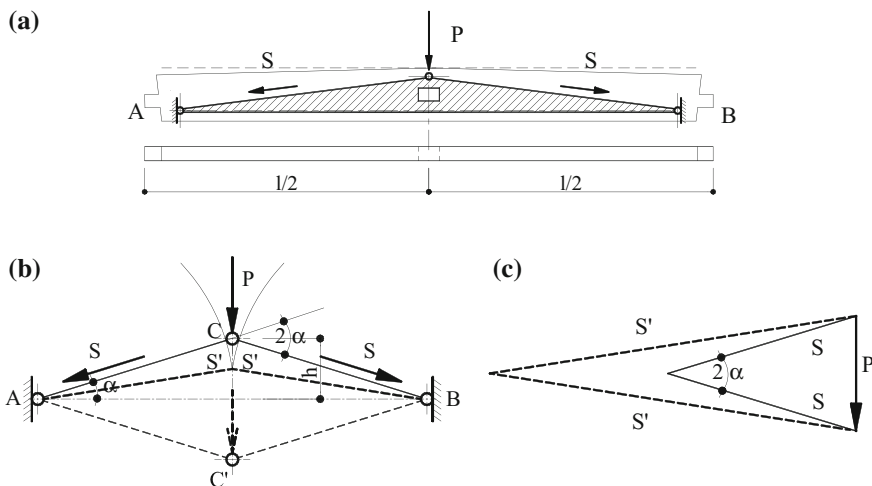


Fig. 7.16 Analysis of a node from ‘crossheads’—illustration of the geometry and the effect of the node snap-through **a** the von Mises’ truss inscribed into the shape of the arch centres used for the building of gridshell domes from wood, **b** the node snap-through effect in the von Mises’ truss. $S' \gg S$, **c** rise of forces caused by the shortening of a bar from the von Mises’s truss

Mises’ truss, who noticed the problem of the node snap-through, however, did not explain the drastic increase of forces in nodes at the impact of the load on the node [10, 11].

The axial forces can locally change in wood due to shrink or swelling at the impact of moisture as well as deformations caused by creep. The shortening of a bar results in the movement of a node to the inside of the sphere and a non-linear increase of forces within the node. It may be presumed that the designers of gridshell domes from crossheads, aware of the impact of the moisture content and temperature and a change in the length of bars from wood rom resulting from it perfected the shape of ‘ribs-crossheads’ so as to ensure the natural shift of wooden bars in nodes and to provide, at the same time, the stability of the shell. **The rhombic gridshell, the structure of the crosshead and that of the node connecting them allows to match the bars from wood in the situation of load variations, including also the thermal-moisture adaptation.** In the von Mises’ truss, inscribed into an arch centre, Fig. 7.16a, there follows a considerable exchange of bending for axial forces. **This mechanism fosters the decrease of wood creep since the smallest creep occurs at forces acting along the fibres when those forces are lower than the minimum axial critical load capacity.** The highest creep is caused by transverse forces, particularly unfavourable for wood.

The above-described phenomenon of the node snap-through was quoted due to the fact that it can appear in the structures of wooden domes built from other elements, as the diameter of the sphere’s horizontal projection increases.

7.9 Conclusions

It follows from the performed review of the bibliography that historical, gridshell domes from solid wood were built on a rhombic network of ribs-crossheads. The gridshell of the sphere of such domes were built from a perfected arch centre, provided at its ends with tangs and an opening in the middle of its span. In each node three ribs of the shell were connected. After putting on and consolidating the shell with the rhombic gridshell structure, the multi-layer, ribbed shell of the dome constituted a geometrically invariable and internally statically undeterminable structure capable of transferring non-symmetrical external loads from wind and snow, as well as from own load and thermal and moisture-related impacts.

A next stage was the structure of the rhombic gridshell from flat laid planks. Very important for the development for the building technology of domes was the application of flat planks laid spirally on the nodes of rhombuses, preventing the node snap-through of the gridshell built from flat planks of a fixed section. A multi-layer planking was applied on the protected grid, creating a geometrically invariable and reliable construction of domes with the minimum wood consumption.

The building technology of wooden domes of a rhombic gridshell structure from ribs-crossheads or flat planks and a multi-layer plank shell worked well, which is evidenced by lack of reports of the catastrophes of such domes.

An essential disadvantage of the axially symmetrical gridshell domes is the non-standardness of crossheads whose dimensions and setting vary as they approach the upper ring of the dome. A conclusion was drawn from the testing made on actual and computer models that it is possible to standardize the shape of ribs of only one latitudinal chord of the dome's shell at one level. Probably, for this reason, it was preferred to build gridshell domes in form of closed sectional vaults, stiffened with chords, among which it was possible to standardize all ribs of the rhombic gridshell. The structures in which it was possible to reach the full standardization of arch centres are shown in Figs. 7.2, and 7.4.

Notice-worthy is the fact that the first gridshell steel domes imitated the rhombic structure of gridshell wooden domes. Kersten C. in his publication [4] quotes after the German Building Journal (1926, p. 366.) the description of a steel dome for the building of the Customs Office as demonstrated in Fig. 7.17. The gridshell structure of the steel dome of a 17.0 m diameter was developed according to the rules for gridshell domes from wooden ribs-crossheads. Undoubtedly, in order to hinder the node snap-through. The creators of the later accomplishments of wooden and steel domes, while building domes from bars of a fixed section, forgot the principal rules of the building of geometrically invariable gridshell structures.

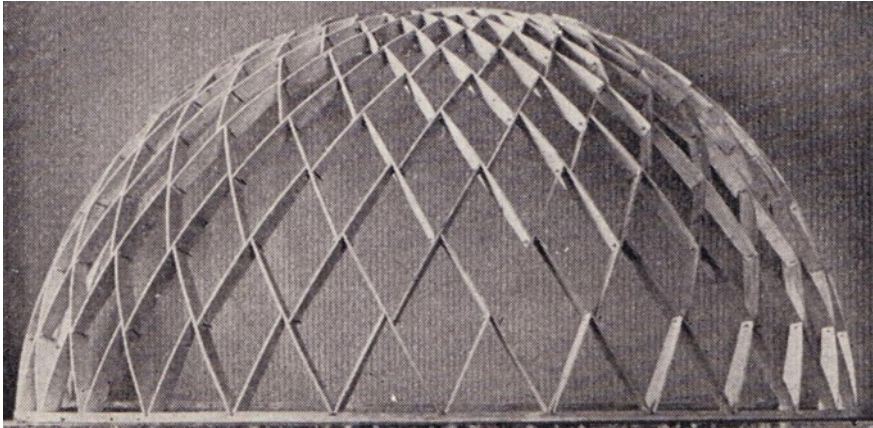


Fig. 7.17 Model of a steel dome of a 17.0 m diameter from 1926 [4]

References

1. Mischke D. *Konstrukcje drewniane*. P. W. N. Warszawa 1959.
2. Jean-Denis Godet *Atlas drewna*, Multico, Oficyna Wydawnicza, Warszawa 2008.
3. Karlsen G. G., Bolszakow W.W., Kagan M. E., Świencicki G., *Kurs dieriewiannykh konstrukcij* cz. I i II, G. I. C. L. Moskwa, Leningrad 1943.
4. Kersten C., *Freitragende Holzbauten*, Verlag von Julius Springer, Berlin 1926.
5. Klejmienow B. *Postrojka Kupola*, Stroitielnaja Promyszliennost, nr 9, str.47-48 Moskwa, wrzesień 1935.
6. Kokociński W., Poliszko S., Raczkowski J., *Pełzanie drewna w warunkach wymuszenia dynamicznego*, Reologia drewna i konstrukcji drewnianych – Sympozjum Akademii Rolniczej w Poznaniu, materiały, Zielonka 21-22 października 1982.
7. Czichacziew H. A. *Dieriewiannyje konstrukcji* Gosplanizdat, Moskwa 1947.
8. Kowal. E. A. *Kopuła kościoła w Gostyniu*, praca doktorska, Wydział Architektury, Politechnika Wrocławska, 1999.
9. Augustyn J., Śledziewski E., *Awarie konstrukcji stalowych*. Arkady, Warszawa 1976.
10. Gawęcki A. *Mechanika materiałów i konstrukcji prętowych, cz. 4*, Wydawnictwo Politechniki Poznańskiej 2003, biblioteka elektroniczna.
11. Kowal Z. Słowik J., Wawszczak W., *Zasady projektowania kopuł prętowo-żebrowych*, Inż. i Bud. 7/1992, s. 247–251.

Chapter 8

Selected Examples of Domes from Glued Laminated Timber

8.1 Introduction of Wood Gluing to Structures

In the 20th century, dome structures got separated as stand-alone systems to cover free-standing public utility building facilities. Examples of such building facilities of a ribbed construction built in Germany and Russia have been discussed in Chap. 5. One of the first stand-alone object is the dome of the circus in Ivanov (Russia), designed by Minofiev S. and Lopatin B. in 1931. The unique object is an eminent example of the soviet constructivism. It represents new elements this trend has inputted into the development of architecture throughout the world.

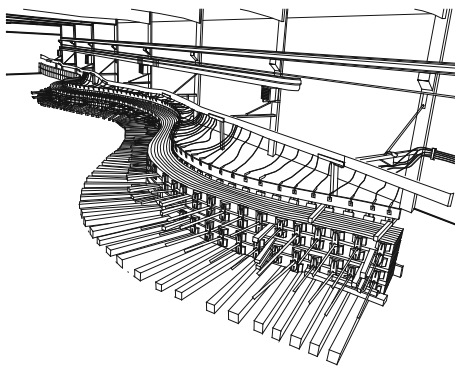
In the forties of the 20th century, the gluing technology of wood from selected sawn timber was developed in America. This material obtained from planks glued with natural casein glues, has been known since long time, also from its application in the construction of light and durable boats. In the American inland waters navigation wooden barges to convey heavy military equipment were commonly built. Light ships built from wood were characterized by a high deadweight tonnage required to float a heavy load. Shown in Fig. 8.1 is the glued ribbing of a warship that participated in the War of Secession in 1861–1865 and was used to convey the army and military equipment. The construction of the ship hull stiffenings was made from planks of white pine, glued using casein glue. During war activities the ship was sunk in the waters of the Mississippi. It was raised as late as in the second half of the 20th century. The preserved elements were reconstructed and the vessel is exhibited in the Vicksburg Battlefield Museum, USA. The photograph of the warship taken by the author in the museum is presented in Fig. 8.1.

After World War II, waterproof resorcinol glues [1] were manufactured in the USA. Owing to them, a gluing technology came into being, to glue straight planks into large-size load-bearing elements of a differentiated form. The invention of waterproof glues resulted in a quick development of the industrial building trade from wood. While also using the achievements from other field of the building

Fig. 8.1 Warship in Vicksburg. Photograph by the author



Fig. 8.2 Building schematic of glued girders



trade, including steel structures in the building of nodes, the building of large-size glued structures from wood was started. Bridges, multi-storey facilities as well as domes of diameters over 100.0 m were built. The planks dedicated to the production of glued structural elements were thoroughly selected, whilst planks of a worse quality were rejected. Before gluing, their quality was checked, the natural defects, e.g. knots, being cut out. The selected material was glued using mechanical clamp. Shown in Fig. 8.2. is the shaping of high-dimensional girders of a curvilinear form from straight planks.

Glued laminated timber was used until the second half of the 20th century for the building of large-size domes fulfilling the function of sports and exhibition halls, swimming-pool roofings, ice rinks, tennis courts, hippodromes, warehouses and manufacturing halls, sacred objects, stock-breeding buildings, public utility facilities, towers and masts, road and railway bridges, circuses, stadium stands, umbrella roofs, etc.

8.2 Examples of Prestigious Domes from Glued Laminated Timber Built in the USA

The introduction into the building trade of waterproof glues and the associated development of glued laminated timber structures concurred with the intensive development of steel structures. The combination of the achievements in those fields led to the completion of large-spatial, double-curvature wooden-steel gril-lages of a circular projection, having the form of domes. Various load-bearing systems of domes operating as stand-alone large-cubature facilities were built. Local cultural, sports, trade, hotel centres, in which the society was organized, both at the stage of the erection and operation of objects, were built around the domes.

The first large-cubature domes from glued laminated timber throughout the world were formed in the USA in the seventies of the 20th century. The cities in which the first American domes were built, such as Portland, Flagstaff, Marquette, Tacoma, acquired their recognizability in the global space. Attractive scientific and culture-creating centres developed around large-cubature American domes. The objects appearing all around them changed the image of the city and that of the life culture of their inhabitants.

Described below are the first large-cubature domes built in the USA in the 20th century by the Western Wood Structures company having its headquarters in Portland, USA. Shown in Fig. 8.3 is the location of the greatest domes from glued laminated timber built in America.

In 1977, Western Wood Structures built the first dome of a 96.96 m diameter. It was built in Portland, Oregon. The dome is shown in Fig. 8.4. In Portland, Oregon, two domes were built. In 1977, an unrepeated, distinguished by the red colour of the covering dome of a diameter of 305 ft, i.e. 96.96 m, for the University of Oregon was erected. In 1983, a dome of a lower span of ca. 40.0 m was built as well. The author took the liberty to decide about erroneous data included in the bibliography. For instance, the author Heinle and Schlaich [2] *Kuppeln aller Zeiten - aller Kulturen* (1996) specified the information about the dome in Portland using the image of the Skydome in Arizona.

The first dome, which exceeded the diameter of 100.0 m, called Skydome, is the dome presented in Fig. 8.5. The facility was commissioned in the town of Flagstaw on 17 September 1977. The dome was designed at the Rossman and Partners Design Office (architecture) and the John K. Parsons Design Office (structure). The diameter of the horizontal projection of the Skydome totals 502 ft (153.11 m),¹ the height is 142 ft (43,584 m).

¹The contemporary American feet is 0.305 m.



Fig. 8.3 Location of the largest domes built in the USA in the 20th century

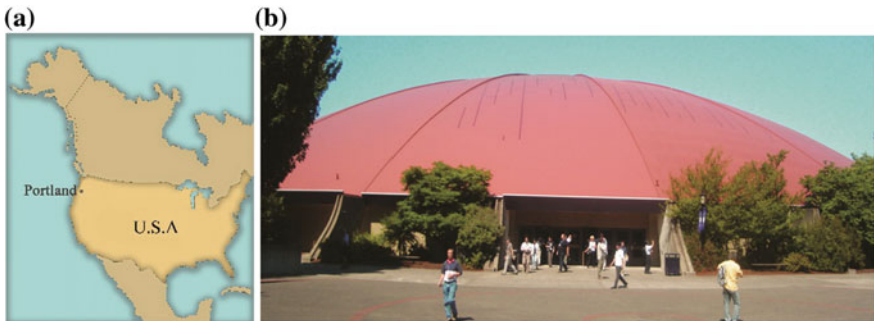


Fig. 8.4 Dome in Portland, 1977, of a 96.96 m diameter, **a** location, **b** photograph by the author of 2006

The auditorium accommodates 15,000 seats. The dome structure is made up of beams from glued laminated timber, connected with steel nodes, building triangles from the beams into spherical ones. The whole constitutes a beam grillage, characteristic of the solutions for American dome structures.

Another dome, shown in Fig. 8.6, was built in 1983 as an multi-functional facility or the academic centre in Tacoma, Washington, USA. The dome of the

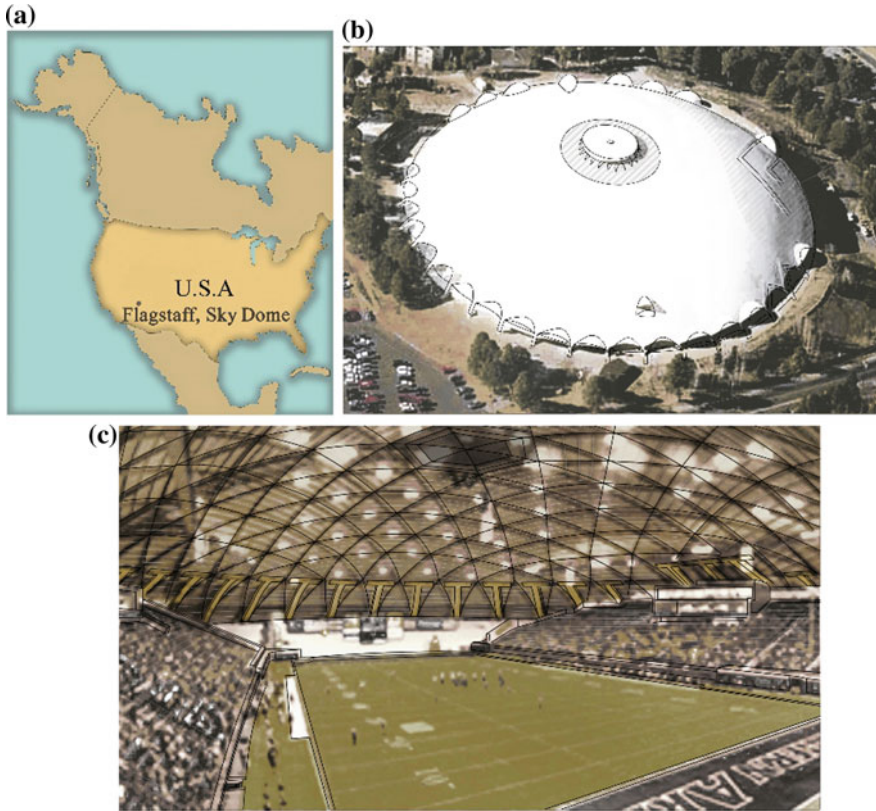


Fig. 8.5 View of the Skydome in Flagstaff, Arizona, year of construction: 1977, diameter: 153.11 m, height 43.58 m [3], **a** location, **b** view of the dome, **c** view of the structure, architect: Rossman and Partners, designed by: John K. Parsons

horizontal projection's diameter of 530 ft (160.0 m), 152 ft (46 m) high, was designed at the Mc Granahan Messenger Associates Design Office. The structure of the dome is made up of spherical triangles, whose bars were made from glued laminated timber and connected with steel nodes. Six bars were connected in each node. The bars-beams have the following dimensions: 170–230 mm wide, 750 mm high, up to 15.0 m long. The beam grillage of a duplicated curvature was built around with boards from a 5.0 cm thick plywood. The base of the spherical beam grillage constitutes a circumferential, reinforced concrete ring, transferring the forces from wooden structures onto the foundations. The structure of such a ring was recognized from materials applicable to Japanese domes.

The highest dome from glued laminated timber built to date is the object of a 536 ft (163.4) diameter, 143 ft (44 m) high, shown in Fig. 8.7. The building was commissioned on 14 September 1991, in the Northern Michigan University in

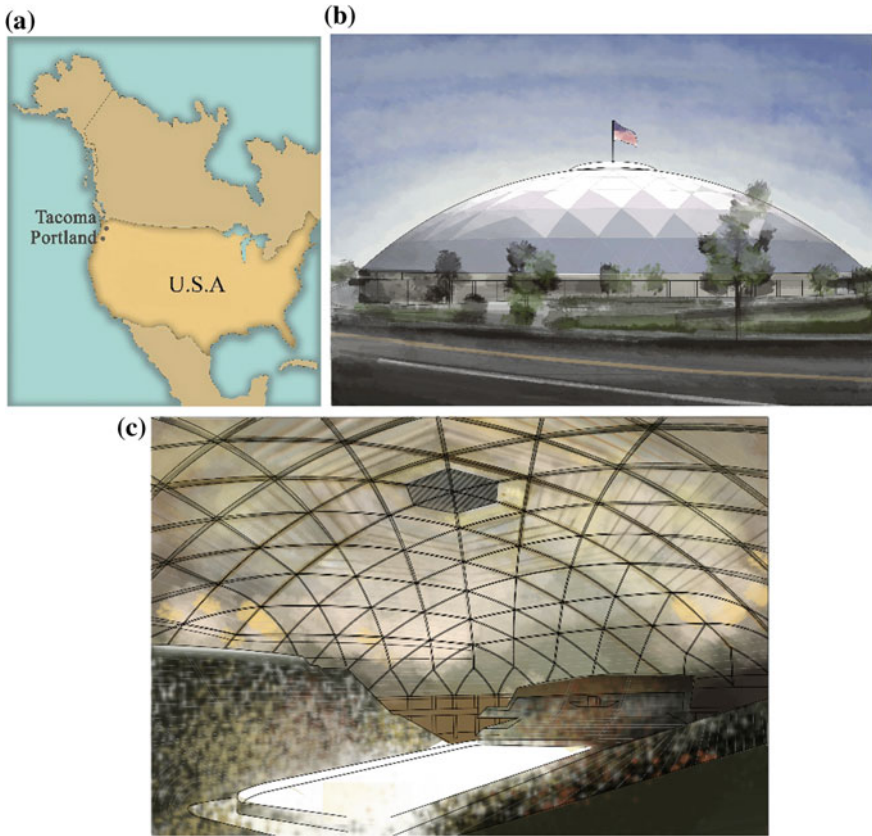


Fig. 8.6 Dome in Tacoma, 1983, diameter: 161.54 m, height: 46.0 m [3], **a** location, **b** view of the dome, **c** view of the structure, Mc Granahan Messenger Associates Design Office

Marquette, Michigan. The dome was built by Western Wood Structures, likewise the domes in Portland, Flagstaff and Tacoma.

The geodesic vision of the sphere into polygons, whose basis element is the triangle, is characteristic of all American domes. Like in domes from steel bars, bars from glued laminated timber have a constant section, and the connection of the bars of the triangular gridshell is made using steel nodes. The schematic of the node and that of the connection using wooden bars is shown in Fig. 8.8.

The bars from wood of ca. 15×76 cm dimensions, like in the Tacoma dome, connected with steel plates are shown in Fig. 8.8. The node made from steel sheets having the form of a prism with a hexagonal base connects the six main bars of the gridshell. The lateral walls of the prism are connected with perpendicular steel plates that are used to fasten wooden beams concurring in the node.

This solution is typical of the US domes and was also used in other domes built by Western Wood Structures, e.g. in the dome in Ashiro, Japan, built in 1986.

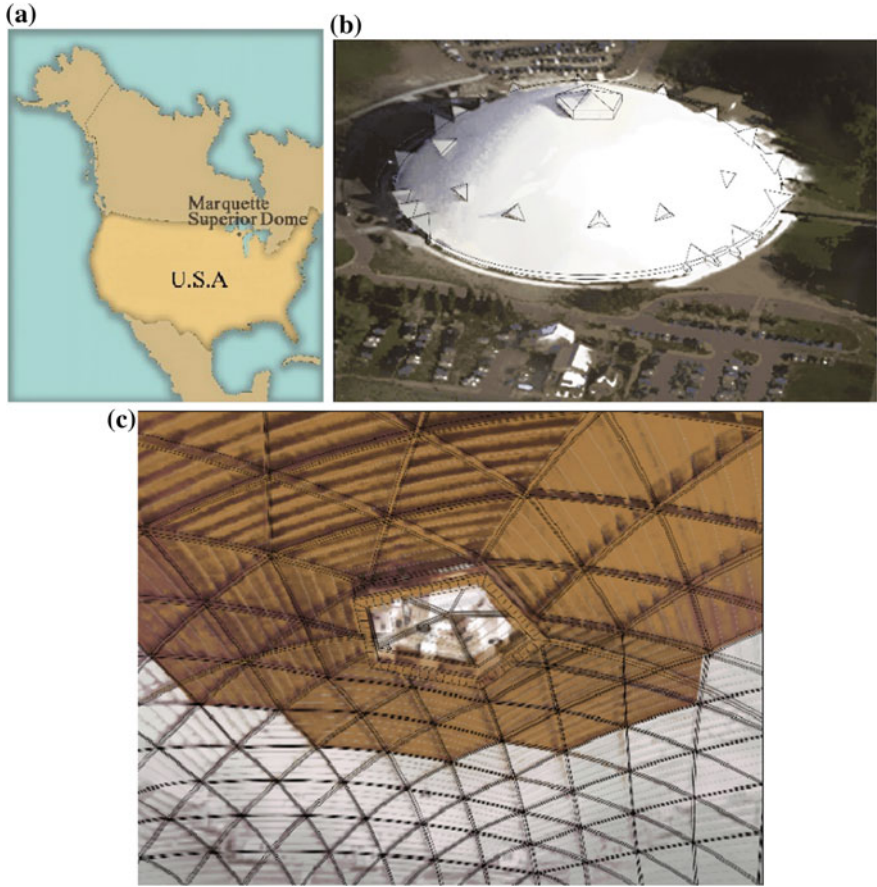
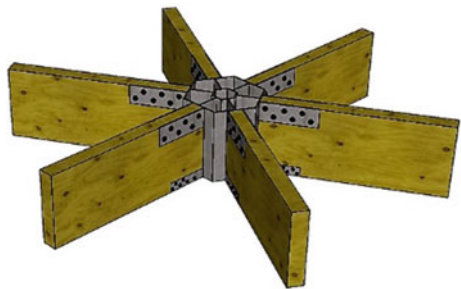


Fig. 8.7 Superior Dome in Marquette, Michigan, USA, year of construction: 1991, diameter: 163.4 m, height: 44.0 m [3], **a** location, **b** view of the dome, **c** view of the gridshell structure on the inside

Fig. 8.8 Schematic of the steel node used in American domes [4]



The construction method of bar domes from glued laminated timber, connected with massive steel nodes, as applied in American domes has been maintained and propagated throughout the world.

8.3 Examples of Domes from Glued Laminated Timber Built in Europe of a Diameter Higher Than 100.0 m

In Europe there are several design and execution centres of structures from glued laminated timber. Large-cubature facilities were created at those centres. One of the first and most beautiful domes, not only in Europe but in the world as well, is the dome shown in Fig. 8.9. The dome was built in 1980–1986 in Žilina, Slovakia, according to the design project by the engineer architect Ľudovít Kupkovič and the engineer architect Andrej Bašista [5].

The structure of the axially symmetrical dome of a 105.0 m diameter and a 18.50 m height, in the axis of the upper ring that connects the load-bearing ribs, is made of 44 bipolar ribs shown in Fig. 8.9f. The ribs were made as semi-arches of a 53.232 m length of a rectangular section of a constant width: 230 mm and a variable height up to 800 mm in the supporting section up to 1800 mm in the highest section of the meridional rib. The meridional ribs were connected with latitudinal beams, the largest of which being on the axis of ordinates +12.0 m, constituting simultaneously, “a breastwork” of windows located on the dome’s circumference—Fig. 8.9c. The whole gives an impression of a gigantic space flying saucer. The individualism of the design project is emphasized by subtly selected proportions. The construction of the dome was mounted on the central scaffolding to support the circumferential upper ring, being, at the same time, a base for the ventilator shown in Fig. 8.9b.

The designers and executors of the authors of the Žilina dome put into effect the difficult formula of the unity of form, structure and function within one architectural facility. Demonstrating a large competence in statics and architecture, they built an exceptional object of the sacral architecture. Unfortunately, despite its exceptionality, the building is not used anymore and deteriorates, which is evident from the attached photographs.

In 1985, in Oulu, Finland, a dome of a 115 m diameter, 25.0 m high, as shown in Fig. 8.10 [8] was built. The dome, like the US domes, was built in a gridshell structure from plywood of a constant section—Fig. 8.10c. The nodes were made from steel plates pasted into the wooden section—Fig. 8.10d. Upon completion of the assembly of the triangular gridshell of the dome sphere’s structure, the nodes to connect the gridshell bars were inundated with polymer concrete.

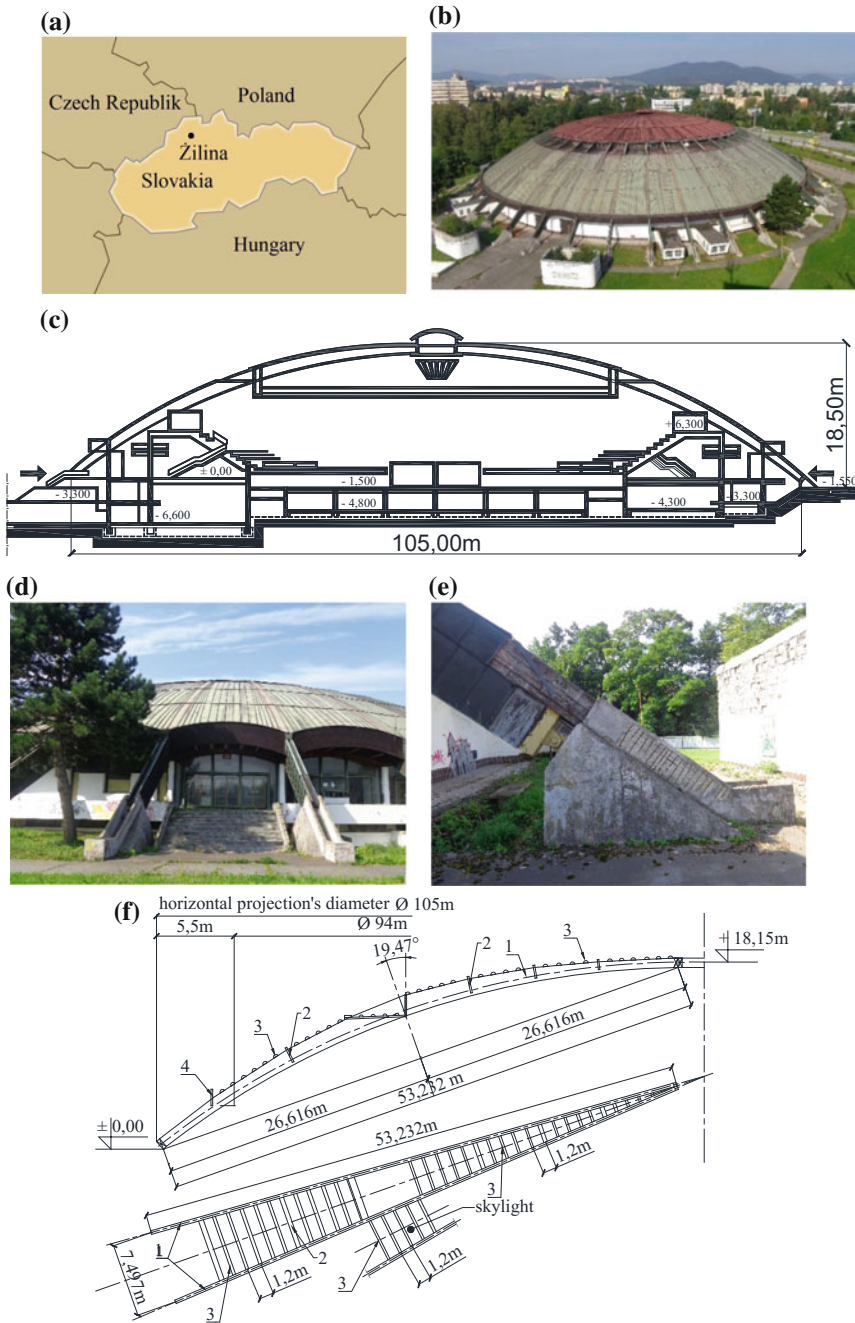


Fig. 8.9 Dome in Žilina, Slovakia. Ribbed structure of a 105 m diameter, 18.50 m high [6], **a** location, **b** view of the dome, **c** section of the dome [7], **d** entrance zone, **e** outside support of the load-bearing ribs, **f** structure and dimensions of the dome's load-bearing ribs [7]: 1—meridional load-bearing rib, 2—latitudinal stiffening ribs, 3—beams of the latitudinal planking, 4—outside beams from glued laminated timber. Photograph by the author, 2016

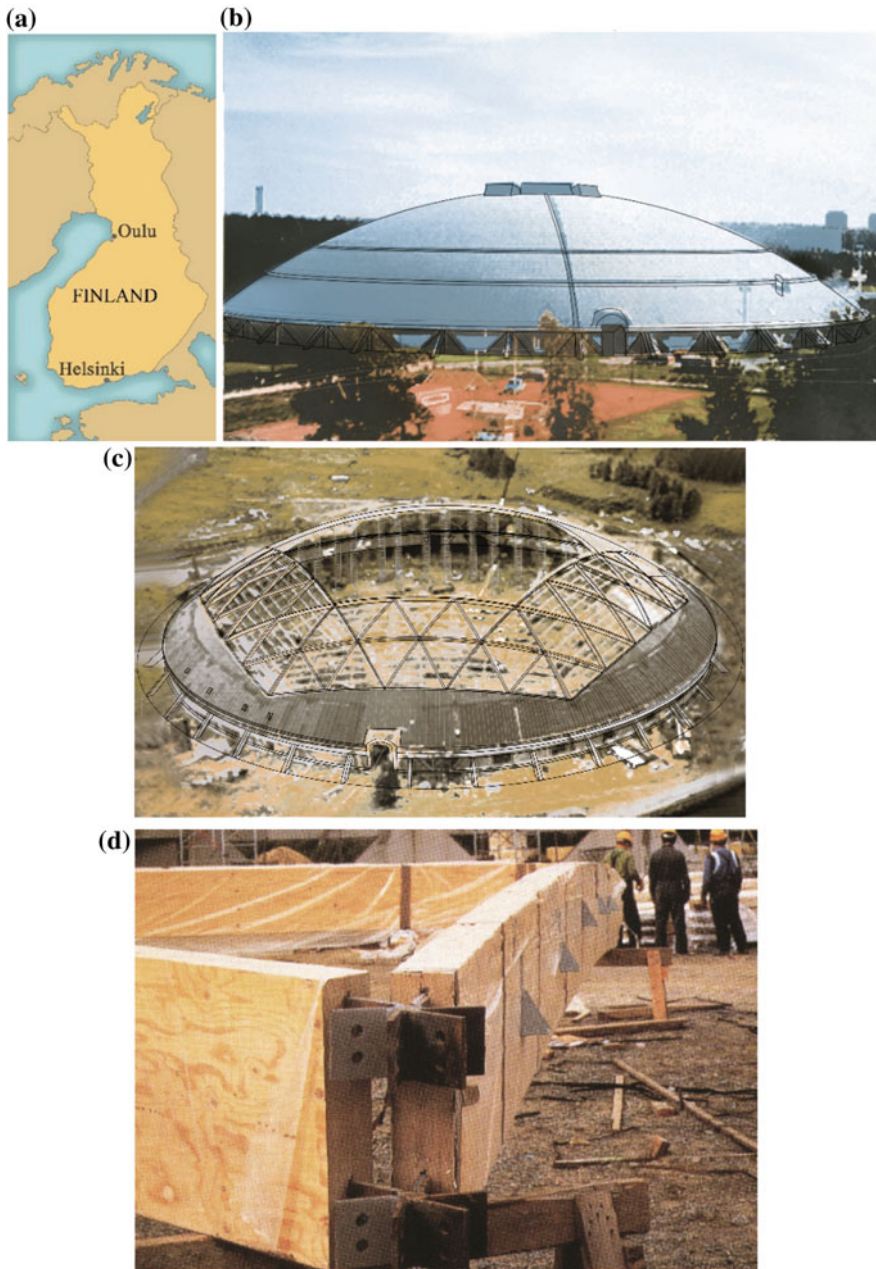


Fig. 8.10 Dome in Oulu [8] **a** location, **b** view of the dome built in 1985 of a 115.0 m diameter, 25 m high, **c** view of the gridshell structure, **d** view of the structure's nodes and bars of the dimensions: length: 12.5 m, height 70 cm, width 20.4 cm

8.4 Examples of Prestigious Domes from Glued Laminated Timber Built in Japan

On the turn of the 20th and the 21st century, large-cubature domes in the Japanese cities Izumo, Odate and Miyazaki were built. Inspired by the tradition, the architectural forms of the Japanese domes constitute eminent examples of the sacral architecture.

The Japanese domes are characterized by an individual form and structures. In Japan, three large-spatial domes were built in the cities: Izumo, Odate and Miyazaki. In order to present the original solutions of the steel-wooden structures of the Japanese domes, drawings were made and the photographs developed on the basis of the paperwork obtained by courtesy of the Director of Miyazaki Prefectural Wood Utilization Research Center, Mr. Yutaka Imura, were quoted.

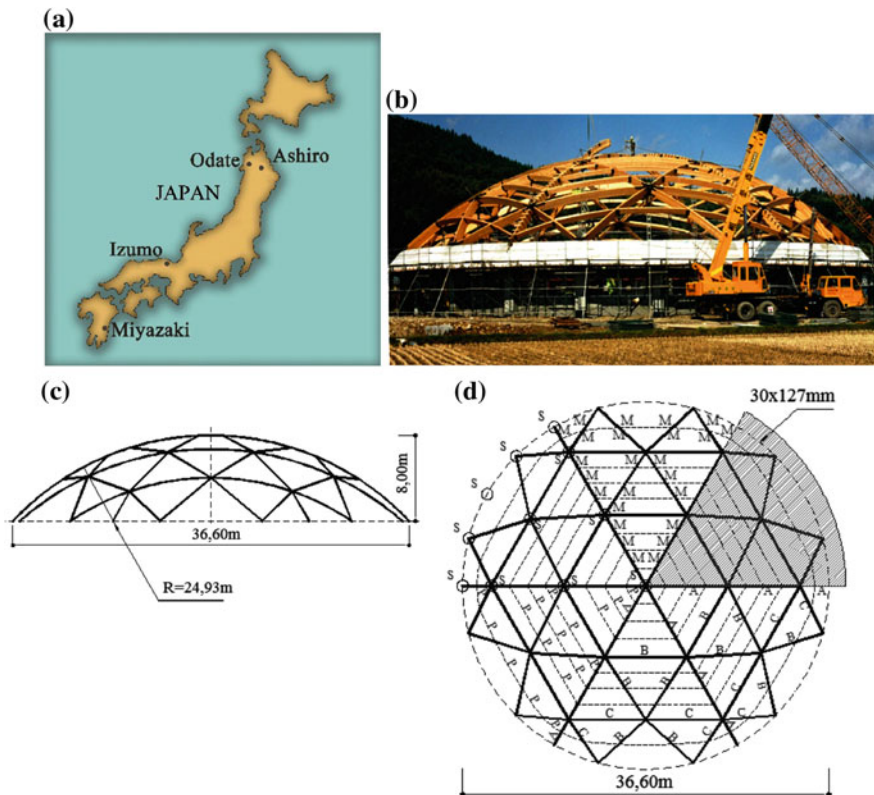


Fig. 8.11 The first dome built in Japan in 1986 according to [9] **a** location of the largest domes in Japan, **b** the dome in Ashiro during construction, **c** side view of the bar gridshell, **d** top view of the bar gridshell

In the eighties of the 20th century, Prof. Marshal Turner along with his assistant, Yutaka Imura, imported wood gluing technologies to Japan. In 1986, the US company, Western Wood Structures, built the first dome from glued laminated timber in Japan, using the constructional solutions typical of American domes.

When implementing the patents purchased from Western Wood Structures, in 1988, in the city of Ashiro in northern Japan [9] the first dome having a construction from glued laminated timber, as shown in Fig. 8.11, was built. The dome, imitating the American solutions, had a diameter of 36.0 m and a height of 8.0 m. The gridshell structure of the dome was made from beams of a rectangular section. The sectional dimensions over the length of beams are constant. The nodes, typical of the US solutions, are massive steel prisms, like in Fig. 8.8. Six bars from glued laminated timber were connected in steel nodes.

The spherical bars of the structure's gridshell were made as glued bars from wood of a 130 mm × 610 mm section, 3377 mm to 8340 mm long. The glued elements were made from planks from common Douglas fir (*Pseudotsuga menziesii*) growing in North America. The weight of the wooden construction without the casing and steel nodes per square metre of the projection amounts to 26.10 kg/m² [9].

The dome was designed for high values of the snow load and earthquake waves.

The experience acquired during the construction of the first dome in Ashiro constituted a basis for successive accomplishments, referring to the inspirations from the Japanese culture. In 1990, in Japan, the first large-size axially symmetrical dome in the city of Izumo [9], as shown in Fig. 8.12, was built. Wooden elements were made from planks from common Douglas fir (*Pseudotsuga menziesii*) growing in North America. The volume of the glued laminated timber from which the structure was made is 2150.0 m³. The diameter of the structure projection totals 49.483 m. The height of the dome including the lantern amounts to 58.783 m. The structure of the dome is made up of 36 pairs of meridional ribs. The area roofed by the dome is 16,277.00 m².

The weight of the wooden structure (without the casing) converted per m² of the projection totals 60.80 kg/m² [9]. The assembly, structure and view of the Izumo dome are shown in Fig. 8.12. Demonstrated in Fig. 8.12a is the location, and in Fig. 8.12b the view of the dome.

The erection of the semi-arches of the dome's structure shown in Fig. 8.12 followed from the building yard level on the basis of the 'opening of an umbrella'. The structure erection stages are shown in Fig. 8.12c. When lifting the central ring of a 22.0 m diameter, it was positioned at a height of 49.483 m above the floor level, and 36 meridional ribs from glued laminated timber connected pair-wise, were set up on 36 reinforced concrete posts, arranged over the circumference of the dome. At the top, the meridional ribs were anchored in the central upper steel ring of a 22.0 m diameter (Fig. 8.12g).

In this structure, a diaphanous Teflon cloth was used for the first time to make the covering of the building facility over such a large area. The structure of the dome of such large dimensions was also pre-stressed with steel tension members for

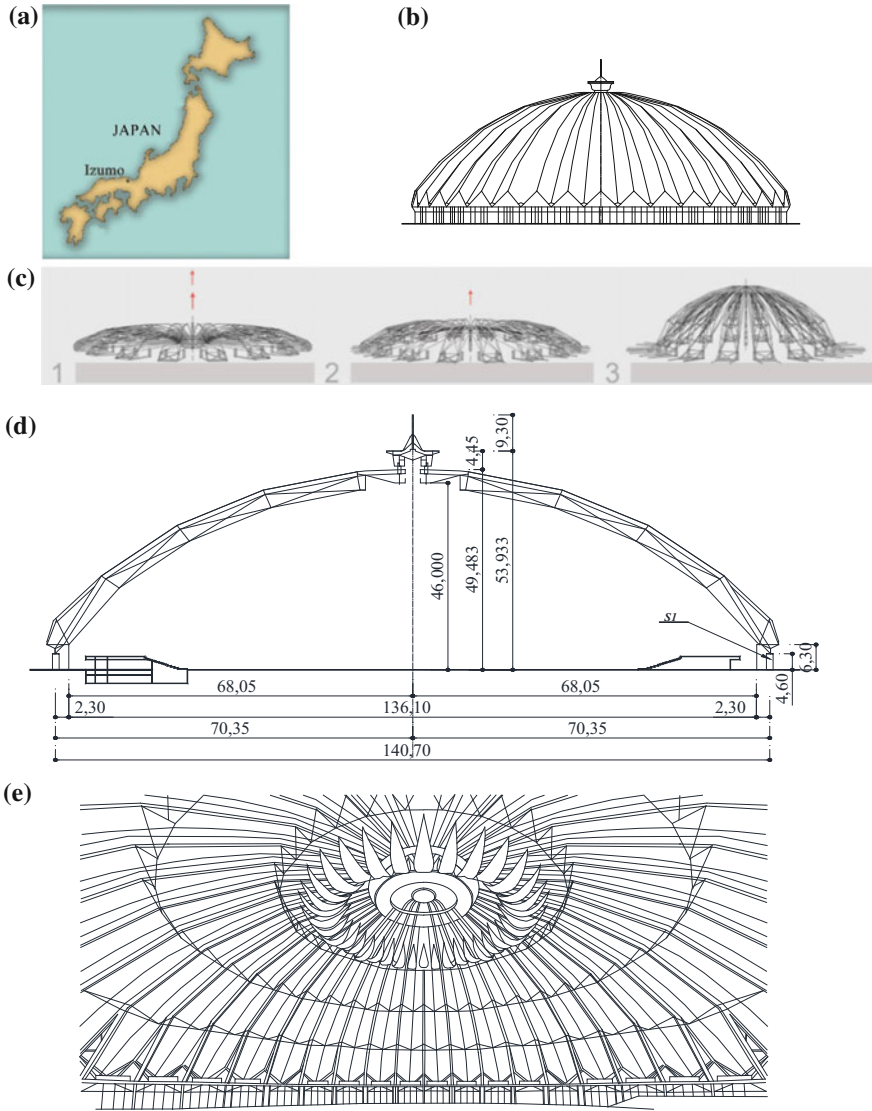


Fig. 8.12 Dome in Izumo, Japan, built in 1990 according to [9], **a** location, **b** view of the dome, **c** schematic of the assembly of load-bearing arches, **d** cross-section of the structure, **e** view of the Izumo dome's interior, **f** meridional load-bearing rib, **g** pair of meridional ribs, **h** upper steel central ring of a 22.0 m diameter, **i** node of a load-bearing rib

the first time. The semi-transparent covering with the cloth provides, at the same time, an additional illumination of the object's interior. The diaphanous Teflon covering was applied in successive accomplishments of high-cubature Japanese domes.

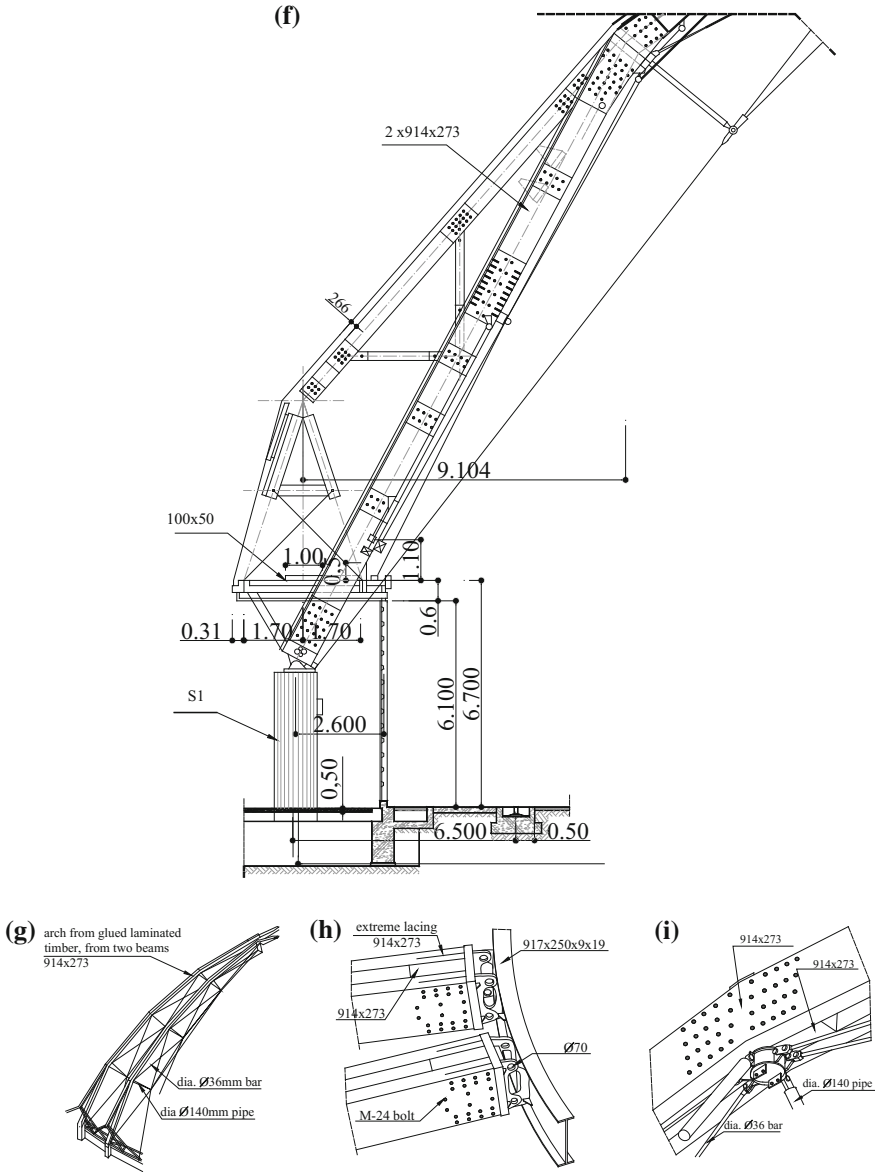


Fig. 8.12 (continued)

Shown in Fig. 8.12d is the vertical section of the structure and the basis dimensions of the object. Demonstrated in Fig. 8.12e–i are the details and the basic dimensions of some elements of the Izumo dome’s structure.

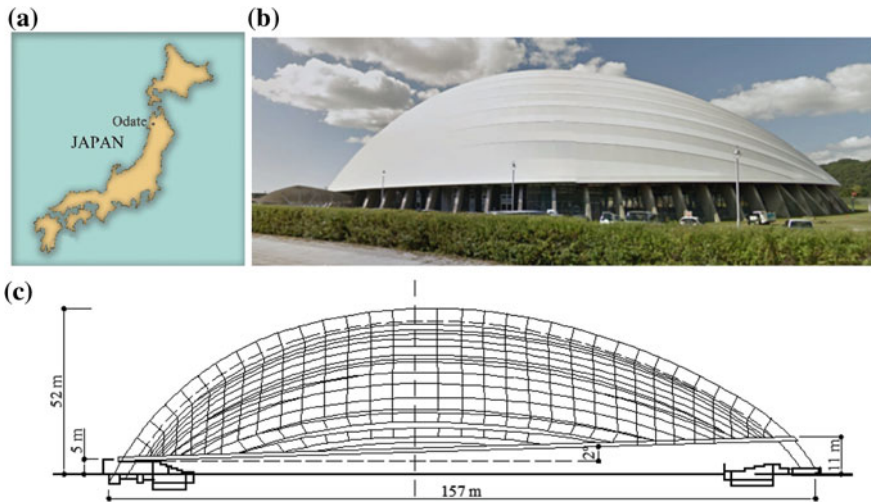


Fig. 8.13 Dome in Odate, Japan—1997 [9] **a** location, **b** view of the Odate dome in <https://www.google.pl/maps>, **c** schematic of the dome's longitudinal section

In the Izumo dome the translucent Teflon covering was used for the first time to fabricate the covering of a building facility over such a large surface. The structure of a dome of such large dimensions was also prestressed for the first time. The translucent cloth covering provides, at the same time, an additional lighting of the facility's interior. The translucent Teflon covering was applied at a later time in the accomplishments of large-cubature Japanese domes.

The largest dome from glued laminated timber was built in Japan in the city of Odate. The facility is shown in Fig. 8.13. The author of the design project is the architect Toyo Ito. The dome was built from sugi wood (*Cryptomeria japonica*) growing in the Akita Prefecture. The dome was constructed in the period of July 1995 up to June 1997. The prestigious facility accommodates many sports and spectator functions, including a football pitch. The dome has a horizontal projection of an elliptic shape and the dimensions: 153.0×157.0 m, being 52.0 m high. The total area of the horizontal projection is $21,911.0 \text{ m}^2$. The volume of the glued laminated timber from which the structure was made amounts to 4273.0 m^3 . The weight of the wooden construction converted per m^2 of the projection is $80.60 \text{ kg}/\text{m}^2$ [9].

25,000 sugi trees, growing longer than 60 years, were cut down. The planks obtained from logs were subjected to a thorough technical inspection, and damaged elements and natural wood defects were eliminated. Using due diligence, structural glued elements were made from planks.

The structural solution as shown in Figs. 8.13 and 8.14, consisting in the production of main load-bearing arches **1** in the longitudinal direction of the horizontal projection, was adopted. Those are trusses of duplicated parallel chords from glued laminated timber, connected with lacings, posts from rectangular pipes and girders

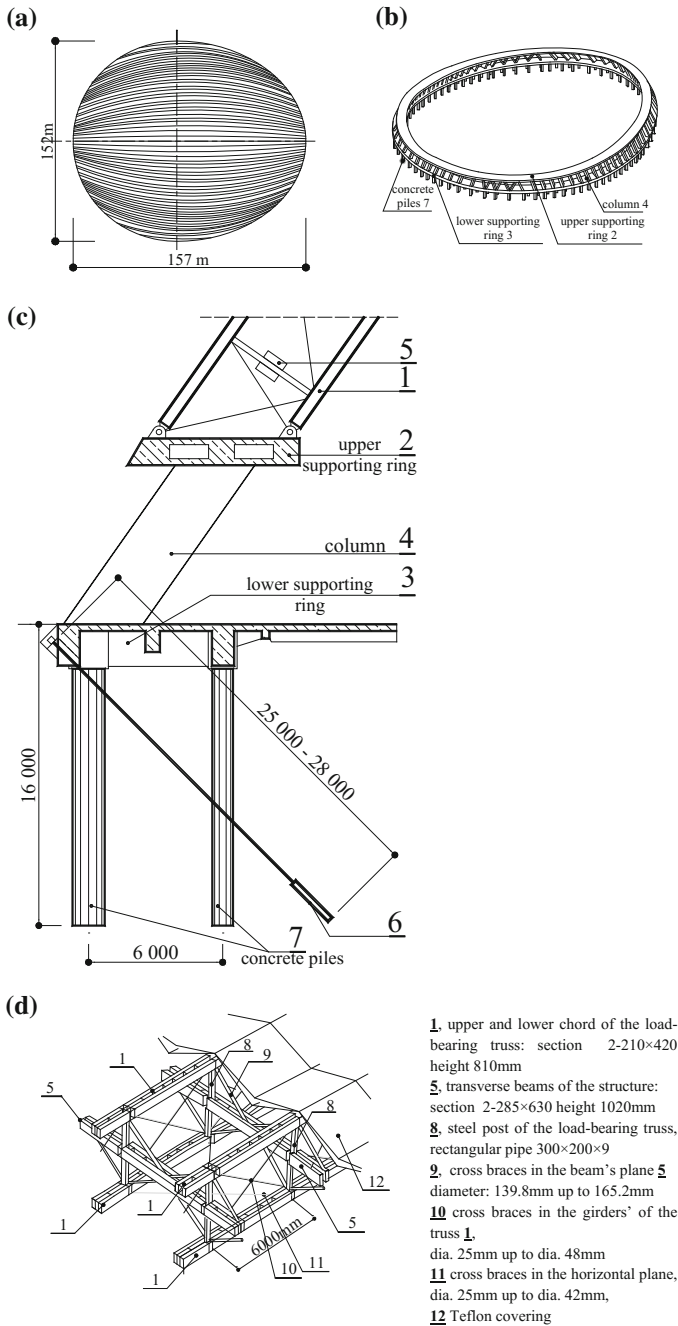


Fig. 8.14 Structure of the Odate dome according to [9], **a** schematic of the bar structure, **b** reinforced concrete structure on logs, **c** section of the lower ring of the dome's supporting structure with the view of foundations, **d**, **e** exemplary dimensions of selected steel nodes and wooden bars, **f** visualizations of bars, nodes and the covering

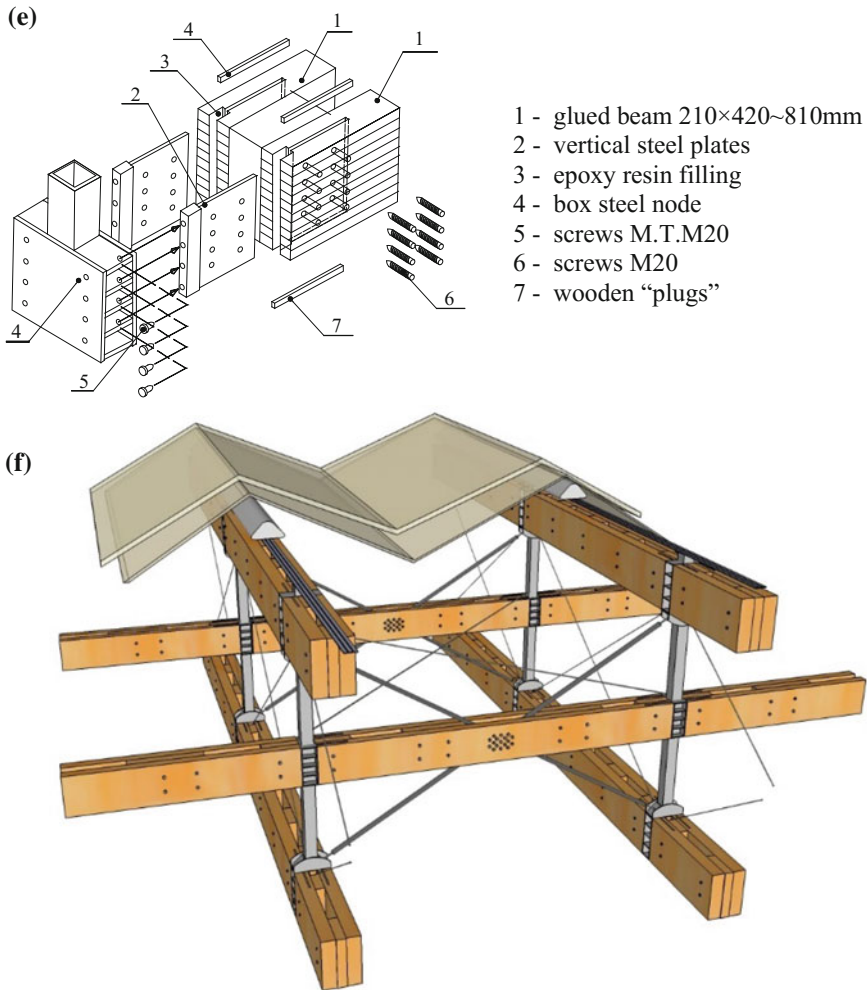
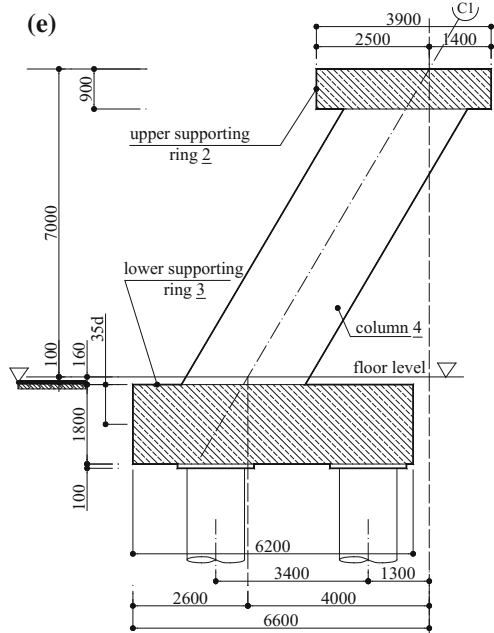
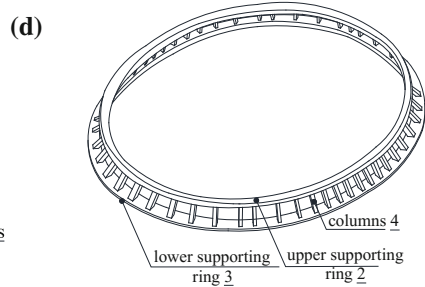
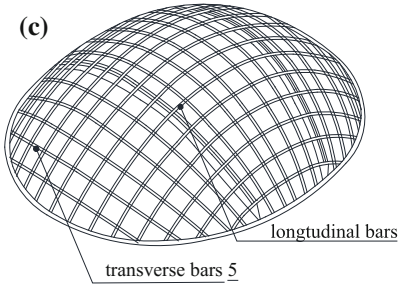
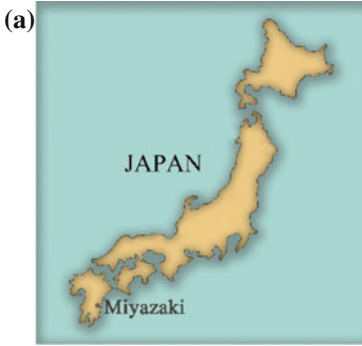


Fig. 8.14 (continued)

from steel bars. Stiffening ribs **5** from wooden beams, duplicated and connected with lacings, were introduced in the transverse direction, of a lower span of the hall. Shown in Fig. 8.14d are the selected elements and their dimensions.

The wooden bar structure built from trusses **1** and cross beams **5** is based on the duplicated lower supporting ring **2** and **3** (Fig. 8.14b). The chords of the reinforced concrete ring **2** and **3** were connected with a sloping reinforced concrete post **4**. The lower supporting ring is settled on logs—**7**, 16.0 m long. In order to reduce the strutting forces from the structure and to strengthen the anchoring of the dome in the ground, ground nails—**6**, of a length up to 28.0 m were used.



◀**Fig. 8.15** The Konohana Dome, Miyazaki, Japan [10], **a** location of the dome, **b** view, **c** schematic of the bar structure, **d** reinforced concrete supporting structure, **e** section of the duplicated ring of the supporting structure with the view of the inclined post and the foundations [10], **f** steel node connecting the wooden bar with the outside pipe for the Teflon tensioning: 1—duplicated wooden bar of a $2 \times 150 \times 1200$ mm section, 7—lacing 150×1200 mm, 6—steel bar to tension the Teflon covering according to [10], **g** photograph of the node taken by the author, **h** wooden structure with a Teflon cloth, photograph taken by the author, **i** view of the interior under the dome, photograph by the author

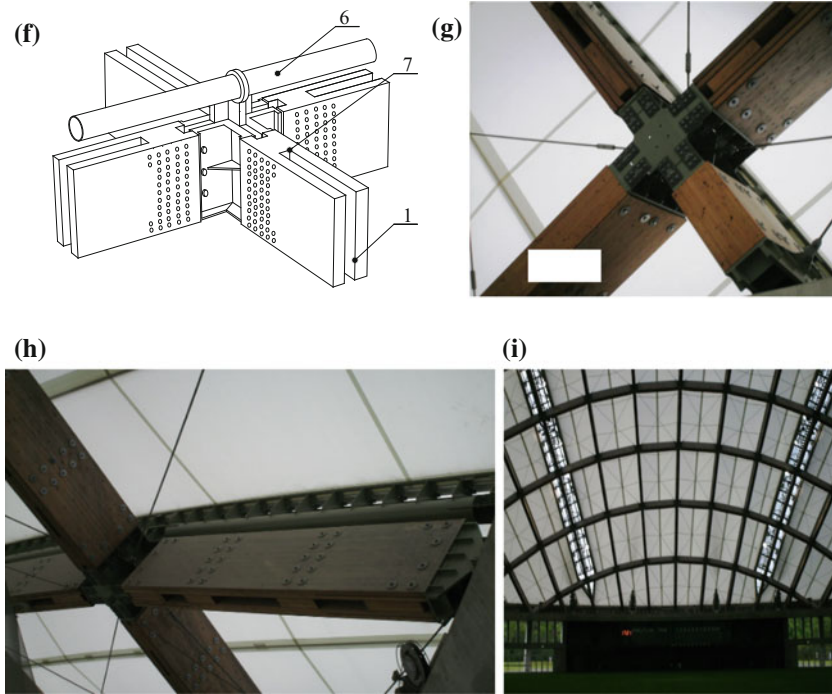


Fig. 8.15 (continued)

For his eminent achievements in the field of architecture, Toyo Ito, as the sixth designer from Japan, was awarded with the globally most prestigious Pritzker Prize [3].

In the years from December 2002 until March 2004, the wooden dome, Konohana, as shown in Fig. 8.15, was built in the city of Miyazaki, Japan. The dome of an elliptic shape of the projection has the dimensions in its interior: 122.0×104.5 m, and is 38.0 m high. The total area of the horizontal projection is $10,966.0 \text{ m}^2$. The dome was built from sugi wood (*Cryptomeria japonica*) growing in the Miyazaki Prefecture. The volume of glued laminated timber from which the wooden structure was made totals 1381.0 m^3 . The weight of the wooden structure

converted per m^2 of the projection is 42.80 kg/m^2 , and the weight of the steel from which the nodes that connect wooden bars were made amounts to 44.70 kg/m^2 [10].

The structure of the dome is made up of 17 longitudinal arches in the direction parallel to the longer diameter of the horizontal projection and 15 transverse arches in the direction of the shorter diameter. The arches, straight in some segments, are made up of duplicated glued beams of a $2 \times 150 \times 1200 \text{ mm}$ cross section, connected with wooden lacings over the bar's length (Fig. 9.14a). The bar structure was made from bars of a different length and the constant section over the given segment. The steel structure of nodes is similar and differentiated depending of the dimensions of the bars connected. The connection of beams in nodes was made using steel fasteners. Pipes were conducted through a steel loop moved out from the node to the outside of the structure, (Fig. 8.15f, h), as elements to make possible the tension of the Teflon covering. This type of compression protects the shape of the covering against deformation caused by external loads, as well as hindered the node snap-through. In the paper [10] no information is specified whether the critical load capacity was developed from the condition of the node snap-through.

The duplicated bars from glued laminated timber were connected using box steel nodes by means of 12 mm thick steel plates introduced in the wooden section. The load from the structure of the dome (Fig. 8.15c, d) as described by Iimura Yutaka in [10] (2008), is transferred by a duplicated supporting ring from reinforced concrete seated on logs. Steel bars prestress the wooden structure.

The Japanese domes as described in Sect. 8.4 are the monuments of the contemporary engineering art. They show the valuable contribution of Japan, inputted in the building of large-spatial glued laminated timber structures. Such facilities require a precise construction execution and assembly technology. The monumental structures of the Japanese domes are the synthesis of the theoretical and experimental output in this field.

The Japanese domes arouse admiration both for the architecture and the constructional solutions. For their further development, it might be advantageous to learn the problems raised in Chap. 9.

8.5 Conclusions

The accomplishments of the large-spatial domes from glued laminated timber, built in America in the second half of the 20th century appeared in the period of the intensive development of steel structures. The solutions taken from the steel structures were applied in single-layer bar structures of domes from glued laminated timber. The wood-steel, double-curvature systems of grillages of a triangular arrangement of bars over the dome's sphere came into being. The highest diameter of the horizontal projection of 163.40 m was attained in the American Superior Dome in Marquette, Michigan, USA, in 1991. The compilation of the largest domes built throughout the world is to be found in Table 8.1.

Table 8.1 Compilation of the high-cubature domes of a diameter above 100.0 m built in America, Europe and Japan

Facility designation	Location	Date of commissioning	Projection diameter [m]	Height [m]	Area of the horizontal projection [m ²]	Structure description	Wood species
Sky Dome	Flagstaff, Northern Arizona, USA	1977	153.00	43.30	18,400.0	Sphere's gridshell from triangles from glued beams	Pine, <i>Pinus palustris</i>
Tacoma Dome	Tacoma, Washington State, USA	1982	161.50	48.00	20,500.0	Sphere's gridshell from triangles from glued beams	Common Douglas fir, <i>Pseudotsuga menziesii</i>
Superior Dome	Marquette, Michigan, USA	1991	163.00	49.00	20,900.0	Sphere's gridshell from triangles from glued beams	Common Douglas fir, <i>Pseudotsuga menziesii</i>
Oulu Dome	Oulu, Bothnia, Finland, Europe	1985	115.00	23.90	10,400.0	Sphere's gridshell from triangles from glued beams connected with a coating from LVL boards (spruce wood)	Plywood
Žilina Dome	Žilina, Slovakia, Europe	1980–1986	105.00	18.50	8655.0	Meridional ribs from glued laminated timber	–
Izumo Dome	Izumo, Shimane Prefecture, Japan	1992	143.00	49.00	16,277.0	Meridional ribs, prestressed with steel, opened like umbrella ribs, Teflon covering	Common Douglas fir, <i>Pseudotsuga menziesii</i>

(continued)

Table 8.1 (continued)

Facility designation	Location	Date of commissioning	Projection diameter [m]	Height [m]	Area of the horizontal projection [m ²]	Structure description	Wood species
Odate Jukai Dome	Odate, Akita Prefecture, Japan	1997	Ellipse 178.00 × 157.00	52.00	23,218.0	Grillage: steel-wooden trusses and duplicated beams from glued laminated timber, Teflon coating	Sugi <i>Cryptomeria japonica</i>
Konohana Dome	Miyazaki, Miyazaki, Prefecture, Japan	2004	Ellipse 122.00 × 104.5	38.00	10,966.0	Beam grillage with steel nodes, Teflon nodes	Sugi <i>Cryptomeria japonica</i>

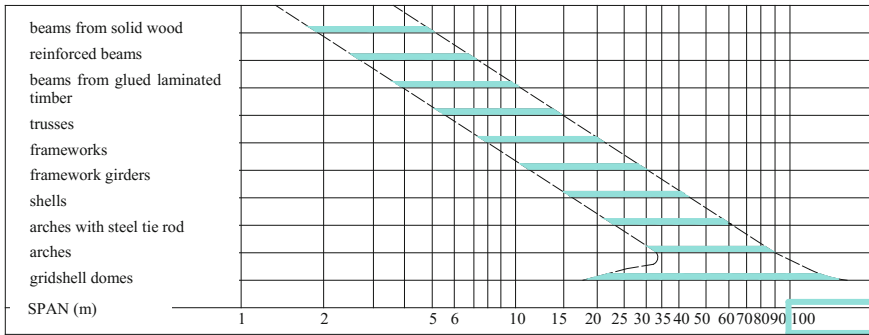


Fig. 8.16 Types of structural systems from wood and corresponding spans applied in a structure from glued laminated timber according to [9]

The fascination with new technologies caused that previous structural solutions and systems of domes from solid wood have been forgotten jointly with people who created them. The conviction of the prestigious nature of domes resulted in abandoning the building of advantageous small-cubature domes from solid wood for domes from glued laminated timber, steel and reinforced steel domes.

In the building of prestigious domes from glued laminated timber, nodes of a massive steel construction are commonly used. Steel nodes were applied in wooden-steel structures, such as Sky Dome, Tacoma, Superior Dome or domes in Izumo, Odate and Miyazaki.

Shown in Fig. 8.16 is the compilation of structural systems from wood acquired from the Japanese documentation [9] and various achievable spans owing to contemporary building technologies. As seen from the compilation, the building of a gridshell dome of a diameter of circa 200.0 m is forecasted in Japan.

Beside the objects of large-spatial domes, small-cubature domes are presently created. Those are, most often, dwelling or servicing facilities. The structure of such domes repeats the solution of large-cubature domes from glued laminated timber, which hinders its propagation. Those are objects of a diameter from several up to a dozen or so metres and their structure can be split into: (1) ribbed, (2) geodesic gridshell structure, (3) shell structure from sheet elements as shown in Fig. 8.17a. The examples propagated in the literature to promote domes demonstrate how far away sank into oblivion the skill of building domes from wood. To illustrate this, two from many examples of promoted structures of dwelling domes have been selected. Shown in Fig. 8.17a is the example characteristic of the contemporary conception of shell domes, whereas demonstrated in Fig. 8.17b is the dwelling geodesic dome from wooden bars connected with steel nodes from plates, introduced into the section of a wooden bar. The first example exhibits a dome made from plywood constituting the casing and the construction, the other example demonstrates the application of plywood as the casing for the bar construction of the geodesic dome. A structure, which was demonstrated by failures of bar domes from steel (Fig. 7.14), is not resistant to the node snap-through.

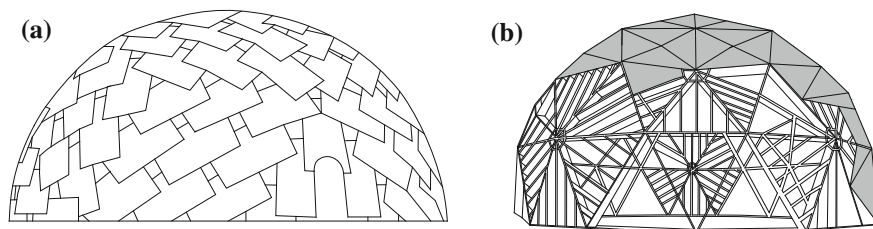


Fig. 8.17 Examples of contemporary wooden small-cubature domes (*Geodesic Domes* International paper by Giulio Neri), **a** a modern shell dome from plywood boards, **b** a dwelling geodesic dome with steel nodes

As shown in Fig. 8.17, the contemporary structures of small-cubature domes look modestly against the background of the domes from solid wood accomplished in the past: ribbed domes without steel nodes of a span up to 67.0 m (Chap. 5), and shell domes of a span up to 60.0 m (Chap. 6). **Even wood of a common quality was used to the building of the subtle constructions of domes discussed in Chaps. 4, 5, 6 and 7, thus they were built less expensively and with a lower amount of waste.**

As demonstrated by the analysis of the examples quoted, the contemporaneous spatial structures built from glued laminated timber with steel nodes consume an enormous amount of wood. According to the Japanese data [9], 60% of the best logs for the production of planks are selected from the wood acquired from a forest. From the amount of the planks obtained, 67% are selected for the gluing of structural elements. The further treatment of planks before gluing consists in the cutting-out of knots, the finish cutting of edges, whereby the amount of waste is increased. **In effect, 37.8% of wood acquired from a forest are used for the gluing of elements of the load-bearing construction, and 62.2% of wood acquired from a forest are waste.**

The result is the destruction of forests and the creation of a high amount of waste. The recycling of waste and the production of wood-based materials therefrom also is an expensive process. The structures built from glued laminated timber, including large-spatial domes are very expensive and energy-consuming investment projects.

The energy-consuming and expensive technologies allow the recycling of wooden waste into various wood-based materials. However, as demonstrated in Chap. 12 of this publication, the majority of them, plywood excluded, are not suitable for the building of durable engineering structures. The production of elements from glued laminated timber is accompanied, as it can be seen, by a high consumption of wood and high financial outlays. The connection of wooden bars using box steel nodes also enhances the energy consumption, hence the construction cost as well.

Compared in Fig. 8.18 are the sections of structural elements used for the building of domes of similar dimensions in various historical periods of time.

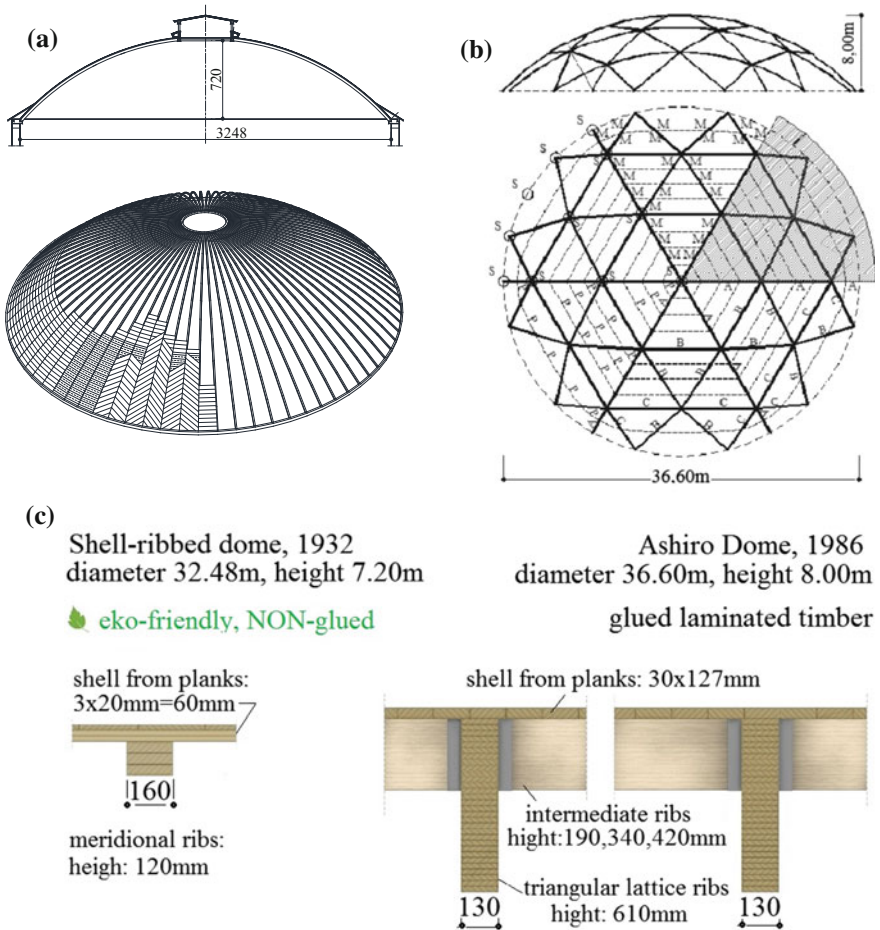


Fig. 8.18 Comparison of the dimensions of the structural elements of domes from massive wood and glued laminated timber of the similar dimensions of the horizontal projection and height, **a** The Berezhtkovskaya dome built in 1932, **b** The dome built in Ashiro, Japan, 1986, **c** sections of load-bearing elements: of ribs and the shell

The dome shown in Fig. 8.18a is a shell-ribbed dome from 1932, and was discussed in Chap. 6. The dome in Fig. 8.18b was built in the city of Ashiro, Japan, in 1986 from glued laminated timber under the US licence by Western Wood Structures and is discussed in the Sect. 8.4. The historical shell-ribbed dome shown in Fig. 8.18a impresses with a minimum consumption of wood for the structure and the timber lining, besides, of a common quality.

Collated in Table 8.2 are shell domes and shell-ribbed domes from solid wood, built until the thirties of the 20th century (lines 1 to 3) and domes of a structure from glued laminated timber, built on the turn of the 20th and 21st century (lines 4

Table 8.2 Comparison of the weights of domes from massive wood and glued laminated timber

		No.	Object	Diameter [m]	Weight of wood per m ² of projection [kg/m ²]	Weight of steel [kg/m ²]	Year of construction
Wooden domes from	Massive wood	1	Shell dome, Fig. 6.4	17.50	30.00	1.50	1907
		2	Berezniki Dome, Fig. 6.11	32.48	33.0	?	1932
		3	Moscow Dome, Fig. 6.14	59.50	58.30	1.71	1933
	Glulam timber	4	Ashiro Dome, Japan, Fig. 8.11	36.30	26.10	?	1986
		5	Izumo Dome, Japan, Fig. 8.12	140.70	60.80	?	1990
		6	Odate Dome, Japan, Figs. 8.13 and 8.14	157.0 × 152.0	80.60	?	1997
		7	Miyazaki Dome, Japan, Fig. 8.15	122.0 × 104.5	42.80	44.70	2002

to 5). The diameter of domes, the year of construction, the mass of wood and steel used up for the execution of the sphere on a per square metre basis of the dome projection are specified. It is worth noticing that in the historical domes the consumption of solid wood comprises both the structure and the timber lining of the building facility. In the domes made from solid wood, such as those in Izumo, Odate and Miyazaki, the wood consumption applies to the supporting structure only since the covering of the building facilities was made from Teflon technical fabrics. In the dome built in Miyazaki the consumption of glued laminated timber is comparable to that of steel (line 7). The mass of the steel appearing in the structures of domes from glued laminated timber exceeds many times the steel consumption in the historical domes.

While comparing the structures of the contemporary and historical domes from massive wood, it may be stated that the contemporary domes are wooden-steel, high-curvature beam grillages. **The creation and development of domes from glued laminated timber are affected by the solutions from within the scope of steel structures, omitting the whole many hundred years old output in the**

building of domes until the first half of the 20th century. The historical domes from solid wood were developed gradually. Their construction was thoroughly perfected. The natural properties of wood were considered therein it: the fibrous structure and visco-elastic features.

Despite the negative processes accompanying the building from glued laminated timber, the cubature domes discussed in this chapter became independent prestigious objects. The minimalist dome of domes is well inscribed in the scenery in each geographical position, starting with America up to Japan. The cities that invested in the building of high-spatial domes from glued laminated timber became recognizable in the global space.

Discussed in Chap. 9 are the issues affecting the further development of wooden structures, including domes from glued laminated timber.

References

1. Mielczarek Z., *Budownictwo drewniane*. Wydawnictwo Arkady, Warszawa 1994.
2. Heinle E., Schlaich I. *Kuppeln aller Zeiten - aller Kulturen*. Stuttgart. Deutsche Verlags-Anstalt 1996.
3. www.Timberline Geodesics.
4. www.takenaka.co.jp/takenaka.
5. Kupkovič L., *Sportowa hala w Žilinie*.
6. Roszyk E., Moliński W., *Pełzanie drewna w warunkach cyklicznych zmian wilgotności ściskanej strefy zginanych belek. Badania wstępne*. Annals of Warsaw Agricultural University SGGW, Forestry and Wood Technology No 53, Warszawa 2003.
7. Kuzniecowa A., W. *Tektonika i Konstrukcja Cienriczeskich Zdzanij*, Gosudarstwiennyje Izdatielstwo Architektury i Gradostroitelstwa, Moskwa 1951.
8. FINFOREST – *Viitesuunnitelmat Reference Structures*, Finforest Modular Office 2002.
9. Iimura Y., *Dokumentacja projektowa 17 kopuł z drewna wybudowanych w Japonii od roku 1986r*. Archiwum prywatne.
10. Iimura Y. *Performance Evaluation of the "Konohana Dome" built with fast – Growing Sugi* WCTE 2008 czerwiec 2-5 2008 Miyazaki Japan.

Chapter 9

Issues of the Load Capacity and Stability of Compressed Wooden Bars

9.1 Introduction

In the dome statics the interference of compressive forces is essential. As shown in the previous chapters, the builders of historical domes knew about it and used construction solutions preventing the negative effects accompanying the compression of wooden bars. The execution method of bars and of their connections in nodes takes into account the specificity of the static operation of domes and the properties of wood. The analysis of domes from solid wood in Chaps. 3–7, as well as observations arising after the juxtaposition of some fragments of the paperwork of several large-volume domes in Chap. 8, show how many difficulties have still remained to identify the model of the material, unsolved issues of the statics, stability, strength and materials science. The abandonment of the building trade from solid wood in the second half of the 20th century delayed for many years their theoretical solution.

Presently, modest attempts to introduce small-volume domes are observed (Fig. 8.17). Against this background the historical domes are attractive facilities for various methods of their utilization. In order to meet the appearing demand, also to propose structural solutions ensuring the minimum wood consumption, forgotten dome systems are discussed in Chaps. 3–7. They constitute examples of light, economical, ecological facilities, suitable also contemporarily for general use.

Since the reminder itself of the subtle structure of historical domes is insufficient, subjects of the most urgent research work, necessary for their further development, are presented in the next chapters. The issues have been stated precisely, the solution of which will affect the development of domes from solid wood.

In the present-day development of wooden dome structures, both in the case of the use of solid wood and glued laminated timber, a growing impact of solutions typical of steel structures and the introduction of steel elements is noticed.

The interoperability of wood and steel pasted into a wooden section was examined by many researchers. Starting with the 60's of the 20th century, the following authors, among others, published their results: Bondin [1], Szczuko [2], Dziuba [3]. The strengthening of a section with pasted, stiff steel elements and composites was tested by: Mielczarek [4], Dzbeński [5], Jasieńko [6]. A closer analysis of research work, especially experimental work demonstrates that the connection of steel with wood happens to be also burdened with negative effects requiring a theoretical solution.

In the optimization, essential factors to evaluate the effectiveness of domes from solid wood are the below-presented issues:

- (1) impact of the variations of the model¹ of the material of wooden bars in function of load,
- (2) use of the analogy of the loss of stability of wooden bars to the loss of stability of bars from composites reinforced longitudinally with fibre,
- (3) taking into account the essential impact of transverse forces on the critical load capacity of wooden bars,
- (4) taking into account the impact of compressive forces on the delamination of fibres at wooden bars' ends (phenomenon of 'splitting' of bar ends),
- (5) occurrence of the impact of compressive forces on the longitudinal stiffness of wooden bars,
- (6) taking into account the impact of steel sheets glued in dome nodes (rigid reinforcement) on the load capacity of wooden bars,
- (7) taking into account the concentration of shape distortions on the fibre surface in the transversely bent and compressed wooden bars,
- (8) natural warning properties of wood (acoustic emissions before the loss of load capacity), occurring on exceeding the neutral critical load capacity,
- (9) use of the paradox of the non-symmetrical strengthening of compressed wood bars under load.

9.2 Static Balance Paths of Wooden Bars in Function of Axial Load

It follows from the observation that the classic mechanics used in the calculation of wooden structures does not properly describe their behaviour in time. Wood is a fibrous material and behaves according to the rules of the wood mechanics specific for it. Wood is a natural composite of wood fibres flooded in a visco-elastic matrix. Dzbeński W. in his work [7], while conducting the testing of various wood species, adopts the visco-elastic models shown in Fig. 9.1. Described in [7] are the test

¹The model is understood as a symbolic notation of the material's properties, and not as the form of an element of a facility. The model can change along with the change of the element's or the structure's effort.

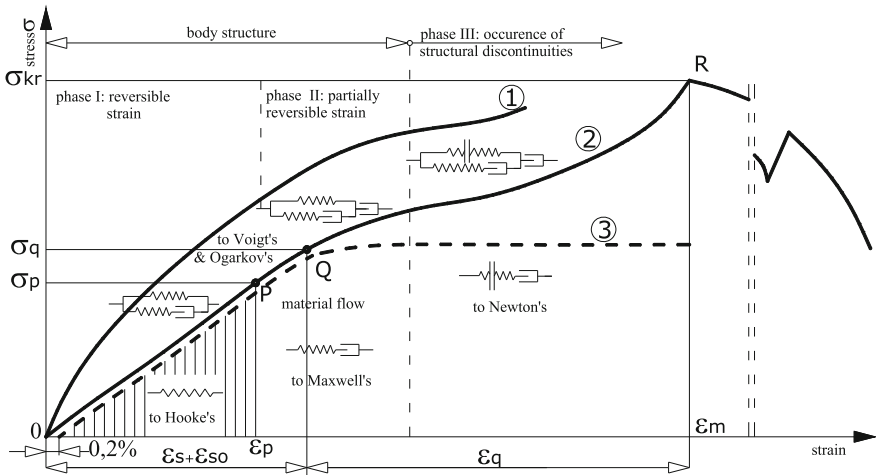


Fig. 9.1 Chart of the anisotropic material stretching under static and dynamic loads in the rheological approach from the work [7]; 1—dynamic load; 2—short-term static load; 3—long-term load

results of ca. 26,000 wood samples, as well as above 60,000 designations of structural features and physical and mechanical properties. The wood extension model has also been developed, as shown in Fig. 9.1, with assigned visco-elastic models at various extension stages until the rupture of samples. Dzbeński W. demonstrated that on the full path of the static balance of wood the model of the material changes: from the elastic Hook’s model, through the visco-elastic Maxwell’s model up to the Ogarkov’s model.

Shown in Fig. 9.1 are three SBP’s² $\sigma(\epsilon)$ dependent on the wood sample stretch ratio. The curve (1) is for high load speeds. The curve (2) is for static temporary testing. The curve (3) is for a long-term load. Dzbeński W. considers that in phase I, the behaviour of wood in the stretching test may be approximated using the Zener model for dynamic loads and the Hook model; for temporary loads. The Zener model and the standard model are the smallest visco-elastic models useful in the analysis of wood. The author recommends the Ogarkov model for the description of long-term processes. The testing by Dzbeński W. collated in the work [7] confirm that for the description of the wood behaviour description the theory of visco-elastic materials is suitable. Similar changes of the wood model in the effort build-up process should be expected in the case of compressed bars.

Dzbeński W. compared the relationships between the moduli of direct elasticity, as determined on the basis of deflections of models loaded with bending and

²Static Balance Paths (SBPs) are a commonly adopted description of the function that binds the relocation with the load of an element or a structure from any material.

shearing and those determined with ultrasonic methods using the AE³ measurement. He conducted the testing of the propagation of elastic waves in timber on the models of beams of a 11 ÷ 20 mm thickness and a 20 ÷ 80 mm width. He tested the acoustic wave propagation speed and the frequency of cross vibration of a beam on the basis of the resonance excitation of the model vibration. He developed the substitutive modulus of direct elasticity, taking into account the reduction of the modulus of direct elasticity due to shape distortions. It should be, however, emphasized that **to assess the deflections of beams from wood loaded transversely it is rational to sum up the relocations from deflection (y_M) and from shearing (y_Q): $y = y_M + y_Q$** , and not to use the substitutive modulus of direct elasticity of wood.

9.3 Analogy of the Loss of Stability of Wooden Bars to that of Composites Reinforced Axially with Fibre

In the bar wooden domes the compression is the dominant effort. Shown in Fig. 9.2 from the work by Kowal [8] are **three types of cracking of compressed composite bars reinforced longitudinally with fibre**. Such destruction forms also appear in compressed wooden bars. The greatest problems with the description and explanation were created by the case demonstrating a crack perpendicular to the axial load of thickset bars (Fig. 9.2c) of a slenderness lower than the coordinate λ_B of bifurcation.

The phenomenon of critical bifurcation of fibre-reinforced composites is shown in the chart in Fig. 9.3 acc. to [9].

Illustrated in Fig. 9.3 is the impact of the slenderness on the destruction forms of longitudinally compressed composite bars of a circular section, reinforced longitudinally with fibre. **According to [9] short bars [within the slenderness range ($0 - \lambda_B$)] cracks transversely. Bars of an average slenderness within the range of ($\lambda_B - \lambda_Q$) delaminate longitudinally. Bars of a slenderness above λ_Q undergo the destruction due to the conventional, global loss of stability.** It was shown in the paper by Kowal and Trąbski [10] that below **the coordinate λ_B of bifurcation transverse cracks of composite thickset bars appear** (Figs. 9.3 and 9.4).

An illustration of the bifurcation, understood as the split of the form of static balance and the destruction form of short composite compressed bars at the point with the coordinates (σ_B, λ_B) is the chart of the critical strength in function of slenderness $\lambda = l_w/i$ shown in Figs. 9.3 and 9.4.

³AE—acoustic emission.

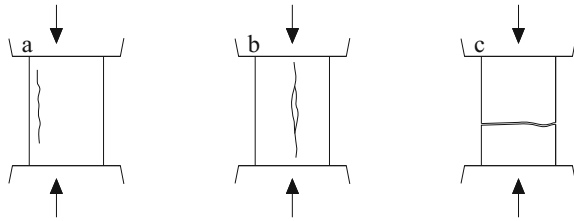


Fig. 9.2 Destruction forms of wooden bars [8]

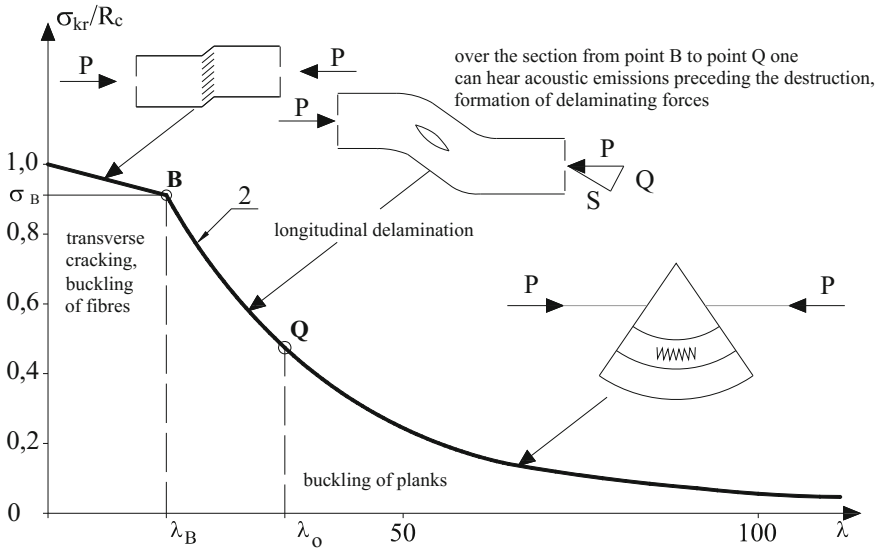


Fig. 9.3 Destruction models in various slenderness ranges of composite bars according to [9], σ_B , λ_B —coordinates of bifurcation [10]

The asymptotic regression curve 2 (Fig. 9.4) intersects in the point B the regression straight line 1. The bifurcation point B has the coordinates: σ_B and λ_B . The coordinates of the bifurcation point B segregate the destruction of compressed bars due to the local loss of stability of fibres in the composite from the destruction due to the delamination of the matrix caused by the concentration of tangential stresses between fibres (resulting in the longitudinal cracking of the compressed bar according to Figs. 9.2b and 9.3). In the range λ_B to λ_Q (Fig. 9.3) the regression curve 2 depicts the impact of transverse forces on the global buckling of the bar. The delamination of fibres may be prevented using a circumferential spiral reinforcement, for instance rowing—Kowal [11].

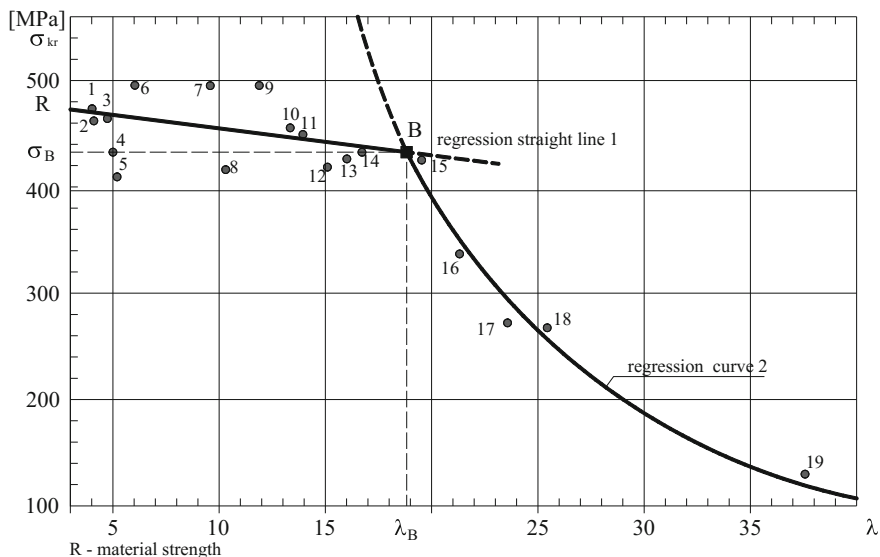


Fig. 9.4 Bifurcation (change of the balance form of a compressed bar) of the strength of composite bars reinforced longitudinally with fibre glass [10]

9.4 Impact of Transverse Forces on the Critical Load Capacity of Wooden Bars

The impact of the transverse forces accompanying the buckling on the critical load capacity of compressed bars is particularly important for wooden bars due to the low shear modulus. Timoshenko [12] resolved the issue of the impact of transverse forces on the critical load capacity of compressed bars using the Eq. (9.1):

$$\frac{1}{\sigma_{kr}} = \frac{1}{\sigma_e} + \frac{1}{G_{zr}}, \tag{9.1}$$

where: σ_e —Euler’s critical stress of a compressed bar, G_{zr} —reduced modulus of transverse elasticity depends on the shape of the cross section.

Kowal Z. in his papers [8, 13–16] and others, analysed the impact of transverse forces on the critical load capacity and limit strength of compressed composite bars. As the ratio E/G increases, the critical load capacity of bars, in particular wooden bars in which E/G is of an order of ~20 to ~25, gets reduced [17] (e.g. in steel E/G is 2.6). In reality, due to the significant dispersion of wood properties resulting from its anatomical structure, the E/G ratio is considerably higher. Shown in Fig. 9.5 according to [18] is the generation of transverse forces due to the

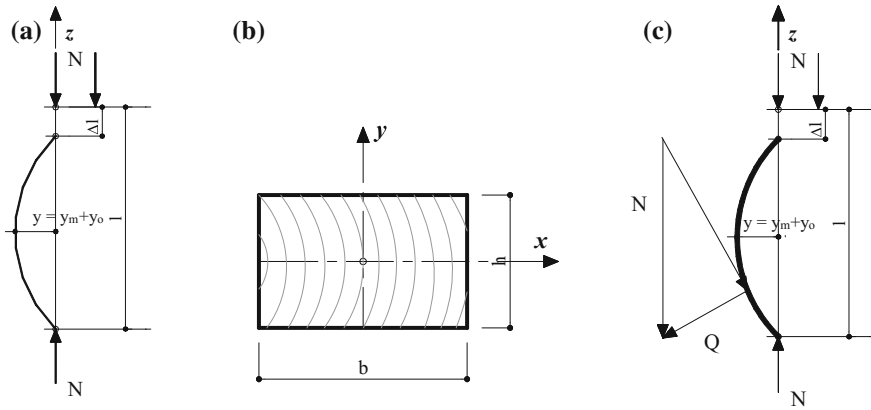


Fig. 9.5 Generation of transverse forces when compressing a wooden bar burdened with a preliminary bending [18], **a** buckling diagram, **b** bar section, **c** generation of a transverse force, y_0 —preliminary bending of a bar, y_m —translocation locating from the shortening of a bar

amplification⁴ of the preliminary bending y_0 of a bar. In Table 9.1 (Kowal [18]) the coefficients η of the impact of transverse forces on the global critical load capacity of wooden bars in function of E/G and the slenderness λ are placed.

The phenomenon of higher elasticity moduli of wood to stretching than to compression and bending was described by Dzbeński W. in his work [7]. The issue of differences in the values of wood elasticity moduli is explained by Kowal Z. in his work [18] as related to **the buckling of compressed wooden fibres in a weaker visco-elastic matrix**. Kowal Z. in the Eq. (9.2) considered, beside static translocations y_q the geometric imperfection δ_0 of the bending of wooden posts:

$$EJy^{IV} + N\left(y + y_q + \delta_0 \sin \frac{n\pi z}{l}\right)'' = 0 \tag{9.2}$$

where: $\delta = \delta_0 \sin \frac{n\pi z}{l}$ —sinusoidal geometric imperfection in compressed bars, y_q —translocation from transverse forces, EJ —sectional stiffness, N —axial load. From the Eq. (9.2) the critical load capacity N_{kr} was obtained, taking into account the impact of transverse forces to [18]:

$$N_{kr} = \frac{N_e}{1 + \frac{N_e K}{A G_{zr}}} = \frac{N_e}{\eta} \tag{9.3}$$

where: N_e —Euler’s critical load capacity, K —dimensionless coefficient of shape of the bar section ($K = 1.2$ for a rectangular section, $K = 1.195$ for a circular section), A —bar section, G_{zr} —reduced modulus of transverse elasticity.

⁴Amplification—enlargement of the transverse translocation due to the longitudinal compression of a bar.

Table 9.1 Coefficient η to reduce the critical load capacity of wooden bars of a rectangular section depending on E/G [18]

$\frac{E}{G}$	$\lambda = 10$	$\lambda = 20$	$\lambda = 30$	$\lambda = 40$	$\lambda = 50$	$\lambda = 60$
8	1.947	1.237	1.105	1.059	1.038	1.026
10	2.184	1.296	1.132	1.074	1.047	1.033
15	2.777	1.444	1.197	1.111	1.071	1.049
20	3.369	1.592	1.263	1.148	1.095	1.066
25	3.961	1.740	1.329	1.185	1.118	1.082
30	4.553	1.888	1.395	1.222	1.142	1.099
40	5.737	2.184	1.526	1.296	1.189	1.132
50	6.922	2.480	1.658	1.370	1.237	1.164
60	8.106	2.777	1.790	1.444	1.284	1.197
$\frac{E}{G}$	$\lambda = 70$	$\lambda = 80$	$\lambda = 90$	$\lambda = 100$	$\lambda = 110$	$\lambda = 120$
8	1.019	1.015	1.012	1.009	1.008	1.007
10	1.024	1.019	1.015	1.012	1.010	1.008
15	1.036	1.028	1.022	1.018	1.015	1.012
20	1.048	1.037	1.029	1.024	1.020	1.016
25	1.060	1.046	1.037	1.030	1.024	1.021
30	1.070	1.056	1.044	1.036	1.029	1.025
40	1.097	1.074	1.058	1.047	1.039	1.033
50	1.121	1.093	1.073	1.059	1.049	1.041
60	1.145	1.111	1.088	1.071	1.059	1.049

The dimensionless coefficient η of the impact of transverse forces to reduce the critical load capacity calculated from the formula (9.4) is placed in Table 9.1:

$$\eta = 1 + \frac{\pi^2 EK}{G_{tr} \lambda^2}, \quad (9.4)$$

where: $\lambda = l_w/i_{\min}$, l_w —buckling length of a bar, i_{\min} —radius of inertia of a section (Fig. 9.6).

The effort of a compressed wooden bar burdened with a preliminary bending totals:

$$\max \sigma = \frac{N}{A} + \frac{M h}{J 2} = \frac{N}{bh} \left(1 + \frac{(1 - \eta) \frac{N}{N_e} 6 \delta_0}{1 - \eta \frac{N}{N_e} h} \right) = \omega \frac{N}{bh}, \quad (9.5)$$

where: N —compressive force, δ_0 —preliminary bending of a bar, η —coefficient of the impact of transverse forces calculated from the formula (9.4) or taken from Table 9.1.

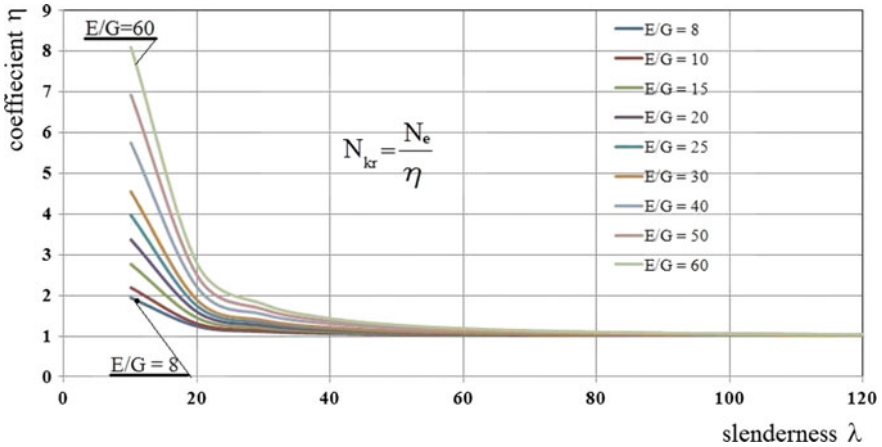


Fig. 9.6 Chart of the coefficient η to reduce the critical load capacity $N_{kr} = \frac{N_e}{\eta}$ according to Table 9.1

The longitudinal bending M of the compressed bent bar, taking into account the impact of transverse forces is determined according to [18] from the formula (9.6):

$$M = N(y_0 + \delta_0) = N\delta_0 \frac{1 + (1 - \eta) \frac{N}{N_e}}{1 - \eta \frac{N}{N_e}} \tag{9.6}$$

where: η —coefficient calculated from the formula (9.4), or from Table 9.1.

The curve 1 in Fig. 9.7 depicts an SBP (Static Balance Path) without taking into account the impact of transverse forces. The curve 2 depicts the example of an SBP taking into account the impact of transverse forces for $E/G = 20$ and the slenderness $\lambda = 40$.

The curve 3 depicts the impact of the matrix degradation that increases the translocation $y_0 + \delta_0$ on an SBP. This phenomenon is described in Sect. 9.11 on the degradation of the matrix of wooden bars at the impact of thermal treatment.

The lower is the modulus of transverse elasticity G in relation to the coefficient of direct elasticity E of material, the lower is the critical load capacity of bars from wood. The elasticity moduli E and G of wood specified in the standard [17], and papers on the basis of the standard, suggests the ratio of the coefficient of direct elasticity to the modulus of transverse elasticity of circa 20. In reality, this ratio varies depending on the wood species and individual features of the microscopic structure, also dependent on the environment. Actually, due to the considerable dispersion of the strength features of wood, the E/G ratio may be higher. Hence, an important conclusion is drawn that: **the critical load capacity of compressed wooden bars ($\sigma_{kr} = \sigma_e/\eta$) should be determined taking into account the impact of transverse forces** (shape distortions).

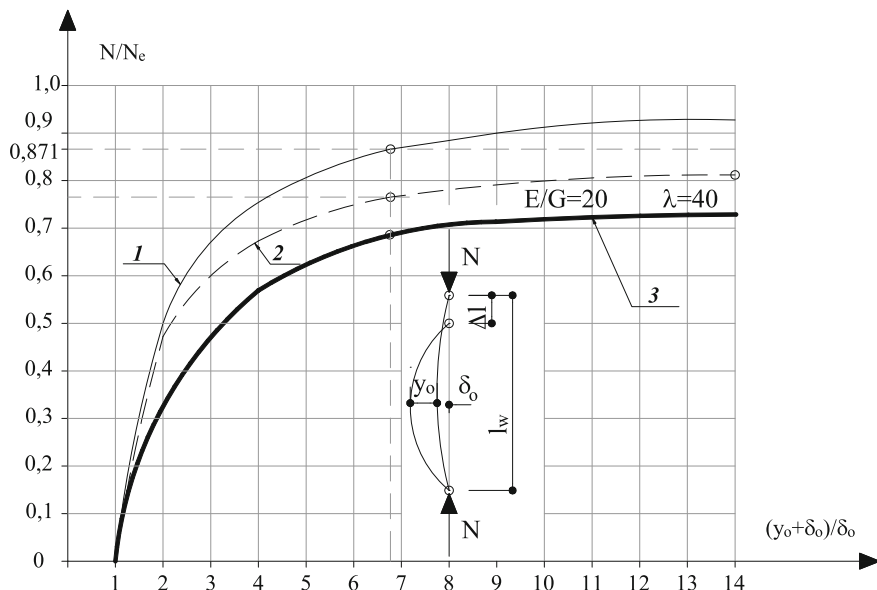


Fig. 9.7 Example of an SBP: curve (1) without impact of transverse forces, curve (2) with the impact of transverse forces, curve (3) with the impact of transverse forces and thermal treatment of wood, δ_0 —random imperfection of a wooden element [19]

Attention should be called that **the protection of wood against biologic corrosion, e.g. thermal treatment or vacuum-pressure impregnation causes the matrix degradation in wood.** The matrix degradation reduces the load capacity, especially that of wooden bars, this being depicted by the curve 3 in Fig. 9.7.

9.5 Impact of Compressive Forces on the Destruction of Wooden Bar Ends in Nodes—Cleavage of Compressed Bars' Ends

The properties of wooden bars subjected to compression are revealed not only over the length of bars. The faces of the compressed wooden bars are exposed to the preparation of fibres (Fig. 9.8) reducing the load capacity of a bar (Kowal [8]). This phenomenon may be particularly dangerous connections with the steel nodes of wooden domes (Figs. 9.11 and 9.15).

The phenomenon of the cleavage of fibres at the pale ends known from the driving of pales was resolved theoretically in the paper by Kowal [20]. The author developed the issue of the reduced load capacity of the ends of composite compressed bars, reinforced longitudinally with fibre. The behaviour of fibres inundated in the matrix is illustrated in Fig. 9.8.

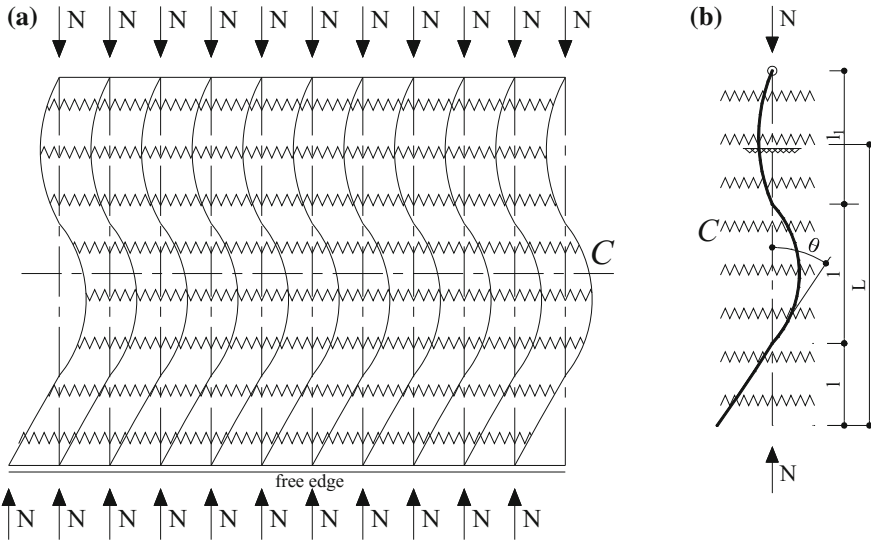


Fig. 9.8 Model of the loss of statics of fibres on the free end of a wooden bar [8], **a** on the free edge, **b** of a single fibre according to [8]. L —length of the free end of a bar

The critical load capacity of a composite bar—formula (9.7) depends to an essential degree on the coefficient K_1 —transverse stiffness of the matrix falling on one fibre:

$$N_{cr} = m \frac{\pi^2 EJ}{l_{1w}^2} + mK_1, \tag{9.7}$$

where: m —number of fibres in section, l_{1w} —buckling length of a single fibre, K_1 —transverse stiffness (shape stiffness) of the matrix falling on one fibre, E —fibre’s modulus of elasticity, J —moment of inertia of the fibre’s section.

The effect of the free edge appears in strongly loaded wooden bars of a low slenderness. **In order to avoid the reduction of the load capacity of composite bars’ ends, they should be protected with a steel ferrule (Fig. 9.9a) or a circumferential reinforcement (Fig. 9.9b, c).** Carpenters had the awareness of the need to protect the face sections of compressed wooden bars, protecting the extreme sections with ferrules and cast-iron clamps. Depicted in Fig. 9.9 is the historical solution of the protections of wooden compressed bars’ ends according to Obmiński [21], G. G. Karlsen with his team [22], Warth [23].

In the paper [11], the author demonstrated the need to protect the ends of compressed composite bars. **Thus, the historical protection of wooden bars’ ends has a sense and is worth recommending also in domes from glued laminated timber.** In [11], the method of distortion analysis and the assessment of the impact of a spiral reinforcement on the effort of compressed bars is specified.

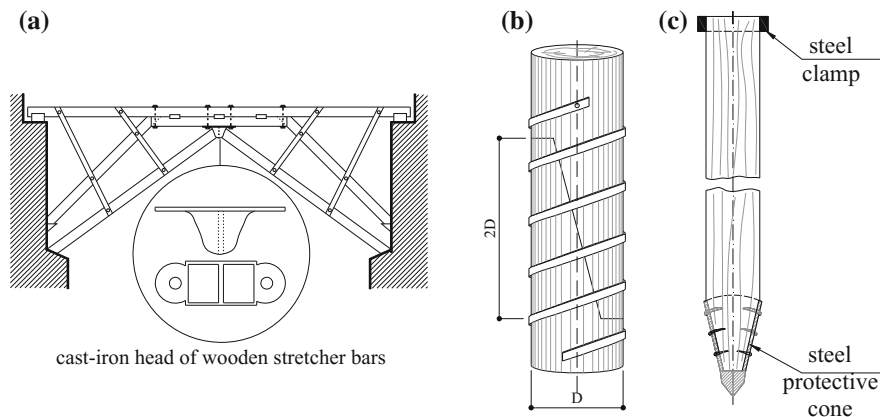


Fig. 9.9 Historical protection methods of bar ends against delamination, **a** protection of compressed bars with a cast-iron head according to Obmiński [21], **b** longitudinal connection of wooden bars' end according to [22], **c** cast-iron elements to protect the ends of a wooden log according to [23]

Shown in Fig. 9.10a is the chart of the local loss of the stability of fibres. It is shown in Fig. 9.10b that the ends of a wooden bar should be so protected with a ferrule that the Poisson effect in the fastening does not result in the cutting of fibres (Fig. 9.10b) and the matrix destruction (as in Fig. 9.11). Figure 9.10d demonstrates the generation of transverse forces caused by compressive forces.

Designated in Fig. 9.10 are: R_s —strength of a fibrous composite to compression, of a bar protected against the local loss of the stability of fibres, R_1 —strength of a fibrous composite from the condition of the preparation of a bar's fibres, (the strength drops from R_s to R_1), R_p —failure of the impact of transverse forces on the critical strength of a bar.

The occurrence of the phenomena illustrated in Fig. 9.10 is confirmed by the papers of other authors. Lachiewicz-Złotowska A., Orłowicz R. in the paper [24] described the destruction of supporting arches from glued laminated timber of a sports hall in Lodz (expertise of 2002). It is a typical delamination of the type a and b from Fig. 9.10 according to [8] that results in the reduction of the load capacity as shown in an SBP (Fig. 9.10c). The deformation as shown in Fig. 9.11 is characteristic in the supporting sections of arches where the highest compressive forces appear and are in line with the model shown in Fig. 9.8 [8]. The authors [24] made the photographs that are cited in Fig. 9.11.

The negative effects of the phenomena forecasted in the paper [8] and shown in Fig. 9.11 from the paper [24] may be eliminated with the circumferential reinforcement of bar ends with steel spirals [25] or strips from composite fibres (rowing) [11] with an alignment to the oval section. The scheme of the spiral reinforcement is shown in Fig. 9.12.

The circumferential spiral reinforcement of bar ends affects (1) the reduction of the impact of micro-fissures on the wood strength, (2) the increase in the load

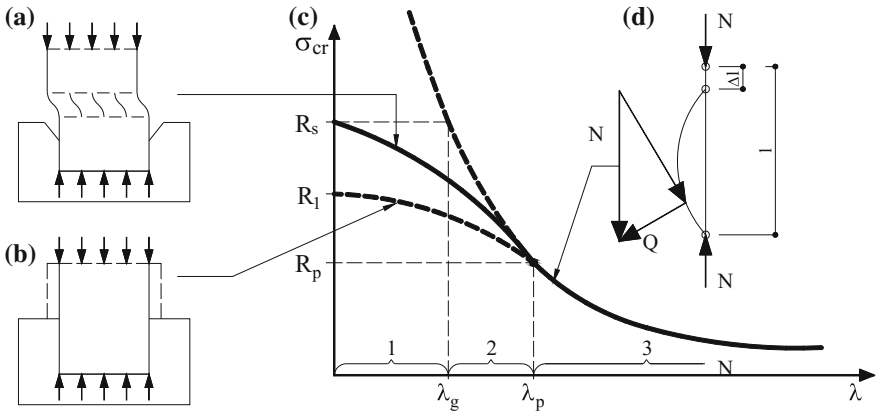


Fig. 9.10 Critical strength of composite bars according to [11]

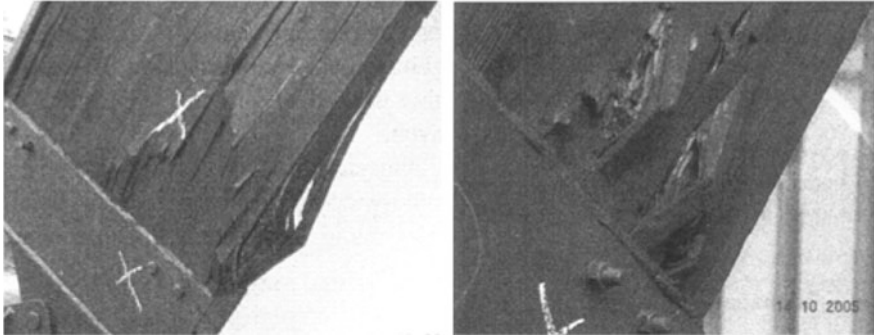


Fig. 9.11 Delamination of the fibres of arches' supporting zones [24]

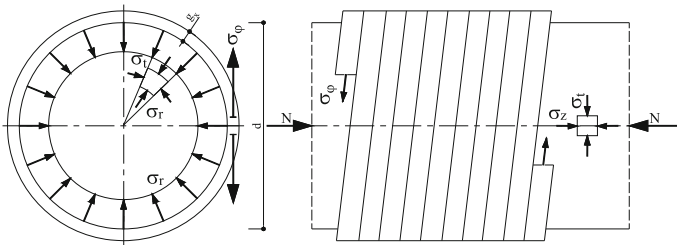


Fig. 9.12 Scheme of the spiral reinforcement with a rowing of a composite bar [11] instead of a cast-iron ferrule. σ_ϕ —circumferential stress in a rowing, σ_t —circumferential stress in the matrix, located in a distance r_i from the section centre, σ_r —stress along the radius r of the section

capacity of a wooden bar to compression, (3) counteracts the longitudinal cracking of a compressed bar from wood.

While watching the presently used solutions of wooden bars' connections in the steel nodes of high-size domes from layer-wise glued laminated timber, one gets the impression **that the awareness of the need to protect the ends of compressed wooden bars in the construction nodes has vanished.**

9.6 Impact of the Pasting of Steel Nodular Sheets on the Load Capacity of Wooden Bars

9.6.1 *Effects Accompanying the Pasting of Steel Sheets into the Extreme Section of Compressed Bars*

In the presently built wooden domes the use of nodes to connect wooden bars with steel sheets inserted into the wood section is common. Wood is sectioned with chases—Figs. 9.14 and 9.15 necessary to install node steel sheets. Stiff, steel sheets intersect the section from the bar's face, increasing the buckling effect of fibre ends, already known as the delamination of the free edge of a wooden bar. **The destruction of fibres and of the matrix caused by the intersection of the wooden section with steel sheets reduces the load capacity of compressed bars from wood.** The tightening with bolts of node steel sheets to wood also contributes to this (Fig. 9.15). **The pasting of 'stiff' steel sheets intersects fibres, destroys the matrix and intensifies the fibre buckling processes. This is supplemented by the buckling of the steel sheet or the pasted bar being compressed, expanding the wood, initiating the propagation of longitudinal cracks of bars.** These phenomena reduce the load capacity of compressed elements from wood.

The inserts of the stiff pasted reinforcement should have a sufficient critical load capacity so as not to produce as a result of the buckling the delaminating disruption of a wood bar. This is the case of the potential loss of the load capacity of a bar caused by the intersection and impact of the buckling on the load capacity of bars and beams from wood. The issue occurring in the connection of the steel sheet inserted into the wooden section is illustrated in Fig. 9.13. An example to confirm this may be the state of connections shown in Fig. 9.15 after the testing for the compression of wooden bars with pasted-in sheets of the dome in Odate, Japan. It is possible to explain, on the basis of the work [26], the behaviour of the compressed sheet burdened with a preliminary bending $\delta_0 \sin n\pi x/l$ pasted into a visco-elastic medium. The differential Eq. (9.8) of the balance of forces from load and the interference of the medium has the form:

$$EJy^{IV} + N\left(y + \delta_0 \sin \frac{n\pi x}{l}\right)^{II} + Cy = 0 \quad (9.8)$$

where: $y^{IV} = d^4y/dx^4$, $y^{II} = d^2y/dx^2$,

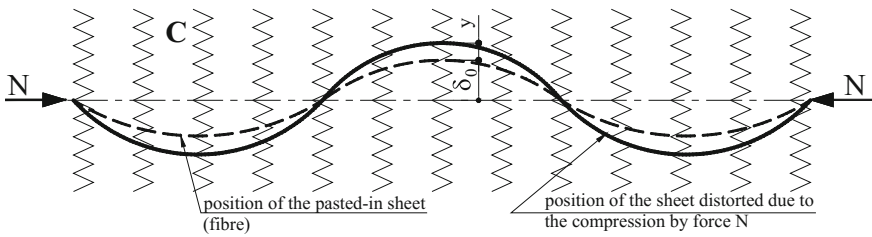


Fig. 9.13 Buckling of the compressed bar burdened with the preliminary bending δ_0 in the visco-elastic medium [26]

The solution of the Eq. (9.8) for $\delta_0 = 0$ is the formula (9.9) for the critical load capacity of the pasted-in steel sheet:

$$N_{kr} = 2\sqrt{CEJ}, \tag{9.9}$$

where: C —elasticity modulus of the wood used in the construction calculated in the transverse direction to the pasted-in steel sheet, EJ —stiffness of the steel sheet, E —modulus of direct elasticity of steel, J —moment of inertia of the steel sheet section.

The wood disrupting forces caused by the buckling of the pasted-in sheet increase when geometric imperfections δ_0 of the steel sheet grow and there is the freedom of the outside wood surface distortions.

In order to convince the reader about the importance of the issues of the impact of the placement of steel elements in wooden elements, the example made available by courtesy of the Miyazaki Prefectural Wood Utilization Research Centre and the Rothoblaas company was used, as discussed in the next chapter.

9.6.2 Examples of the Destruction of Wooden Bars' Ends Fastened in Steel Nodes

Shown in Fig. 9.14 is the connection of bars in the nodes of the Konohana dome in Miyazaki (Japan), built in 2002. Figure 9.14a depicts the section of the original load-bearing bar of the dome. The load-bearing bar from glued laminated timber is made up of the branches each 15.0 cm wide and is connected with lacings of the same thickness. The total dimensions of the section of the forces of the lacing are $\times (150 + 150 + 150) \times 1200$ mm.

12 mm thick steel sheets were inserted into the supporting sections of the beam branches (Fig. 9.14b) over the whole height of the beam. The steel sheets were used to connect the wooden bar with the steel node of the dome. The pasted-in steel sheets were connected with the branches of the wooden section with dia. 16 mm and dia. 24 mm bolts. In the photograph—(Fig. 9.14a) the dimensions of the

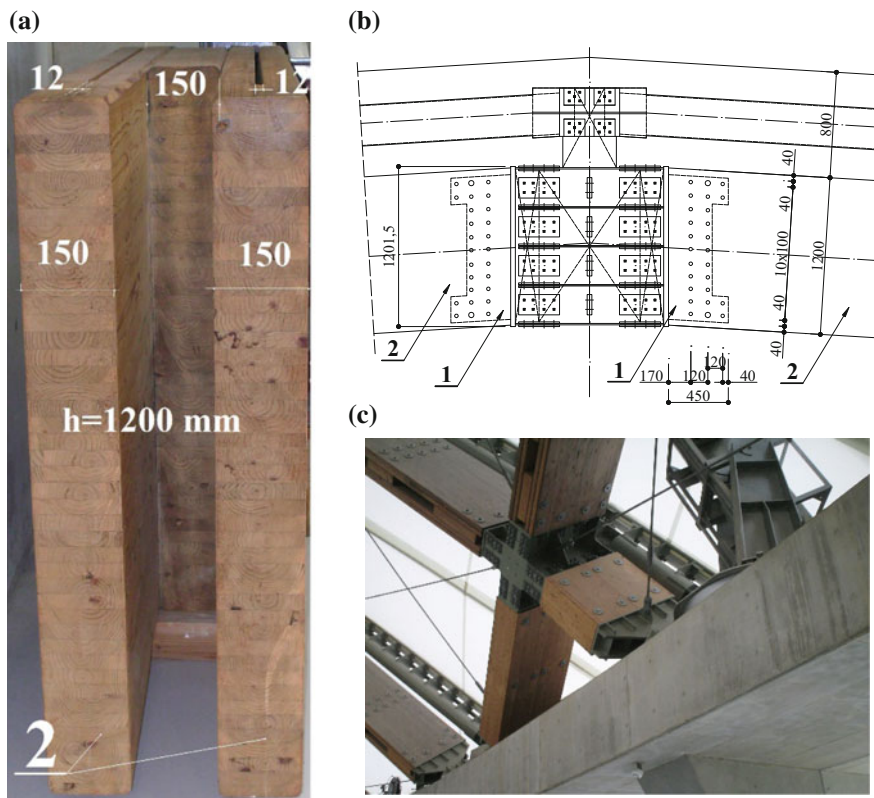


Fig. 9.14 Steel node of the Konohana dome in Miyazaki, Japan, from 2002, photo by the author; **a** section of the wooden $3 \times 150 \times 1200$ mm with cuts for node sheets, **b** design of the steel node to [27], **c** view of the node on the lower reinforced concrete thrust ring; 1—pasting in steel sheet, 12.0 mm thick, 2—bar of $3 \times 150 \times 1200$ mm dimensions

section and of the chases prepared for the steel sheets of the wooden structure of the Konohana dome were brought onto the section of the bar.

The chases prepared for steel sheets were cut in the extreme section of the wooden bar, intersecting fibres in the most disadvantageous for fibrous composite place—on the free edge of the bar. This solution, as it follows from the works by Kowal Z., reduces the load capacity of the connected ends of the bars and in consequence, the load capacity of the whole structure.

The confirmation of this solutions constitute the photographs in Fig. 9.15 [28] of the bars from glued laminated timber (*Cryptomeria japonica*) of the dome in Odate (Japan), as described in Chap. 8. They show the destruction forms of the ends of wooden bars, connected with steel inserts using bolts. The photographs from the laboratory testing illustrate the effects of the buckling of the stiff pasted-in reinforcement, occurring on the ends of the compressed wooden bars. These

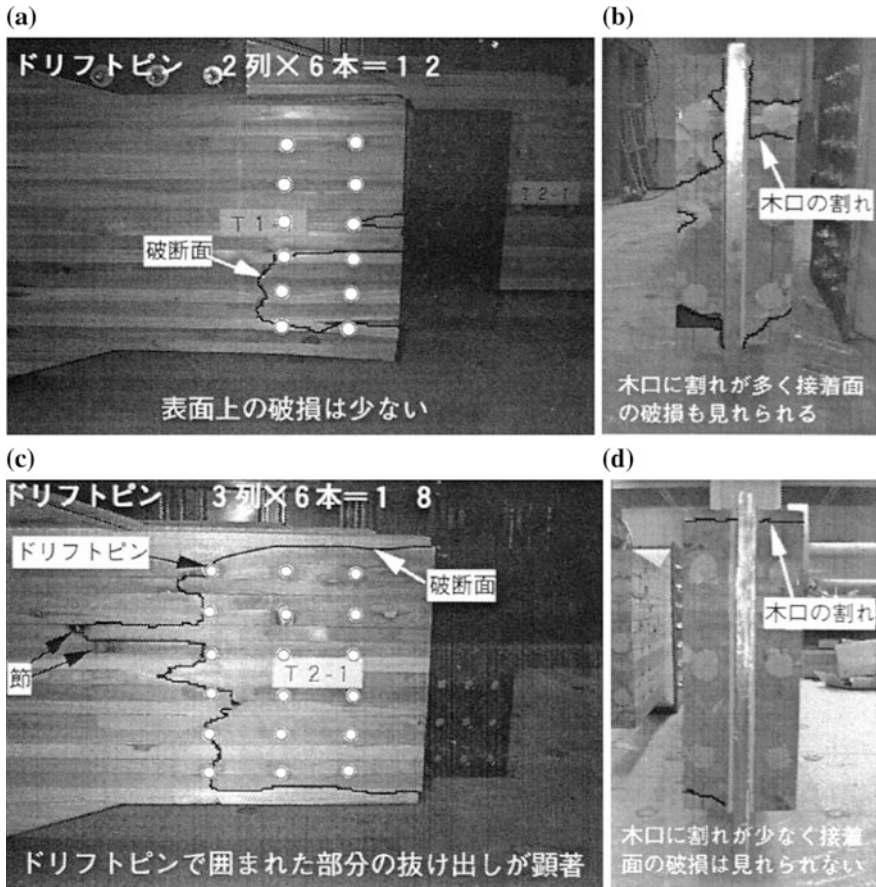


Fig. 9.15 Destruction forms of woods from layer-wise glued laminated timber with stiff steel sheets, used in the Odate dome, Japan [28]; **a, c** side view, **b, d** front view

phenomena confirmed by the wood destruction picture in Fig. 9.15, shows the urgent need for their further research.

The irregular picture of cracks of wooden bars' ends with pasted-in steel inserts, as shown in Fig. 9.15, results from the random distribution of clamp and shear strength of the matrix on which the impact of the thermal treatment and vacuum-pressure treatment of wood can be imposed. The load capacity of wooden bars' ends clamped in the nodes on the free edge, especially intersected with pasted-in sheets, used in the contemporary domes, from glued wood, can be lower than expected on the basis of the assumed limit load capacity of the bars being connected.

The wood destruction picture is also affected by low-size elements, such as steel bolts and screws. Shown in Fig. 9.16 are wooden nodes after the strength testing conducted by the ROTHOBLAAS company, specialized in the production of

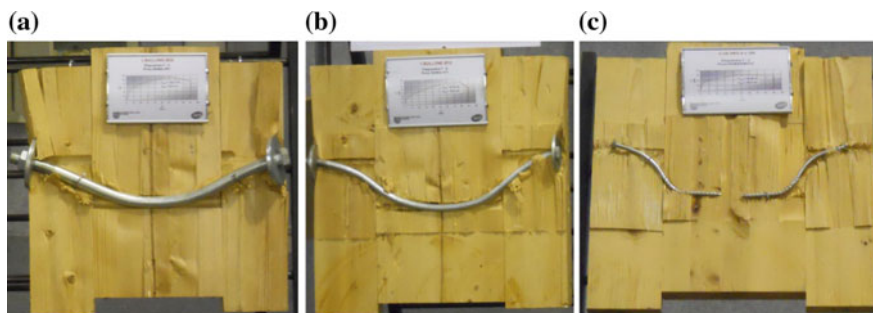


Fig. 9.16 Effects of the load of wooden elements connected with steel fasteners of various diameters (Photographs of the models exposed by the ROTHOBLAAS company at the WCTE 2010 conference, made by the author, Riva del Garda, Trentino, Italy, June 20–24, 2010), **a** connection with a dia. 12 bolt, **b** connection with a dia. 8 bolt, **c** connection with a dia. 4 screw

fasteners for wood. The test results of the elements shown in Fig. 9.16 were presented at the international conference WCTE 2010.

Visible in Fig. 9.16 are the effects occurring in the connection section of the interference of steel connectors in form of cracks in wood, the separation of fibres as well as the bending of steel fasteners. **The distortion of the steel fastener, due to the translocation of the bar with respect to the node, causes additional damages, such as: cracking, crushing of the matrix and wood fibres.**

9.7 Impact of the Longitudinal Stiffness Reduction of Compressed Bars on the Dome Node Snap-Through

9.7.1 Impact of the Bar-Compressing Strength on the Bar's Longitudinal Stiffness

In the paper [29] by Kowal Z. the formula for the coefficient κ of the longitudinal stiffness reduction of compressed bars (9.12) used to assess the reduced stiffness K of compressed bars according to the formula (9.10) was introduced:

$$K = \kappa K_0, \quad (9.10)$$

where: $K_0 = EA/l$ —conventional longitudinal stiffness of a wooden bar.

Shown in Fig. 9.17 is the increment of deflection $y + \delta$ that increases the shortening of a bar

$$\Delta l = \Delta l_0 + \Delta l_m, \quad (9.11)$$

where: Δl_0 —shortening of a bar from the axial force, Δl_m —shortening of a bar from the bending caused by the transverse translocation $\delta + y$.

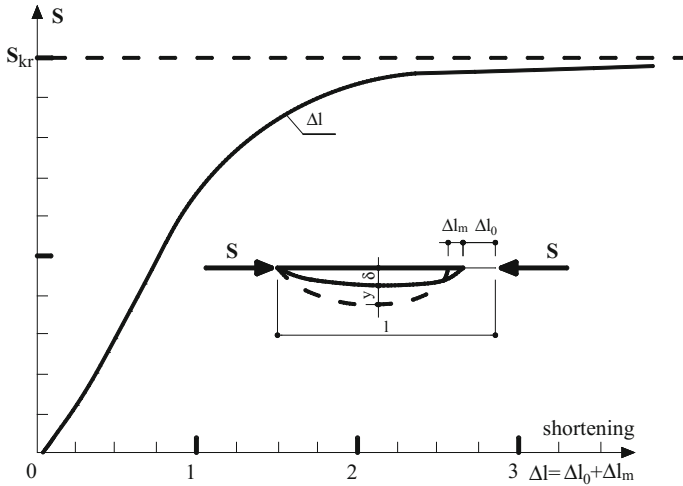


Fig. 9.17 Static Balance Path $S(\Delta l)$ of compressed and bent bars according to [29]

The coefficient κ of the longitudinal stiffness reduction in function of $\sigma = \frac{S}{A}$ totals:

$$\kappa = \frac{\left(1 - \frac{\sigma}{\sigma_{kr}}\right)^2}{\left(1 - \frac{\sigma}{\sigma_{kr}}\right)^2 + c \frac{\sigma}{\sigma_{kr}}}, \tag{9.12}$$

where: $\sigma = S/A$ —average axial stress in a bar, σ_{kr} —critical effort of a bar taking into account the impact of transverse forces, σ_e —Euler’s critical stress, B —the geometric imperfections coefficient totals:

$$B = \delta^2 / 4i^2 \tag{9.13}$$

where: δ —preliminary bending of a bar (Fig. 9.17) caused by geometric imperfections, y —deflection caused by transverse bending, i —minimum radius of inertia of the bar section.

The coefficients κ are placed in Table 9.2. The coefficient of imperfection C occurring in Table 9.2 and in Fig. 9.18 is calculated from the formula:

The coefficients κ are placed in Table 9.2. The coefficient of imperfection C occurring in Table 9.2 and in Fig. 9.18 is calculated from the formula:

$$C = B\sigma_{kr} / \sigma_e \tag{9.14}$$

Table 9.2 The reduction coefficient κ of the longitudinal stiffness of bars in function of σ/σ_{kr}

$\frac{\sigma}{\sigma_{kr}}$	C = 0.0001	C = 0.001	C = 0.01	C = 0.05	C = 0.1	C = 0.2	C = 0.5	C = 1
0	1	1	1	1	1	1	1	1
0.1	1	0.9999	0.9999	0.9939	0.9878	0.9759	0.9419	0.8901
0.2	1	0.9997	0.9969	0.9846	0.9697	0.9412	0.8649	0.7619
0.3	0.9999	0.9994	0.9939	0.9703	0.9423	0.8909	0.7656	0.6203
0.4	0.9999	0.9989	0.9890	0.9474	0.9	0.8182	0.6429	0.4737
0.5	0.9998	0.9980	0.9804	0.9091	0.8333	0.7143	0.5	0.3333
0.6	0.9996	0.9963	0.9639	0.8421	0.7273	0.5714	0.3478	0.2105
0.7	0.9992	0.9923	0.9278	0.7200	0.5625	0.3913	0.2045	0.1139
0.75	0.9988	0.9881	0.8929	0.625	0.4545	0.2941	0.1429	0.0769
0.8	0.9980	0.9804	0.8333	0.5	0.3333	0.2	0.0909	0.0476
0.85	0.9962	0.9636	0.7258	0.3462	0.2093	0.1169	0.0503	0.0258
0.9	0.9911	0.9174	0.5263	0.1818	0.1	0.0526	0.0217	0.0110
0.93	0.9814	0.8405	0.3451	0.0953	0.0501	0.0257	0.0104	0.0052
0.95	0.9634	0.7246	0.2083	0.05	0.0256	0.0130	0.0052	0.0026
0.97	0.9027	0.4813	0.0849	0.0182	0.0092	0.0046	0.0018	0.0009
1	0	0	0	0	0	0	0	0

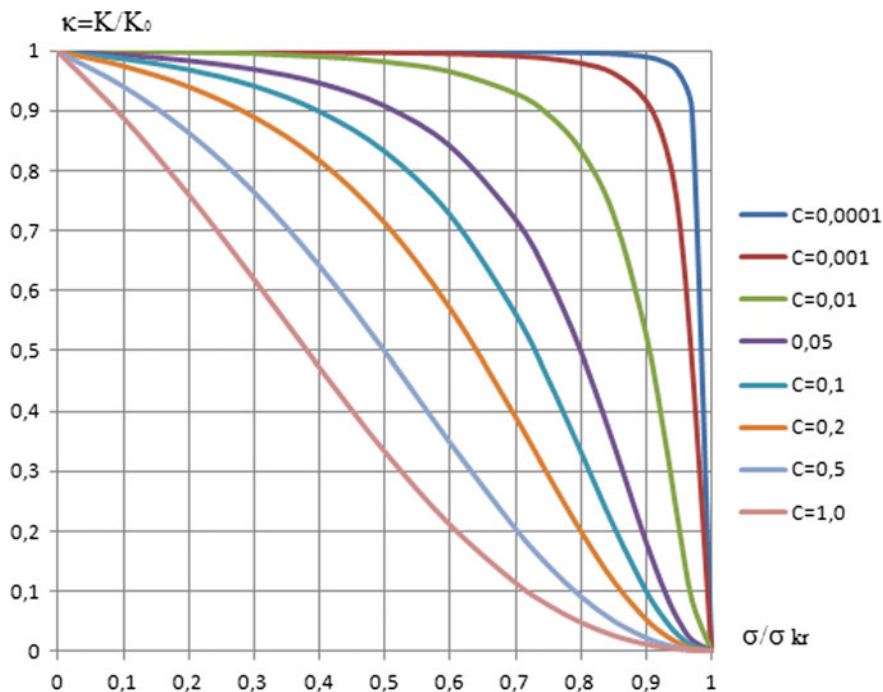


Fig. 9.18 Charts of the longitudinal stiffness coefficient $K = \kappa K_0$, $K_0 = EA/l$

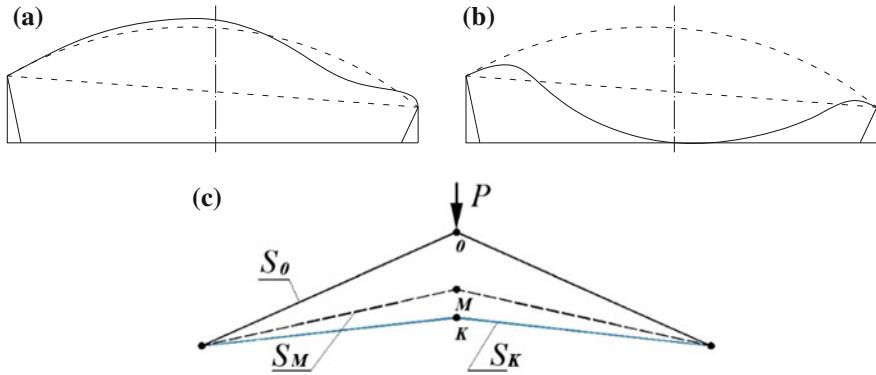


Fig. 9.19 Dome destruction mechanism due to the node snap-through; **a** node snap-through, **b** node collapse to the inside, **c** successively occurring position of bars of a node in the node snap-through process: S_θ —forces in bars designed following the rule of stiffening, S_M —forces in bars according to R Mises, S_K —forces in bars according to Kowal Z

The longitudinal stiffness of a bar is reduced as the longitudinal effort of bars $S/N_{kr} = \sigma/\sigma_{kr}$ is increased, and the geometric imperfection coefficient C is increased C (Fig. 9.18). The phenomenon as described in the work by Kowal [29] of the reduction of the longitudinal stiffness of composite compressed bars is recommended to be introduced to assess the reduction of the longitudinal stiffness of compressed wooden bars. This is of utmost importance for wooden bars that are naturally burdened with preliminary geometric imperfections.

For instance, if $C = 0.0001$, then imperfections are low, for $C = 1$ the bar is preliminarily strongly bent. The coefficient C as specified in Table 9.2 and Fig. 9.18 is calculated from the formula (9.14) according to [29].

In the calculations of bar wooden domes the reduction in the longitudinal stiffness of bars caused by compressive forces should be taken into account.

Until to date, **in the static calculations of domes, both wooden and reinforced concrete as well as steel domes, the reduction in the longitudinal stiffness of compressed bars was not taken into account.** This was the cause of many **disasters** of single-layer, bar structures of steel domes due to the ‘snap-through’ of nodes (Figs. 7.16b and 9.19c). It should be emphasized that the random clearances of bars’ connections of single-layer domes have also impact on the risk of a node snap-through. As the diameters of gridshell domes from solid wood increase, the potential for a node snap-through should be considered, thus the collapse of the coating, like in Fig. 9.19a, b.

9.7.2 Effect of the Node Snap-Through in Domes as a Cause of Catastrophes

In single-layer domes the phenomena of the dome node snap-through may occur, as illustrated in Fig. 9.19. The snap-through of one node may provoke an avalanche reaction of the other. The node snap-through is strongly affected by the inter-nodal bending of compressed bars.

As a result of the action of loads P concentrated in nodes, axial compressive forces S in the bars of the structural grid occur (Figs. 9.19 and 9.20). According to the stiffening rule, when a node is loaded with a concentrated force, forces S_0 will occur. Richard von Mises considered using conventional methods that impact of the translocations of nodes caused by the shortening $\Delta l = PL/EA$ of bars, achieving increased axial forces S_M (Fig. 9.19c). The authors: Kowal Z. in his work [30] and Gawęcki A. in his work [31] studied this phenomenon more precisely. Mises R. did not consider the impact of the reduction of the longitudinal stiffness of compressed bars on their shortening.

Kowal Z. in his work [29] assessed the reduction of the longitudinal stiffness of compressed bars—Fig. 9.19c. The consideration of this reduction significantly influences the significant rise of the axial forces in domes' bars leading to the node snap-through. The increased axial forces S_K are marked in Figs. 9.19c and 9.20 with blue colour. These forces may provoke a node snap-through, which is repeatedly noticed in single-layer, bar steel domes—Fig. 9.19a, b.

The node snap-through in single-layer bar constructions starts with a slow lowering of the most loaded node. The effects of the action of the load increase the rheological features of wood and wood-based materials. The translocations of nodes are signalled by a damage to the coating and covering. Cracks visible from the outside and inside of the facility appear on the coatings. The author demonstrated in Fig. 9.21 the photographs of the cracks characteristic of the lowering of a node were noticed in a dome of a 96.96 m diameter built in Portland (USA) in 1977, made in 2006.

In 2006, the author took photographs of the damages to the dome covering shown in Fig. 9.21. Visible in Fig. 9.21a are cracks on the outside covering, and in Fig. 9.21b—damages to the plates' contact points creating the coating, visible in the dome inside. The compression of rectangular plates caused by the lowering of node results in the tear-off and destruction of connections between the plates. These damages are the largest in the vicinity of the declining node of the gridshell dome construction.

Attention should be drawn to the fact that the disturbed balance of forces on one node of the dome construction under the impact of the distortion of bars entails the

Fig. 9.20 Build-up of forces in bars due to the translocation of the node

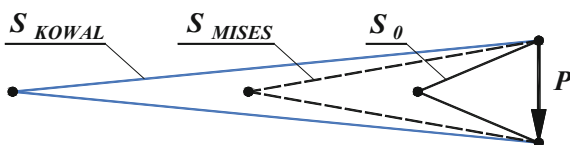




Fig. 9.21 Effects of the lowering of a node occurring in the dome in. Photographs of the authors taken in 2006, **a** cracks on the covering, **b** damage to the connections of plates around the node visible from the inside

overloading of neighbouring nodes and leads to the catastrophe of the system of the two-curvature, single-layer bar lattice.

In bar two-curvature structures the node snap-through can be counteracted using:

1. stiff nodes,
2. tensioning of the bar grid with an outside covering,
3. two-layer bar construction.

9.8 Concentration of Tangential Stresses on the Surface of Fibres in Wooden Beams Loaded Transversally and Axially

The particular feature of the composites reinforced with a parallel beam of fibres is that a bent fibre generates the shape distortion γ and the tangential stress τ (Fig. 9.22). The concentration of tangential stress occurs on the surface of fibres. Kowal Z. in his work [32] assessed the concentration of tangential stresses in fibrous composites. Shown in Fig. 9.22 is a separated single fibre placed in the visco-elastic matrix subjected to the compression with the force N_1 generating the transverse force Q_1 .

The critical load capacity of a fibre not stiffened with the matrix is close to zero. The increase in the load capacity of fibres is the result of taking over by the matrix of transverse forces Q_1 generated with axial forces N_1 in fibres.

$$Q_1 = \frac{N_1 \delta_1 \pi}{1 - \frac{N_1}{N_{1cr}} l_1} \quad (9.15)$$

where: Q_1 —transverse force associated with the buckling of a fibre, l_1 —length of the semi-wave of the buckling of a fibre, δ_1 —preliminary bending of a fibre, N_1 —axial force compressing one fibre, N_{1cr} —critical load of one fibre in the matrix (the matrix increases the critical load capacity of a fibre).

The destruction of a fibrous composite can be caused by the damage of the matrix due to the concentration in it of tangential stresses on the surface of fibres. In the paper [32] the concentration of tangential stresses for two types of the packing of fibres: square packing (Fig. 9.23) and triangular packing. Table 9.3 specifies the solution from the paper [32] for the square packing of fibres (Fig. 9.23).

The average tangential stress $\overline{\tau_{zy}}$ in the matrix resulting from the average shape distortion of the bar section can be assessed using conventional methods.

The maximum concentration of tangential stresses τ_m in the matrix with a square packing assessed on the basis of shape distortion totals according to [32]:

$$\tau_m = k \overline{\tau_{zy}} = \frac{b+d}{b} \overline{\tau_{zy}}, \quad (9.16)$$

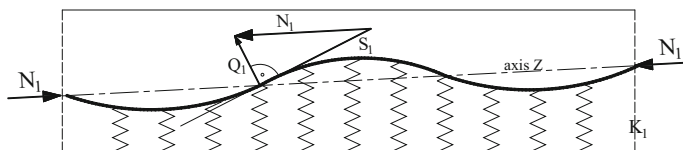


Fig. 9.22 Schematic of the generation of transverse forces associated with the buckling of fibres according to [32]

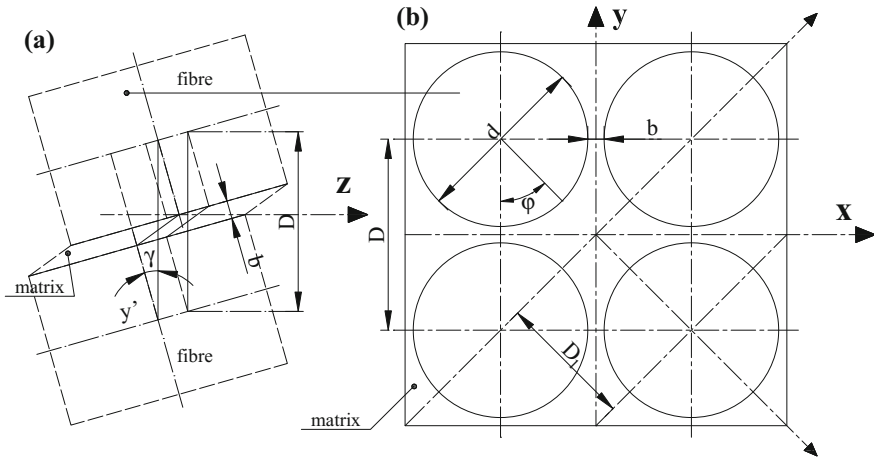


Fig. 9.23 Schematic of the square packing of fibres in the matrix according to [32], **a** translocation of fibres in the matrix, **b** square type of fibre packing

Table 9.3 Coefficients **k** of the concentrations of shape distortions and tangential stresses at the square packing of fibres [32]

No.	$\beta = \frac{d+b}{d}$	V_{wl}	$k_m = \frac{d+b}{b}$	$\bar{k} = \frac{1}{\beta} + \ln \frac{\beta}{\beta-1}$
1	1.02	0.755	51	4.912
2	1.05	0.712	21	4.000
3	1.10	0.649	11	3.307
4	1.15	0.594	7.(6)	2.9065
5	1.20	0.545	6	2.6251
6	1.25	0.503	5	2.409
7	1.30	0.465	4.(3)	2.766
9	1.35	0.431	3.857	2.0906

where: $\bar{\tau}_{zy}$ —average tangential stresses in the matrix, k_m —maximum coefficient of stress concentration according to the column 4 of Table 9.3.

Placed in the column 4 of Table 9.3 are the maximum coefficients **k** of the concentrations of shape distortions and tangential stresses in the plane *zy* of the translocation of fibres in the matrix, for the packing thickness β of fibres according to the formula (9.17):

$$\beta = (b + d)/d, \tag{9.17}$$

ranging 1.02–1.35, specified in the column 2, Table 9.3, where: *b*—spacing between fibres, *d*—diameter of fibres, $D = d + b$ (Fig. 9.22).

Specified in the column 3 are the fibre volume coefficients V_{wl} in the matrix. Specified in the column 4 is the maximum, in the column 5—the average coefficient of stress concentration **k**.

The maximum coefficient of the concentrations of shape distortions for the triangular packing of fibres in the matrix from plastics according to [32] can be assessed from the formula (9.18):

$$\max k = \frac{d+b}{2b}, \quad (9.18)$$

The described process of the concentration of shape distortions and in the consequence of tangential stresses on the fibre surface has its reflection in the buckling of compressed bars reinforced longitudinally with fibre. The shape distortions increase k -times, and the increase in the load Q_1 (formula 9.15) leads to the longitudinal cracking of the matrix between the fibres of bars of an average slenderness—see Figs. 9.2 and 9.3.

In wood the packing of fibres similar to the polar packing occurs. The packing of fibres in wood has not been principally tested. It follows from the vision of wood that this packing is essentially different depending on the wood species, time and place of growth. It follows from the perfunctory vision of samples that in the constructional wood species, e.g. pine wood, the concentration of shape distortions and tangential stresses on the surface of fibres in the matrix will also occur.

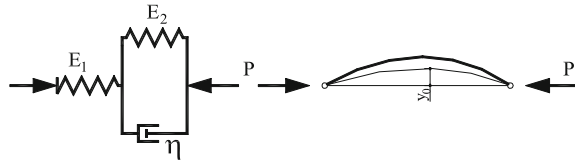
A conclusion is drawn from the papers discussed in Sect. 9.8 that the for the testing of the shape distortions in wood the theory developed for fibrous composites may be used. **One should take into account in the analysis of mechanical properties of wood the occurrence of various properties of the matrix that stick together fibres in annual rings and the matrix between the annual rings as well as the occurrence of a significant impact of moisture and temperature on the physical properties of matrices.** Therefore the concentration of shape distortions should be considered, as the origin data to assess the concentrations of tangential stresses.

An example of the significance of the impact of fibres' packings on the wood strength may be the approval in Japan of wood for the construction of domes, with the standard pre-defined spacing between the annual accruals—Fig. 11.1. The higher is the annual accrual, the lower is the wood strength. Attention should be drawn to the fact that the visco-elastic properties of the matrix allow the permanent distortion of wood.

9.9 Warning Properties of Wood Accompanying the Exhaustion of the Load Capacity of Compressed Bars

The phenomenon of the warning cracks of compressed wooden posts was learnt in salt mines. Due to the overloading of wooden props supporting the ceiling of the rock mass cracks were occurring with which wood warned about the growth of rock mass loads and the disaster to follow. This was described by Krzysik [33] on the

Fig. 9.24 Visco-elastic standard model of wood [34]



basis of the research by Stebnicka E.⁵ In accordance with the research by Stebnicka E., 45–50–85 s elapse between the moment of the occurrence of the critical force, signalled by noisy cracks of the cracking wood, with the collapse of pine wood props in mines. Often, this was the time sufficient for the evacuation and saving the life of miners. The wood species used in the mining trade may be categorized by the warning capacity in the following order: spruce, larch, pine, beech, birch, oak, locust. The longest acoustic emission tie is demonstrated by spruce.

Kowal Z. in his work [34] explained this phenomenon on the basis of the analysis of the standard visco-elastic model of wood. Using the elastic—visco-elastic analogy, taking into account the impact of transverse forces, Kowal Z. used the standard model to determine the critical load capacity of compressed wooden bars, including the creep of wood (Fig. 9.24). It follows from the analytical solution [34] that in such a model two critical load capacities appear: neutral N_{kr} and shock load capacity N_{sh} . The neutral load capacity is lower from the shock capacity $xN_{sh} > N_{kr}$.

The creep buckling with acoustic signals occurs under the load P included within the limits of $N_{kr} < P < N_{sh}$. The shock critical load capacity of the creep buckling totals [34]:

$$N_{sh} = \frac{\omega^2 E_1 J}{l^2 + d^2 \omega^2}, \tag{9.19}$$

where: $d^2 = EJ/GA$ —coefficient of the influence of shape translocations on the critical load capacity, ω —coefficient dependent on the boundary conditions of the bar being compressed.

The neutral, lower, critical load capacity may be assessed from the formula according to [34, 35]:

$$N_{kr} = \frac{\omega^2}{l^2 + d^2 \omega^2} \left(\frac{E_1 E_2}{E_1 + E_2} \right) = \frac{N_{sh} E_2}{E_1 + E_2} < N_{sh} \tag{9.20}$$

⁵Stebnicka E., *Usefulness of the dried-up wood for the production of mine wood pit-props*, 1953, (typescript).

The creep translocation is expressed with the formula [34, 35]:

$$w = y_0 e^{-at}, \quad (9.21)$$

The creep speed is expressed with the formula:

$$\dot{w} = -ay_0 e^{-at}, \quad (9.22)$$

where: t —time, y_0 —initial deflection, $a = \frac{E_0}{\eta}$ coefficient of creep speed, η —viscosity.

Shown in Fig. 9.25 are exemplary charts of the speed of the transverse creep of compressed bars upon exceeding the neutral critical load capacity N_{kr} .

The creep buckling of a bar occurs upon exceeding the initial (neutral) critical load capacity. At that time the process of the transverse creep of the bar begins, accompanied by the emission of the acoustic wave of the material associated with the cracking of single fibres caused by the buckling and the concentration of tangential stresses on the surface of fibres. When the load P reaches the shock critical load capacity, the process of the avalanche tearing of fibres and the total destruction of the bar begins. The initial critical load capacity (neutral balance) decides about the permanent load capacity of the construction. Wood under the load P higher than the neutral load capacity cracks, thus signalling the excess of the permanent critical load capacity.

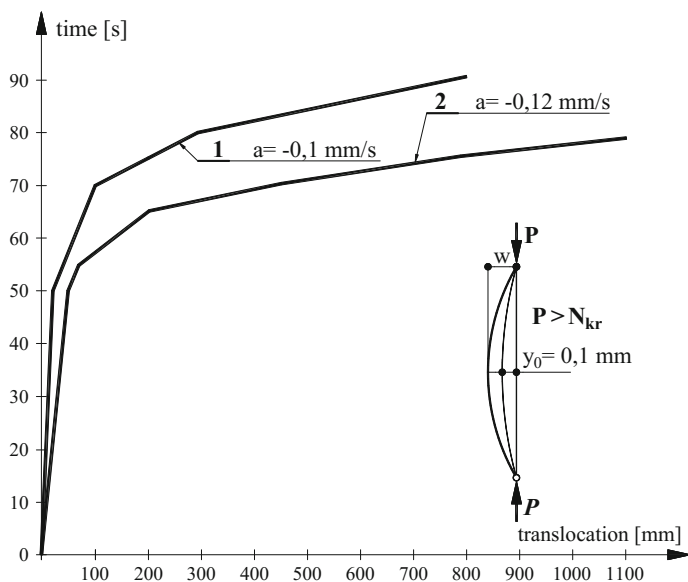


Fig. 9.25 Exemplary translocation in the function of time of wooden bars for the coefficient of creep speed $a = 0.1 \text{ mm/s}$ and for $a = 0.12 \text{ mm/s}$ [34, 35]

It follows from Sect. 9.9 that the compressed wooden bar that occur in domes should be designed for the initial critical load capacity from the formula (9.20). In the opinion by Kowal [34], the standard model is the smallest model useful for the analysis of wooden constructions. Similar results may be obtained on the basis of the model by Zener, also resolved in the paper [34, 36]. In those solutions the impact of transverse forces on the critical load capacity was taken into account.

9.10 Strengthening of Compressed Wooden Bars Under Load

The advantage of compressed bars from solid wood is the ease of their strengthening under load. Those methods often were the unique way to extend the technical efficiency of wooden props in mines. Shown in Fig. 9.25a–c is the strengthening of bent compressed bars as described in the paper [25]. The historical solutions preferred a non-symmetrical strengthening of compressed wooden elements.

The paradox of the advantageous non-symmetrical strengthening of compressed bars under load was explained by Kowal Z. in his paper [37]. Placed in it are effective formulas to determine the global limit load capacity of wooden posts. Kowal Z., basing on the statement that the actual conditions of the balance of forces (equations of statics) apply to the constructional systems after the displacement of the structure, in the assessment of the bending of a post takes into account the impact of transverse forces on the conventional transverse translocation. He introduces the summation of deflections taking into account the impact of shape distortions caused by transverse forces:

$$\delta = \delta_i + \delta_P + \delta_Q \quad (9.23)$$

where: δ_i —preliminary deflection, δ_P —translocation from the bending using the load P, δ_Q —shape distortions from transverse forces, K—coefficient of sectional shape. The assessment of the amplification of translocations using the formula (9.23) is controlled by the global critical load capacity N_{kr} :

$$y + \delta = \frac{\delta}{1 - \frac{S}{N_{kr}}} \quad (9.24)$$

The critical load capacity N_{kr} taking into account the shape stiffness GA is calculated from the formula (9.3) discussed in Sect. 9.4.

It follows from the comparison of the load capacity of a bent post strengthened symmetrically and non-symmetrically that better strengthening effects are obtained through the non-symmetrical strengthening of bent posts—Fig. 9.26c.

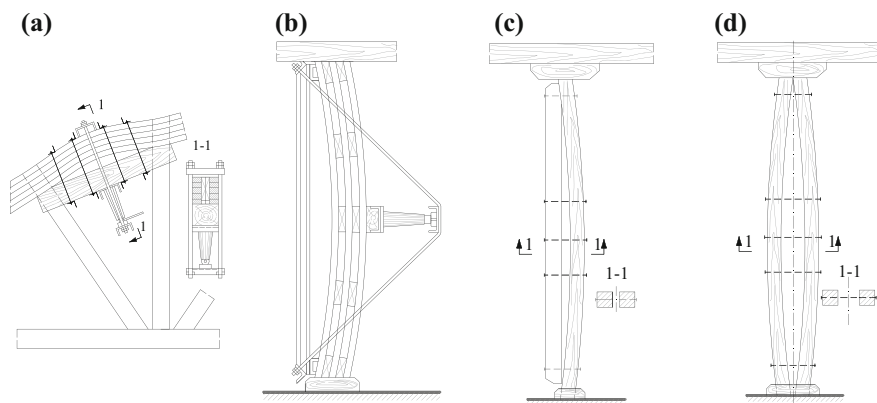


Fig. 9.26 Strengthening of wooden elements under load, **a** compressed truss chord, **b** multi-branch post, **c** single-branch post, **d** two-branch post

The highest strengthening effect is obtained when the axis of the strengthened post overlaps with the direction of the compressive force action—Fig. 9.26d, and the direction of the force passes through the centre of gravity of the post's section after the strengthening. In the assessment of the load capacity of wooden posts the impact of transverse forces on the critical load capacity [35] N_{kr} and dependency according to Timoshenko [38] should be taken into account.

The actual critical load capacity σ_{kr} of compressed bards according to Kowal Z. should be calculated from the formula:

$$\frac{1}{\sigma_{kr}} = \frac{1}{\sigma_e} + \frac{1}{R_e} + \frac{1}{G_{zr}}, \quad (9.25)$$

where: $G_{zr} = G A_{sr}/A$ —modulus of transverse elasticity of wood, A_{sr} —section of the web, A —section of the bar, σ_e —Euler's critical stress, R_e —yield strength of the material.

At this moment there is no recognition in the area of the yield strength of wood.

9.11 Impact of the Wood Protection Technology on the Load Capacity of Wood

The susceptibility of wood to the interference of environment produced that for centuries various methods of its protection have been used. In order to increase the durability of facilities from wood, chemical and physical methods have been used to counteract the harmful factors of the environmental impact. Chemical preparations that destroy the biological pests of wood were used: fungi, moulds and insects. Also physical methods were used, including cooking, for instance, of

planks for painting supports [39]. Usually, what was destructive for pests was handled, and less the impact of the preparation or the protection method on the properties of wood resulting from its structure.

The authors Kozakiewicz P., Matejak M. in their paper [39] described the chemical composition and the fibrous structure of wood. The dimensions of a single wooden fibre deciding about the strength of wood were specified. Depending on the species, wood fibres have various dimensions. In constructional species the typical dimensions total circa: length $\sim 3500 \div 4000 \mu\text{m}$, diameter $\sim 1/15$ to $1/20$ of the fibre length. Wooden fibres of a various packing are placed in the mass of parenchymatous cells (Fig. 9.27). Both the features of fibres and those of parenchymatous cells depend on the species and the growth conditions of a tree. It is common, however, that parenchymatous cells as live cells are characterized by the visco-elastic susceptibility, on the other hand, the cells that create wooden fibres are dead cells, stiffening the composite. Wood is built from cells with walls from cellulose and hemi-cellulose, strengthened with lignin fibres. Cellulose and hemi-cellulose are polysaccharides of the general chemical formula $C_nH_{2n}O_n$, or otherwise $C_n(H_2O)_m \rightarrow$ hence the name of hydrocarbons. In each glucose unit in the cellulose chain there appear free hydrocarbon groups with a high affinity to water. This is the cause of a high absorbability of wood, whereby water particle are additionally bound between the cellulose chains. This process weakens the interference between the cellulose chains, leading to the swelling of wood and the lowering of its strength.

The cellulose present in wood produces that wood also is an attractive nutrient medium ensuring the development of various micro-organisms feeding with glucose. The wood paralysis mechanism by pathogenic fungi is described in the paper [33]. Fungus spores, present in environment, of an increased moisture content, settle in wood, leaving ejecting hyphae that pegridrate to the mass of parenchymatous cells. The decomposition process of cellulose and lignin starts under the impact of enzymes emitted by hyphae: cellulose and ligninase. This is the biochemical process

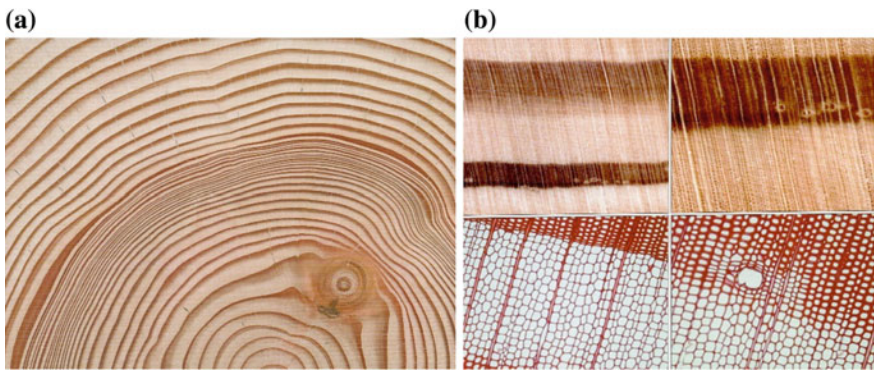
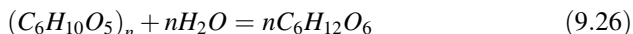
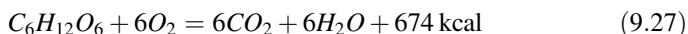


Fig. 9.27 Fibrous structure of douglas fir (*Pseudotsuga menziesii*), **a** cross-section, **b** tangential section (Jean-Denis Godet *Atlas of Wood*, Multico, Oficyna Wydawnicza, Warszawa 2008) [25]

occurring in the humid environment. In the presence of cellulase the decomposition of cellulose into simple sugar—glucose occurs according to the reaction:



Glucose is used by the fungus to all vital processes. The action of other enzymes, air and room temperature produces the glucose oxidation reaction:



It follows from the reaction (9.26) that the simplest method to block the biological degradation of wood is to ensure the continuous offtake of moisture from environment and to prevent the outdropping of water on the surface or in the close vicinity of elements from wood. It follows from the reaction (9.27) that water and carbon dioxide are the glucose disintegration products. These products deepen the destruction of parenchymatous cells.

The microscopic pictures of the activity of the parasitic fungus *Piptoporus betulinus* in the growing birch tree are discussed in the paper [40]. Shown in Fig. 9.28 are hyphae pegrigrating to the next cells of wood through not closed cell cavities. Gradually, hyphae occupy next cells, providing the fungus with alimentary ingredients through the secretion of enzymes and the production of glucose. The cellulose decomposition process $(C_6H_{10}O_5)_n$ occurs in the presence of enzymes excreted by hyphae and in the presence of water. Therefore the biological corrosion of wood, both the growing wood and in a construction, always starts with its moistening.

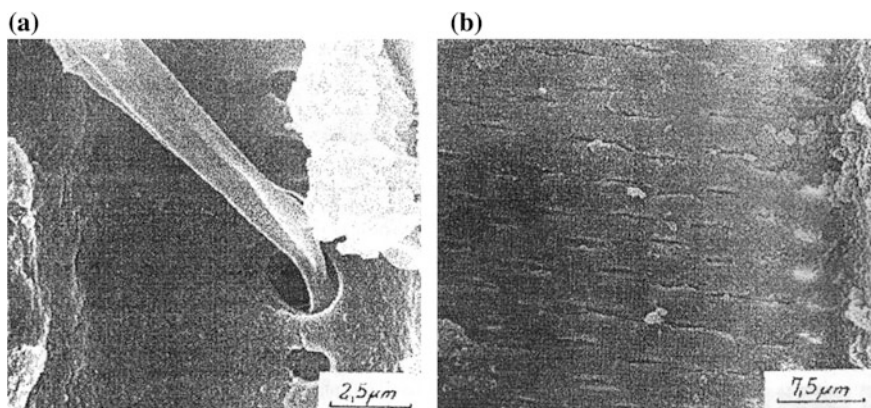


Fig. 9.28 Picture of the paralysis with the fungus *Piptoporus betulinus* of the birch tree according to [40], **a** hypha outgrowing a cavity cell, **b** closure of cavity cells in a live birch tree trunk, infected with the fungus in the northern part of the trunk

The natural defence form of the growing tree against fungi is to cut off the infected zone from the sound part of the trunk. In Fig. 9.28b there are photographs taken of well visible numerous cell cavities in the cellular wall of the vessel that are closed. The cellular walls with closed cell cavities constitute a mechanical lock for the growing spawn in the pegridration to neighbouring cells. The natural reaction to the pegridration pulse of hyphae in a live tree is the closure of cell cavities in the sound vessels, not attacked yet by the fungus. Shown in Fig. 9.28b is the view how in wood, infected by the fungus *Piptoporus betulinus* such a natural, defensive barrier looks like.

This process was described in order to call attention to the recognition of natural mechanisms, for the rational handling and application of wood. The fibrous structure allows to treat wood as a fibrous composite of a visco-elastic matrix. For the needs of the use of wood for the building of engineering constructions it is important to recognize the impact of the protection methods of wood against corrosion on the properties of fibres and the matrix. The data on the wood strength after the vacuum-pressure impregnation with a salt preparation at the temperatures of 20, 50, 100, 150, 200, 230 °C is described by the team Bednarek Z., Kaliszek-Wietecha A. in their paper [41]. Samples were tested statically and dynamically. In the static testing the following tests were performed: bending test, compression test along fibres, compression test across fibres, tensile test along fibres. In the dynamic testing the strength to dynamic bending and wood impact strength were verified. It has been demonstrated that the use of vacuum-pressure impregnation methods with a salt preparation reduces the strength of wood samples impregnated in relation to those not impregnated. The authors explain that this is associated with the violation of the wood structure due to the variations pressure during the saturation with the impregnating substance [41].

Changes in the wood structure due to the action of pressure and temperature are also illustrated by the results of the testing conducted by the Finnish Thermowood Association specified in Thermowood Handbook [42].

The samples of pine wood and spruce wood subjected to vapour bath at a temperature 190–240 °C under pressure were tested. The photographs (Fig. 9.29a, b) quoted in the paper [42], show the changes in the structure of pine wood before and after the vapour bath process at 215 °C. When comparing them, it is possible to notice the loss of the matrix material between wood fibres.

The decrease in the wood density in the vapour bath process is accompanied by changes in strength properties. The soaking of wood at increased temperatures momentarily increases the compression strength, however, the destruction form changes from quasi-plastic to fragile. Wood samples subjected to compression after the Thermowood process go to pieces [42]. This fact may be explained by the degradation, even the loss of the matrix that binds wooden fibres. The effect of this is the lack of a sufficient anchoring of fibres in the matrix, which due to the lack of fastening crack avalanche-wise when compressed.

The impact of the matrix degradation to the critical strength of wood after thermal treatment may be explained on the basis of the model of a composite fibre-reinforced longitudinally. The behaviour of a fibre inundated in the visco-elastic matrix was

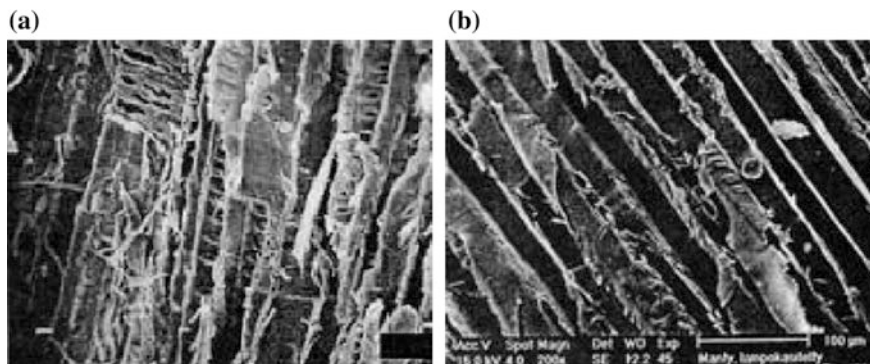
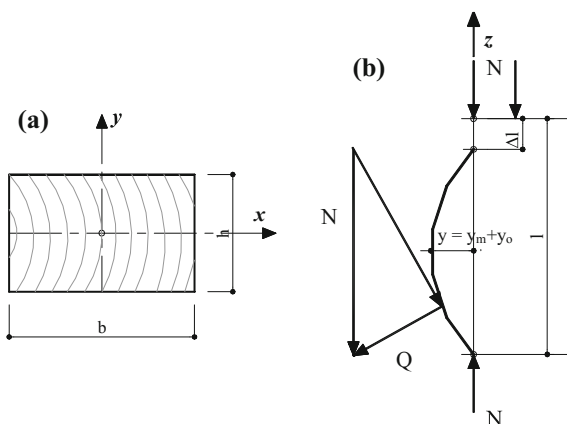


Fig. 9.29 Microscopic picture of the pine wood structure [42], **a** before thermal treatment **b** after thermal treatment

described by Kowal Z. in his paper [32], as a phenomenon dependent on geometry and the properties of the matrix. Demonstrated in Fig. 9.22 according to [11] is the generation of transverse forces as a result of the amplification of the transverse preliminary bending y_0 of a single fibre. The buckling associated with compression applies both to a bar and a single fibre. Illustrated anew in Fig. 9.30 is the generation of a transverse force in the compression process of a single fibre. The transverse forces associated with the compression of fibres, generate the accumulation of shape distortions on the surface of fibres and the tangential stress in the matrix. **Lack of a damage of the matrix caused by the vapour bath at 215 °C, additionally under pressure, produces the avalanche-like crumbling of fibres during the sample compression.** The effects intensify for short samples, due to the free edge phenomenon, described in Sect. 9.3 (Fig. 9.3).

The charts from the wood strength testing in the Thermowood process, as developed in [42] and quoted in Fig. 9.31, illustrate a change in the mechanical

Fig. 9.30 Generation of transverse forces in a compressed wood fibre with a preliminary bending [11]



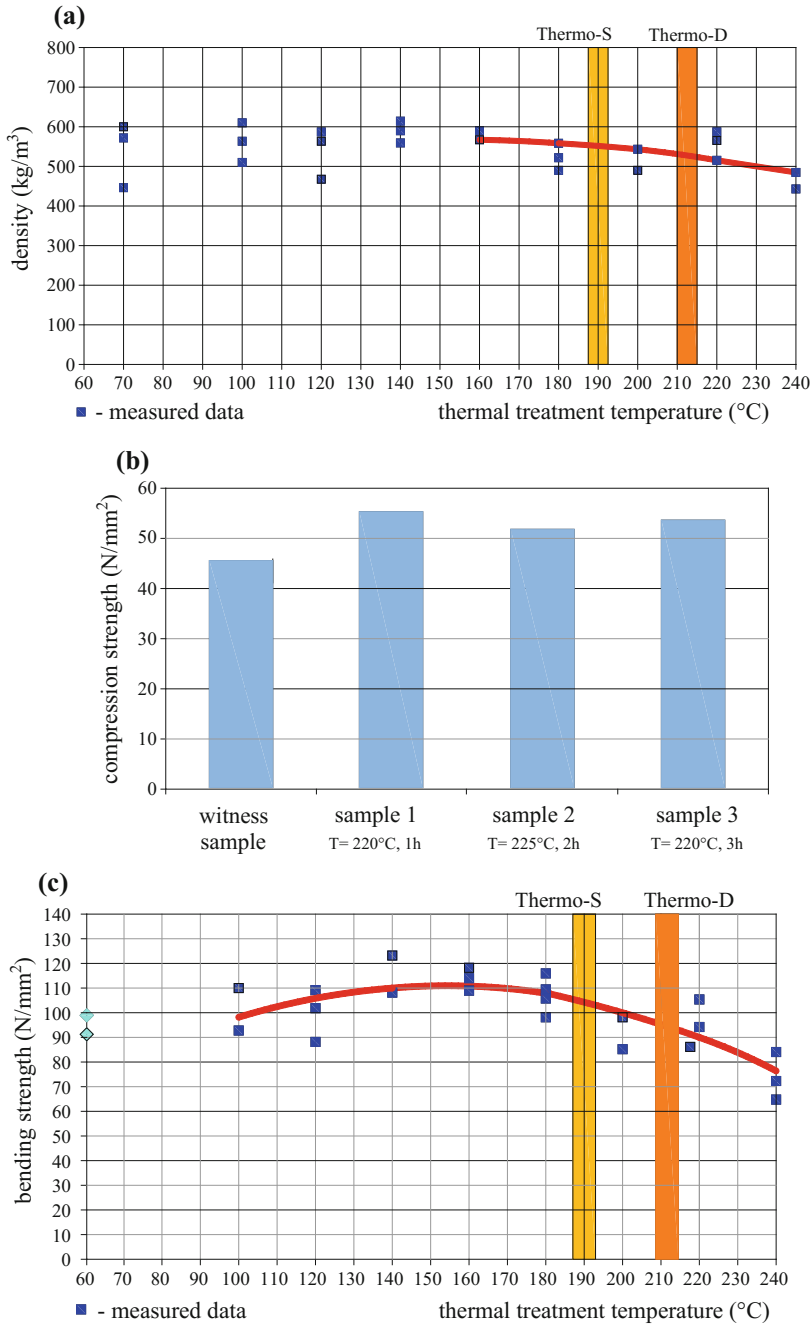


Fig. 9.31 Change in the properties of wood as a result of thermal treatment according to [42], **a** dependence of the pine wood thickness on temperature, **b** bending strength of spruce wood of a thickness 4.2 kN/m³ after vapour bath, **c** dependence of the bending strength of pine wood, **d** dependence of the coefficient of direct elasticity of pine wood

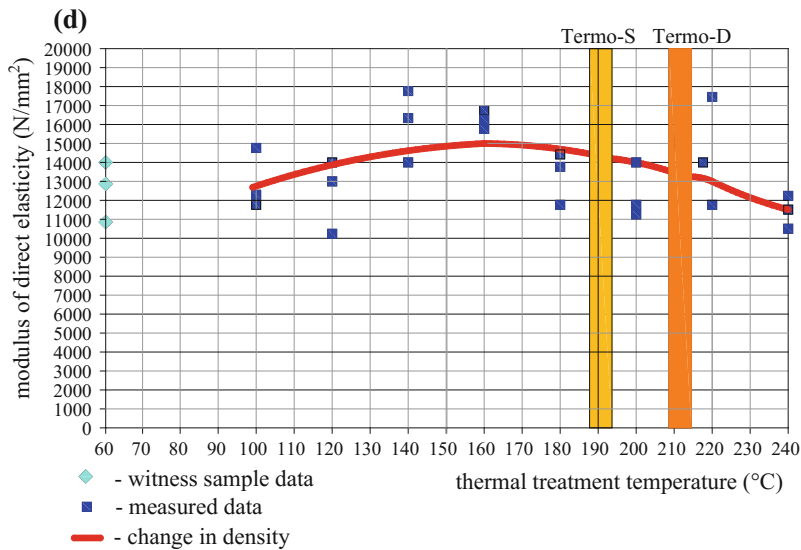


Fig. 9.31 (continued)

properties of wood. In Fig. 9.31a the continuous line depicts the chart of the pine wood thickness reduction caused by the vapour bath of planks at high temperatures under pressure. The higher is the treatment temperature, the higher is the reduction in wood thickness. Probably, the wet visco-elastic matrix is destroyed in the first order, this being visible in Fig. 9.29b.

The decrease in wood thickness after the vapour bath process is accompanied by the changes to strength properties. The soaking at an increased temperature changes to compression strength and the bending strength of wood—Fig. 9.31b, c. It follows from short-term wood strengths trials, developed in [42], that there occurs a change in the compression strength of samples from spruce wood, vapour-bathed at 220 °C for 1 h (sample 1) and for 3 h (sample 3), and at a temperature of 225 °C for 2 h (sample 2), in relation to the witness-sample not subjected to thermal treatment.

Shown in Fig. 9.31c is the drop in the compression strength of pine wood after a vapour bath at a temperature not higher than 160°. Visible in Fig. 9.31d is the decreasing of the coefficient of direct elasticity caused by a temperature rise.

The load capacity of single fibres affects the global load capacity of the whole bar and is described in Sect. 9.7. The degradation of parenchyma, live cells, that is the visco-elastic matrix in which wooden fibres are inundated decides about the load capacity of the composite. The decrease in the density of pine wood (Fig. 9.31a) upon completion of the steaming process suggests the decrease in the modulus of direct elasticity E of eccentrically bent wooden bars. Also, a significant

decrease in the modulus of transverse elasticity G due to the matrix degradation should also be expected. Visible in the Fig. 9.31d is the decrease of the elasticity modulus of pine wood subjected to thermal treatment in relation to samples not treated thermally. The higher is the treatment temperature, the lower is the coefficient of direct elasticity. In the paper [42] the phenomena occurring in bars of a low slenderness⁶ were not considered.

It is important that the modulus of direct elasticity of wood affects the critical load capacity of bars of an average and high slenderness,⁷ which was studied in Sect. 9.4. The decrease in the coefficient of direct elasticity by circa 11% results in the decrease in the load capacity of wood by circa 20%. The curve 3 demonstrates this on the chart from Fig. 9.7.

The decrease in the modulus of elasticity of wood subjected to thermal treatment results in the decrease of the global critical load capacity of compressed bars.

To summarize, it should be emphasized that the degradation of the matrix may be explained by the crumbling of wooden bars, which was tested in the short-term compression and noted down in the paper [42]. The losses of the matrix provoke the insufficient fastening of fibres, which produces that wooden fibres crack avalanche-wise under the impact of compression. **The phenomenon of the buckling of a single fibre in the visco-elastic matrix is translated into the global load capacity of compressed bars from wood, especially those of a low slenderness.**

It follows from the papers [11, 32, 35] that the load capacity of a fibrous composite depends on the fastening of fibres in the visco-elastic matrix. **In order to maintain the strength of wood care should be taken of the matrix in which wood fibres are naturally placed. In the modern methods the preparation of planks for the construction of bars from glued laminated timber the fact is omitted despite the fact that some researchers signal the problem of the decrease in the strength of wood protected with presently used methods.**

The methods of designing, building and protecting facilities from wood should consider the features of the anatomic structure of the building material which wood is.

For the needs of the use of wood for the building of engineering construction it is important to learn the possibilities of the use of the natural defensive properties of wood. It becomes urgent to recognize the acquisition methods of wood as a building material on its durability. The development of the methods to ensure the maintenance of the properties of wooden fibres and the visco-elastic matrix is essential for the further development of structures from wood.

⁶Bars of a small length are those of a slenderness $\lambda < \lambda_B$, where λ_B —slenderness of the point of bifurcation.

⁷Bars of an average slenderness are those with a slenderness of $\lambda_B < \lambda < \lambda_Q$, bars of a high slenderness are those of $\lambda > \lambda_Q$. Figure 9.3.

References

1. Bondin W. *O obliczaniu zbrojonych belek drewnianych*. Zeszyty Naukowe Nowosybirskiego Instytutu Inżynieryjno-Budowlanego. Nr.624.011.6.072.2.04. 1968.
2. Moliński W., Raczkowski J., *Wpływ promieniowania ultrafioletowego na pęczanie drewna*. Reologia drewna i konstrukcji drewnianych, Sympozjum Akademii Rolniczej w Poznaniu, materiały, Zielonka 21–22 październik 1982.
3. Dziuba T., *Nośność graniczna belek drewnianych jednostronnie zbrojonych prętami stalowymi*. Praca doktorska pod kierunkiem prof. dr hab. inż. R. Ganowicza., Poznań 1980.
4. Mielczarek Z., *Budownictwo drewniane*. Wydawnictwo Arkady, Warszawa 1994.
5. Dżeński W., *Przydatność drewna do wyrobu kompozytów sprężanych stalą*. Wydawnictwo SGGW, Warszawa 2003.
6. Jasieńko J. *Połączenia klejowe i inżynierskie w naprawie, konserwacji i wzmacnianiu zabytkowych konstrukcji drewnianych*, Dolnośląskie Wydawnictwo Edukacyjne, Wrocław 2003.
7. Dżeński W., *Nieniszczące badania mechanicznych właściwości iglastej tarcicy konstrukcyjnej wybranymi metodami statycznymi i dynamicznymi*, Wydawnictwo SGGW-AR, Warszawa, 1984.
8. Kowal Z. *Kaskadowy model utraty stateczności prętów w ośrodku lepkosprężystym*. Politechnika Krakowska, Monografia 194, Kraków 1995.
9. Kowal Z. *Nośność krytyczna a wyboczenie pęczające metalowych prętów ściskanych w podwyższonych temperaturach* Konferencja Naukowa Komitetu Inżynierii Lądowej i Wodnej PAN i Komitetu Nauki PZiTB, Warszawa – Krynica 12–17 września 2004. t. II, str. 245–252.
10. Kowal Z., Trąbski L. *Brittle Fracture of Compressed Composite Rods*, V International Symposium on Brittle Matrix Composite (BMC5), Warszawa 13–15 październik 1997, s. 409–416.
11. Kowal Z. *Kompozytowe pręty ściskane zbrojone podłużnie i spiralnie*. XLII Konferencja Naukowa Komitetu Inżynierii Lądowej i Wodnej PAN i Komitetu Nauki PZiTB, Kraków – Krynica, wrzesień 1996.
12. Warth Otto *Die Konstruktionen in Holz* Gedruckt von A. Th. Engelhardt, Leipzig 1900.
13. Kowal Z., *Stateczność osiowo ściskanego pręta w ośrodku lepkosprężystym*, Archiwum Inżynierii Lądowej 2/1964, t. X., s. 37–45, 197–204.
14. Kowal Z. *Wyboczenie pęczające osiowo ściskanych prętów lepkosprężystych*, III Sympozjum PTMTS poświęcone reologii, referaty t. i, Wrocław 1966, s. 209–218.
15. Kowal Z. *Parametry losowej wytrzymałości prętów ściskanych i współczynniki wyboczenia*. Archiwum Inżynierii Lądowej nr 1/1981.
16. Kowal Z., Radoń U. *Propozycja modelu konstytutywnego prętów ściskanych do obliczania nośności granicznej rzeczywistych konstrukcji prętowych*. *Inż. i Bud.* 12/1995, s.679–683.
17. Kajima Corporation *Materiały firmowe*.
18. Kowal Z. *Nośność krytyczna słupów drewnianych jako kompozytów włóknistych*. Sympozjum - Drewno i materiały drewnopochodne w konstrukcjach budowlanych. Szczecin-Międzyzdroje 05–06 września 1996.
19. Misztal B., *Pomiary dynamiczne w diagnostyce stropów drewnianych* REMO 2004 r. XI Konferencja Naukowo Techniczna Problemy Remontowe w Budownictwie Ogólnym i Obiektach Zabytkowych, Wrocław Zamek Kliczków, 9–11 grudnia 2004.
20. Kowal Z., Szychowski A. *Nośność graniczna prętów ściskanych pod interakcyjnym obciążeniem poprzecznym*, *Inż. i Bud.* 7/1996, s. 399–404.
21. Obmiński T. *Budownictwo ogólne II Atlas* Wydanie i nakład Związku Studentów Inżynierii Politechniki Lwowskiej. Lwów 1925.
22. Karlsen G. G., Bolszakow W.W., Kagan M. E., Świencicki G., *Kurs dierewiennych konstrukcji cz. I i II*, G. I. C. L. Moskwa, Leningrad 1943.
23. Timoszenko S. P. *Teoria stateczności sprężystej*. Arkady, Warszawa 1996.

24. Orłowicz R. B., Lachiewicz-Złotowska A. *Zachowanie się stref przypodporowych dźwigarów lukowych i belkowych z drewna klejonego*. Czasopismo Techniczne B, Wydawnictwo Politechniki Krakowskiej, z. 1–8/2007.
25. Jean-Denis Godet *Atlas drewna*, Multico, Oficyna Wydawnicza, Warszawa 2008.
26. Kowal Z. *The limit load bearing capacity of composite rods from the condition of the material stability loss*. International Conference on Lightweight Structures in Civil Engineering, Warszawa, 25–29 wrzesień 1995.
27. Iimura Y. *Performance Ewaluation of the "Konohana Dome" built with fast – Growing Sugi* WCTE 2008 czerwiec 2–5 2008 Miyazaki Japan.
28. Iimura Y., *Dokumentacja projektowa 17 kopuł z drewna wybudowanych w Japonii od roku 1986r*. Archiwum prywatne.
29. Kowal Z. *Redukcja sztywności podłużnej kompozytowych prętów ściskanych*. XLIV Konferencja Naukowa Komitetu Inżynierii Lądowej i Wodnej PAN i Komitetu Nauki PZiTb, t. III Poznań – Krynica 1998.
30. Kowal Z. Słowik J., Wawszczak W., *Zasady projektowania kopuł prętowo-żebrowych*, Inż. i Bud. 7/1992, s. 247–251.
31. Gawęcki A. *Mechanika materiałów i konstrukcji prętowych, cz. 4*, Wydawnictwo Politechniki Poznańskiej 2003, biblioteka elektroniczna.
32. Kowal Z. *Koncentracja odkształceń i naprężeń stycznych w ściskanych prętach kompozytowych zbrojonych podłużnie włóknem*, Księga Jubileuszowa Profesora Zbigniewa Kaczkowskiego, Warszawa 1996, s. 233–240.
33. Krzysik F., *Nauka o drewnie*, Państwowe Wydawnictwo Rolnicze i Leśne, Warszawa 1957.
34. Kowal Z. *Wyboczenie pełzające kompozytowych prętów ściskanych o właściwościach ostrzegawczych*, Problemy Budownictwa, Księga Jubileuszowa 70-lecia prof. T. Bilińskiego, Zielona Góra 2003, s. 293–300.
35. Kowal Z. *Wpływ sił poprzecznych na nośność krytyczną i pełzanie lepko-sprężystych prętów ściskanych*, w XLIX Konferencja Naukowa Komitetu Inżynierii Lądowej i Wodnej PAN i Komitetu Nauki PZiTb, Warszawa – Krynica 14–19 września 2003.
36. Kowal Z. *The effect of transverse forces on creeping buckling of viscoelastic compressed columns*. Arch. of Civil and Mechanical Engineering. Vol. V, No 2/2005, s. 13–23.
37. Kowal Z. *Nośność graniczna słupów wzmocnianych pod obciążeniem*, IX Konf. NT Problemy remontowe w budownictwie ogólnym i obiektach zabytkowych REMO 2000, Wrocław-Szklarska Poręba, 7–9.12.2000 r, s. 279–286.
38. Taras J. *Sacral Wooden Architecture by Ukrainians of Carpathians*. National Academy of Sciences of Ukraine. The Ethnology Institute. Lviv 2007.
39. Kozakiewicz P., Matejak M., *Klimat a drewno zabytkowe*, Wydawnictwo SGGW, Warszawa 2002.
40. Krutul D., Kozakiewicz P., *Właściwości fizykochemiczne oraz cechy budowy mikroskopowej drewna brzozy porażonej przez *Piptoporus betulinus**. SYLWAN 4: 49–59, Warszawa 1998.
41. Bednarek Z., Kaliszek-Wietecha A., *Wytrzymałość drewna impregnowanego ogniochronnym środkiem solnym metodą próżniowo- ciśnieniową*. 50-ta Jubileuszowa Konferencja Naukowa Komitetu Inżynierii Lądowej i Wodnej PAN i Komitetu Nauki PZiTb „Krynica 2004” 12–17 września 2004 roku.
42. Finnish Thermowood Association *Thermowood handbook*, Helsinki, Finland, 08.04.2003 www.thermowood.fi Kowal Z. *Koncentracja odkształceń i naprężeń stycznych w ściskanych prętach kompozytowych zbrojonych podłużnie włóknem*, Księga Jubileuszowa Profesora Zbigniewa Kaczkowskiego, Warszawa 1996, s. 233–240.

Chapter 10

Effect of Time on the Mechanical Properties of Wood

The historically shaped wooden domes from solid wood, still built until the thirties of the 20th century, have a diameter up to 67.0 m—Kaszkarow [1] (1937). The constructions of such domes were built without applying steel nodes and wood gluing.

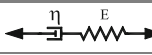
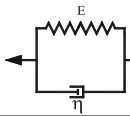
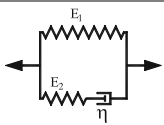
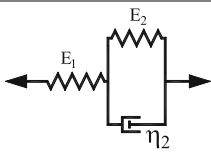
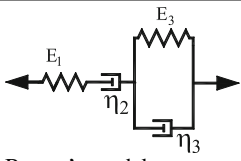
The increase of the dome diameters up to a span of 163.0 m, as discussed in Chap. 8, was obtained owing to the application of bars and girders from glued laminated timber connected with massive steel nodes, as well as such materials, such as concrete or polymer concrete. The completion of such domes became, in terms of computations and technology, more and more difficult and expensive. **New problems also come into being, being of significance for the experiments on the structures of domes from wood as well as other materials.**

The development of knowledge and numerical methods of the computation of constructions inspire for the completion of next domes of record-breaking diameters. However, the application of the conventional models of an elastic body in the calculations of wooden constructions yields, sometimes, unexpected results.

The differences between the classic results of theoretical calculations conducted on the basis of the models of an elastic body and the effects observed after years of operation, as described by Misztal B., reach up to 30% [2] (1999). This applies especially clearly to the limit states of the use. The identification of an visco-elastic model of wood is difficult due to various behaviours of wood depending on the direction of load and shift: longitudinal, flexible and crosswise.

It was demonstrated in the paper [3] (1966) by Kowal Z. and the paper by Kowal and Surkont [4] (1978) that time-dependent deformations and forces in constructions of rheological properties may be determined on the basis of the identified models of visco-elastic materials. In the paper [4] (1878) the authors deal with the analysis of spatial structures built from linear-visco-elastic bars, coupled articulated in nodes. They specify the formulae to assess the creeping shifts of visco-elastic bars, stretched by a load invariable in time. The authors also demonstrate that the elastic—visco-elastic analogy maintains its validity in the case of a random load of structure's nodes. Compiled in Table 10.1 are various visco-elastic models taken

Table 10.1 Compilation of basic rheological models of materials [4] (1978)

Model of the bar	k	u(t) elongation
 <p>Maxwell's model</p>	$\frac{EA}{l}$	$\frac{P}{k} \left(1 + \frac{E}{\eta} t \right)$
 <p>Voight's model</p>	$\frac{EA}{l}$	$\frac{P}{k} \left(1 - e^{-\frac{E}{\eta} t} \right)$
 <p>Zener's model</p>	$\frac{E_1 A}{l}$	$\frac{P}{k} \left[1 - \left(1 - \frac{E_1}{E_1 + E_2} \right) e^{-\frac{E_1 E_2}{\eta_2 (E_1 + E_2)} t} \right]$
 <p>Standard model</p>	$\frac{E_1 A}{l}$	$\frac{P}{k} \left(1 + \frac{E_1}{E_2} - \frac{E_1}{E_2} e^{-\frac{E_2}{\eta_2} t} \right)$
 <p>Burger's model</p>	$\frac{E_1 A}{l}$	$\frac{P}{k} \left(1 + \frac{E_1}{E_3} + \frac{E_1}{\eta_2} t - \frac{E_1}{E_3} e^{-\frac{E_3}{\eta_3} t} \right)$

into account. Shown in column 1 is the geometry of the models, in column 2 the elastic longitudinal stiffness, in column 3 the change u(t) of the elongation of bars in time.

Determined in Table 10.1: E—modulus of direct elasticity, A—section of the bar, η—damping parameter, k = EA/l—elastic longitudinal stiffness, l—length of the bar.

Theoretical and experimental research on the static and dynamic analysis of visco-elastic constructions have been conducted since the fifties of the 20th century. The basic theoretical papers in this direction (in the understanding of the operation of creep-exhibiting constructions) were conducted in Poland by: Nowacki [5] (1963), Kisiel [6] (1967), Kowal [7] (1964) et al.

In his paper [5] (1963) Nowacki W. formulates the mathematical fundamentals of statics and dynamics of linearly visco-elastic structures, the solutions of statics and dynamics of visco-elastic systems as well as the propagation of visco-elastic waves. He subjects the variation in time to the mathematical analysis, as well as the responses of materials and building constructions to load, a long-lasting load in particular. He demonstrates that the model of a perfectly elastic body is insufficient to the description of the state of stress and strain of the majority of building materials.

In his paper [6] (1967) Kisiel I. defines several basic rheological models, anticipating the option of their introduction to theoretical analyses in the building industry, in geotechnics (M/V model) in particular. He describes the operational mechanism of external forces as static loads on the soil. He introduces the mathematical analysis on the basis of two-parameter rheological models according to the rules of creep theory, elasticity and plasticity theory. He resolves, on the basis of rheological models adopted, rheological tasks for soils. It should be emphasized that the creep of soil has its impact on the creeping distortion of constructions seated on the soil, including wooden constructions.

In [8] (1982) Ganowicz R. demonstrated that the theoretical description of the creep process using determinist methods is impossible. In the opinion of the author, neither does the visco-elasticity theory reflect the behaviour of wood. The creep curves of visco-elastic materials are smooth, on the other hand, the experimental curves of creeping distortions of wood and visco-elastic materials being tested exhibit random variations of creeping distortions caused by random effects that can be described using the modified Poisson's process.

In her paper [2] (1999) Misztal B. noticed on the basis of own research and that conducted by other authors that the use in the analysis of wood of visco-elastic models leads to the observed variations in time of constructional elements from wood, wood-based materials and steel. She called attention to the fact that the creep of wood, wood-based materials and complex trusses from wood, wood-based materials and steels follows with a time-variable speed. At the first stage of the transverse load the creep speed is the highest. At the next stages of the creep process, the creep speed decreases. Deflections increase more and more slowly since in the creep process the deflection increments decrease.

In [9] (2002) Socha T. described the experimental testing of wooden beams of 5×11 cm dimensions being bent under the action of long-term static loads. He describes the results of the testing using several rheological models. The author is of the opinion that the basic rheological models, also including the Burger's model, do not describe the observed creeping distortions of beams. He proposes, however, the use of the Kelvin-Voight's model that in the opinion of Misztal B. neither describes well the behaviour of wood under the impact of a dynamic coercion.

In the paper [10] (2006) Rautenstrauch K, Doehrer A. and Harnack R. suggest the series connection of one-parameter and two-parameter models to calculate the creep coefficient of wooden compressed posts of 16/16 cm dimensions.

In the opinion of the author, the adoption of such an expanded model, as shown in Fig. 10.1, increases the difficulties in the assessment of the stiffness moduli of an element or a construction in the long-term testing. For the model shown in

Fig. 10.1 Rheological model applied by the author of the paper [10]

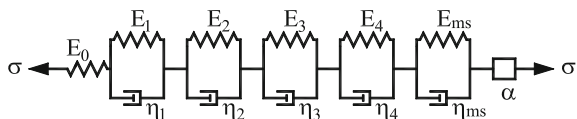


Fig. 10.1, the number of constituent values of the modulus of direct elasticity E_i after the time $t \rightarrow \infty$ of the construction's operation is difficult to determine:

$$\frac{1}{E_t} = \frac{1}{E_0} + \frac{1}{E_1} + \frac{1}{E_2} + \frac{1}{E_3} + \frac{1}{E_4} + \frac{1}{E_{ms}} \quad (10.1)$$

It is evident from the formula (10.1) that the higher is the quantity of E_i in the computational model, the more difficult is the assessment of the construction's stiffness in the time t .

In his paper [11] (1982) Pożgaj A. describes the trials of the long-term, 3000hrs-lasting bending of beams from spruce wood, of 11×11 mm and 20×20 mm sectional dimensions. It follows from the testing that a higher relative creep is demonstrated by samples of a larger section. **At the ratio of the sides of a rectangle such as 1:4, the creep of samples of a larger section is by 20–30% higher than that of samples of a smaller section. This information should be verified whether it operates in relation to high-dimensional domes built from glued elements of massive sections operates—as discussed in Chaps. 8 and 9, Figs. 9.14 and 9.15.** Pożgaj A. also demonstrated that the rise in the moisture content of the tested sample results in a decrease of deflection and vice versa. He notes down that deflection variations occurred with a various intensity. It points out to a sample that responded differently. The author suggests that abnormalities are caused by the wavy course of the fibre. Besides, he points out that larger samples respond to moisture content and air temperature variations with a delay as compared to smaller samples—he calls it inertia. As regards the impact of air temperature, he expresses an idea that temperature affects creep to a lower degree than moisture content. He is of the opinion that under the given ambient conditions, the impact on the creeping deflection of wood is exerted by the magnitude of load and the time of operation, moisture content, wood density and dimensions of the cross-section area of the sample. The author states that he did notice the creep process stabilization after 3000 h of the experiment.

In the paper the authors [12] (1982) Moliński W., Raczkowski J. tested the effect of ultra-violet radiation on the creep process of samples from pine wood, of 11×11 mm dimensions and a height of 110 mm. The experiments were conducted at the constant value of the tensile force amounting to 0.40 of the temporary rupture force. After the testing it was found that UV radiation eminently intensifies the creep process. The increase in creeping distortions due to the action of UV rays followed from the beginning of the application of the set static load. **UV radiation, in the set creep period, produces a sudden increase in the creep speed, exceeding up 6–8 times the creep speed before the exposure to illumination. The stabilization of the creep process after the switch-off of the illumination was noticed. The term of photo-mechanic creep was introduced.** The authors also specify that after the testing of the samples from an early wood of a fir-tree, after 8 h of radiation, the tensile strength dropped by 30%. In their opinion, the lowering of the strength gives evidence of the destruction of cellulose fibres on

which the tensile strength of wood depends. **In the opinion of Misztal B., the drop in the tensile strength after the UV exposure results from the destruction of the matrix and the weakening of the fastening of fibres in the visco-elastic matrix.**

In their paper [13] (2003) the authors Drelich R., Karczmarek M., Kubik J. describe the examination of the impact of ultrasonic waves on the creep of pine wood, in three different directions. The authors did not describe the effect of the wave on the creep process of wood.

In the paper [14] (2003) the authors Kasprzyk H., Wichłacz K. examined the chemical composition of pine wood at a temperature of 120–172 °C, as well as that exposed to gamma rays by doses of $\gamma = 20\text{--}11000$ kGy.¹ **It was found that the carbohydrate constituents of wood exhibit a significantly lower resistance to high temperature and high γ radiation does than lignin.** At the dose of 4500 kGy cellulose undergoes a full degradation and the content of pentosanes drops down to 70%. The content of lignin practically did not change, as it did not change for samples soaked at 172 °C, for 114 h, and those exposed to the radiation dose of 11000 kGy. The content of extraction substances abruptly rose both in cold and hot water, at 1% of NaOH, in the benzene-methanol mixture, with the rise of the radiation dose and temperature.

The impact of wood density on the propagation of ultrasonic waves along fibres was examined by the authors Marcinkowska A., Moliński W. in their paper [15] (2003). The experiment was conducted on samples of pine, oak and beech wood. It was found that the propagation speed of ultrasounds along fibres, in the mature wood tissue, of pine and beech wood, decreases, and for beech wood it rises along the rise of its density. It was noticed that **the length of anatomical elements (e.g. length of fibres) and not its density is an essential factor affecting the sound transmission along fibres.**

The authors Roszyk E., Moliński W. [16] (2003) described the results of the wood creep testing under the cyclic conditions, the non-symmetrical variations of the moisture content of the compressed zone of beams being bent. The testing was conducted on samples from the whitish part of pine wood, on the model of a free-supported, single-span beam, burdened with two forces concentrated in the span. The comparative testing of beams of an 8% moisture content and wet beams was conducted. It was found that wet wood features, in comparison with dry wood, an increased susceptibility to creep, especially in the initial period of the process. Besides, it was stated that **the wetting of the compressed zone of the beam being bent since the moment of its loading intensifies the creep process to a higher degree than in the case when the wetting process occurs in the period of the settled creep.**

The results of this testing may be used to determine the parameters of rheological models. In the opinion of the author, the sufficient forecasting of the behaviour of actual constructions is provided by models of several parameters, for instance, the

¹1KGy—kilo Grey—radiation dose unit.

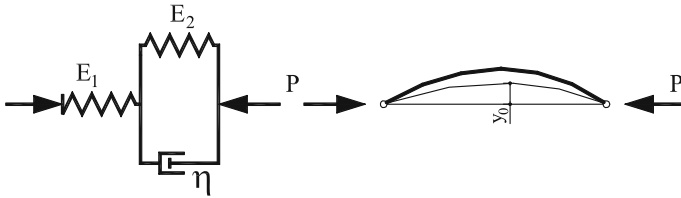


Fig. 10.2 Standard model adopted for the analysis of compressed bars from wood [17]

standard model or the Zener’s model. An example of the application of the standard model for the examination of the creep of an axially compressed post is shown in Fig. 10.2.

The module E_t of the standard model shown in Fig. 10.2 after the time $t = \infty$ amounts according to [17] to:

$$\frac{1}{E_t} = \frac{1}{E_1} + \frac{1}{E_2}, \rightarrow E_t = \frac{E_1 E_2}{E_1 + E_2} \tag{10.2}$$

The standard model, like that of Zener, is a sufficient model to control the regression curve of creeping shifts for constructional wood species, e.g. pine and spruce.

Worth noticing is the observation described in [18] of actual constructional systems from wood, confirming the durability and reliability of wooden constructions. In his publication [18] (2007) the author Ajdukiewicz A. describes the disaster of a steel roof caused by the action of snow bags. Due to the overloading, this roof fell on a wooden roof operated for sixty years, of a constructional schematic as shown in in Fig. 10.3 and dimensions: 44.60 m wide, 102 m long, made from wooden, single-pitch truss of a 22.26 m span. A damage to the wooden roof followed, but this roof did not collapse.

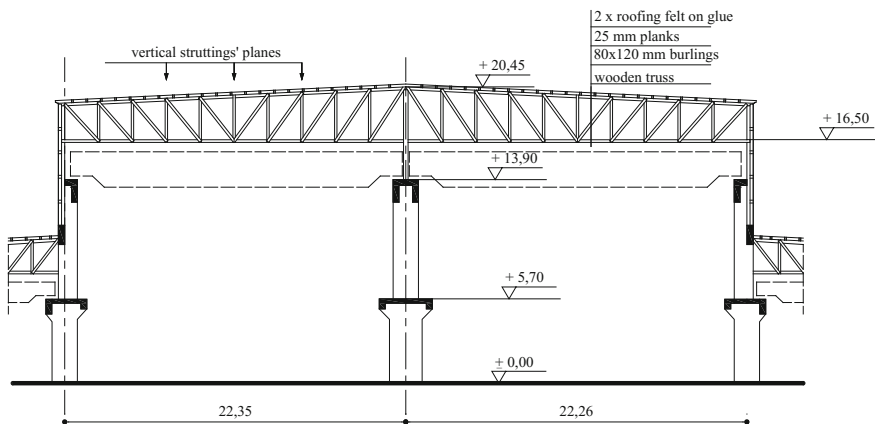


Fig. 10.3 Cross-section of the wooden roof according to [18] on which the steel roof fell

The problem of the assessment of the physical properties materials necessary for the objective calculation of wooden constructions grows along with the development of materials engineering, the wood gluing technology in particular.

For millennia, wood has been known for its rheological features. In the building of domes in which load-carrying elements are subject to high permanent, dynamic and climatic loads, the factors intensifying the wood creep process are of special importance. As follows from the publications discussed, the following factors belong to them: effect of the exposure to UV radiation, gamma radiation, the dynamic interference of environment, moisture content variations, even the dimensions of structural elements. These factors can provoke both creeping distortions, permanent, local cracks, as well as they can initiate the growing degradation of a material up to the destruction of the structural system. The effects of this process can be noticed, while watching historical facilities in which various deformations of elements and the whole wooden architectural forms followed. The increase of axial and transverse forces results in the deflection and shortening of wooden bars. The accompanying phenomenon of wood creep can initiate the node-through process and the loss of the load-capacity of wooden domes, especially gridshell domes. This should be taken into account in the course of the calculation of wooden constructions, including domes of diameters larger than 67.0 m.

It follows from the description of the testing included in Chap. 10 that in the engineering practice the methods of a quick, non-destructive diagnostics of constructional elements from wood are essential. The author shows in Chaps. 11 and 12 the possibility of using the dynamic testing to determine the physical properties of wood and wood-based materials as well as for the evaluation of the technical state of the constructional elements of the domes discussed in the papers [19] (2004), [20] (2006), [21] (2008), [22] (2009), [23] (2010).

References

1. Kaszkarow K., P. *Kopuły* Sprawocznik projektrowszczyka promyszlennych sooruzienij. Dieriewannyje konstrukcji. Kuzniecowa G. F. Gławnaja riedakcija stroitielnoj literatury. Moskwa-Leningrad 1937.
2. Misztal B., *Kratowe dźwigary z drewna, materiałow drewnopochodnych i stali*, Praca doktorska, Politechnika Szczecińska 1999.
3. Kowal Z. *Wyboczenie pełzające osiowo ściskanych prętów lepkosprężystych*, III Sympozjum PTMTS poświęcone reologii, referaty t. i, Wrocław 1966, s. 209–218.
4. Kowal Z. Surkont B., *Wyznaczanie losowych przemieszczeń i sił wewnętrznych w lepkosprężystych strukturach przestrzennych* VII Sympozjum poświęcone reologii PAN i PTMTS, PWr Wrocław 1978, s.146–156.
5. Nowacki W., *Teoria pełzania*, Arkady, Warszawa 1963.
6. Kisiel I., *Reologia w budownictwie*, Arkady, Warszawa 1967.
7. Kowal Z., *Stateczność osiowo ściskanego pręta w ośrodku lepkosprężystym*, Archiwum Inżynierii Łąkowej 2/1964, t. X., s. 37–45, 197–204.

8. Ganowicz R. *Zastosowanie teorii procesów losowych do opisu pełzania tworzyw konstrukcyjnych*, Reologia drewna i konstrukcji drewnianych – Sympozjum Akademii Rolniczej w Poznaniu, materiały, Zielonka 21–22 października 1982 r.
9. Socha T. w *Liniiowo lepko sprężyste modele reologii drewna*. V Konferencja Naukowa “Drewno i materiały drewnopochodne w konstrukcjach budowlanych”. Szczecin 17–18 maja 2002.
10. Rautenstrauch K., Doehrer A., Hartnack R., *Long-term load of wooden columns influenced by climate and stochastic material parameters* WCTE 2006 - 9th World Conference on Timber Engineering, Portland, OR, USA, August 6–10, 2006.
11. Pożgaj A. *Wpływ wymiarów przekroju poprzecznego próbek na ich pełzanie w naturalnych warunkach atmosferycznych* Reologia drewna i konstrukcji drewnianych – Sympozjum Akademii Rolniczej w Poznaniu. Materiały. Zielonka 21–22 październik 1982.
12. Moliński W., Raczkowski J., *Wpływ promieniowania ultrafioletowego na pełzanie drewna*. Reologia drewna i konstrukcji drewnianych, Sympozjum Akademii Rolniczej w Poznaniu, materiały, Zielonka 21–22 październik 1982.
13. Drelich R., Karczmarek M., Kubik J., *Propagacja fal ultradźwiękowych w drewnie jako naturalnym kompozycie*. Annals of Warsaw Agricultural University SGGW, Forestry and Wood Technology No 53, Warsaw 2003.
14. Kasprzyk H., Wichlacz K., *Comparative studies on the chemical composition of heat treated and gamma irradiated Pinus sylvestris wood*. Annals of Warsaw Agricultural University SGGW, Forestry and Wood Technology No 53, Warszawa 2003.
15. Marcinkowska A., Moliński W. *Wpływ gęstości drewna na propagacje fal ultradźwiękowych wzdłuż włókien*. Annals of Warsaw Agricultural University SGGW, Forestry and Wood Technology No 53, Warsaw 2003.
16. Roszyk E., Moliński W., *Pełzanie drewna w warunkach cyklicznych zmian wilgotności ściskanej strefy zginanych belek. Badania wstępne*. Annals of Warsaw Agricultural University SGGW, Forestry and Wood Technology No 53, Warszawa 2003.
17. Kowal Z. *Nośność krytyczna słupów drewnianych jako kompozytów włóknistych*. Sympozjum - Drewno i materiały drewnopochodne w konstrukcjach budowlanych. Szczecin-Międzyzdroje 05–06 września 1996.
18. Ajdukiewicz A., Brol J., Hulimka J., Węglorz M., *Awaria wielkopłociowego dachu o konstrukcji drewnianej* Awarie budowlane 2007, XXIII Konferencja Naukowo Techniczna Szczecin – Międzyzdroje, 23–26 maja 2007.
19. Misztal B., *Pomiary dynamiczne w diagnostyce stropów drewnianych* REMO 2004 r. XI Konferencja Naukowo Techniczna Problemy Remontowe w Budownictwie Ogólnym i Obiektach Zabytkowych, Wrocław Zamek Kliczków, 9–11 grudnia 2004.
20. Misztal B., *Forecasting in Time of Rheological Defections of Truss Girders, Consolidated from Wood, Wood-based Material and Steel*. WCTE 2006 - 9th World Conference on Timber Engineering, Portland, OR, USA, August 6–10, 2006.
21. Misztal B., *Comparison of the Vibration Frequency and Damping of Beam Models Made of Dry and Wet Pine Wood*, WCTE 2008, 10th World Conference on Timber Engineering, Miyazaki, JAPAN, June 2–5, 2008.
22. Misztal B. *Wpływ degradacji matrycy na nośność krytyczną ściskanych prętów drewnianych* REMO 2009 r., XII Konferencja Naukowo Techniczna Problemy Remontowe w Budownictwie Ogólnym i Obiektach Zabytkowych., Wrocław Zamek Wojanów, 2–4 grudnia 2009.
23. Misztal B., *Dynamic Parameters of the Free Vibrations of Various Wood Species* WCTE 2010, 11th World Conference on Timber Engineering, Riva del Garda, Trentino, Italy, June 20–24, 2010.

Chapter 11

Testing Wooden Elements for the Building of Domes

11.1 Introduction

The selection and choice of wood for the building of domes is a difficult task. Neither objective criteria for the choice of a wood species nor the best planks for the building of dome structures have been developed. Globally, the application of various wood species, most often the local ones, is noticed, and the choice of the best planks follows manually. The choice of wood species most useful for the building of structures on the basis of a tradition and the choice of planks on the basis of visual methods is worth supplementing with the physical testing methods taking into account the conditions and the operational life of constructions. It is suggested in this chapter **to supplement the recognition of the usefulness of wood for the building of domes on the basis of the free vibration measurement.**

The wood used for the building of prestigious wooden domes have to exhibit good physical properties, including strength parameters to ensure the required durability of the construction. Therefore, an effective selection of wood is necessary so as to choose from the mass of the best planks for the most strenuous elements of the construction, and to use planks of a worse quality in secondary elements, or to reject them.

In the daily practice the choice of wood for construction follows on the basis of a visual inspection. For instance, the Japanese Miyazaki Prefectural Wood Utilization Research Center responsible for the production of the Konohana Dome in the town of Miyazaki in 2002 (described in Chap. 8) made the choice of the best planks according to the measurement of the spacing between the fibres in the wood section [1]. Shown in Fig. 11.1 is the section glued from planks cut out from 45-year-old sugi trees. Planks were so selected that the spacing between rings were included within the range of 4–14 mm.

Demonstrated in Fig. 11.2 is the testing consisting in the sending of acoustic waves in the upper zone of the ceiling beam. Two sensors are installed on the

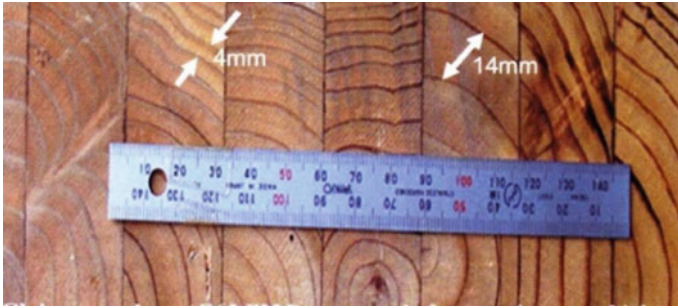


Fig. 11.1 Planks selected on the basis of the spacing criterion between rings [1] by Yutaka Imura (2002)

section of the wood being tested. With a hammer blow in one of the sensors the acoustic wave flowing to the next sensor is excited. The measurement of the wave flow resistance multiplied by the coefficient adopted in the measurement method is a conventional value of the modulus of direct elasticity of the material. It is assumed in this method that the acoustic wave flow rate also allows to make a comparative assessment of damages to the specimen being tested.

Shown in Fig. 11.2 is the FAKOPP Microsecond Timer device. The formula for the coefficient v suggested in [2]: v [m/s] = $1000 \times l_a / \text{FAKOPP} [\mu\text{s}] - 4.5$,

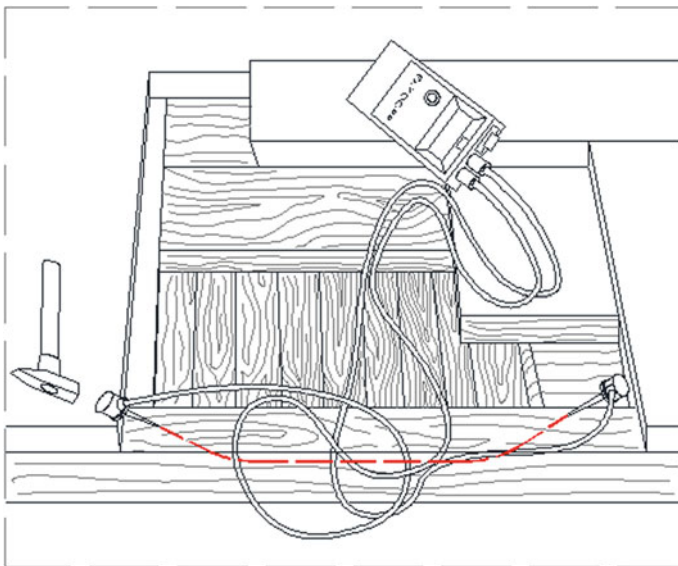


Fig. 11.2 Testing schematic of the beam through the measurement of the acoustic wave flow rate in wood between the sensors. The wave flow path is marked with a red dotted line

where “ v ”—wave flow rate [m/s], l_a —spacing between the measurement sensors as measured in [mm]. “ v ” is the coefficient read on the device demonstrated in Fig. 11.2.

In this method it is recommended to calculate the dynamic module of direct elasticity (E_d) at the known wood density of the beam being tested “ ρ ” from the formula:

$$E_d = v^2 \times \rho.$$

where: v —coefficient read out on the device, “ ρ ”—density of wood being tested.

As known from the paper [3], the flow rate of the acoustic wave depends mainly on the length of the fibres of the wood being tested. It does not depend on the wood density. The properties of the structural wood depend not only on the length of its fibres, as demonstrated in Chap. 9. The properties of wood depend on many factors, among others, on the properties of the matrix in which wood fibres are inundated and the quality of their fastening in the said matrix.

The methods presented allow, in the opinion of the author, to make local measurements and a local assessment of the individual features of the wood sample being tested. **Most often, beside the local data, the global information about the technical state of the element and the value of, e.g., of the modulus of elasticity E for a wooden beam or post, is required. To this aim, the author recommends short dynamic tests for the selection, evaluation and determination of the stiffness of elements, as well as the modulus of direct elasticity E from various wood species.**

Many authors were dealing with the issues of dynamics of visco-elastic structures. Among others, Nowacki W. in his monograph [4] (1972) specifies the solutions related to the dynamics of some visco-elastic systems and the propagation of visco-elastic waves. The author presented the mathematical fundamentals for the dynamics of linear visco-elastic constructions.

The work tasks of the loss of the stability of visco-elastic compressed bars are formulated and resolved by Kowal Z. in his papers [5] (1966) and [6] (2005) and other papers. In the paper [5] (1966), he resolves the issue of the buckling of a compressed bar in a visco-elastic medium. The author analyses the vibration: of a visco-elastic and a stiff beam on the supports: viscous, visco-elastic and stiff. He determines the dynamic coefficients to determine the maximum vibration amplitude and the maximum forces within the system. Kowal Z. describes the free vibration measurement method in his paper [7] (1983) for a practical application. It was used for the comparative detection of girders damaged in a flat roof having the construction from prestressed concrete girders. Upon excitation up to vibration of successive girders, the frequency of their free vibration was measured. The lowest frequencies were exhibited by damaged girders of a lower stiffness. This allowed to conclude about the need of their replacement or strengthening. This method is also suitable to detect damaged planks and wooden beams.

Langer J. in his paper [8] (1980) on the subject of the vibration of flat bar systems as well as the vibration of solids on an elastic substrate called attention that

the free vibration of constructional systems of a low damping are described in practice by an equation derived for the Kelvin-Voigt model. The author stated, however, that the Kelvin-Voigt model does not describe sufficiently the statics and dynamics of building constructions. Like Kowal Z., he demonstrates in his numerous publications that in the Kelvin-Voigt model there is no element to reflect the immediate deflection of a construction under the influence of loads, and this model used so far yields increased values of forces and a decreased assessment of the shifts of a construction. On the other hand, the Maxwell model shows increased amplitudes and reduced forces within the system.

The testing of the free vibration allows the comparative analysis of the vibration parameters of construction elements. On the basis of the comparison of the measured circular speeds of the own free vibration α of similar beams there is a possibility to detect dry and wet beams, and to differentiate damaged beams from undamaged beams. To this aim, the logarithmic vibration damping decrements Δ on the basis of dimensional damping coefficients ρ should be calculated. For the first time, the author recommended the dynamic testing in the diagnostics of wooden constructions in her paper [9] (2004).

The authors Kokociński W., Poliszko S., J. Raczkowski [10] (1982) described the creep of wood under the conditions of a dynamic extortion. The authors do not define the practical conclusions resulting from the dynamic testing. They specify that:

1. the dynamic extortion activates the process of the static creep of wood,
2. the creep speed at low cycles (3 cycles per minute) is comparable to that of static creep,
3. at higher frequencies >30 cycles per minute the creep speed is higher than that of static creep,
4. as the amplitude of translocations from applied load rises, the difference between the static creep and the vibro-creep increases,
5. according to [10], the static and dynamic forced distortions are subject to a description using the same function of creep.

They called attention to the missing dynamic testing of wooden structural elements. The authors have demonstrated that: (1) in the case of statically loaded wooden constructions, the introduction of vibrational load produces enhanced distortions and creeping translocations, (2) the wood creep model changes under the influence of moisture variations.

Jakowluk A. in his paper [11] (1993) examined the vibro-creep of samples from materials with a plastic stop (metals). The author describes the impact of harmonic vibration on the creeping process. The samples of materials were loaded statically and subjected to a harmonic load. The author defines the vibro-creep as the process of the impact of a dynamic load, of a low stress amplitude A_{σ} in metals, on the process of static creep. He assumes that vibration does not produce the fatigue of a material, but jointly with the action of a static stress brings about a creep leading to destruction.

The hypothesis about the use of the dynamic testing to the calculation of the modulus of elasticity of wood and the evaluation of the technical state of wood was formulated for the first time in the experimental works by Misztal B. [9] (2004), [12] (2008), [13] 2010.

These hypotheses were presented in the testing of models from wood and wood-based materials, as described in this chapter and Chap. 12 of this publication.

11.2 Dynamic Testing Oriented Towards the Choice and Selection of Wood for the Construction of Domes

It is suggested to measure the free vibration parameters of wooden, plank-supporting elements, instead of the commonly applied long-term testing or visual inspection as discussed in the preface. This will allow the verification whether the testing of the free variation of wooden elements is suitable for the selection of wood for the construction for domes.

The recognition of the features of wood on the basis of a dynamic testing, yielding clear results, instead of visual inspections, long-term testing or the measurement of flow speed of acoustic waves was suggested.

The measurement and calculation method of the free vibration parameters following the examples of dry and wet models of beams from wood: pine, spruce, larch and oak is demonstrated in this chapter. The aim of the testing was to determine the degree of the suitability of various wood species for the building of constructions, domes in particular.

The rate of the deflection reduction upon removal of the load was adopted as one of the criteria of the suitability of wood for the building of domes.

Models of dry and wet planks, of a 10×40 mm section, 1200 mm long were prepared for the testing. The models were made from pine, spruce, larch and oak wood. Before the experiment, the planks were weighed in a dry-air state. After the dynamic testing of dry planks, they were soaked in water for 24 h. After the wetting, the planks were re-weighed, and their moisture by weight was calculated. Planks loaded with a fixed mass of 250 g, cantilever-wise, like in the figure, were set in a vibrating motion. The extortive load was applied at the end of the support perpendicularly to the plane of the lower stiffness of the beam (Fig. 11.3).

The frequency n and the damping ρ of the free vibration extorted by a pulse via the load $P = 250.0$ g suspended on a thread at the end of the support was tested. The vibration was extorted through the cutting of the load-maintaining thread. After the wetting in water, the testing of the impact of the wetting of wooden beams on the frequency n and the damping ρ of free vibration and the creep of beams was carried out.

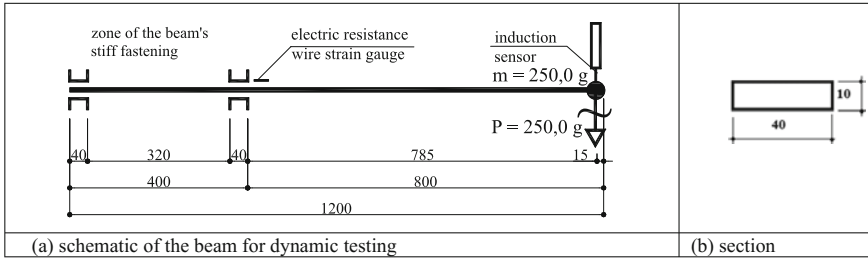


Fig. 11.3 Model of the beams being tested

In all cases, the damped free vibration measured, regardless of the wood species, was well described by the function (11.1) [14]:

$$y_t = y_0 e^{-\rho t} \cos(t\omega + \varphi) \Rightarrow y_t = y_0 e^{-\rho t} \cos\left(t\sqrt{\alpha^2 - \rho^2} + \varphi\right), \quad (11.1)$$

where:

- α circular frequency of own vibration,
- ρ dimensional vibration damping
- φ phase displacement

$$\omega = \sqrt{\alpha^2 - \rho^2} \quad \text{circular frequency of damped vibration} \quad (11.2)$$

Placed below are the vibrating motion parameters as measured on the models from dry and wet planks and as assessed according to the formulae as follows:

- vibration frequency:

$$n = \frac{1}{T} \left[\frac{1}{s} \right], \quad (11.3)$$

- vibration period T measured in [s],
- circular speed ω of damped vibration speed was calculated from the formula:

$$\omega = 2\pi n \quad (11.4)$$

- logarithmic damping decrement Δ was calculated from the formula:

$$\Delta = \ln \frac{A_i}{A_{i+1}} = \ln \frac{e^{-\rho t}}{e^{-\rho(t+T)}} = \rho T \quad (11.5)$$

- where A_i, A_{i+1} are successive vibration amplitudes
- dimensional damping coefficient ρ totals:

$$\rho = \Delta/T[1/s]. \tag{11.6}$$

For each of dry and wet beams the vibrating motion parameters were calculated: for dry models with an index “s”: $T_s, y_0, \rho_s, n_s, \omega_s, \Delta_s$, and for wet models with an index “m”: $T_m, y_0, \rho_m, n_m, \omega_m, \Delta_m$, where: n —vibration frequency, T —vibration period, ρ —damping coefficient, Δ —logarithmic damping decrement.

The vibration chart of the model from a dry pine-wood plank is presented in Fig. 11.4. This is an exemplary chart of the free damped vibration of a pine-wood plank during 10 s of the testing (Table 11.1).

The vibration chart of a model from a pine wood plank is presented in Fig. 11.5. This is an exemplary chart of the damped vibration of a pine wood plank of a 56.62% moisture by weight, during 10 s of the testing (Table 11.2).

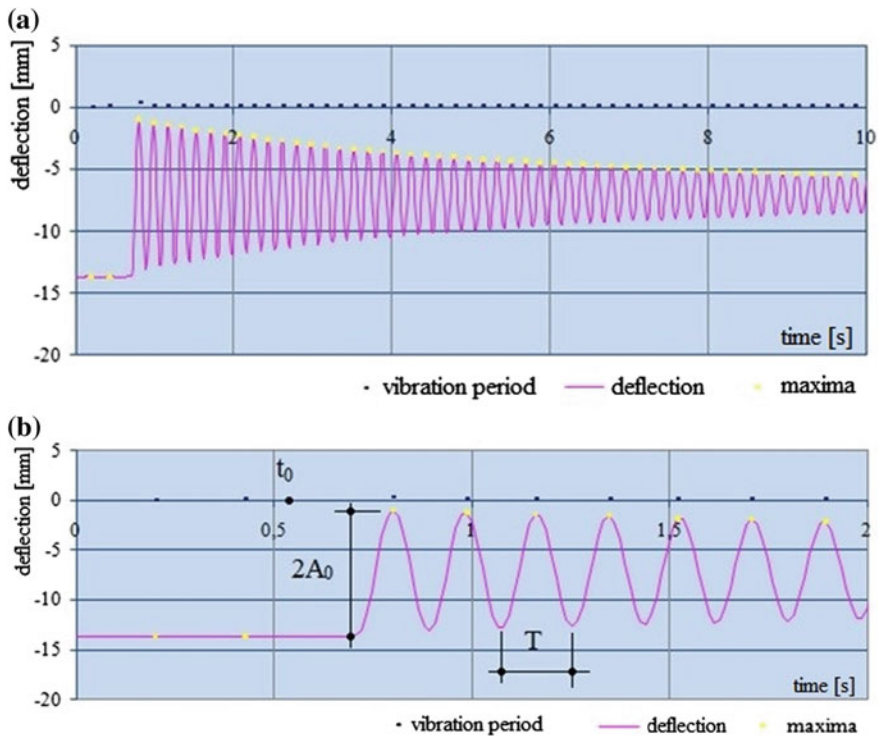
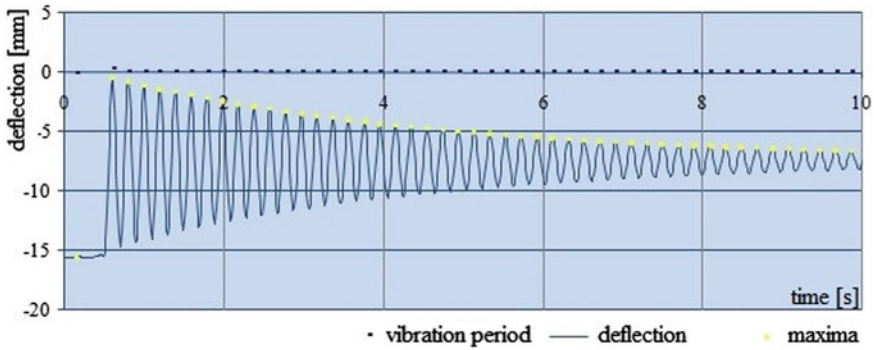


Fig. 11.4 Vibration chart **a** of the pine-wood model in dry-air state during 10 s of the testing, **b** during the first 2 s of the testing

Table 11.1 Parameters of the vibrating motion of the model tested according to Fig. 11.3 from pine wood in a dry-air state, burdened with a concentrated mass at the end

T_s [s]	t_0 [s]	y_0 [mm]	ρ_s [1/s]	$n_s = 1/T$ [1/s]	ω_s [1/s]	φ [°]	Δ_s
0.186	0.5733	13.68	0.14	5.38	33.8	11.15	0.026

**Fig. 11.5** Record of the vibrating motion of a model from pine wood burdened at the end during 10 s**Table 11.2** Vibrating motion parameters of a model according to Fig. 11.3 from wet pine wood of a 56.62% moisture, burdened with a concentrated mass at the end

T_m [s]	t_0 [s]	y_0 [mm]	ρ_m [1/s]	$n_m = 1/T$ [1/s]	ω_m [1/s]	φ [°]	Δ_m
0.1117	0.506	15.57	0.2411	5.076	31.811	3.21	0.04112

Table 11.3 The vibrating motion parameters of a model according to Fig. 11.3 from spruce wood in a dry-air state, burdened with a concentrated mass at the end

T_s [s]	t_0 [s]	y_0 [mm]	ρ_s [1/s]	$n_s = 1/T$ [1/s]	ω_s [1/s]	φ [°]	Δ_s
0.17	0.2667	13.99	0.172429	5.8823	35.35994	-3.49754	0.029313

Placed in Table 11.3 are the parameters of the vibrating motion T_s , y_0 , ρ_s , n_s , ω_s , Δ_s and in Fig. 11.6 an exemplary chart of the damped free vibration of a spruce wood plank model in a dry-air state.

Placed in Table 11.4 are the vibrating motion parameters as well as in Fig. 11.7 an exemplary chart of the damped free vibration of a spruce wood plank model of a 34.92% moisture content.

Placed in Table 11.5 are the vibrating motion parameters T_s , y_0 , ρ_s , n_s , ω_s , Δ_s as well as in Fig. 11.8 an exemplary chart of the damped free vibration of a larch wood plank model in a dry-air state.

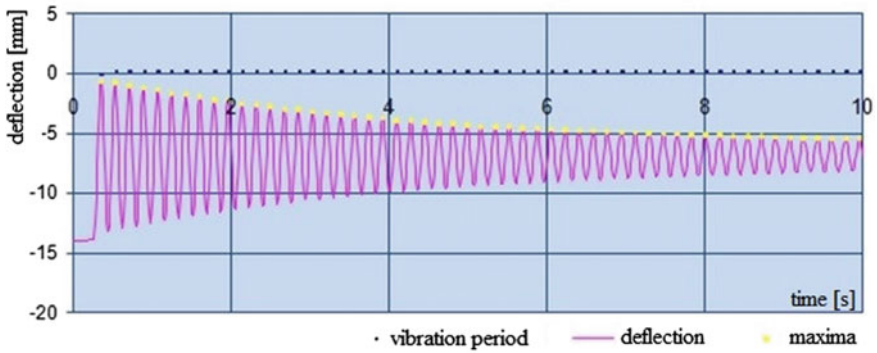


Fig. 11.6 Record of the vibrating motion of a model from spruce wood burdened at the end during 10 s

Table 11.4 The vibrating motion parameters of a model according to Fig. 11.3 from wet spruce wood of a 34.92% moisture content, burdened with a concentrated mass at the end

T_m [s]	t_0 [s]	y_0 [mm]	ρ_m [1/s]	$n_m = 1/T$ [1/s]	ω_m [1/s]	φ [°]	Δ_m
0.187	0.4667	14.85	0.263616	5.3475	34.11056	-3.51436	0.0493

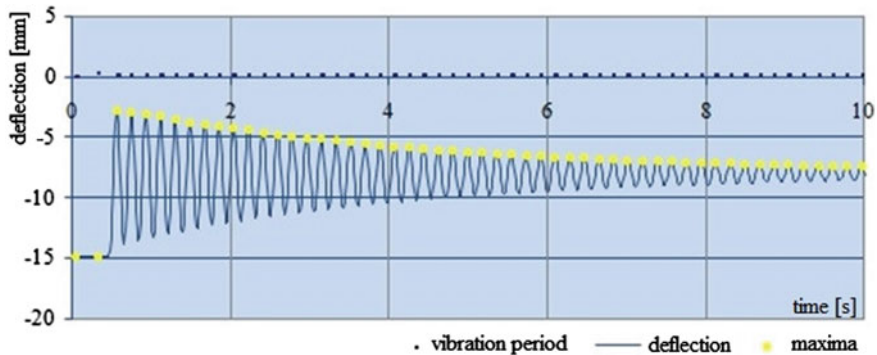


Fig. 11.7 Record of the vibrating motion of a model from wet spruce wood burdened at the end during 10 s

Table 11.5 Vibrating motion parameters of a model according to Fig. 11.3 from larch wood in a dry-air state, burdened with a concentrated mass at the end

T_s [s]	t_0 [s]	y_0 [mm]	ρ_s [1/s]	$n_s = 1/T$ [1/s]	ω_s [1/s]	φ [°]	Δ_s
0.21	0.72	18.76	0.148506	4.7619	30.01375	21.70679	0.0312

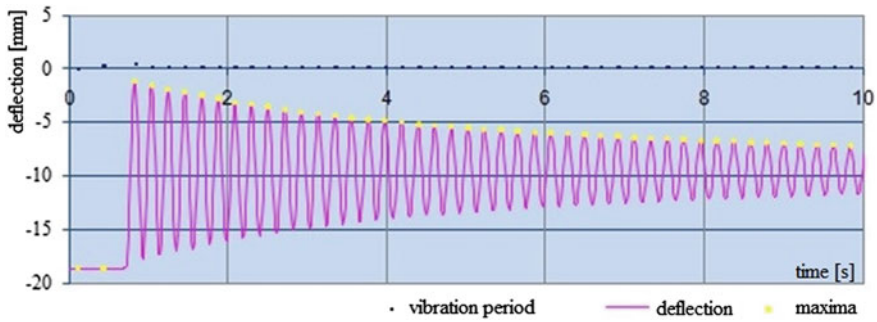


Fig. 11.8 Record of the vibrating motion of a model from larch wood in a dry-air state during the first 10 s of the testing

Table 11.6 The vibrating motion parameters of a model from wet larch wood of a 25.93% moisture content, burdened with a concentrated mass at the end

T_m [s]	t_0 [s]	y_0 [mm]	ρ_m [1/s]	$n_m = 1/T$ [1/s]	ω_m [1/s]	φ [°]	Δ_m
0.22	0.4533	21.16	0.256217	4.54	28.5664	9.524647	0.0564

Placed in Table 11.6 are the vibrating motion parameters of a larch wood plank of a 25.93% moisture content by weight. Figure 11.9 presents an exemplary chart of damped vibration during the first 10 s of the testing.

Placed in Table 11.7 are the vibrating movement parameters T_s , y_0 , ρ_s , n_s , ω_s , Δ_s as well as in Fig. 11.10 an exemplary chart of the damped free vibration of an oak wood plank model in a dry-air state. Figure 11.10 demonstrates an exemplary chart of damped vibration during the first 10 s of the testing.

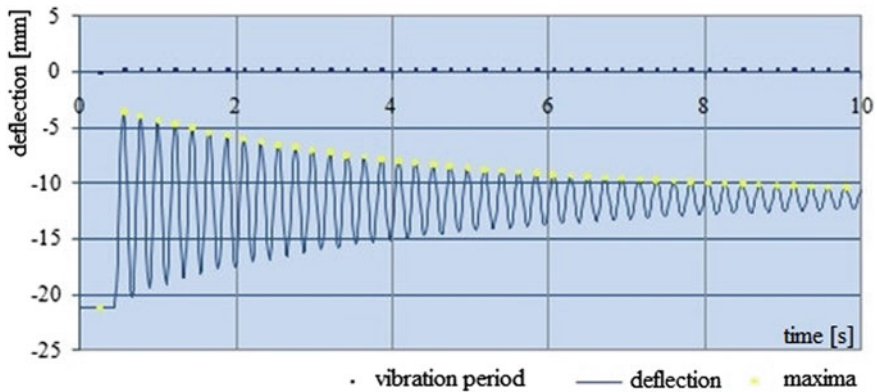


Fig. 11.9 Record of the vibrating movement of a model from wet larch wood during the first 10 s of the testing

Table 11.7 The vibrating motion parameters of a model tested according to Fig. 11.3 from oak wood in a dry-air state, burdened with a concentrated mass at the end

T_s [s]	t_0 [s]	y_0 [mm]	ρ_s [1/s]	$n_s = 1/T$ [1/s]	ω_s [1/s]	φ [°]	Δ_s
0.253	0.11067	25.77	0.1673	3.953	24.835	2.251	0.0423

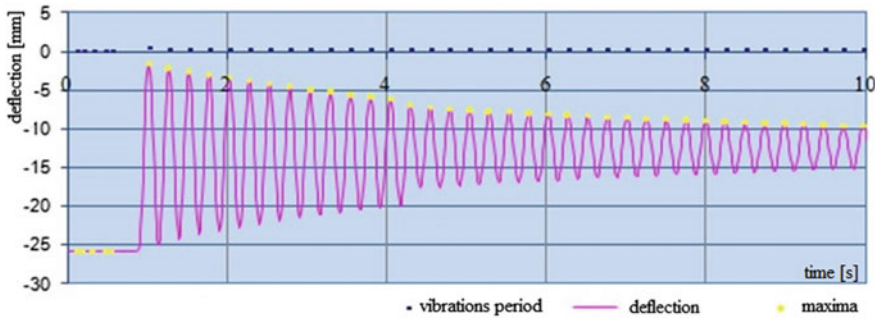


Fig. 11.10 Vibration chart of a model from oak wood in a dry-air state during the first 10 s of the testing

Placed in Table 11.8 are the vibrating motion parameters of an oak wood plank of a 23.00% moisture content. Figure 11.11 demonstrates the damped vibration charts of a wet oak wood plank during the first 10 s of the testing.

Table 11.9 demonstrates the impact of the increase in moisture content of beams from pine wood on the free vibration parameters of the models. Pine wood was selected as a representative of coniferous construction wood species, oak wood as a representative of deciduous wood species.

Presented in Table 11.10 are the ratios of the vibration parameters of wet models versus the vibration parameters of dry models characterizing the impact of the increase in moisture content on beams from oak wood. The determination of the vibration parameters is like in Table 11.9.

The models of small beams from wood were also subjected to a testing consisting in the six-fold pulse excitation with a force of 250.0 g, (each model separately) according to the scheme as in Fig. 11.3. For each model, after the testing, the residual deflection was observed. The total deflection upon completion of six excitation trials of one model was adopted as residual deflection. After a variable time for the given model, the deflection was decreased down to a value that did not decrease any more (Table 11.11). Such a deflection was called a permanent deflection.

Table 11.8 The vibrating motion parameters of a model tested according to Fig. 11.3 from wet oak wood of a 23.00% moisture content burdened with a concentrated mass at the end

T_m [s]	t_0 [s]	y_0 [mm]	ρ_m [1/s]	$n_m = 1/T$ [1/s]	ω_m [1/s]	φ [°]	Δ_m
0.267	0.6	30.98	0.236	3.745	23.5325	15.876	0.063

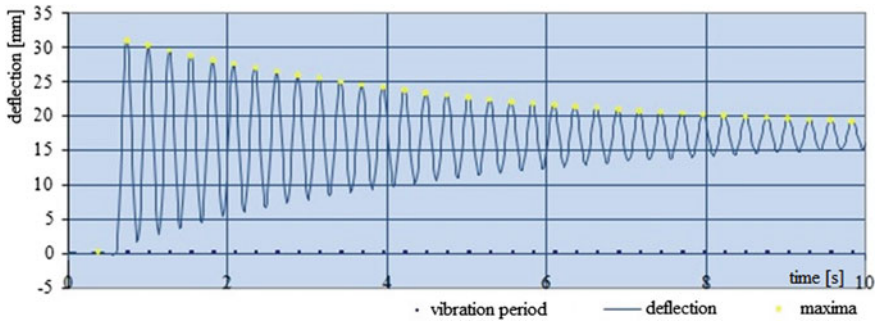


Fig. 11.11 Record of the vibrating motion of a model from wet oak wood burdened at the end during 10 s

Table 11.9 Ratios of the free vibration parameters of wet pine wood versus dry pine wood

Pine wood						
1	2	3	4	5	6	7
$\frac{n_m}{n_s}$	$\frac{T_m}{T_s}$	$\frac{\rho_m}{\rho_s}$	$\frac{\Delta_m}{\Delta_s}$	α_s	α_m	$\frac{\alpha_m}{\alpha_s}$
0.9435	1.0511	1.785	1.822	33.8[1/s]	31.8[1/s]	0.94

where

n_m —vibration frequency of a wet plank

n_s —vibration frequency of a dry plank

T_m, T_s —vibration period of a wet plank and a dry plank

ρ_m, ρ_s —vibration damping coefficient of a wet plank and a dry plank

Δ_m, Δ_s —logarithmic damping decrement of a wet plank and a dry plank

α_m, α_s —circular speed of the undamped free vibration of a wet plank and a dry plank,

$$\alpha = \sqrt{\omega^2 + \rho^2}$$

Table 11.10 Comparison of the free vibration parameters of a dry oak wood plank versus a wet oak wood plank

Oak Wood						
1	2	3	4	5	6	7
$\frac{n_m}{n_s}$	$\frac{T_m}{T_s}$	$\frac{\rho_m}{\rho_s}$	$\frac{\Delta_m}{\Delta_s}$	α_s	α_m	$\frac{\alpha_m}{\alpha_s}$
0.947	1.0553	1.41	1.488	24.836 [1/s]	23.534 [1/s]	0.9476

The models from wood subjected to the six-fold pulse excitation during several dozens of minutes exhibited such residual deflections like after a long-term static testing. The pulse-excited vibration allowed a preliminary discrimination of visco-elastic models of various wood species during a dozen or so minutes, and several dozens of months, like in the case of the long-term testing for static creep.

Table 11.11 Comparison of deflections and vibration periods of four wood species after six excitation cycles up to vibration using a 250.0 g mass

Wood species	Residual deflection of the support's end after 6 excitations using a 250 gf force	Permanent deflection of the support's end	Dry beams	Wet beams
			Vibration period	Vibration period
1	2 [mm]	3 [mm]	4 [s]	5 [s]
Pine	0.29	0.05	0.07	0.18
Spruce	0.13	0.02	0.07	0.17
Larch	0.39	0.07	0.074	0.21
Oak	2.93	2.01	0.106	0.253

The least residual deflection after 6 cycles of pulse-excited vibration is exhibited by coniferous trees' species. Among the coniferous species, the highest permanent deflection is demonstrated by larch wood.

The lowest vibration period is owned by pine wood, the highest vibration period by oak wood. The vibration period depends on the mass of a construction. The significant difference in the vibration periods specified in columns 4 and 5 of Table 11.11 results from a different mass of dry planks and wet planks. To a low degree, it follows from a various vibration damping. It has also been noticed that each element tested differed insignificantly by the free vibration period. **The vibration period within one trial of each of the planks tested was a fixed value.**

The models from wood were also tested in order to assess the moduli of direct elasticity E_s in a dry-air state and after a 24-h soaking in water. The description of the testing and the statement of the results are specified in Sect. 11.3.

11.3 Dynamic Testing Results Oriented Towards the Determination of the Modulus of Direct Elasticity E of Wood

On the basis of the dynamic testing conducted on a test stand presented in Sect. 11.2 according to the schematic shown in Fig. 11.3 it is recommended to determine the frequency n and the damping ρ of free vibration in order to assess the modulus of direct elasticity of wood. The vibrating motion parameters T , ρ , ω , Δ , shown in Tables 11.1, 11.2, 11.3, 11.4, 11.5, 11.6, 11.7, and 11.8 were determined on the basis of the numerical measurement results using EXCEL spreadsheets. Vibration was excited through the cutting of a thread maintaining a load of $P = 250.0$ g suspended at the end of the support. After soaking in water, the testing of the impact of the wetting of wooden beams on the frequency n and the damping ρ of free vibration and the modulus of direct elasticity of beams was performed.

The testing of the models of pine, spruce and larch wood planks representing coniferous species of construction wood and that of an oak wood plank, as the representative of deciduous species was carried out. The testing was done on dry models and after a 24-h soaking in water.

In all cases the damped free vibration, as described by the function (11.1) are discussed in Sect. 11.2. For each of the beams the free vibration parameters were calculated using the formulae (11.2) through (11.6) and compiled in Tables 11.1 through 11.8. The calculated modulus of elasticity E is compiled in Tables 11.12 and 11.13, in columns: 9 and 10, developed in this chapter.

Kowal Z. specified in his paper [14] (1966) the relationships between the stiffness K , the mass— m_z , the vibration speed ω and the damping ρ . The dependence was derived from the equation of the motion of a visco-elastic body written in form of the formula (11.7):

$$m_z^{**} y + K_\eta y + Ky = 0 \quad (11.7)$$

$$m_z^{**} y + K_\eta y + Ky = 0/m_z \quad (11.8)$$

$$y + \frac{K_\eta}{m_z} y + \frac{K}{m_z} y = 0 \quad (11.9)$$

$$\alpha^2 = \frac{K}{m_z} \quad (11.10)$$

$$\rho^2 = \frac{K_\eta}{m_z} \quad (11.11)$$

$$\alpha^2 = \omega^2 + \rho^2 \quad (11.12)$$

In the absence of damping, there is the equation of the free vibration of a spring:

$$m_z^{**} y + Ky = 0/m_z \quad (11.13)$$

The assessment of the stiffness $K = \alpha^2 m_z$ is understated since the actual stiffness will be slightly higher as damping occurs:

$$\omega^2 = \alpha^2 - \rho^2 \quad (11.14)$$

In the elastic system of one degree of freedom the relationship occurs:

$$Ky = P \quad (11.15)$$

Table 11.12 Comparative compilation of the modulus of direct elasticity E of the tested in a dry-air state

Dynamic parameters in a dry-air state tested according to Fig. 11.3									
Material	Model's mass [g]	Evenly distributed mass [g/m]	ρ_s		Own vibration	m_z [g]	$K = m_z \alpha_s^2$ [g/s ²]	E _s of models in dry-air state [GPa]	E as per the standard [GPa]
			ρ_s^2 [1/s]	ω_s^2 [1/s ²]					
1	2	3	4	5	6	7	8	9	10
Pine wood	260.70	178.15	0.14	33.80		285.498	326,170.1	17.98	11-14
Spruce wood	224.58	153.46	0.0196	1142.44	1142.46	280.578	370,065.5	20.40	
Larch wood	267.60	182.86	0.0297	1318.91	1318.94	286.437	258,035.6	14.23	
Oak wood	314.42	214.85	0.1673	24.835	900.847	292.811	180,607.3	9.96	No data
			0.028	616.777	616.805				

Table 11.13 Comparative compilation of the moduli of direct elasticity E_m of the tested models after a 24-h soaking in water

Material	Dynamic parameters of wet models tested according to Fig. 11.3						m_z [g]	$K = m_z \alpha_g^2$ [g/s ²]	Moisture content [GPa]	E_m [GPa]	Reduction of E [%]
	Model's mass [g]	Evenly distributed mass [g/m]	ρ_m^2 [1/s]		ω_m^2 [1/s]	$\alpha_m^2 = \rho_m^2 + \omega_m^2$ [1/s ²]					
			ρ_m^2	ω_m^2							
1	2	3		4	5	6	7	8	9	10	11
Pine wood	408.30	279.00		0.2411	31.811		305.594	309,260.05	56.6	17.05	5.0
Spruce wood	308.52	210.82		0.0581	1011.94	1011.998	292.008	329,685.65	34.9	18.18	10.9
Larch wood	337.00	230.28		0.2636	33.6		295.886	241,474.01	25.9	13.31	6.5
Oak wood	386.70	264.23		0.0695	1128.96	1129.0295	302.650	167,618.73	23.0	9.24	7.2
				0.2562	28.5664	816.106					
				0.06565	816.04						
				0.236	23.5325						
				0.0557	553.78	553.836					

Disregarding the viscosity η due to the low impact of damping on the stiffness of an element from wood (Table 11.13) on vibration frequency, one may assess the local stiffness \mathbf{K} of the bar directly from the formula:

$$K = m_z \alpha^2 \approx m_z \omega^2 \quad (11.16)$$

The moduli of elasticity \mathbf{E} were assessed from the below-specified algorithm.

When calculating the reduced mass of the test models, the actual, effective local stiffness of the tested beams was counted. The elastic stiffness K_{ef} , associating the load with the shift, $K_{ef} = P/y$, is related to the measured vibration speed ω and the damping ρ with the formula from the paper [14].

$$\alpha^2 = \omega^2 + \rho^2 = \frac{K_{ef}}{m_z} \quad (11.17)$$

where: ω —measured frequency of damped free vibration [radians], ρ —measured damping of free vibration, α —frequency of own vibration (undamped) [radians].

The immediate shift under the load $P = m_z \cdot g$ can be determined from the formula:

$$y_o = P/K_{ef} \quad (11.18)$$

where: $K_{ef} = m_z \alpha^2$ effective stiffness of the beam as measured on the model.

The circular speed of undamped free vibration, required to assess the elastic stiffness of dry and wet planks, was calculated from the formula (11.12).

$$\alpha = \sqrt{\omega^2 + \rho^2} [1/s] \quad (11.19)$$

where: α —own vibration, ω —free vibration, ρ —vibration damping.

The local stiffness \mathbf{K} of the support model was assessed on the basis of the substitutive concentrated mass m_z at the end of the support, as well as the measurement of the support's free vibration measurement α from the formula (11.16).

The square of the free vibration frequency $\alpha^2 = \omega^2 + \rho^2$ calculated after the testing on models is placed in Tables 11.12 and 11.13 (column 6).

The substitutive concentrated mass m_z resulting from the own mass of the support (of the tested model) was calculated from the formula (11.20) according to [15]:

$$m_z = 0.243 ql + 250 \quad (11.20)$$

where: q —measured weight per running metre of the support.

The stiffness \mathbf{K} of the models determined from the relationship $K_{ef} = m_z \alpha^2$ is placed in Tables 11.12 and 11.13—column 7.

The relationship between the stiffness K and the load P has the form from the Eq. (11.15), therefore:

$$y = \frac{P}{K} \Rightarrow K = \frac{P}{y} \quad (11.21)$$

The shift y was determined from the formula:

$$y = \frac{Pl^3}{3EJ} = \frac{P}{K} \quad (11.22)$$

The modulus of direct elasticity E was obtained from Eq. (11.21):

$$E = \frac{Kl^3}{3J} \quad (11.23)$$

According to Fig. 11.3, the length of the support $l = (785 + 20 + 15) \text{ mm} = 0.82 \text{ m}$ was assumed for the calculations of E .

In Tables 11.12 and 11.13 the measured vibration parameters and the calculated stiffness values K and the moduli of direct elasticity E are compiled. The stiffness values K and the moduli of elasticity E of the tested wood species from dry and wet models were compared. In column 9 of Table 11.12 the assessment of the moduli of elasticity E_s of the tested dry models are compiled. In column 10 of Table 11.13 the assessment of the moduli of elasticity E_m of the tested wet models are compiled. The moisture content by weight of the models is specified in column 9 of Table 11.13.

The columns of Tables 11.12 and 11.13 were numbered and the following data were placed therein: in column 1—name of the material from which the model was made, in column 2—the mass 1 of the model, in column 3—mass in [g/m] of the support, in column 4—dimensional damping ρ , in column 5—square of free vibration frequency ω^2 , in column 6—square of own vibration frequency α^2 , in column 7—substitutive mass m_z , in column 8—stiffness of the support K , in column 9—modulus of elasticity of dry models E_s , Table 11.12 in column 10—modulus of elasticity of wet models E_m , Table 11.13 in column 11—percentage reduction E_m after a 24-h soaking in water after a 2-h soaking in water.

11.4 Conclusions

Presented in Figs. 11.4, 11.5, 11.6, 11.7, 11.8, 11.9, 11.10, and 11.11 are the charts of the damped free vibration of plank models: from pine, spruce, larch and oak wood during the first 10 s of the testing. The comparison of the vibration of dry and wet planks allowed to determine significant differences in the vibration damping. **For each species of dry and wet planks the rations were calculated and placed in Tables 11.1, 11.2, 11.3, 11.4, 11.5, 11.6, 11.7, 11.8, 11.9, 11.10, 11.11, 11.12,**

and 11.13: —free vibration frequency of a wet plank n_m versus dry plank n_s : n_m/n_s , —vibration periods of a wet plank T_m versus a dry plank T_s : T_m/T_s . —damping coefficients of a wet plank ρ_m versus a dry plank ρ_s : ρ_m/ρ_s , —logarithmic damping decrements of a wet plank Δ_m versus a dry plank Δ_s : Δ_m/Δ_s .

It is possible to classify qualitatively, on the basis of the vibration measurements, the usefulness of the wood of the tested models for the application in construction according to the listing: pine, spruce, larch, oak. The highest vibration frequency was exhibited by a spruce, pine wood, the lowest vibration frequency by an oak wood plank.

The following can be done on the basis of the vibration damping magnitude of wooden elements:

1. to detect mechanically or biologically damaged elements within the set of similar elements,
2. to assess the usefulness of elements from various wood species for the construction of wooden constructions,
3. to detect wetted elements,
4. to select the usefulness of the same timber from the same wood species for the building of structures, especially those of prestige.

It is known from the engineering practice that wetted elements from wood have a lower resistance to biological elements and in such elements the reduction of load capacity and of the stiffness of wooden elements in time may be expected. It follows from the testing that wooden beams, of an increased moisture content, have a lower own frequency n and a significantly higher damping ρ . One may anticipate that the high damping within the group of similar elements indicates the wet elements most exposed to the destruction by biological corrosion.

The conclusions deriving from the dynamic testing demonstrated in the publication may be used:

- (1) to compare the creep speed and relaxation speed in combined elements from various wood species,
- (2) to assess the rheological models of wood on the basis of vibro-creep,
- (3) to assess the impact of moisture content on the mechanical properties of wood.

The conventional selection of wood species and wooden elements useful for the building of domes on the basis of visual inspections and traditions is worth supplementing by a dynamic testing since **the deviations of the vibration frequency and the vibration damping from the expected values are a significant indicator of hidden defects of an element.**

It follows from the analysis of the damping on the frequency of undamped vibration of dry models from wood that the damping has no essential impact on the stiffness of dry-air models from wood. The local actual stiffness K may be securely determined on the basis of the square of damped free vibration measured $\alpha^2 \sim \omega^2$ from the formula $K_{ef} = \omega^2 m_z$. For wood the assessment error of the tested wood does not reach 1%.

The lowest reduction of the modulus of elasticity of wood due wetting may be adopted as a criterion of the usefulness of wood for a long-term operation.

It is possible to forecast, on the basis of the dynamic testing of elements made from dry and wet elements from wood, their physical properties, thus their usefulness for the application in construction. The dynamic testing can be used for various purposes, including, for instance, the selecting of planks for the building of constructions, especially prestigious facilities. The planks of a higher damping should be rejected, and those exhibiting higher vibration frequencies and a lower logarithmic damping decrement can be used when a higher durability of a construction is required.

The dynamic testing allows a quick comparative qualitative analysis of the physical properties of wood. They allow to assess the fitness of wood for the use in constructions just after a few minutes, and not after several days, or even years, as in the case of the long-term testing. They allow a better recognition of the features of the wood being analysed, like the applied visual inspection of planks.

It follows from the analysis of the free vibration of models from wood that **species of a greater usefulness for construction exhibited lower vibration periods, higher vibration frequencies, a lower damping and a lower logarithmic damping decrement.**

The following occurred in the wet wood models: (1) the beams' mass increased, (2) the creep rose, (3) the damping increased, (4) the modulus of elasticity E decreased.

It follows from the dynamic testing conducted that the information obtained therefrom about the properties of wood are more unambiguous than that obtained after a long static testing. The recognition of the properties of wood is more precise than that on made on the basis of the static testing. Therefore, in the next chapter, the usefulness of the dynamic testing for the recognition of the mechanical properties of wood-based materials has been verified.

A short dynamic testing may be recommended for the selection of wood for the building of dome structures as well as to determine damaged elements in the wooden structures already built.

References

1. Iimura Y. *Performance Evaluation of the "Konohana Dome" built with fast-growing Sugi* WCTE 2008 czerwiec 2-5 2008 Miyazaki Japan.
2. Zielski A., Krąpiec M., *Dendrologia*, PWN, Warszawa 2004.
3. Marcinkowska A., Moliński W. *Wpływ gęstości drewna na propagacje fal ultradźwiękowych wzdłuż włókien*. Annals of Warsaw Agricultural University SGGW, Forestry and Wood Technology No 53, Warsaw 2003.
4. Nowacki W., *Dynamika budowli*, Arkady, Warszawa 1972.
5. Kowal Z. *Wyboczenie pelzające osiowo ściskanych prętów lepko-sprężystych*, III Sympozjum PTMTS poświęcone reologii, referaty t. i, Wrocław 1966, s. 209-218.

6. Kowal Z. *The effect of transverse forces on creeping buckling of viscoelastic compressed columns*. Arch. of Civil and Mechanical Engineering. Vol. V, No 2/2005, s. 13–23.
7. Kowal Z., Sendkowski J., Walasek A., *Wykrywanie porównawczą metodą dynamiczną elementów zarysowanych populacji belek strunobetonowych*, Politechnika Rzeszowska, Mechanika z.5, Rzeszów 1983.
8. Langer J., *Dynamika budowli*, Wydawnictwo Politechniki Wrocławskiej, Wrocław 1980.
9. Misztal B., *Pomiary dynamiczne w diagnostyce stropów drewnianych REMO 2004 r.* XI Konferencja Naukowo Techniczna Problemy Remontowe w Budownictwie Ogólnym i Obiektach Zabytkowych, Wrocław Zamek Kliczków, 9–11 grudnia 2004.
10. Kokociński W., Poliszko S., Raczkowski J., *Pełzanie drewna w warunkach wymuszenia dynamicznego*, Reologia drewna i konstrukcji drewnianych – Sympozjum Akademii Rolniczej w Poznaniu, materiały, Zielonka 21–22 października 1982.
11. Jakowluk A. *Procesy pełzania i zmęczenia w materiałach*, WNT, Warszawa 1993.
12. Misztal B., *Comparison of the Vibration Frequency and Damping of Beam Models Made of Dry and Wet Pine Wood*, WCTE 2008, 10th World Conference on Timber Engineering, Miyazaki, JAPAN, June 2–5, 2008.
13. Misztal B., *Dynamic Parameters of the Free Vibrations of Various Wood Species* WCTE 2010, 11th World Conference on Timber Engineering, Riva del Garda, Trentino, Italy, June 20–24, 2010.
14. Kowal Z. *Dynamika nieważkiej belki na podłożu lepkosprężystym*, Archiwum Inżynierii Lądowej nr 1/1966, tom XII, s. 29–42.
15. Banasiak M. *Ćwiczenia laboratoryjne z wytrzymałości materiałów*. Praca zbiorowa. Warszawa 1985 PWN, Wydanie III zmienione.

Chapter 12

Assessment of the Physical Properties of Wood-Based Materials on the Basis of the Measurement of Free Vibration Parameters

12.1 Introduction

The current **economic pressure resulting from the need to recycle waste formed during the production of wood**, (including the layer-wise glued laminated timber), **has an impact** (in many cases) **on the incorrect use of wood-based materials in building constructions**.

Wood-based materials are characterized by a considerable spread of mechanical features, in particular strength. Some of them exhibit an unlimited creep in time, which was already described by Nożyński V. in his paper [1] (1978). In the statistical studies a large impact of moisture on the properties of wood-based materials, especially creep, was noticed [2–4]. It follows from the dynamical testing of vibro-creep [5] that in various material brands the impact of vibration on the creep process under load is different.

It was noticed during the preliminary testing that the periodical load substantially accelerates the creep of wood-based materials and allows to assess the creep model of a material. In order to learn the properties of wood-based materials the testing on the models was performed: those of coniferous plywood, beech wood plywood, OSB, fibreboard and chipboard, as materials most often used in the construction.

12.2 Dynamic Testing of Models from Wood-Based Materials

The dynamic testing to reveal the properties of wood-based materials in the vibro-creep process were performed on the models like for wooden beams.

The models from wood-based materials had an identical section 10×40 mm and a length 1200 mm, and the reach of the bracket during the testing was 785 mm, like in Fig. 11.3. before the testing, the beams were weighed and a series of tests on

beams in a dry air state was performed. After the testing and a six-time excitation with the mass $m_2 = 250.0$ g, the models suspended at the end of the bracket were soaked in water during 24 h. After the soaking, the models were re-weighed and their moisture content by weight was calculated. Each model was excited six times to vibration by the cutting-off of the mass $m_2 = 250.0$ g, suspended on the free end of the support, already burdened with the mass $m_1 = 250.0$ g.

Wet models were also excited to vibration by the cutting-off of the mass $m_2 = 250.0$ g, but once since the considerable residual deflections of the models from wood-based materials hindered successive excitations.

The record of the vibrating movement of dry beams and wet beams is specified in Figs. 12.1 through 12.9.

The comparison of the following free vibration parameters of the models was made:

1. damping of the vibration of dry and wet vibration in order to reveal the impact of moisture on the properties of materials,
2. vibration period of the models tested,
3. initial stiffness \mathbf{K} of the models from wood-based materials, on the basis of the measurement of free vibration,
4. creep of the models tested on the basis of residual deflections.

Presented in Tables 12.1 through 12.14 is the compilation of the test results developed for various wood-based materials. The vibration parameters of the models $T, y_0, \rho, n, \omega, \Delta$ were calculated from the formulae specified in Sect. 11.2.

The vibration movement parameters were calculated for each of the beams tested under the statistical scheme of the bracket, made from the specified wood-based materials, both in the dry and wet state: for the dry models with the “s” index: $T_s, y_0, \rho_s, n_s, \omega_s, \Delta_s$, and for the wet models with the “m”: $T_m, y_0, \rho_m, n_m, \omega_m, \Delta_m$, where: n —vibration frequency, T —vibration period, ρ —damping coefficient, Δ —logarithmic damping decrement.

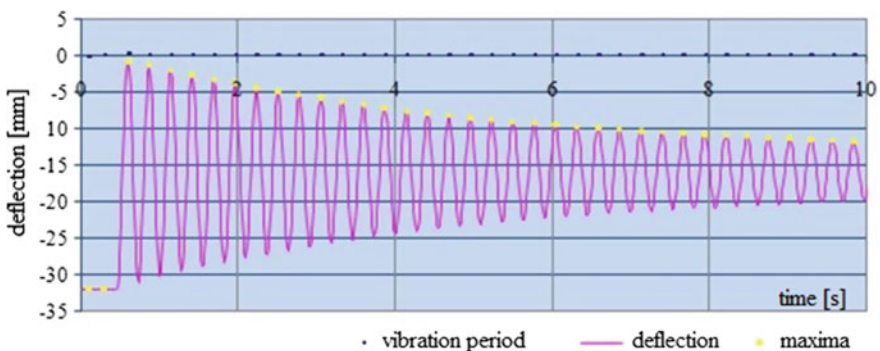


Fig. 12.1 Record of the vibrating movement of a model from coniferous pine plywood during the first 10 s of the testing

Table 12.1 Free vibration parameters of the model from dry coniferous plywood, burdened at the end with a concentrated mass $m_1 = 250$ g

T_s [s]	t_0 [s]	y_0 [mm]	ρ_s [1/s]	$n_s = 1/T$ [1/s]	ω_s [1/s]	φ [°]	A_s
0.2666	0.4667	31.96	0.1381	3.75	23.15182	40.64	0.0368

Placed in Table 12.1 are the vibrating movement parameters measured and calculated from the formulae: (11.2–11.5), and presented in Fig. 12.1 is the chart of the free vibration of the model made from coniferous plywood in a dry-air state.

Placed in Table 12.2 are the vibrating movement parameters measured and calculated from the formulae: (11.2–11.5), and in Fig. 12.2 the chart of the free vibration of a model from a coniferous plywood after a 24-hour soaking in water.

Placed in Table 12.3 are the vibrating movement parameters as measured and calculated from the formulae: (11.2–11.5), as well as in Fig. 12.3 the vibration chart of a model from broadleaf beech plywood in a dry-air state.

Placed in Table 12.4 are the vibrating movement parameters as measured and calculated from the formulae: (11.2–11.5), and in Fig. 12.4 the chart of the free vibration of a model from a broadleaf plywood after a 24-hour soaking in water, of a moisture content by weight of 40.21%.

Table 12.2 Free vibration parameters of a model from wet coniferous plywood, of a moisture content $w = 31.93\%$ burdened at the end with the mass $m_1 = 250$ g

T_m [s]	t_0 [s]	y_0 [mm]	ρ_m [1/s]	$n_m = 1/T$ [1/s]	ω_m [1/s]	φ [°]	A_m
0.291667	2.371	37.741	0.30	3.4285675	21.52142	43.50573	0.0875

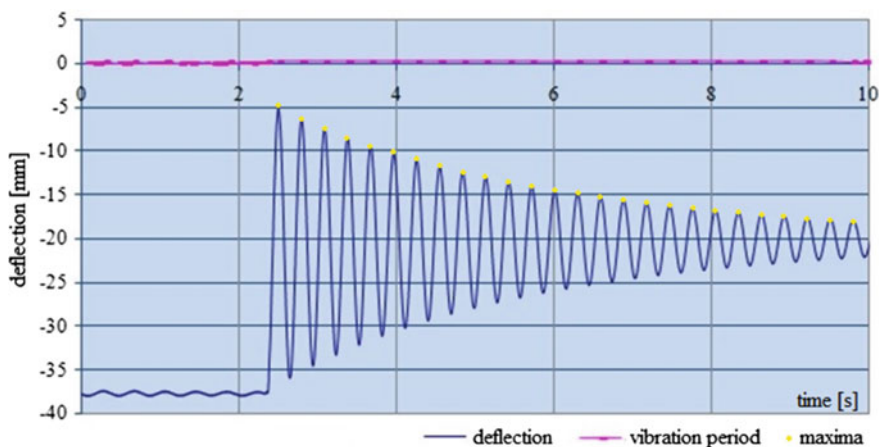


Fig. 12.2 Record of the vibrating movement of a model from a wet coniferous pine plywood, of a moisture content of 31.93%

Table 12.3 Free vibration parameters of a model from a dry broadleaf beech plywood, burdened at the end with a mass $m_1 = 250$ g

T_s [s]	t_o [s]	y_o [mm]	ρ_s [1/s]	$n_s = 1/T$ [1/s]	ω_s [1/s]	φ [°]	Δ_s
0.29	1.8133	36.83	0.14848	3.44823	21.73074	3.0428	0.043

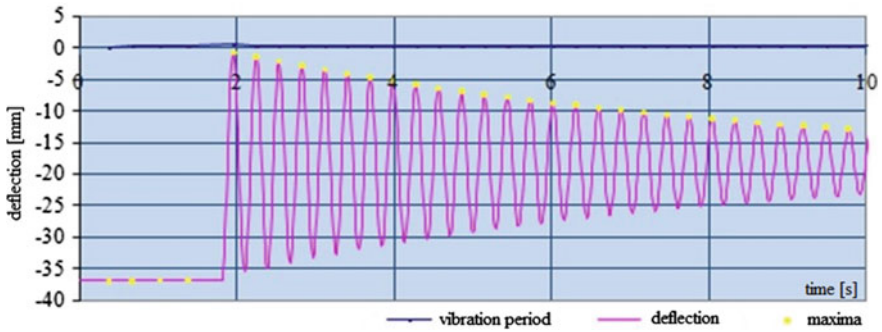


Fig. 12.3 Record of the vibrating movement of a model from a broadleaf, beech plywood during the first 10 s of the testing

Table 12.4 Free vibration parameters of a model from a broadleaf, beech plywood of a moisture content $w = 40.21\%$ burdened at the end with a mass $m_1 = 250$ g

T_m [s]	t_o [s]	y_o [mm]	ρ_m [1/s]	$n_m = 1/T$ [1/s]	ω_m [1/s]	φ [°]	Δ_m
0.31	5.60667	42.722	0.30	3.2258	20.26	-1.5	0.093

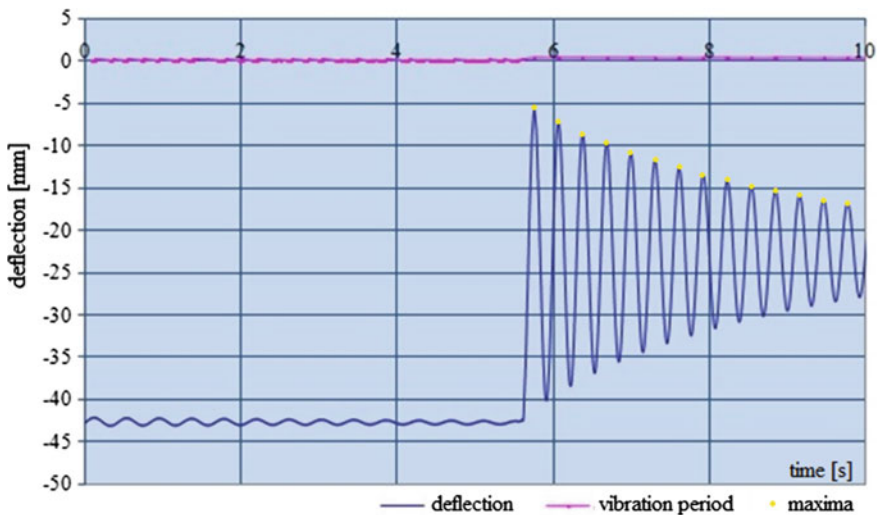
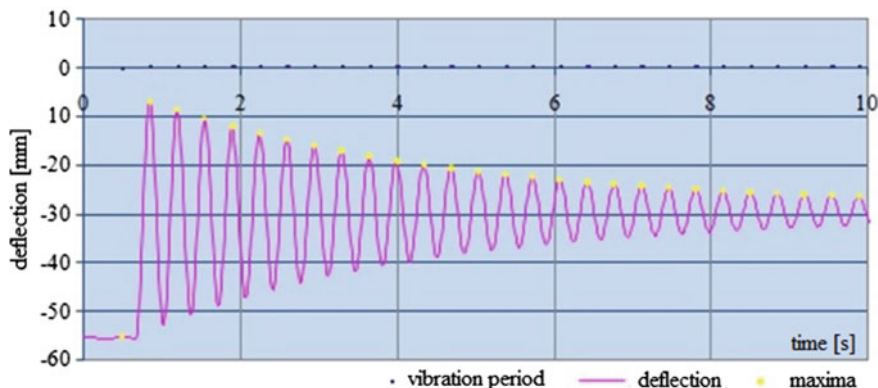


Fig. 12.4 Record of the vibrating movement of a beam from a broadleaf, beech plywood of a moisture content of 40.21%

Table 12.5 Parameters of the free vibration of a model from an OSB, burdened at the end with a mass $m_1 = 250$ g

T_s [s]	t_0 [s]	y_0 [mm]	ρ_s [1/s]	$n_s = 1/T$ [1/s]	ω_s [1/s]	φ [°]	Δ_s
0.3466	0.68	55.31	0.245985	2.885	18.0801	22.03447	0.0853

**Fig. 12.5** Record of the vibrating movement of a model from an OSB board during the first 10 s of the testing

Placed in Table 12.5 are the parameters of the vibrating movement as measured and calculated from the formulae: (11.2–11.5), as well as in Fig. 12.5 the chart of the vibration of an OSB board in a dry-air state.

Placed in Table 12.6 are the parameters of the vibrating movement as measured and calculated from the formulae: (11.2–11.5), and in Fig. 12.6 the chart of the free vibration of a model from an OSB board after a 24-hour soaking in water, of a moisture content by weight $w = 57.382\%$.

Placed in Table 12.7 are the parameters of the vibrating movement as measured and calculated from the formulae: (11.2–11.5), and in Fig. 12.7 the chart of the vibration of a model from a fibreboard in a dry-air state, burdened at the end with a mass $m_1 = 250$ g.

Placed in Table 12.8 are the parameters of the vibrating movement as measured and calculated from the formulae: (11.2–11.5), and in Fig. 12.8 the chart of the free vibration of a model from a fibreboard after a 24-hour soaking in water, of a moisture content of 44.932%.

Table 12.6 Parameters of the free vibration of a model from an OSB board, of a moisture content of $w = 57.382\%$, burdened with a mass at the end

T_m [s]	t_0 [s]	y_0 [mm]	ρ_m [1/s]	$n_m = 1/T$ [1/s]	ω_m [1/s]	φ [°]	Δ_m
0.4367	1.74	89.266	0.47	2.2899	14.48965	31.33439	0.2052

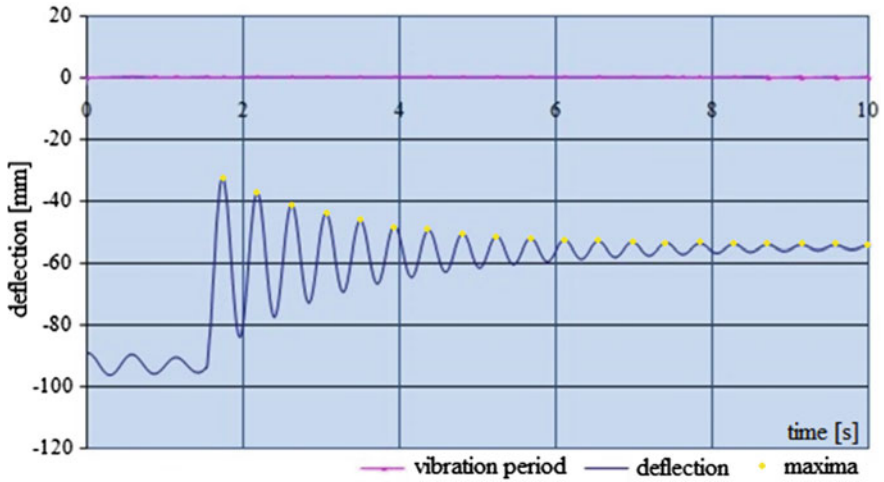


Fig. 12.6 Record of the vibrating movement of a model from a wet OSB board, of a moisture content 57.382%

Table 12.7 Parameters of the free vibration of a model from a fibreboard, burdened at the end with a mass $m_1 = 250$ g

T_s [s]	t_0 [s]	y_0 [mm]	ρ_s [1/s]	$n_s = 1/T$ [1/s]	ω_s [1/s]	φ [°]	Δ_s
0.4133	0.50667	74.10	0.25598	2.42	15.01267	28.44077	0.1058

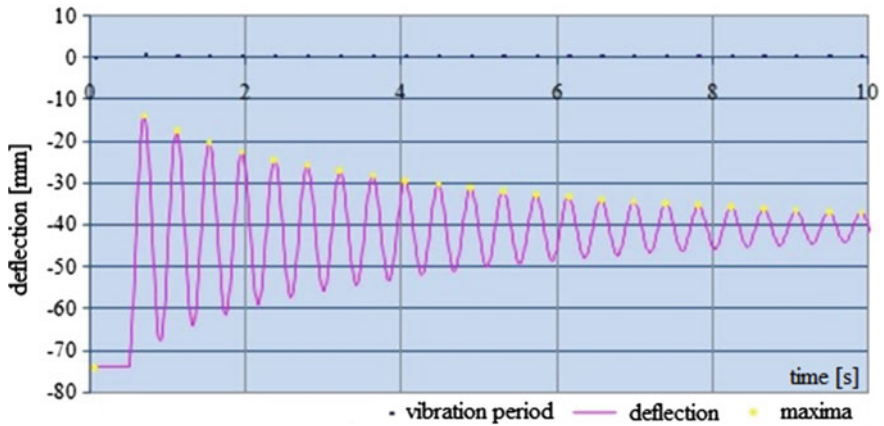


Fig. 12.7 Record of the vibrating movement of a model from a fibreboard during the first 10 s of the testing

Table 12.8 Parameters of the vibrating movement of a model from a fibreboard, of a moisture content $w = 44.90\%$, burdened at the end with a mass

T_m [s]	t_0 [s]	y_0 [mm]	ρ_m [1/s]	$n_m = 1/T$ [1/s]	ω_m [1/s]	φ [°]	Δ_m
0.57	1.74	71.66	0.4517	1.75	11.2511	74.52	0.2575

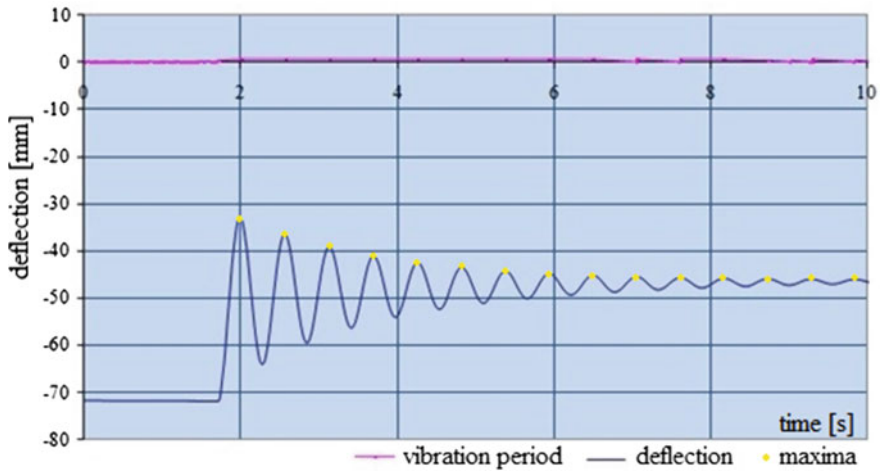


Fig. 12.8 Record of the vibrating movement of a model from a fibreboard of a moisture content $w = 44.90\%$

Table 12.9 Parameters of the free vibration of a model from a chipboard, burdened with a mass at the end $m_1 = 250$ g

T_s [s]	t_0 [s]	y_0 [mm]	ρ_s [1/s]	$n_s = 1/T$ [1/s]	ω_s [1/s]	φ [°]	Δ_s
0.32	0.48204	48.67	0.36971	3.125	19.79352	9.393215	0.1183

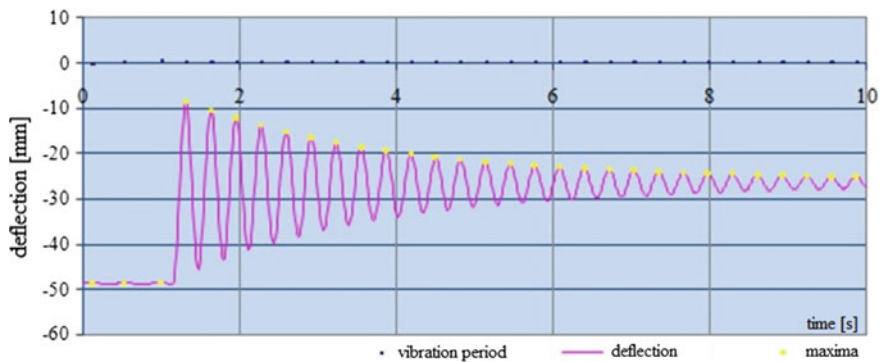


Fig. 12.9 Record of the vibrating movement of a model from a fibreboard during the first 10 s of the testing

Shown in Table 12.9 are the vibrating movement parameters as measured and calculated from the formulae: (11.2–11.5), as well as in Fig. 12.9 the chart of the vibration of a model from chipboard in a dry-air state, burdened with a mass at the end $m_1 = 250$ g.

The parameters of the free vibration of a model from a wet chipboard, after a 24-hour soaking in water, were indeterminable due to the destruction at the first trial of the loading. A beam from a chipboard of a moisture content $w = 77.54\%$, burdened at the end with a mass $m_1 = 250$ g, was unfit for the dynamic testing. During a trial to excite the vibration using an additional mass $m_2 = 250$ g, it broke under the load.

12.3 Comparison of the Vibration Period of the Tested Models

Compiled in Table 12.10 are the vibration periods and the vibration period ratio of the wet model to the dry model T_m/T_s , from wood-based materials.

Arranged in Table 12.10, in column 1, are the models from wood-based materials according to their fitness to the building trade, starting with the most useful model—line 1 up to the model unfit to the building of a construction. The criterion according to which wood-based materials are specified in the first column is the growing value of the ratio $\frac{T_m}{T_s}$, where T_m —vibration period of a wet beam, T_s —vibration period of a dry beam.

It follows from the comparison that the models from wetted materials have a higher vibration period: $T_m > T_s$, than dry models due to the higher mass of the wet models. The model from the chipboard of a moisture content 77.5% was destroyed under a static load. The lowest period of vibration T and the highest vibration

Table 12.10 Comparison of the vibration period of dry and wet models from wood-based materials

Material	Vibration period [s]		Coefficient t_m/t_s
	Dry models	Wet models	
Coniferous plywood	0.266	0.292	1.10
Beech plywood	0.290	0.31	1.07
OSB	0.347	0.437	1.26
Fibreboard	0.416	0.57	1.37
Chipboard	0.320	After the excitation with the force $P = 250$ g—destruction	

frequency n , both for the dry model and the wet model, was demonstrated by a coniferous plywood. During the performance of one free vibration testing, according to the scheme in Fig. 11.2, was a constant magnitude.

12.4 Comparison of the Vibration Damping of Dry and Wet Models in Order to Reveal Wetted Materials

For each dynamically tested model the dimensional damping of the free vibration ρ was calculated using Excel spreadsheets. Also, the dimensionless logarithmic damping decrement was calculated from the formula $\Delta = \rho T$.

Compiled in Table 12.11 is the magnitude of the damping ρ and that of the logarithmic damping decrement Δ for each model of the beams tested.

Arranged in Table 12.11 are wood-based materials according to the magnitude of the dimensional logarithmic damping coefficient ρ_s and of the logarithmic damping decrement Δ . The lowest ρ_s and Δ , both in the dry and wetted state, was exhibited by a beam from a coniferous plywood.

The damping ρ and the logarithmic damping decrement Δ increase as the moisture content of the beam grows.

Table 12.11 Comparison of the damping coefficients and the logarithmic damping decrements of dry and wet models

Compilation of the damping of models from wood-based materials						
Material	Dry models		Wet models		Comparison of the damping	
	Damping coefficient	Logarithmic damping decrement	Damping coefficient	Logarithmic damping decrement	$\frac{\rho_m}{\rho_s}$	$\frac{\Delta_m}{\Delta_s}$
	$[\frac{1}{s}]$	$[\frac{1}{s}]$	$[\frac{1}{s}]$	$[\frac{1}{s}]$		
	ρ_s	Δ_s	ρ_m	Δ_m		
Coniferous plywood	0.1381	0.0368	0.30	0.0875	2.17	2.38
Beech plywood	0.14848	0.043	0.30	0.093	2.02	2.15
OSB	0.245985	0.0853	0.47	0.2052	1.91	2.41
Fibreboard	0.25598	0.1058	0.4517	0.2575	1.76	2.43
Chipboard	0.36971	0.1183	After the excitation with the force P = 250 g —destruction			

12.5 Comparison of Residual and Permanent Deflections of the Tested Models from Wood-Based Materials

Each model from wood-based materials in a dry-air state was excited to vibration six times using a mass $m = 250$ g. The models after a 24-hour soaking in water was excited to vibration once.

It was noticed that in each case after the testing of models having a static scheme of the support, the free end of the supporting beam, upon removal of loads, remained deflected. This deflection was called a residual deflection and designated as y_r . After a certain time, the residual deflection was reduced. Finally, it reached a value that did not change any more. This magnitude of the deflection, measured in [mm], was considered as a permanent deflection and designated as y_t . The compilation of residual and permanent deflections of dry and wet beams is placed in Table 12.12. Placed in column 6 of Table 12.12 is the increase in the permanent deflection due to the rise in the moisture content of the beam. After the soaking in water, a model from a chipboard was destroyed under a static load.

The residual and permanent deflections in wet models are several times higher than those in dry models.

The lowest residual deflection and permanent deflection was exhibited by the models from a coniferous plywood. The ratio of permanent deflections y_t to residual deflections y_r can be used to forecast the vibro-elastic model from a wood-based material.

Table 12.12 Compilation of residual and permanent deflections after 6 measurement tests of the free vibration of dry models and a one-time excitation of the vibration of wet beams

Models tested according to Fig. 11.3							Deflection ratio of wet and dry models	
Material	Dry models after 6 vibration cycles			Wet models after 1 vibration cycle			$\frac{y_{tm}}{y_{rs}}$	$\frac{y_{tm}}{y_{ts}}$
	Residual y_r [mm]	Permanent y_t [mm]	$\frac{y_t}{y_r}$	Residual y_r [mm]	Permanent y_t [mm]	$\frac{y_t}{y_r}$		
Coniferous plywood	0.48	0.36	0.75	2.967	1.367	0.46	6.18	3.79
Beech plywood	0.99	0.48	0.485	3.908	2.325	0.60	3.95	4.84
OSB	3.53	1.62	0.46	15.69	11.673	0.74	4.44	7.21
Fibreboard	5.84	2.97	0.51	39.644	35.257	0.89	6.67	11.87
Chipboard	3.94	1.97	0.50	After excitation with the force $P = 2.5$ N—destruction				

12.6 Dynamic Testing Oriented Towards the Determination of the Coefficient of Direct Elasticity E of Wood Derived-Materials

On the basis of the measurement of the free vibration of dry and wet models, the free vibration parameters and the moduli of direct elasticity E were assessed and compiled in Tables 12.13 and 12.14. Specified in the tables are also the calculated stiffness K and the moduli of direct elasticity E of dry and wet models made from: coniferous and broadleaf plywood, OSB board, fibreboard and chipboard. The local stiffness K of the supporting model was assessed on the basis of the measurement of a substitutive concentrated mass m_z at the end of the support, and the measurement of the free vibration frequency of the support α from the formula 11.8 in Chap. 11: $K = m_z \alpha^2$.

The square of the own vibration $\alpha^2 = \omega^2 + \rho^2$ calculated after the testing performer on the models is placed in Tables 12.13 and 12.14 in column 6.

The substitutive concentrated mass m_z resulting from the on mass of the support of the model tested and the mass suspended at the end was calculated from the formula (12.1) according to [6]:

$$m_z = 0.243ql + 250 \quad (12.1)$$

where: q —weight measured per running metre of the support, l —length of the support.

The stiffness K of the models determined from the relationship $K = m_z \alpha^2$ is placed in Tables 12.13 and 12.14 (column 7).

The relationship between the stiffness K and the load P has the form (12.2):

$$y = P/K \rightarrow K = P/y \quad (12.2)$$

The translocation y of the laden model's end of the support totals:

$$y = \frac{Pl^3}{3EJ} = \frac{P}{K} \quad (12.3)$$

The moduli of elasticity E were assessed according to the algorithm specified below from the Eq. (12.3):

$$E = \frac{Kl^3}{3J} \quad (12.4)$$

The length of the support's reach was adopted in the calculations (Fig. 11.3) $l = (785 + 20 + 15) \text{ mm} = 0.82 \text{ m}$. The following was placed in Tables 12.13 and 12.14 in the columns: 1—name of the material from which the model was made, 2 and 3—mass of the model, 4—dimensional damping ρ , 5—square of the free

Table 12.13 Assessment of the moduli of direct elasticity E_s of the models tested in a dry-air state

Material	Model's mass [g]	Evenly distributed mass [g/m]	ρ_s		ω_s	Own vibration		m_z [g]	$K = m_z \rho_s^2$ [g/s ²]	E_s assessed after the testing of models in a dry-air state [GPa]	E as per standard [GPa]
			ρ_s^2 [1/s]	ω_s^2 [1/s]		$\rho_s^2 = \rho_s^2 + \omega_s^2$ [1/s ²]					
Coniferous plywood	313.96	214.54	0.1381	23.152	536.01	536.03		292.75	156922.8	8.65	-
			0.0191	536.01							
Broadleaf plywood	291.54	199.22	0.1485	21.731	472.223	472.25		289.70	136810.8	7.54	7.0
			0.0221	472.223							
OSB	369.80	252.70	0.246	18.080	326.890	326.95		300.35	98199.4	5.42	5.0
			0.0605	326.890							
Fibreboard	459.56	314.03	0.256	15.0127	225.386	225.45		312.57	70468.9	3.86	3.1
			0.0655	225.386							
Chipboard	392.48	268.19	0.3697	19.794	391.783	391.92		303.44	92075.8	5.08	3.2
			0.1367	391.783							

Table 12.14 Assessment of the moduli of direct elasticity E_m of the models tested after a 24-hour soaking in water

Material	Dynamic parameters of wet models tested according to the scheme in Fig. 11.3				m_z [g]	$K = m_z$ α_s^2 [g/s ²]	Moisture content [%]	E_m assessed after the testing of wet models [GPa]	
	Model's mass [g]	Evenly distributed mass [g/m]	ρ_m	ω_m					Own vibration $\alpha_m^2 = \rho_m^2 + \omega_m^2$ [1/s ²]
			ρ_m^2 [1/s]	ω_m^2 [1/s]					
Coniferous plywood	414.20	283.04	0.30	21.52	306.4	141955.1	31.9	7.83	
			0.09	463.2					
Broadleaf plywood	408.76	279.32	0.30	20.26	305.7	125520.4	40.2	6.92	
			0.09	410.5					
OSB	582.00	397.70	0.47	14.49	329.2	69197.8	57.4	3.82	
			0.221	209.9					
Fibreboard	666.05	455.13	0.452	11.25	340.7	43200.8	44.9	2.38	
			0.204	126.6					
Chipboard	696.81	476.15	Destruction		344.9		77.5		

vibration frequency ω^2 , 6—square of the own frequency vibration α^2 , 7—substitutive mass m_z , 8—stiffness of the support K , column 9 in Table 12.13—modulus of elasticity of dry models E_s , column 9 in Table 12.14—moisture content, column 10 in Table 12.14—modulus of elasticity of wet models E_m .

It follows from the analysis of the impact of damping on the vibration frequency of dry wood-based materials that the damping has no essential impact on the stiffness K of dry-air models. The local stiffness can be safely determined directly on the basis of the square of the measured frequency of free vibration damped $\alpha^2 \sim \omega^2$ from the formula $K = \omega^2 m_z$. For wood and wood-based materials the assessment error does not reach 1%.

12.7 Conclusions

In all the testing performed on wood-based materials under a static and dynamic load no full reversibility of the creep model was achieved. **After each test the permanent deflection remained.** The lowest residual and permanent deflection after a six-fold excitation was exhibited by the coniferous plywood. The highest one was exhibited by the fibreboard and the chipboard. The highest vibration frequency was presented by the coniferous plywood, the lowest one by the fibreboard and the chipboard.

It follows from the analysis of the free vibration of models from wood-based materials that **the materials of a higher durability demonstrated in the dynamic testing lower vibration periods, higher frequencies, a lower dimensional damping and a lower logarithmic damping decrement.**

The following occurred in wet models: (1) an increase in the mass of beams, (2) the material was becoming brittle, (3) the creep was growing, (4) the damping was rising, (5) the residual and permanent deflections in wet models were several times higher than in dry models, (6) the reduction in strength was higher than the one expected on the basis of the creep.

In all the testing of wood-based materials under static and dynamic load **no full reversibility of the creep model was achieved.** After each testing the permanent deflection remained.

As demonstrated by the testing of wet beams from wood-based materials, some of them: chipboard, fibreboard, lose their load capacity after soaking in water already after 24 h. It follows from the testing that the chipboard degrades fastest, the second in the succession is the hard fibreboard. **The coniferous plywood demonstrates the highest durability, close to that of wood.** The broadleaf exhibits in relation to the coniferous plywood the highest permanent deflection. The wetted wood and the coniferous plywood preserve the technical parameters for the longest time. The water absorption of such wood-based materials as fibreboard and chipboard leads, in a short time, to the destruction of constructions fabricated from those materials. **It is possible to determine, on the basis of the measurement of vibration, the fitness degree of the materials of the models tested for the**

application in construction in the following order: (1) coniferous plywood, (2) beech plywood, (3) OSB board, (4) fibreboard, (5) chipboard. The last two materials in the series actually are unfit for the consolidation with permanent constructions.

Structural elements consolidated with wood-based materials, like for instance steel-wooden girders with box chords from wood and wood-based materials, beams with chords from wood and webs from wood-based materials, are particularly susceptible to a premature destruction due to wetting. This results in a need to repair or replace them during the operation of a facility.

On the basis of the dynamic testing of the models of elements made from dry and wet wood-based materials it is possible to anticipate their physical properties and to recommend their use for various purposes, also including their selection for the building of constructions, especially prestigious facilities.

The dynamic testing points out to the need to improve the physical properties of wood-based materials.

References

1. Nożyński W. *Wyniki badań belek z materiałów drewnopochodnych pod obciążeniem długotrwałym*. Sympozjum Badania nad zastosowaniem drewna i materiałów drewnopochodnych we współczesnych konstrukcjach budowlanych. Szczecin czerwiec 1978.
2. Misztal B., *Kratowe dźwigary z drewna, materiałów drewnopochodnych i stali*, Praca doktorska, Politechnika Szczecińska 1999.
3. Misztal B., *Ugięcia pełzające zespolonej belki o przekroju skrzynkowym z drewna i płyty wiórowej*, Konferencja Naukowa K.I.L i W Polskiej Akademii Nauk i K.N. PZiTB, Wrocław – Krynica 2000, t. 3.
4. Misztal B., *Prognozowanie w czasie ugięć reologicznych dźwigarów kratowych z drewna i stali*. Konferencja Naukowo – Techniczna, Konserwacja, wzmacnianie i modernizacja budowlanych obiektów historycznych i współczesnych, Kielce, 22–23 lutego 2001.
5. Jakowluk A. *Procesy pełzania i zmęczenia w materiałach*, WNT, Warszawa 1993.
6. Banasiak M. *Ćwiczenia laboratoryjne z wytrzymałości materiałów*. Praca zbiorowa. Warszawa 1985 PWN, Wydanie III zmienione.

Summary

The prestigious buildings of the East and the West were crowned with domes. The domes belong to the works of architecture presenting the technical culture and the technological capabilities of their epoch. They are the synthesis of the knowledge of societies who built them. The form of a dome was shaped over centuries, finding for it various constructional solutions, depending on the material used for the construction. The properties of the material imposed optimum, proven for centuries of experience, constructional systems. At the same time, constructions from wood developed, which as scaffoldings supported the building of various concrete and masonry domes, undergoing transformations towards light and durable constructions. There are several directions of the evolution of scaffolding constructions from which a meridional-latitudinal system of bars developed, characteristic of the form of wooden domes.

One of them, described in Chap. 2 derives from the transformations of scaffoldings from wood used for the construction of heavy masonry vaults into a shell-ripped system of the vault (Fig. 3.1). The basis and development element of a scaffolding were outside wooden arch centres giving the shape to the shell, built from several layers of planks.

In Chap. 3 the lasting for several centuries experimenting in which from the scaffoldings supporting various outside shielding constructions from wood of masonry domed were described, the most eminent being:

1. a two-layer Dome on the Rock of a 20.40 m diameter, from the years 687–691, (Fig. 3.6),
2. a two-layer Al Aqsa dome of a 11.50 m diameter from 715, (Fig. 3.7),
3. a two-layer wooden dome of the Il Redentore Church in Venice by arch. Palladio A., of a 14.50 m diameter from 1546 (Fig. 3.19),
4. a wooden outside dome, shielding the masonry dome against wind in the Schönborn Chapel, by the architect Neumann B. in Würzburg of a 20.0 m diameter from 1722 (Fig. 3.16),
5. a two-layer wooden dome by the architect Weinbrenner F. of a 30.0 m diameter, built in 1808–1814 (Fig. 3.21),
6. a dome by the architect G. Moller of a 33.5 m diameter (Fig. 3.23) of a ribbed, meridional-latitudinal construction from 1827.

The transformation of the covering structures of wooden domes into a legible meridional-latitudinal system of load-bearing elements was a breakthrough in the shaping of wooden domes. The meridional ribs, developed over the centuries of experimenting, from trusses of arched outside straps, were stiffened with latitudinal trusses. The meridional-latitudinal system of trusses was transformed, over time, into a simple ribbed system from arch centres, as in the ribbed dome by G. Moller in Darmstadt. The meridional-latitudinal construction by G. Moller from wooden arch centres, developed over time into various load-carrying systems of ribbed domes from solid wood.

A next link in the chain of transformations of the constructions characteristic of the dome form is the evolution of thick-wall coverings as described in Chap. 4. Starting with various dome-like coverings from halved logs, through coverings from short quartering elements connected with foreign connectors, domes of a massive shell were shaped. The last link of their development are the examples described in Sect. 4.6 of thick-wall domes of a 20.05 m diameter (Fig. 4.21) from 1934, and a 60.0 m diameter (Fig. 4.24) described in 1937. Such large diameters of a facility were obtained using outside, meridional load-carrying ribs, directing, at the same time, the geometry of the dome. The thick-wall domes were an essential achievement in the development of constructions. The following may be classified among its advantages: (1) building the dome without a central supporting scaffolding, (2) use for the construction of planks of a worse quality, (3) good thermal insulation of load-carrying ribs and of the shell, (4) a smooth surface of the dome inside, freed from the protruding constructional elements, (5) a smooth surface resulting from the missing inside construction and associated higher fire resistance of the facility.

The construction method of thick-wall wooden domes as described in Sect. 4.6 did not remain, however, it was an important experience on the way of the construction development of domes from solid wood.

Described in Chap. 5 are the first, built in the 30s of the 20th century domes of a load-bearing structure from meridional ribs, as bipolar trusses. The realization of the domes described in Chap. 5 required a central scaffolding to support meridional ribs. The ribs of such domes were dimensioned analogically to three-joint ribs loaded with a covering and spatially stiffened using meridional ribs.

The dome of the circus theatre in Baku (Fig. 5.5) of the largest among the historical domes diameter of the horizontal projection amounting to 67 m was built in 1930. The meridional load-carrying ribs of the dome of a bipolar shape were stiffened spatially with latitudinal truss ribs. To connect wooden elements low-size steel connectors in form of 5.00 mm thick lashes, dia. 5 mm nails and dia. 13 mm bolts were used. The box shell from planks, introduced for the first time in history, made on the straps of meridional ribs spatially stiffened the construction, although, as specified by its author Eng. Kashkarov K.P., it was not considered in the calculations of ribs. The shell was calculated independently, for the load with the covering, and the outside load with wind and snow. The solution of the dome in Baku is distinguished by the grid of ventilation ducts built from planks on the outside of the shell. They were made in parallel over the construction of main ribs,

along the meridians and the lines of latitude. This ventilation prevents the corrosion of wood and the occurrence of distortions caused by changes in humidity and temperature.

In the thirties, the use of steel in the building trade became widespread. Steel was also used in the solutions of the nodes in the dome of a projection diameter of 50.0 m built in Ivanov in 1931. While introducing steel to the wooden construction, the fibrous structure of wood was still remembered. Steel elements were made as cast-iron castings comprising wooden elements by strengthening them with a mechanical clamp. The fibres and the matrix of the wooden load-carrying bars of the domes were not intersected with steel sheets, especially in the extreme sections, as it happens in almost all contemporary wooden domes.

After World War II, these constructions vanished, and new, wooden-steel spatial constructions of domes from glued laminated timber appeared.

Presented in Chap. 6 are four dome systems of the least wood consumption, called rotary shells. They were built on the turn of the 19th and 20th century. **The structure and the construction technology of shell thin-wall domes built until the 30s of the 20th century were reconstructed on the basis of fragmentary historical sketches. The drawings of the structures as shown in Figs. 6.2, 6.5, 6.8, 6.11, 6.13, 6.14 were made. Through the construction of the models shown in Figs. 6.1, 6.3, 6.4, 6.12 the stability of the systems reconstructed was verified.**

The thin-wall, axially symmetrical shell domes (Figs. 6.1, 6.2) were built on the meridional ribs from 3.0 cm thick planks, being a scaffolding, joined afterwards with the plank shell using nails. In this way the lightest axially symmetrical, smooth shell domes of a diameter up to 20.0 m were built. As the diameters of such domes were increased, the ribs were modified, from several bent planks up to planking of a variable moment of inertia of the section and variable form of bipolar girders. The meridional process ribs were used to keep the shape of the spherical canopy and to eliminate the deviations in assembly. Also, the mutually advantageous arrangement of the layers of the covering planks was practiced, creating a quasi-continuous spherical dome, shaping the dome form and mating the ribs to carry over loads. The improvement of the construction led to the minimum consumption wood and steel fasteners. In the domes from 1907 (Fig. 6.4) and 1933 (Fig. 6.14) the use of materials calculated per square metre of projection is so small that its repetition in presently realized wooden domes is not successful (Table 8.1).

The domes built according to the above-described ideas constitute an essential and technological change in the quality of wooden domes in the history of their development. The shell system allows to build domes of a small eminence amounting from 0.25 to 0.15 of the projection diameter. The bending of planks to the required shape of the shell and the increase in the load capacity by nailing successive layers of the covering layers allowed to increase the diameter of domes without changing the construction technology. Despite many advantages, they were not built until the second half of the 20th century

Shown in Chap. 7 are special solutions of axially symmetrical domes in which the shells from planks are joined with the rhombic grid made from crossheads of a variable height, connected at the highest section of a bar with two other crossheads.

The transformation of arch centres into crossheads of a variable height, ended with tangs and provided with an opening (in the highest section), prepared to make a node, constitutes an important stage in the development of shell-gridshell coverings. The grid from crossheads splits the sphere into rhombic polygons characteristic of wooden domes. The shape of a crosshead protected the shell nodes against the node snap-through and allowed the elimination on the construction yard of random geometric deviations in assembly. The structure of nodes also fostered the neutralization of distortions caused by the thermal-humidity effects caused during the operation of the facility. A drawback of axially symmetrical shell-gridshell domes is the non-standard nature of crossheads. However, it is possible to standardize crossheads on each separate line of latitude. The advantage of such domes is (1) the stiffness of the shell resulting from the junction of the plank shell with ribs from crossheads, (2) the possibility of the additional lighting of the inside with windows built into the fields between the ribs of the dome's grid (Fig. 7.6).

The erection technology of shell-gridshell wooden domes on a self-supporting scaffolding from 'crossheads' passed the examination, which is evidenced by the lack of reports about the disasters of such domes.

Described in Chap. 8 are selected domes from glued laminated timber. The contemporary realizations of domes developed towards high-cubic capacity prestigious facilities. The wood applied is protected with industrial methods. Bars—beams are connected with massive, steel box nodes, bolts and metal sheets pasted into wooden bars. However, the steel nodes that connect bars from glued laminated timber have not been adapted to the natural structure and the properties of wood.

Due to the considerable consumption of wood and steel (Table 8.2, line 7), the solutions of steel-wooden bar structures are energy-consuming. **Attention was drawn to the high amount of waste and the high consumption of wood associated with the building of glued structures. In the highly advanced Japanese technology there occur circa 62.2% of waste, from the wood acquired from the forest.**

Formulated in Chap. 9 is the issue important from the point of view of the further development of the constructions of domes from solid wood presented in Chaps. 4 through 8. The most urgent research subjects were shown since the development of domes from solid wood stopped on the shell-ribbed domes of diameters up to 67.0 m. **The need for further research work is visible in the contemporary realizations from layer-wise glued laminated timber, which revealed the omission of various issues associated with the structure and properties of wood.**

The recognition of the following problems is urgent:

- (1) change of the model of compressed and stretched bars in function of load (W. Dzbeński, Fig. 9.1, [1]);
- (2) the consideration of the impact of shape distortions on the critical load capacity of wooden bars in which the predominant load are compressive axial forces. The impact of shape distortions is more essential in wooden constructions than in steel constructions since in wooden bars the E/G ratio

reaches high values, depending on the wood species. **The reduction of the critical load capacity depending on E/G is described by the coefficient η specified in Table 9.1, Fig. 9.6;**

- (3) compressed bars of a low slenderness $\lambda < 20$ are destroyed due to the local loss of stability of fibres, which is demonstrated by the transverse cracking of thickset bars (the ends of thickset bars should be strengthened, e.g. using a spiral reinforcement over the circumference);
- (4) the critical load capacity of wooden fibres is dependent on the coefficient of transverse stiffness of the matrix (Sect. 9.5, Formula 9.7). The phenomenon of the buckling of fibres in wood is the cause of the lower strength of wood not burdened by the presence of knots to compression than to stretching. A particular intensification of this phenomenon occurs on the ends of wooden bars (“cleavage” of bar ends);
- (5) the dependence of the destruction form of compressed wooden bars may be assessed on the basis of the analogy to the destruction of fibre-reinforced composite bars (Kowal Z., [2]). In bars of a slenderness λ_Q lower than 30 it is recommended to use a circumferential reinforcement with a rowing or steel clamps, especially the most loaded bar ends. The ferrule should be so formed that the Poisson effect (Figs. 9.10b, 9.11) does not result in the sectioning of fibres, but so as to protect against the “cleavage” the extreme sections of wooden bars;
- (6) in the compressed bars of domes there occurs the phenomenon of the reduction in the longitudinal stiffness as the effort of the bar increases. The reduction in stiffness κ (Table 9.2, Fig. 9.18), depends on the ratio σ/σ_{kr} , and the coefficient of imperfection C of a compression-loaded bar. This issue applies to all bar constructions, not only wooden ones. **The reduction in the longitudinal stiffness of compressed bars should be considered in the analysis of the load capacity of bar domes, especially those built from bars of a permanent section because it may initiate the snap-through of nodes;**
- (7) in wooden bars transversely **a strong concentration of tangential stresses between fibres** occurs. Stresses τ from shearing in the matrix may lead to its destruction. Specified in Table 9.3 are the coefficients of the concentrations of tangential stresses in the matrix between fibres for the square packing of fibres;
- (8) due to the structure of wood in form of fibres placed in the visco-elastic matrix, **two critical load capacities occur in bars: the neutral (lower) load capacity and the shock (temporary) load capacity** [3]. Compressed wooden bars should be dimensioned on the basis of the stable (lower) critical load capacity since the load comprised between the neutral and the shock critical load capacity produces a continuous transverse creep of wood until its destruction;
- (9) letting in massive nodal steel sheets into the ends of wooden bars of the constructions of domes reduced their load capacity. Such connections of bars with nodes require an additional strengthening;
- (10) an advantageous feature of wood is the possibility of the repair of damaged or bent compressed bars without disassembling the dome, using a non-symmetrical reinforcement of the element being compressed;

- (11) the contemporaneously used protection methods of wood against corrosion produce the degradation of the matrix in the natural fibrous composite, which wood is. The degradation of the matrix reduces the load capacity of wooden bars.

The insufficient propagation of the knowledge and the research on the detailed phenomena described in Sects. 9.1 through 9.11 in Chap. 9 constitutes a barrier to increase the span of domes from solid wood.

Presented in Chap. 10 are the reconnaissance research works of the wood creep models conducted by various researchers, aiming at the theoretical forecasting of the creep of wooden constructions basing on visco-elastic models.

Related in Chap. 11 are own research works on the dynamic models from pine, spruce, larch and oak wood. It has been demonstrated that on the basis of the measurement of free vibration of wooden beams it is possible **to assess the stiffness of the elements of constructions from wood, the free vibration parameters, the coefficient of direct elasticity of wood.** The test results included in Chap. 11 of free models from wood point out to the possibility of their use in the diagnostics of the elements of wooden constructions for:

- (1) the selection of both the best elements and the elimination of defective elements within the area of similar elements from the same wood, (2) the comparison of the properties of elements from various wood species, (3) the preliminary recognition of the rheological models of wood on the basis of micro-creep, (4) the testing of the impact of moisture on the mechanical properties of wood, (5) the detection of moistened elements in the sets of similar elements, (6) the detection of hidden defects in wooden construction.

In Chap. 12 the possibility of using wood-based materials in the construction of domes and responsible engineering constructions were examined. **As the first criterion of usefulness of wood-based for the construction of domes the reversibility of the creep model, after the removal of the load, was adopted. The second criterion is the identical durability of elements made as a load-bearing construction built from various materials.**

It follows from the measurement of free vibration of dry and wet models from coniferous plywood, beech plywood, OSBs, fibreboards and chip boards that: the chip board undergoes the quickest degradation, the fibreboard degrades in the second order. The coniferous plywood exhibits the highest durability close to that of wood. Wetted wood and plywood maintained the required technical parameters longest. It follows from the research work that fibreboards and chip boards as well as OSBs are not useful for the construction of fundamental elements of dome constructions. The soaking of the tested wood-based materials with water led in a short time to the destruction of the models made from those materials. **Wooden-derived materials, subjected to the strong degradation of physical properties, are fit for the use as supplementary element and the outfit of permanent building facilities with large consequences of their destruction.**

It has been demonstrated in Chaps. 1 through 7 how the development of structures proceeded, from multi-layer arches made from arch centres up to the systems characteristic of wooden domes.

The typology of the structures of wooden domes has been introduced. Dome-like forms from logs, domes on scaffoldings, domes of a ribbed, shell and gridshell structures have been presented, occurring in the building trade from wood only. Among ribbed domes, domes of meridional ribs from arch centres and of truss ribs, in form of arches with bipolar coordinates, have been discussed. Shell domes of a massive and a thin-wall shell: smooth, shell-ribbed and ribbed-shell domes have been reviewed.

The axially symmetrical structures of smooth shells from naturally pre-stressed planks are distinguished by an unparalleled until today minimum consumption of wood and steel fasteners in relation to the area being covered. Attractive structures of a rhombic grid built from ribs, whose shape secures the sphere against the node snap-through, a known cause of geodesic failures of steel gridshell domes, have been reminded. The typology introduced is illustrated in the compilation.

The development of constructions, starting with simple post-beam systems up to arches and dome forms including wooden domes, has lasted for millennia. Unfortunately, many solutions of dome constructions from solid wood sank oblivion. Many dome construction systems have been restored in this book, basing on the scarce, residual data. Many of the structural solutions referenced by the author has preserved until this day an economical, engineering and eco-friendly justification. Different sources of the origin of domes have been described: starting with dome-like coverings up to wooden scaffoldings.

The typology of wooden constructions has been introduced. The domes of a ribbed, shell and netlike construction, characteristic of the building trade from wood, have been presented. Among ribbed domes, the domes on meridional ribs from arch centrings and with lattice ribs, having the form of arches of bipolar coordinates have been discussed. Shell domes with a massive and thin-wall shell: smooth, shell-ribbed and ribbed-shell have been discussed. The axially symmetrical constructions of smooth shells from naturally compressed planks are distinguished by an unparalleled until this day minimum consumption of wood and steel fasteners in relation to the area being covered. Attractive constructions of a rhombic grid built from ribs, whose shape protects the sphere against the node snap-through, a known cause of geodetic failures of netlike domes from steel, has been reminded.

It has been presented how to use the natural properties of wood for the building of aesthetic and eco-friendly constructions from wood of an average quality and without the expensive selection applied in the building of glued constructions. It has been demonstrated that a significantly better use of solid wood than in domes from glued wood is possible. The domes from solid wood are an attractive proposal for the general building trade taking into account their aesthetics and ecology.

Attention was drawn to the analogy of wood to fibrous composites. Computational models and computational proposals for constructions from solid wood have been shown. The topics of the most urgent research, necessary for the further development of this knowledge domain, have been indicated.

The book presents the results of theoretical analyses to be used in the designing and building of constructions from wood, as well as their use in the teaching at technical universities.

Basic types of wooden domes

Dome-like coverings



pyramidal



stepped pyramidal



pyramidal on
a hexagonal projection



segmentally cylindrical



lantern

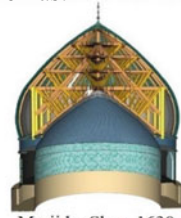
Multi-layer domes built in the Middle East



Dome of the Rock, 691,
D=20.40m



Al-Aqsa Mosque, 715,
D=11.50m



Masjid-e Shan, 1630,
D=21.40m

Domes on scaffoldings



Venice,
Saint Mark's Basilica,
1094, D=10m



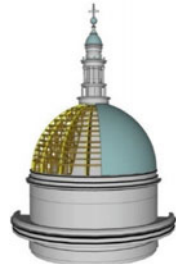
Venice,
Il Redentore,
1592, D=14.5m



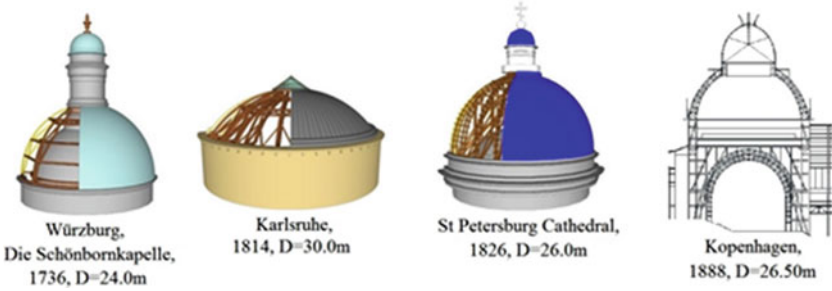
Venice,
Santa Maria della Salute,
1687, D=20.5m



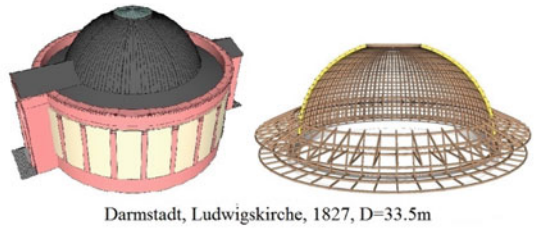
Paris,
Saint-Louis-des-Invalides,
1693, D=29.0m



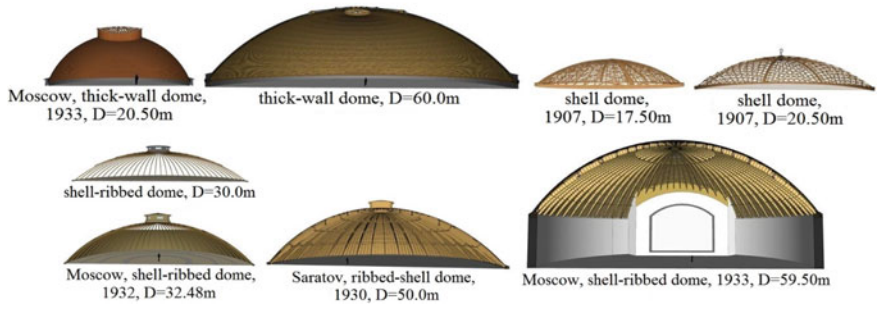
London,
Saint Paul Cathedral,
1715, D=32.0m



Domes on ribs from arch centres



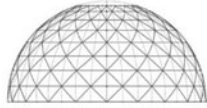
Shell domes



Gridshell domes



Moscow, 1932, D=32.0m



Sakura, 1927, D=20.0m



Zollbau, 1928, D=15 to 20.0m

Greim, 1st half of the 20th century,
D=15.0 to 20.0m

Ribbed domes



Munich, 1925, D=21x24.20m



Baku, 1930, D=67.0m



Ivanovo, 1932, D=50.0m

Domes having a glulam structure

Flagstaff, 1977,
D=150.6mTacoma, 1983,
D=161.54mMarquette, 1991,
D=163.4mOulu, 1985,
D=115.0mŽilina, 1986,
D=105.0mIzumo, 1992,
D=140.7mOdate, 1997,
D=153,0x157,0mMiyazaki, 2004,
D=122.0x104.5m

References

1. Dzbeński W., *Nieniszczące badania mechanicznych właściwości iglastej tarcicy konstrukcyjnej wybranymi metodami statycznymi i dynamicznymi*, Wydawnictwo SGGW-AR, Warszawa, 1984.
2. Kowal Z. *Kompozytowe pręty ściskane zbrojone podłużnie i spiralnie*. XLII Konferencja Naukowa Komitetu Inżynierii Lądowej i Wodnej PAN i Komitetu Nauki PZiTb, Kraków – Krynica, wrzesień 1996.
3. Kowal Z. *Nośność krytyczna słupów drewnianych jako kompozytów włóknistych*. Symposium - Drewno i materiały drewnopochodne w konstrukcjach budowlanych. Szczecin-Międzyzdroje 05-06 września 1996.

End

Compiled in Table A.1 are the weights of masonry domes, reinforced concrete domes, those from glued laminated timber and natural solid wood, as expressed per m^2 of the dome's horizontal projection.

The data on various domes are specified in lines 1 through 10 of Table A.1. Specified in column 1 are the dome types, in column 3 the dome name and location, in column 4 the diameter of the horizontal projection, as expressed in [m], in column 5 the weight of the material from which the dome was built, calculated per m^2 of the dome's horizontal projection, in column 6 the weight of steel consumed for the reinforcement system of the shell (Tbilisi Sports Palace, Georgia—reinforced concrete shell) or the joining of elements.

The comparison of the weight of domes expressed in $[\text{kg}/\text{m}^2]$ provides a favourable picture of the construction of wooden domes, especially solid wood, as compiled in line 6 and 7.

The weight of wood in domes from solid wood is specified jointly with the weight of the construction and that of the shell being, at the same time, the outside casing of the facility. In the constructions from glued laminated timber—lines 9, 10, 11, just the weight of the ribbing is specified since in the aforementioned domes an outside shell from light technical fabrics was used. Table A.1 does not specify the weight of the wood consumed for the scaffolding to fabricate masonry and reinforced concrete domes. It is also worth noticing that wood and domes made therefrom are, in many aspects, closer to the requirements of environmentally friendly savings. It is known, already at the fabrication stage of a building material, that the production of constructional timber is based on the cultivation of forests that are a 'factory of oxygen'. The production of steel and concrete is associated with the destruction of environment and emissions of harmful gases, mainly CO and CO_2 .

Shown in Fig. A.1 is the chart from the paper [1], depicting the increase in the weight of domes associated with the increase in the diameter of the horizontal projection of domes built from various materials. Curve A applies to masonry domes, B—to reinforced concrete domes of a ribbed construction, C—to reinforced concrete shell domes. The chart in Fig. A.1 was supplemented by curve D depicting the weight of wooden domes: from glued laminated timber and solid wood: shell

Table A.1 Compilation of the weight of stone domes, concrete domes and wooden domes: from solid wood and glued laminated timber

		No.	Facility	Diameter [m]	Weight of material per m ² of projection [kg/m ²]	Weight of steel [kg/m ²]	Year of construction
Masonry concrete Reinforced concrete		1	Temple of Diana, Rome	14.50	7000.00	–	135
		2	Pantheon, Rome	43.30	6000.00	–	125
		3	Saint Peter's Cathedral, Rome	42.52	6800.00	–	1542
		4	Centennial Hall, Wroclaw, Poland	65.00	2030.00	–	1905
		5	Tbilisi Sports Palace, Georgia—reinforced concrete shell	76.00	~ 180.00	16.00	1961
Wooden domes	From solid wood	6	Shell dome, Fig. 6.4	17.50	30.00	1.50	1907
		7	Moscow Dome, Fig. 6.14	59.50	58.30	1.71	1933
		8	Ashiro Dome, Japan, Fig. 8.11	36.30	26.10	?	1986
	From Glued Laminated Timber	9	Izumo Dome, Japan, Fig. 8.12	140.70	60.80	?	1990
		10	Odate Dome, Japan, Figs. 8.13 and 8.14	157.0 × 152.0	80.60	?	1997
		11	Miyazaki Dome, Japan, Fig. 8.15	122.0 × 104.5	42.80	44.70	2002

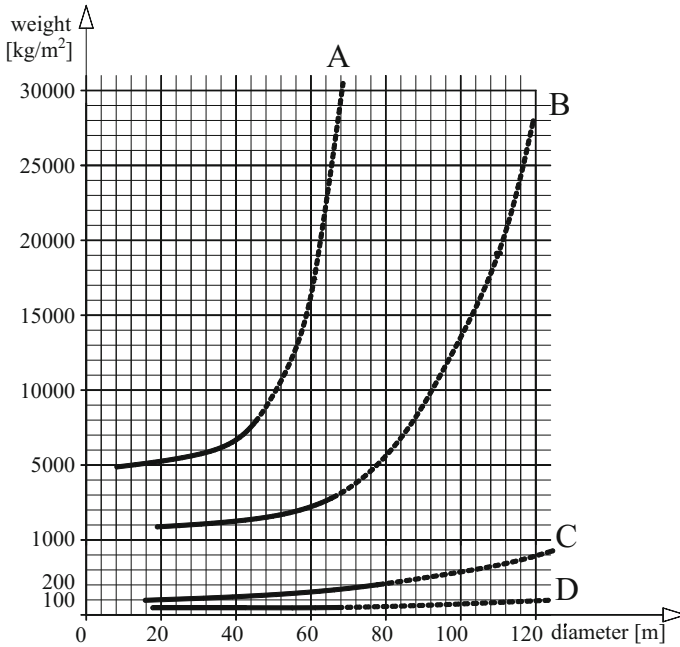


Fig. A.1 Compilation of the weight of masonry domes, reinforced concrete domes, steel domes and wood domes at the same diameter of the horizontal circular projection as expressed in metres according to [2], A—masonry domes, B—reinforced concrete domes, ribbed domes, C—reinforced concrete shell domes, D—wooden domes

domes, ribbed domes and thin-wall domes. The probable weight of the dome accompanying the increase in the projection’s diameter is drawn with a dotted line.

It is demonstrated in Fig. A.1 (curve D) that **wooden domes are lighter and more cost effective than those built from other materials.**

The historically established opinion that domes are prestigious facilities has found contemporaneously its confirmation in the development of domes having a structure from glued laminated timber. This fashion, supported by the development of the constructional mechanics from homogeneous materials, has resulted in the abandonment of the building of less expensive constructions from solid wood suitable for general application.

A large variety of ideas inspiring the correct structural solutions of wooden domes appeared in the history of the building trade. Many among those solutions may form a basis for the continuation of experiments, also for the development of the construction of modern domes from wood and their application in the general building trade.

Compiled in Fig. A.2 on a chart are the curves illustrating the weights of domes from solid wood, as discussed in this publication, including thin-wall, ribbed and shell domes in function of their diameter.

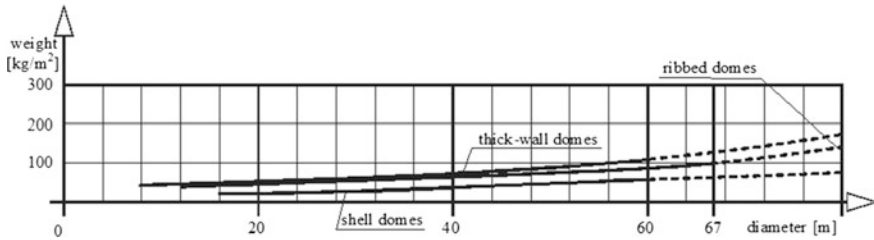


Fig. A.2 Compilation of the weight of domes from solid wood having a thick-wall, ribbed and shell structure

As it can be seen from the comparison of the curves in Fig. A.2, among the domes from solid wood shell domes are distinguishable by an imposingly low consumption of wood expressed per m^2 of the dome's horizontal projection. Such domes are described in Chap. 6 and it was demonstrated that those of a low and medium-sized span, of a diameter of the projection lower than 50.0 m, do not require such a huge outlay of energy and construction costs than domes of a larger diameter. The advantages from the operation of such domes are worth propagation. They are aesthetical, light and simple in assembly. They can also be built in an economic way from cheap wood, even of a common quality.

Wooden domes are well inscribed in the scenery, including also that of a great city. The form and the construction of a dome allow to make savings on the energy used for its execution and operation. Besides, the building of facilities of a weight of the materials required for the construction and the casing amounting to 30.0 kg/m^2 , renewable at the same time and fostering the environment, is favourable and follows at the minimum destruction of that environment.

An important advantage of the domes described in this monograph is **the amount of waste from solid wood generated in the preparation process of a constructional element several times lower than that of waste produced in the building industry of domes from glued laminated timber**. Imura Y., the author of many domes built in Japan, specifies that only 37.8% of wood acquired from a forest are fit for the production of glued elements of the load-bearing construction. A further treatment of planks before gluing additionally increases the amount of waste. The cost of one m^3 of glued laminated timber is about three times higher than that of solid wood.

On the basis of few still preserved bibliography references discussing the examples of domes still built until the thirties of the 20th century as well as fragmentary information the forms of the already forgotten facilities have been reconstructed. The constructional systems recovered delight with delicate proportions and a light structure. They help understand the characteristic subject matter of historically shaped domes from solid wood. They are the set of correctly resolved connections and nodes, in accordance with the properties of wood and the feeling of statics.

It is worth emphasizing that the domes from solid wood have a series of advantages: (1) a slight weight of the construction and the casing when calculating per m^2 of the dome's projection, (2) the simplicity in the construction process, (3) a minimum consumption of wood and metal for fasteners, which is translated into a lower realization cost, (4) the use of thermo-insulating properties of the wood of the construction and the casing, (5) the inclusion of the shell from planks into the mating of ribs constituting the skeleton of the load-bearing structure, (6) the amount of waste several times lower in the preparation process of wood for the building of domes from solid wood than those from glued laminated timber. **Moreover, the dome forms in relation to building facilities of another geometry have additional advantages:** (1) a lower load from wind and snow, (2) an easier drying of the surface after precipitation, (3) the possibility of a natural protection against biological corrosion, (4) the possibility of the surface protection of wood against fire through the use non-flammable shields, (5) a lower weight and a low-positioned centre of gravity of the solid makes the dome more stable in the situation of earthquakes and extreme weathering conditions.

No negative effects of the connections of wooden elements with steel nodes used and observed in the contemporary domes as described in Chaps. 8 and 9, Sect. 9.6, occur in the domes from solid wood.

The constructions of historical domes can be developed using the most recent theoretical papers and the research work discussed in this work. The issues as presented in Chap. 9, on the basis of the papers by Dzbeński W. and Kowal Z. and others, have revealed a series of problems recommended for the inclusion into the analysis of wooden structures.

To sum up, it should be emphasized that:

1. the historically shaped domes from wood constitute an essential set of useful solutions that are favourable taking into account the features of wood,
2. the domes from solid wood of diameters up to 67.0 m are environmentally friendly structures and constitute a good alternative for the construction of domes from other materials,
3. many of the described dome systems from solid wood are suitable for a series production due to the aesthetical, economic, utility values and the simplicity of the assembly,
4. wooden shell domes are exceptionally minimalist forms in which the load-bearing construction is simultaneously a casing of the facility. This allows to maintain low indicators of the consumption of wood and metal fasteners per m^2 of the roofed area,
5. the preparation of wood for the building of domes from solid wood is burdened with a considerable lower amount of waste than the production of glued laminated timber, and it is even possible to use wood of a common quality,
6. the selection methods of wood and wood-based materials as presented in Chaps. 11 and 12 on the basis of the measurements of free vibration provide a legible piece of information on which wood species or which element is suitable to complete the construction of domes,

7. demonstrated in Chaps. 11 and 12 is the method how, using simple testing, to find wetted elements in the sets of similar elements,
8. it has been demonstrated on the basis of the measurement of the free vibration of dry and wet models that **among wood-based models plywood only** is suitable for responsible constructions determining the load capacity of the system,
9. the testing of the impact of wood creep on sectional forces as well as creep buckling of compressed bars constituting the structural elements of wooden domes is important,
10. in the industrial wood treatment process the degradation of the visco-elastic matrix should be taken into account, which, as demonstrated in Chap. 9, affects the strength of structural elements from wood,
11. the experimental analysis of the effect of the longitudinal stiffness reduction in the function of inside force in structure S to critical force S/S_{kr} , is recommended.

It follows from the comparison of various dome constructional systems that the highest wood savings can be achieved by developing the evolutionarily perfected systems. In the constructions shown in Chaps. 4, 5, 6, 7 it is even possible to implement wood of a common quality. The building of such domes is not associated with the cutting-out of hectares of forests like in the case of contemporary domes from glued laminated timber. The recycling of material from technically worn-out facilities does not result in the destruction of environment.

Further research work covering the recognition of the biochemical structure and the resultant properties of wood as a construction material is necessary.

The development of the wood mechanics is an urgent need for the rational development of the production of building elements, wood protection technology and the development of wood-specific structural systems. Dome structures are examples of structures shaped with the minimum consumption of wood and steel fasteners, at the maximum use of strength properties.

Making the building from wood a global undertaking, covering the cultivation of forests may protect the Earth against ecological disaster.

References

1. Lisowski A. *Projektowanie kopuł obrotowych* Biuro Studiów i Projektów Wzorcowych Budownictwa Miejskiego, Warszawa 1955.
2. Łopatin B. *Postroika Zdanija Goscirka w Gorodie Iwanowo*. Dierewo w Stroitielitelstwie, Stroitielnaja Promysliennost, nr 1, s. 46-50, styczeń Moskwa 1934.

Bibliography

1. Coleman E., Hurst T. *Timber Structures Reinforced with Light Gage Steel* Forest Products Journal. vol. 24 No. 7 1974.
2. Cebecauer D., Stubna J., Bitterer L., Sima J. *Vyvoj pretvorenia drevenej nosnej konstrukcie sportovej hały v Žiline*. GaKO, 1987, p. 56–58.
3. Cyrankowski M., Romański M., Osipiuk J., *Wpływ niektórych związków chemicznych na skuteczność zabezpieczenia przeciwogniowego drewna*. Annals of Warsaw Agricultural University SGGW, Forestry and Wood Technology No 55, Warsaw 2004.
4. Durand J. N. L. *Reuceilet Paralele Edifices de Tout Genre Ancien et Modernes*, Chez l'Auteur, à'Ecole Polytechnique. 1800.
5. Dudovsky J., Rohanova A. *Charakterystyka zginania i gęstości drewna świerkowego w związku z klasyfikacją wytrzymałościową*. Annals of Warsaw Agricultural University SGGW, Forestry and Wood Technology No 55, Warsaw 2004.
6. Dzbeński W., Kraińska H., *Drewniane elementy mebli i wyposażenia wnętrz z okresu koptyjskiego (V-VIII w n.e.)* Wydawnictwo SGGW Warszawa 1999.
7. Dzbeński W., Kozakiewicz P., Krzostek S., *Wytrzymałościowe sortowanie tarcicy budowlano-konstrukcyjnej metodą wizualną*. Katedra Nauki o Drewnie i Ochrony drewna. Wydział Technologii Drewna SGGW, Warszawa 2004.
8. Ganowicz R. *Zastosowanie teorii procesów losowych do opisu pełzania tworzyw konstrukcyjnych*, Reologia drewna i konstrukcji drewnianych – Sympozjum Akademii Rolniczej w Poznaniu, materiały, Zielonka 21–22 października 1982 r.
9. Grześkiewicz M., Nowicki G. *Badania właściwo fizyko – mechanicznych drewna bukowego poddanego obróbce termicznej*. Annals of Warsaw Agricultural University SGGW, Forestry and Wood Technology No 55, Warszawa 2004.
10. Hichcocok H. R., *Architecture of the nineteenth and twentieth centuries*, Penguin Books, 1963 (Moller's dome).
11. Hoyle R. J. *Projektowanie drewnianych belek zbrojonych stalą* Forest Products Journal nr 4 kwiecień 1975.
12. Imura Y., Kurita S., Ohatsuka T., *Reticulated Timber Dome Structural System Using Glulam with a Low Specific Gravity and its Scalability* WCTE 2006—9th World Conference on Timber Engineering—Portland, OR, USA—August 6–10, 2006.
13. Iwanow W. F., *Konstrukcja iż dieriewa i plastmas* Izdatielstwo Literatury po Stroitelstvu Leningrad, Moskwa 1966.
14. Jasnyj G. W. *Pokrytija Obszczestwiennych Zdanij*, Izdatielstwo Litieratury po Stroitelstvu, Moskwa 1964.
15. Kowal Z. *“Oszacowanie nośności granicznej i bezpieczeństwa konstrukcji na podstawie teorii niezawodności”* Inżynieria i Budownictwo nr 10/1972, s. 386–390.
16. Kowal Z., Raducki K., *Interaction of random critical load of spatial truss joint loaded at the joint and on the bars*, III International Conference on Space Structures, Guildford 1984.

17. Kowal Z., Malec M., *Wyznaczanie nośności krytycznej swobodnie podpartych belek podsuwnicowych na podstawie pomiaru częstotliwości drgań własnych*, Inż. i Bud. 2/1989.
18. Kowal Z. *Statystyczne osłabienie i wzmocnienie konstrukcji*, Inż. i Bud. 7–8/1995, s. 392–394.
19. Kowal Z. *The Limit Load Capacity of Compressed Rods with Imperfection In Elastics Medium*, Int. Collegium Stability of Steel Structures, IABSE, V.1, Budapest 1995, s. 1/57–1/62.
20. Kowal Z. *Efekt swobodnego brzegu w ściskanych prętach kompozytowych*, ZN PŚK 34, Kielce 1996s. 39–44.
21. Kowal Z. *O siłach odrywających otulinę zbrojenia ściskanych prętów kompozytowych*, Wybrane Problemy Naukowo-Badawcze Mostownictwa i Budownictwa, Wydział Budownictwa Politechniki Śląskiej, Gliwice 1997, s. 135–143.
22. Kowal Z. *O amplifikacji przemieszczeń i zginania prętów ściskanych*. XLII Konferencja Naukowa Komitetu Inżynierii Lądowej i Wodnej PAN i Komitetu Nauki PZiTB, Poznań—Krynica 1997, T 5, s. 49–56.
23. Kowal Z. *Emisja akustyczna towarzysząca wyboczeniu kompozytowych prętów ściskanych*, XLIV Naukowa Komitetu Inżynierii Lądowej i Wodnej PAN i Komitetu Nauki PZiTB, Poznań—Krynica 1999r., s. 55–62, współautor: Gołaski L.
24. Kowal Z. *Nośność krytyczna wielogłęziowych słupów drewnianych zespolonych przewiązkami*. Konferencja Naukowa Drewno i materiały drewnopochodne w konstrukcjach budowlanych, Szczecin-Swinoujście, 27–28.09.1999r., s. 59–66.
25. Kowal Z. *Interakcyjna nośność graniczna słupów drewnianych wzmacnianych dyskretnie nakładkami*, Wrocław—Kliczków 5-7.12.2002, REMO 2002, s. 181–188.
26. Krajewski K., *Use of the stress wave based tomography for testing of wood*, Annals of Warsaw Agricultural University SGGW, Forestry and Wood Technology No 53, Warszawa 2003.
27. Krutul D. *Rozmieszczenie celulozy i ligniny na przekroju poprzecznym i podłużnym sosny zwyczajnej (Pinus sylvestris L.)* 12 Konferencja Naukowa Wydziału Technologii Drewna SGGW Warszawa, 17–18 listopada 1998.
28. Krutul D *Udział celulozy i niektóre jej właściwości badane na przekroju poprzecznym i podłużnym pnia dębowego*. Folia Forestalia, Polonica, Zeszyt B, 1988.
29. Lantos G. *Test Results on Mild Steel Reinforced Glulam Timber Beams*. Civil Engineering, listopad 1964 London.
30. Mazga-Górecka M. *Humanitarna rewolucja w architekturze*. Architektura 04/2016, str. 30–46.
31. Mielczarek Z., Mickiewicz D., *Wzmacnianie belek drewnianych zbrojonych włóknem szklanym*. Inżynieria i Budownictwo nr 12/1973.
32. Mielczarek Z., Misztal B., *The Investigation of Trusses Made from Wood, Steel and Wood-Base Materials Under Long-Term Load*, International Wood Engineering Conference, New Orleans, Louisiana, U.S.A. October 28–31, 1996.
33. Mielczarek Z., Misztal B., *Analiza sztywności dźwigarów drewniano-stalowych z pasem górnym ciągłym z drewna i materiałów drewnopochodnych*. Sympozjum Naukowe Politechniki Szczecińskiej, Wydziału Budownictwa i Architektury, Szczecin-Międzyzdroje 5–6, wrzesień 1999.
34. Misztal B., *Kopuły drewniane*. rozdział 4 w monografii p.t. *Współczesne problemy budownictwa* pod redakcją Lucjana Kurzaka, Jacka Selejda, Wydawnictwo Politechniki Częstochowskiej, Częstochowa 2015.
35. Murray P. *Architektura włoskiego renesansu* Wydawnictwo VIA 1999 r.
36. Natterer J., Gotz K., Hoor D., Mohler K., *Holzbau Atlas*, Institut für internationale Architektur-Dokumentation GmbH, München 1980.
37. Pape M.W.T. *Andrea Palladio 1508–1580 Architect between the Renaissance and Baroque*. Benedict Taschen Verlag, Photographs by Paolo Marton.

38. Paliszko S., Raczkowski J. *Pełzanie drewna w warunkach wielostopniowego programu obciążeń*. Reologia drewna i konstrukcji drewnianych. WSR, Poznań 1984.
39. Stierlin H. *Skarby Orientu. Architektura i sztuka islamu od Isfahanu po Tadż Mahal*. Warszawa, Arkady 2002.
40. Sourdel - Thomine J. von Spuler B. *Propyläen Kunstgeschichte die Kunst des Islam*, II. 102a, 102b, Berlin 1973.
41. Własow W. E., Goldenwiejzer A. L. *Razcziet tonkostiennych swodow- obołocziek*. Sprawocznik projektirowszczyka promysziennych sooruzienij. Dieriewiannyje konstrukcji. Głównaja redakcija stroitielnoj literatury. Moskwa-Leningrad 1937.
42. Wundram M., Pape T., Marton P., *Andrea Palladio. Architect between Renaissance and Baroque*. Verlag, Germany, Kościół II Redentore w Wenecji.
43. www.fakopp.com/site/contact.
44. www.twojebieszczady.pl/ Kaniewska M., *Cerkiewki Lubelszczyzny*, 2005.
45. www.westernwoodstructures.com.
46. <http://www.tvn24.pl>.
47. PN-B-03150:2000, *Konstrukcje drewniane. Obliczenia statyczne i projektowanie*.